Tube hydroforming of steel for automotive applications.

Darlington, Roger

corus

EPSRC

Engineering and Physical Sciences Research Council

DOCTOR OF ENGINEERING (EngD) Degree

'Tube Hydroforming of Steel for Automotive Applications'

Roger Darlington

BEng (Hons) AMIM (GE)

Engineering Doctorate Thesis (EngD)

Academic Supervisor : Prof. J. D. Parker

Industrial Supervisor : Dr. Ir. B. D. Carleer

EPSRC Engineering Doctorate Centre - Wales

Abstract

Tube hydroforming has the potential to produce large structural automotive components which may be utilised for weight reduction in future generation vehicles, by replacing stamped and spot-welded steel assemblies. However, limited implementation of this technology has taken place for Body-In-White (B-I-W) components, due to the complexity of the process and low levels of confidence and knowledge of the technology. This is coupled with assembly issues that this technology presents for B-I-W construction. In contrast the application of this technology for sub-frame and chassis component applications has been successful, principally due to the less stringent assembly requirements and proven cost and performance related benefits.

The tube hydroforming process utilises forming fluid, under high pressure, to stretch a tube blank into the shape of a die cavity. The application of the internal pressure may be accompanied by axial feeding of the tube ends to push additional tube material into the die cavity. Close control of process parameters and the die design are essential to produce successful, defect-free components. However, the behaviour and response of steel and the influence of friction under these forming conditions are unknown entities.

On the basis of a critical review of literature, a research programme was initiated to engage some of the key forming issues inhibiting wide-scale implementation of steel tube hydroforming for BIW automotive applications.

The principal aims of the project were to identify the fundamental influences of steel properties on the tube hydroforming process and to develop a mathematical model of the process for steel tube.

The research programme entailed small-scale formability tests and large-scale experimental trials, accompanied by the development of analytical and finite element (FE) models of the tube hydroforming process for various steel grades. The analytical and FE models could be used as design aids in the development of automotive BIW hydroformed components. The research project identified significant changes in both mechanical properties and surface characteristics as a result of the Electric Resistance Welding (ERW) tube manufacturing process. This in turn had a significant impact upon the hydroforming behaviour of the steel tubes. An analytical forming limit curve (FLC) model evaluated in this thesis was deemed to provided a robust means of predicting splitting or excessive thinning of a tube hydroformed component as a result of die geometry, tube material or processing conditions. The FE models developed, which incorporated the analytical FLCs, illustrated that the tube hydroforming process could be predicted with a high level of confidence for simple components.

Acknowledgements

The author would like to thank the management, technical and administrative staff of Corus, R, D &T, based at the Welsh Technology Centre, Port Talbot and the academic staff of the EPSRC Engineering Doctorate Centre and University of Wales, Swansea. In addition, support from the Engineering Physical Sciences and Research Council (EPSRC) is gratefully acknowledged.

Thanks are due to the author's project supervisors, Professor Jonathon Parker, the late John Godwin and Dr Bart Carleer, who provided technical support and guidance during the term of the research project. Additionally, the author would like to thank Mike Boyles who, as a mentor, provided valuable input into the author's professional development and technical steer into the project.

A special thanks is owed to Clive Broome and the workshop staff at the Welsh Technology Centre, who provided substantial support in terms of test sample machining and preparation of the drawings for the hydroforming research tools.

Dedication

This Thesis is dedicated to my dear wife Emma, to whom I owe a debt of gratitude for her tremendous encouragement and support during the EPSRC Engineering Doctorate programme, despite the difficult times that she faced during the illness of her late father, Leighton Hunt.

Doctorate of Engineering Degree - Record of Training

Overview

The first three and a half years of the EngD programme were spent with British Steel Strip Products and the remaining half year with Corus R, D&T within the Product Engineering Department, at the Welsh Technology Centre, Port Talbot. During this period, a broad appreciation of engineering practice within a high-tech industrial culture was gained. This included experience in health & safety issues, quality assurance and total quality management/principles and techniques, having direct exposure to a strongly customer orientated working culture. In addition, expert knowledge of a specific engineering area has been developed (Tube Hydroforming).

Formal Training

Training was aimed at achieving the technical competencies, professional skills and personal qualities essential for a fulfilling career in industry. The following assessed formal training modules were successfully:

Technical Modules: Steel Process Evolution, Refractories and Steel Structures, Steel Processing, Coated Products, Steel Product Development, Engineering Applications, Environmental Issues, Finite Element Analysis, Statistical Design of Experiments and Training in Windows 95 and Lotus Smartsuite 97.

Professional Development and Management Modules: Development of Personal Skills, Leadership/Teamworking Skills, Investment Appraisal, Business Process Engineering, Graduate Management, Total Quality Management, Effective Management, Employee Relations, Health and Safety Awareness, Financial Awareness and Business Awareness.

Informal Training

In addition to the formal training modules a range of other tasks were completed facilitating the development of a range of competencies. These have included:

Presentations have been made to a range of external groups and senior management within British Steel Plc (upto Executive Board level). Presentations were made to the following groups:

- *Delegation from the DTI, including Lord Sainsbury*
- *Rover Group & BSSP's Steering Group meeting*
- *BSSP's Hydroforming Strategy Group*
- *Simulation Review meeting between Rover and BSSP regarding internal projects*
- *Delegates from Nippon Steel R &D*
- *Newport Metallurgical Society*
- *Management from Product Application Centre, Koninklijke Hoogovens R&D*
- *Managing Director, Ken Bradley and Chief Engineer, Murray Mason from F& P Manufacturing*

Doctorate of Engineering Degree - Record of Training

During the research programme, attendance at an ULSAC forming simulation review meeting held in Heilbronne, Germany was made on behalf of BSSP 14th September 1999. International representatives of the ULSAB-AVC attended this meeting to review the simulation and prototyping status of ULSAC. The meeting concluded with a visit to Krupp Drauz's prototype tool manufacturing facility in Heilbronne.

Conferences/Seminars

Presentations have been made at the following conferences/ seminars, resulting in experience in communicating and defending technical issues with a learned audience:

- *Preparation of poster presentation at the 3rd EngD Annual Seminar, University of Wales, Swansea. Sept. 1997.*
- *Preparation of poster presentation at the 4th EngD Annual Seminar, University of Wales, Swansea. Sept. 1998.*
- *Preparation and oral presentation of Publication (1) at the 5th EngD Annual Seminar, University of Wales, Swansea. Sept1999.*
- *Preparation and oral presentation of Publication (2) at EUROPAM '99 international conference, Darmstadt, Germany. Oct. 1999*
- *Preparation of poster presentation for 3rd International Conference – Materials for Lean Weight Vehicles, Heritage Motor Centre, Gaydon UK. 10-11th November 1999.*
- *Preparation of a poster presentation at the 6th EngD Annual Seminar, University of Wales, Swansea. Sept. 2000.*

The opportunity to attend a wide variety of lectures and seminars/conferences has been taken throughout the duration of EngD programme including:

- *South Wales Metallurgical Association lecture – 'Solidification Processing – The Last Half Century'*
- *Newport Metallurgical Society lecture – 'Materials Requirements for Rover Body and Pressings'*
- *South Wales Metallurgical Association lecture – 'The Challenge to Steel in the Automotive Industry'*
- *Steel Division - Annual Meeting and Dinner, 'Steel Beyond the Millennium, the material challenge', The Belfry, Wishaw, Nr. Birmingham, 5-6th November 1998*
- *International Conference on Hydroforming - Fellbach/Stuttgart, Germany 12-13th October 1999*
- *3rd International Conference – Materials for Lean Weight Vehicles, Heritage Motor Centre, Gaydon UK 10-11th November 1999*

Doctorate of Engineering Degree - Record of Training

Publications

From the research programme carried out, the following papers have been produced entailing a number of days planning and preparation in each case: -

(1) 'Forming Evaluation of Complex Tube Hydroformed Components', Darlington, R., A., Parker, J.D. and Godwin, M. J., Ironmaking and Steelmaking 2000,Vol.27 No.6, pp461-468.

(2) 'Design Considerations for Pre-bending of Tubes for the Production of Hydroformed Components', Darlington, R., A., Hughes, D. and Rees, M., EUROPam '99'. Darmstadt, Germany.

Skills & Competencies

Training has also been received for a variety of test equipment and facilities leading to competence in the following: -

- *Optical metallography techniques including electronic image capture.*
- *Wide range of small scale formability tests and mechanical tests*
- *Circle Strain Analysis*
- *Operation of Anton Bauer High Pressure Hydroform Press*
- *The use of Pamstamp™ to perform Incremental Finite Element Simulations, in sheet metal forming, tube bending and tube hydroforming.*
- *The use of Hypermesh™ to create simple CAD geometry and Finite Element meshes for use in Pamstamp™ forming simulations.*

CONTENTS

References

1.0 Introduction

Tube hydroforming technology provides the potential for significant performance improvements and weight reduction of future generation vehicles. The principal benefits are derived from the closed section properties and part consolidation opportunities that are offered by tube hydroformed parts. Tube hydroforming technology has already proven successful for a number of sub-frame and chassis applications. However, to date B-I-W applications have largely been in niche vehicle models with limited application of this technology to producing B-I-W structural components in volume vehicle manufacture.

The tube hydroforming process uses a fluid medium to apply pressure to the inside of a tube blank in order to deform it in to the shape of a die cavity. The process may be assisted by means of feeding tube metal in to the die cavity from either end of the tube, with the intention of achieving the complex sectional changes of a component.

This thesis focused on investigating the fundamentals of tube hydroforming, including the influence of steel property effects, with the aim of developing a robust mathematical model of the process. An extensive review of literature was conducted to develop a thorough understanding of the tube hydroforming process and its limitations. Throughout the duration of the programme, experience of tube hydroforming technology was gained through technical exposure at the Welsh Technology Centre, visits to tube suppliers, component and vehicle manufacturers and from discussions with technical experts in the hydroforming field.

The thesis details the programme of research performed, which included use of a production high-pressure tube hydroforming unit for experimental research trials with automotive steel grades. A state-of-the-art commercial software code was used to develop FE models of the tube hydroforming process based upon experimental data input.

The aims derived from an extensive review of literature, which provided the definition of the project and new areas of tangible research were highlighted. The findings of the project were of benefit to the automotive manufacturing industry.

In today's manufacturing climate, greater emphasis is placed upon ensuring right first-time design. In the manufacture of hydroformed components using the high pressure hydroforming process the tooling must be made of expensive tool steel as opposed to lower cost tooling alternatives such as kirksite or polymer resins, directly as a consequence of the extreme pressures and forces involved in the forming process. The reworking of die tools, relating to design modifications, are expensive during prototype phase. Reducing lead-time to market and associated costs is particularly beneficial to vehicle manufacturers. It is therefore at the design and development stages that Computer Aided Engineering (CAE) may contribute significantly in the reduction in time to market.

A key element of the research performed in this thesis was in the development of a mathematical model of the process, which included the generation of FE models of the experimental trials and the determination of a suitable failure criterion for the prediction of component necking under various strain modes. During the programme, a further failure criterion was investigated and proposed for more complex components and processing conditions. The analytical and FE models developed indicated that the tube hydroforming process could be modelled with a high degree of accuracy.

The following thesis provided: -

i. A greater understanding of steel Electric Resistance Welded (ERW) tube capability and the limitations regarding hydroform tool geometry and processing conditions.

ii. A robust modelling method that was able to evaluate the tube hydroforming process conditions, material and die design.

2.0 Review of Published Literature

Introduction

The review of literature begins with automotive manufacturing trends that have dominated the 1990's and which have lead to the research, development and growth of new automotive technologies such as tube hydroforming. This chapter outlines the current manufacturing climate and describes how steel, in conjunction with new technologies, may achieve new targets in terms of performance, cost and weight reduction. The review covers the state-of-the-art in tube hydroforming technology, identifying the complex nature of the process, the equipment used to produce hydroformed components, key advantages and limitations, followed by a brief review of reported applications. The review also addresses aspects of formability and friction and how these influence forming conditions. A separate section of the review examines the approaches currently used in component design and describes how FEA plays a key role in tube hydroforming with particular reference to new developments. The review concludes with a summary of findings, which highlight areas where research was required. In the preparation of this review, state-of-the-art search techniques were used and discussions with key members of the hydroforming community were made.

2.1 Automotive Manufacturing Trends

2.1.1 Globalisation

Globalisation has featured strongly in all areas of the automotive industry with activities such as investment in foreign ventures, alliances, and strict licence and supply agreements which ensure delivery of lowest cost supplies to the manufacturers. These practices are apparent throughout the complete automotive supply chain, from the base steel supplier to vehicle manufacturer. Recent joint ventures include plans by Opel and Suzuki Motors Corporation to build the Suzuki Wagon R+ and Opel Agila, on Suzuki's mini-car platform. General Motors (GM) and Isuzu Motors plan to develop a common platform for Isuzu's Rodeo and Trooper and GM's Sport Utility Vehicles (SUVs) aimed at the US market [1]. These types of venture provide for cost-effective production, minimising financial risks and increasing utilisation of manufacturing plants. Hand-in-hand, large-scale foreign investment by the vehicle manufacturers continues with drives

for improved economics and increased market share. An example of such large-scale investments includes Renault's acquisition of the Korean company, Samsung Motors', taking over its assets in April 2000. Another example is Daimler-Chrysler's bid for a 34 percent stake in Mitsubishi Motors [1,2]. Over the last ten years, a high rate of aquisitions of vehicle manufacturers or groups by other larger vehicle manufacturing groups has been seen, such that by 1999 only 20 manufacturers or groups remained. These groups are listed below. Although only twenty groups remain, the brand names of the companies have been preserved, such as Jaguar and Volvo, which belong to Ford Motor Company. The number of vehicle groups/manufactures, however, is expected to continue to decrease.

2.1.2 Vehicle Body Construction

Most vehicle bodies that are produced today have a monocoque (unibody) design or are based upon a body-on-chassis or a 'space-frame' design [3]. The body design has several restrictions, which continue to change with the requirements of the customer, the government. The principal of the vehicle body was to provide occupant space and weather protection. However, today the requirements of the body structure go beyond this and it must achieve high passive safety targets, low manufacturing costs, low vehicle body-mass and adequate aerodynamic characteristics, accompanied by low road noise and good ride and handling. Currently, occupant safety is of prime importance. The legislation for safety performance requirements is derived from three principal domains, North America, Europe and Japan, each having individual standards which must be conformed to.

As the vehicle body provides the most effective means of protecting the passenger or occupant, the large structural members of the vehicle body h are used to manage crash conditions, by either crumpling, and absorbing the impact, or distributing and directing the load from the impact area. These structural members have traditionally been made from steel pressings that have been spot welded together, although increasingly structures are integrating laser-welding techniques for joining the pressings. These closed structures

also have the added capability of providing high body torsional and bending stiffness, which are fundamental in ensuring good ride characteristics.

The bulk of steel vehicle body construction, initiates from sheet steel coil. The press shop shear or blank the coil into an optimum number of flat sheet blanks ready for the individual parts to be pressed. The general vehicle construction then involves spot welding of the individual parts into sub-assemblies, which are built up into large assemblies and married together, generally starting from the floor upwards.

2.1.3 Platform Rationalisation

The vehicle platform is the major structural vehicle base, generally consisting of the nose sub-assembly, the floorpan and the rear sub-assembly. The nose sub-assembly contains the bulkhead and the front suspension and engine mounting, whilst the rear sub-assembly provides the rear suspension mounting points. Due to the large cost of the vehicle platform, rationalisation or platform sharing, as previously mentioned, has become very attractive to the vehicle manufacturer. Examples of platform rationalisation include Renault's Megane family platform, in which the 3 & 5 door hatch, 4 door saloon models, and the Scenic MPV (Multi-Purpose Vehicle) all utilise a common platform [4]. Fiat has pursued a rapid implementation of platform sharing, which also incorporates Alfa Romeos' range. The Fiat Brava, Bravo, Tempra, Coupe, the 146 and Spider all share the same platform [5]. In 1999 Volkswagon's A4 platform was used for 1.3 million vehicles spread over eight different models [6]. Platform strategies play an important role in the economics of vehicle manufacture and where a manufacturer does not produce sufficient volumes of a model or models, as with some of the Off-road and SUV variants, then joint ventures with other vehicle manufacturers/groups must be pursued.

2.1.4 Flexible Manufacture

In volume manufacture of today's vehicles, the assembly operations are carried out with high levels of automation within large purpose built plants. However, the running and maintenance cost of such a dedicated plant is extremely high. Therefore, the next generation of vehicle production plants include high levels of flexibility with the

capability to manufacture many different vehicle models but also to also reduce the cost of product launches [7]. Honda UK planned to extend its factory base in Wiltshire, with the investment of new 'flexible' manufacturing plant [8]. The new plant would provide Honda with a 5th international production plant capable of changing its production line for the manufacture of a completely different vehicle model, costing minimal time and tooling investment [9]. At the hub of this new flexible manufacturing system are multifunctional programmable robots and a general welder (GW) jig, where the vehicle floor sides and roof are assembled.

2.1.5 Modularisation

It is generally accepted that a vehicle module is a component assembly that has been completely built up and therefore is ready for inclusion directly in the vehicle. Modularisation is the use of modules, by the vehicle manufacturers, in preference to performing significant degrees of sub-assembly prior to vehicle assembly. Dana Corporation is one company offering modular and systems assembly. Their philosophy states that the vehicle manufacturer does not have to, 'develop, source, stock, inspect, manage and then assemble all those components into a single system [10]. An example of this approach is their Rolling Chassis ™. This comprises some 30% of a completed vehicle, allowing a significant increase in speed to market. The trend will gradually mean that vehicle manufacturers will tend to become vehicle assemblers or builders of the basic modules. The rationalisation of the vehicle composition into discrete entities or modules provides significant cost reduction opportunities and efficiencies, including improved logistics. The use of modular construction means that different models, within a group, can share part of the same platform, the same gearboxes, exhaust systems or even engines or any combinations of these. Although there are major benefits to be achieved through modularisation, widespread implementation has been progressive and is still developing.

2.1.6 Cost Reduction

Although rationalisation of vehicle platforms and modularisation may provide cost efficiencies, a broad spectrum of strategies are utilised by vehicle manufacturers to enable them to achieve target cost reductions. Global purchasing and a rationalisation of

suppliers are two methods to maintain pressure upon the suppliers to deliver goods at economic prices. The implementation of longer-term supplier contracts provides stability and ultimately improved quality. The use of modularisation , enables suppliers to perform the sourcing and to develop component systems. By accepting modules instead of multiples of individual parts, a major reduction in assembly costs can be realised. The platform sharing method, already mentioned, allows cost reduction by commonising components or modules for different vehicle models. This allows a reduction in the tooling investment and piece price, whilst also reducing the number of suppliers and logistics involved with the components. A major reduction in cost may be realised from the integration of components by using new manufacturing technologies. By integrating components manufacturing and tooling costs may be reduced.

2.1.7 Vehicle Weight Reduction

The principal drivers behind vehicle weight reduction are government and customer pressures. Both the government and customer have been demanding vehicles with improved fuel consumption that release fewer emissions to the environment. One of the determining factors in this has been oil price and its availability. For obvious reasons it has had some control over the car industry's current and future direction. In the 1950's and 1960's the actual price of oil fell. However, in 1971 oil price revisions were made. This coupled with the oil embargo of 1973 increased oil prices significantly and highlighted the car industry's dependency upon oil prices. The oil prices escalated again in 1978 and 1980 [11]. The result of the oil crises was a temporary switch in the demand to more fuel-efficient models and consequently this forced the automotive industry to act.

Thus since the 1970's, government pressure has increased to force motor vehicle manufacturers to reduce fuel consumption and emissions. In North America this legislation entered in the form of the federal government CAFE (Corporate Average Fuel Economy) targets [12] and for Europe in the form of EC directives on fuel emissions [13]. If vehicle manufacturers were to make vehicles with improved fuel consumption this could play a significant role in the global strategy of reducing motor vehicle emissions, until a time when alternative fuels can be tapped on a practical scale.

There are several means of improving fuel consumption but one the single largest means is to reduce the mass of the vehicle, thus reducing emissions.

In addition to the demands of improved fuel economy and reduction in emissions, the customer has also increased pressures on the vehicle manufacturers to provide cars with improved:-

- Safety Features / 'Crash Worthiness'
- Performance
- Comfort and Refinements

The customer pressures for the above, however, contradict the requirements for vehicle – weight reduction and have lead to increases in vehicle weight for the average European vehicle by as much as 20% [14]. Interestingly the average weight of the vehicle has been increasing in light of these customer pressures to include features such as electric door mirrors, heated seats, air conditioning and satellite navigation systems.

As weight reduction in vehicles is the single most effective way of making reductions in fuel consumption, and hence emissions, vehicle manufacturers have been keen to pursue all avenues possible. The conventional fabricated vehicle body, accounts for approximately 30% of the total vehicle mass [3]. Therefore, opportunity exists for a sizeable reduction in vehicle mass. By focusing on the body structure for weight reduction, additional advantages may be achieved including, greater rigidity coupled with higher levels of occupant safety.

As previously mentioned there are two key types of traditional vehicle design, the Monocoque and the Body-on-Chassis. With these designs, mild steel is still the most common metal used today [15]. To achieve further weight reductions in the vehicle body a range of strip steel products were developed specifically for the automobile industry. These have been increasingly incorporated into the vehicle and are discussed later in this

chapter. The aim of each steel product is generally to improve component or component system performance, whilst maintaining satisfactory forming and joining characteristics for vehicle manufacture. For the steel manufacturer these specialised steels provide added product value opportunities and, therefore, potentially greater profit.

With the use of higher strength steels, down-gauging and therefore light-weighting has been possible. However, there have been limits to the extent of thickness reduction, after which crash performance and stiffness are significantly impaired. Changing car design and using different manufacturing technologies, accompanied with the latest steel products, provides one avenue to achieve further reductions in vehicle body mass. However, changing car design is complex and must be evaluated in detail as small modifications can have a considerable influence upon vehicle performance, manufacturing, and ultimately on cost.

2.1.8 Steels for Automotive Structural Members

In the 1970's, the introduction of high strength steels (HSS) for automotive applications began to assist in meeting fuel efficiency targets by reducing vehicle body mass. By the early '80s a typical vehicle Body-In-White was composed of 30% of high strength sheet steels. Traditionally, such components would have been made from hot or cold rolled mild steels, possessing yield strengths in the range 120-230MPa. The incorporation of steels with higher yield strengths meant that a further reduction in material thickness was possible, therefore achieving greater levels of weight reduction. A typical reduction in steel thickness of 0.1mm [16] is permissible, without significantly impairing stiffness or buckling performance, thus allowing a reasonable reduction in vehicle mass. A reduction of 0.1mm of the steel thickness used on a vehicle would translate to approximately a 10% reduction on the mass of the vehicle B-I-W.

In the production of hot rolled strip steel products, rolling reduction of a cast billet is used to control the coil thickness. On completion the strip passes through a bank of water or gas cooling jets and is subsequently coiled. Careful control of the thermo-mechanical processing ensures that the microstructure and properties meet specification. To provide

an adequate surface finish for automotive purposes, the coil must have the blank oxide scale removed by pickling. In the case of cold rolled production, the metal is produced by the same means as for hot rolling before being cold reduced, annealed and then temper rolled (skin passing). The processing of a cold rolled product is more complex than of the hot rolled metal and therefore more costly. In any case the final properties of a steel are controlled by the steel chemistry and processing conditions.

Mild Steels [17]

These steels may be supplied in the hot or cold rolled condition. Hot rolled mild steel is usually supplied in thickness ranges from 1.5 – 8.0mm and typically has yield strengths in the region of 220 - 250MPa, with tensile strengths in the region of 380 - 450MPa. Therefore, these products are more commonly used for structural, reinforcement and chassis components. As these steels are unalloyed, they are also least expensive. Cold rolled mild steels are commonly used on automotive components not requiring a coated finish and are particularly formable, distinguished by the low yield strength (140MPa) to tensile strength (250MPa) ratio, high strain-hardening exponent and tensile elongation. Cold rolled mild steels are typically supplied for automotive applications in thickness ranges of between 0.6mm and 1.5mm.

IF (Interstitial Free) Steels

These steels are used in more demanding automotive applications, where forming severity is high and mild steel would not be suitable. This grade of steel is achieved by vacuum degassing to reduce the carbon levels to less than 50ppm. The remaining carbon is taken out of solution by strong carbide and nitride forming elements, such as titanium and niobium. These steels have characteristically high strain hardening properties and favourable texture properties (anisotropy). Consequently, they are employed in pressing applications where good panel depth is required.

BH (Bake-Hardenable) Steels

Bake hardening steels derive their name from the strengthening achieved from the strain-ageing response of the metal. During the press forming process, the strain in the main

body of a drawn panel may be as much as 2%, which introduces fresh dislocations into the steel. On paint-baking, precipitates form at the dislocation sites. The straining of the component, as a result of forming, may develop as much as a 40MPa increase in strength and the final strength increase after the paint-baking cycle may be as much as 50MPa. Although the initial yield strength of these steels is moderate, the increase is significant and these steels cross the range of low to high strength steels. These products are not commonly used for automotive structural components and are principally used for outer body panels to improve dent resistance. However, the benefits of bake-hardening could be utilised in tube hydroformed components, although the magnitude of the strains developed from starting with strip metal are relatively unknown.

High Strength Steels (HSS)

High strength steels are generally considered to be those grades having yield strengths in the range of 260MPa and to 600MPa, above which steels are usually designated as Ultra-High Strength Steels. Whilst increasing strength does provide thickness reduction, up to certain limits, the inherent nature of these materials is they are less formable than mild and IF steels. Consequently their introduction may cause manufacturing issues during press forming or welding. Therefore, care must be made in the selection of the most appropriate steel for the application, whether it is mild, high strength, or ultra high strength steel.

HSS –IF (High Strength Steel - Interstitial Free)

These steels are based upon the IF steel grade but with the addition of solid solution strengthening elements such as manganese, silicon and phosphorus. These influence the tensile strength more than the yield strength, whilst retaining much of the good formability characteristics of an IF steel. These steels are employed in automotive components where good formability and increased strength are required. Corus strip products could supply HSS - IF steels with yield strengths in the range of 190 – 300MPa., although strip would normally be supplied with either a hot dip or galvanneal (GA) finish to meet corrosion requirements.

Rephosphorised Steels

This particular grade of steel makes use of phosphorus as a solid solution strengthening mechanism to achieve the greater yield strengths than conventional mild steels with minimal impact upon press formability and weldability. Phosphorus is a powerful strengthener for steels, however, the phosphorus additions are limited to 0.1wt %, as above this level it is deleterious, due to grain boundary segregation effects, which can cause serious weldability issues.

HSLA (High Strength Low Alloy Steels)

HSLA steels are fully annealed, precipitation hardened micro-alloyed steel products. Originally, these were developed for greater weldability over Carbon-Manganese based high strength steel grades. To improve weldability the carbon content was lowered. However, the result was a reduction in strength, which was compensated for by refining the grain size. The grain size of these steels can be refined by the production of second phase particles in the steel microstructure, during the strip steels processing. These second phase particles include carbides, nitrides and carbo-nitrides, which are formed from elements such as: Aluminium (Al), Niobium (Nb), Vanadium (V) and Titanium (Ti). Niobium Carbide (NbC) and Niobium Nitride (NbN) were found to be the most effective grain refiners and are commonly used in the lower alloy and lower strength commercially available products. The mechanism of precipitation strengthening in ferrite produces still further strengthening. For this purpose, the most effective strengthener was Vanadium Carbide (VC) or Vanadium Nitride (VN).

Dual-Phase Steels

These steels have a mixed microstructure of consisting of ferrite matrix surrounding islands of martensite. The tensile strength of these steels is directly proportional to the second phase martensite content. These steels are characterised by their comparatively low yield strength (dependent on chemistry & processing), high work-hardening rate and good elongation values, typically 15-30%. The manufacture of these steels requires rapid cooling, which can be achieved in continuous annealing line. Currently, Corus does not supply these products on a commercial basis.

TRIP Steels

Another group of high / ultra high strength steels are TRIP steels. These steels derive their strength from the transformation of phases produced by plastic strain, hence the name Transformation Induced Plasticity (TRIP). Through controlled cooling, at room temperature retained austenite is present, which transforms to hard martensite and or a mixture of upper & lower bainite, thereby developing strength. Consequently this steel has an exceptionally high work hardening rate.

Bainitic and Martensitic Steels

These specialised steels may have strengths in excess of 600MPa [18], and are suitable for application involving very high strength, such as door impact (side intrusion) and bumper beams and reinforcements. Whilst these materials have very high strength, their formability. Consequently, the range of applications for these steels is generally limited to components requiring minimal of low levels forming and therefore have been ideal for roll formed bumper beams.

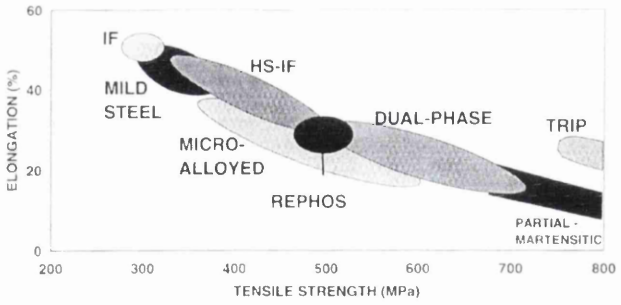

Figure 1: Strip steel grades and their typical mechanical property ranges

An indicator of strip steel formability is the metals total elongation, explained in further detail in section 2.3. For higher strength steels the elongation decreases, Figure 1.

As steel formability / elongation reduces (defined by the total elongation) the range of potential automotive applications becomes reduced but also the components must be designed for the particular steel's forming characteristics.

In Table 2.1 (adapted from Takechi [19], the typical automotive applications utilising high strength steel, are shown against properties required for the particular application and the importance of thickness to the property. This table illustrates the significance of high strength steels and how they may contribute to weight reduction. In the case of structural members component thickness is very important in all major property requirements of stiffness, fatigue strength and impact strength.

Coated Steels

To meet the vehicle manufactures requirements to produce new vehicles with enhanced (increased) anti-perforation corrosion warranties, steel producers have produced a range of coated steel products, tailor-made to meet specific requirements in terms of corrosion performance, weldability, formability and paintability. Those specifically for the vehicle B-I-W are zinc coated (galvanised) steels, although an increase in the use and interest of Organic coated steels by particular vehicle manufacturers is taking place. Essentially three different forms of zinc-coated steel exist, namely [20]:

- ***Hot Dip Galvanised Steel***
- ***IZ (Zn-Fe alloy coated) Steel***
- ***Electro-Galvanised Steel***

The coated steel product that has received most interest over recent years has been Bonnazinc [17, 20]. This is an epoxy-based primer containing zinc particles.

Stainless Steels

This special group of steels has only limited application in current vehicle design. The principal application of stainless steel is for automotive exhaust components. However, increasing interest has grown in stainless steel grades exhibiting high formability and high strength, which may have significant benefits in automotive structural applications.

The stainless steel grade most commonly used in tubular form for exhaust components, hydroformed or otherwise, are the Austenitic grades 301, 304 and 306. Application of stainless steel for potential B-I-W components has been limited due to its significant expense over conventional coated mild steel products.

2.1.9 The ULSAB Project

In July 1994 the ULSAB (Ultra-Light Steel Autobody) was launched. The ULSAB project was a design concept study carried out by Porsche Engineering Services, which was funded by a world consortium of 32 steel companies. The project was a marketing tool for steel products and steel vehicle manufacturing technologies in the automotive industry.

The aim of the project was to design and build a light-weight and efficient body structure. The body structure was to be viable for high volume production, whilst being able to meet a number of high level structural performance and functionality targets, using a holistic design approach. The target for ULSAB was the achievement of a 20% mass reduction [21].

The ULSAB programme was pursued in three phases. Phase I involved a concept design of a medium-to-large saloon (sedan) car. Part of Phase I included a benchmarking exercise of current, medium-to-large saloon models. The purpose of this was to deliver information on their designs, weights and performance, so that the concept car could be ranked. Phase II included the design detail, engineering analysis, building, body demonstration and basic testing. The purpose of phase III of ULSAB was to exploit newly found developments for weight reduction in vehicle design and build programmes [22,23].

In phase I, two preliminary vehicle build designs were investigated. These were a standard Monocoque structure and a Hydroform Intensive Body Structure (HIBS). The Monocoque structure utilised state-of-the-art steel technologies such as tailored welded blanks and tube hydroforms, whereas the HIBS design, although architecturally similar to

the Monocoque, incorporated hydroformed tubular sections. The hydroformed sections would replace spot welded members, where greater structural efficiency or weight saving could be achieved. The main restriction of incorporating tube hydroforms into the HIBS design was due to joining/assembly aspects, i.e. hydroform-to-hydroform and hydroform-to-pressing. In the HIBS design, tube hydroforming technology was originally intended to be for the following structures:

- Fender Supports
- Side Roof Rails
- Pass-Through Beams

Due to the lack of technical knowledge and experience of the process and assembly of such a structure, it was ultimately decided that the final design from Phase I would include the best features of the Monocoque and HIBS designs.

On completion of Phase II, the ULSAB project delivered a concept vehicle, Figure 2.2, that weighed 25 % less than the ULSAB benchmark average vehicles but was 80% stiffer, whilst still attaining the crash performance criteria.

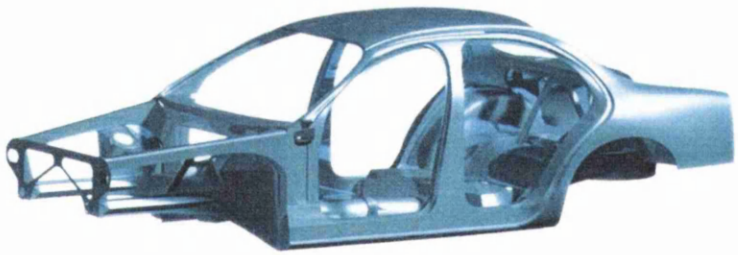

Figure 2: Ultra Light Steel Autobody (ULSAB) – steel concept BIW structure

These achievements were gained by using of a high percentage (approximately 50%) of tailored laser welded blanks coupled with intense use of high strength steels (greater than 90%) The upper strength level of the steel used was 420 MPa. Additionally, two, single piece tube hydroforms made up the ULSAB vehicle roof rails components, providing

effective crash management, mass reduction and assisting the high levels of body stiffness achieved.

2.1.10 Recycling and the End-of-Life Vehicle

Vehicle manufacturers face government pressures, in the form of controls over pollution from vehicles that have reached their end-of-life, not only from exhaust emissions. To uphold these controls, European Industry has made a commitment to improve the environmentally sound disposal of end-of-life vehicles. In 1991 a group was set up to investigate end-of-life vehicle waste, as part of the Priority Waste Stream initiative, and by March 1994 a consensus proposal for a European strategy document was prepared. The document laid down objectives stipulating that by 2002 only 15 percent (weight) per car may be disposed of (landfill or incineration without energy recovery) [24]. From 2002 onwards, for new models, only 10 percent per car may be disposed of and by 2015 only 5 percent [24].

Currently, the way in which vehicles are scrapped means that large amounts of material are being disposed of in landfills. The majority of this material requiring disposal is commonly known as Fluff, which is the term given to resins, fibres, rubber, glass, etc. Fluff is also known as Automotive Shredder Residue (ASR). The quantity of this material has been increasing each year due to the amount of non-ferrous metal and plastics being used in vehicles and also from the increase in the quantity of scrapped vehicles. Due to its nature Fluff has a low bulk density and therefore also causes low transport and landfill efficiencies.

At present the target figure of 15 percent per car is not very challenging as fluff accounts for approximately 15 percent of an average car weight [24]. It is, however, a realistic figure and the overall proposal requires vehicle manufacturers to design with due regard to material choice and recovery potential.

Although weight reduction benefits may be possible with the use of aluminium, the recycling of an all aluminium vehicle costs almost three times that of a steel autobody [25]. The high costs mainly arise through the use of high-grade wrought aluminium for vehicle bodies, which may not be mixed with all alloys if they are to be recycled back into the same high quality wrought alloy products. Disassembly of body parts is a slow and labour intensive process if the correct segregation of metal into its constitutive alloys is to be achieved. Scott of Alcan, stated that the recycling of aluminium at present is costly, both in terms of recycling and collection. However, the cost may be reduced if an increase in aluminium usage continues, as this will cause the recycling infrastructure for aluminium vehicles to strengthen and grow [26].

Due to the increasing plastic content of end-of-life vehicles, the problem of recycling or disposal of the redundant material from these vehicles is also increasing. Recycling of plastics is not an easy task, as it has significantly poorer mechanical properties, as a result of thermal degradation in reprocessing, in addition to significant difficulties for sorting. As a consequence, recycled plastics may only be used in similar automotive applications, or more usually, less critical applications or as fillers [27].

By producing an all steel vehicle it is clear that recycling costs will reduce as the majority of steel in a vehicle can be recycled, particularly the body-in-white, which provides good scrap sorting efficiencies.

2.1.11 Implications for Steel Producers

Part of the ULSAB initiative was driven by the threat of alternative metals and enabling technologies being used by vehicle manufacturers, thereby reducing the steel content in the vehicle. The largest threat to the traditional steel vehicle body, and in particular as a competitor to steel tube hydroforming, has been from aluminium. This fact was reinforced at the beginning of 2000 with the launch of the all aluminium Audi A2, small car. The new A2 utilised a revised form of space-frame technology, ASF® design, which was first used in the construction of the all aluminium Audi A8. The A2 was the worlds' first all aluminium, medium volume production car. The space-frame construction

enabled the vehicle weight to be reduced to 895kg, some 150kg lighter than comparable models in the same class [28]. The Audi A2 space-frame comprised of hydroformed extrusions, aluminium castings and sheet aluminium pressings, Figure 3.

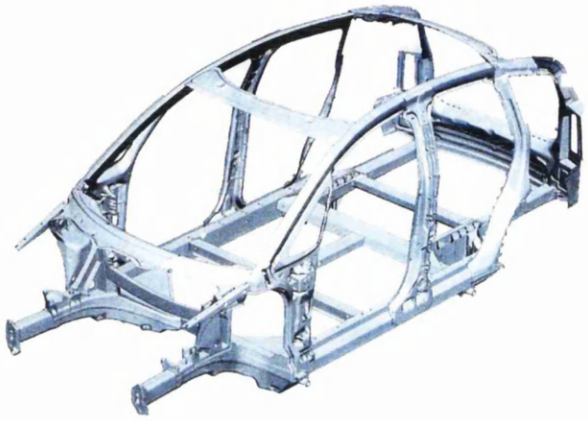

Figure 3: Audi A2 aluminium space frame (ASF®), comprising hydroformed aluminium extrusions, cast nodes and pressings.

To maintain a competitive edge over alternative materials & technology suppliers, steel producers must continue to research new products and technologies, such as tube hydroforming, as these may provide cost, weight reduction and performance enhancing opportunities. To accomplish this, the steel producer must be innovative and target solutions enabled through design and product.

2.2 Tube Hydroforming Technology for Automotive Applications

2.2.1 Introduction

Tube hydroforming technology was originally developed prior to the 1950's for the manufacture of aircraft components and plumbing applications with many of these early developments being patented [29&30]. Over the last decade tube hydroforming has generated significant levels of interest from Original Equipment Manufacturers (OEMs) who have pursued this technology for use in many automotive applications, ranging from exhaust components to structural frame members. The following chapter will review the

current state-of-the-art in tube hydroforming technology used for the manufacture of automotive structural components.

From the perspective of automotive structural components, tube hydroforming technology may provide many benefits over traditional manufacturing methods. Many of these benefits have been proven-out by existing production components found in today's vehicles and are highlighted in section 2.2.4. However, a series of limitations have inhibited wide scale application into vehicle body construction and these reasons are discussed in this Chapter in section 2.2.9.

2.2.2 Tube Hydroforming Process

According to Dohmann et al [31], "the aim of the hydroforming process is to achieve the greatest possible contact between the expanded tube wall and the die tooling at the end of the process, whilst maintaining a specified wall thickness distribution". The tube hydroforming process generally involves the use of a forming fluid, typically an oil-water emulsion, under high pressure to stretch a tube blank to fill the cavity of a die tool. This process may be assisted with the aid of pushing additional tube material into the die cavity. The outline hydroforming process cycle is shown schematically in Figure 4.

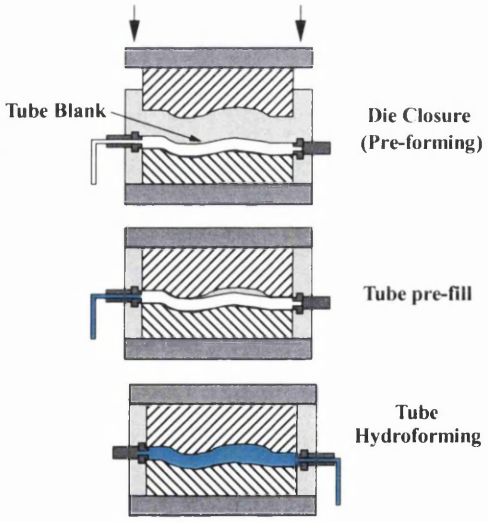

Figure 4: Schematic illustration of the tube hydroforming process (no end feed)

Firstly, the tube blank must be loaded into the die cavity. Secondly, the tube must be filled with the forming fluid, whilst allowing air to escape. Therefore, axial rams with 'end seals' must move in quickly to ensure sealing of the fluid filled tube, whilst allowing sufficient time to remove entrapped air. Purging the tube blank with forming fluid may be necessary in order to achieve good air evacuation. The fluid is normally delivered from one of the axial rams, through a 5-8mm aperture in the end seal. The end seal, as the name suggests, provides the mechanism to close and seal the forming fluid inside of the tube blank. Typically, tube end seals have a cone design and cause the tube to plastically deform onto the cone to provide the sealing conditions required. The next step is the fluid pressure increase in conjunction with the movement of the axial rams in a pre-defined relationship. The actual forming process is usually considered as consisting of two stages, a forming stage (general inflation of the tube blank) and a calibration stage, in which the component definition and geometry fixing is achieved. Following the calibration stage it is also possible to pierce holes into the hydroformed component using one of two methods, inward or outward hole piercing. The most common production method is to punch inward, leaving the slug attached but an additional method is to coin or pre-cut the hole and leave this 'slug' to be removed in a following process [32].

Depending upon the intended geometry of the component, a range of different tube hydroforming processes may be adopted. According to Siegert [33], the tube hydroforming process may be classified under four principal deformation modes dependent upon the applied stresses. These modes include the following:

- Shearing Stress (Displacement)
- Bending Stress (Bending, including hydro-bending)
- Tensile Stress (Expansion or Calibration)
- Tensile-Compressive Stress (Expansion with Axial Force using open or closed dies)

Different components may be subjected to one or more of the above conditions at all or just localised regions of the component. The forming mode, discussed further in section 2.3, may be used to classify the processing conditions. For example, on a component possessing two sharp bends, the application of axial forces to the tube ends may have limited influence upon the material between the bends. Therefore, the region between the two bends would be considered to be subject to a tensile stress, expansion only. In the case of the Audi A2 aluminium extrusions, small levels of deformation were used to apply a calibrating effect, largely to improve the dimensional accuracy of the components over the dimensionally inaccurate extruded profiles.

High Pressure Tube Hydroforming (IHF)

Conventional tube hydroforming utilises internal pressure to stretch the tube blank into the perimeter of the die cavity. Under these conditions an increasing pressure is required to achieve a smaller component corner radius. According to Birkert [34] the relationship between corner radius and internal pressure is a function of the strength coefficient, K and the n-value of the tube metal.

Pressure Sequence Hydroforming (PSH)

However, in contrast a comparatively new method developed by Ti-Variform, a Bundy Group company, utilises the internal pressure during the closure of the hydroforming die tooling. It has been claimed that by doing so the tube blank material is pushed further outward toward the periphery of the die cavity on closure of the die tools. During the PSH process, the component corners are claimed to fill out more easily and under lower pressures, due to lower frictional effects. Consequently, it is claimed that this process therefore, utilises a smaller hydroform press and energy, but also causes the component to thin less during hydroforming than high press hydroforming, thereby improving component strain distribution and potentially performance [35].

Outline of Tube Hydroformed Component Production Process

The manufacture of an automotive steel hydroformed component will involve some or all of the following process operations:

- Cleaning (pre-cut ERW tubular blanks from tube mill, remove mill lubricant & dirt)
- Pre-bending (Bending op., includes self lubrication for tube & internal mandrel tools)
- Measuring / Dimensional Checking (checks to monitor pre-bend accuracy)
- Cleaning (to remove bending lubricant from tube)
- Lubricating
- Pre-forming
- Tube Hydroforming
- Measuring / Dimensional Checking (rework / reject components that do not conform)
- Trimming (e.g. Laser-cut holes that are not punched and remove excess tube metal)
- Cleaning (remove, pre-forming/ hydroforming lubricant)
- Assembly
- Cleaning (degreasing, removal of dirt/debris from assembly processes)
- E-Coating and Painting

Therefore, tube hydroforming may in many instances be considered a multi-stage forming process.

2.2.3 Process Limits

In hydroforming a tubular blank there are process limitations in terms of the combinations of applied axial force (or axial end feed) and internal pressure that may be used to produce a component successfully [36]. These limits include: an upper limiting axial force, due to buckling or wrinkling tendencies; bursting, due to excessive internal pressure; loss of seal, due to insufficient axial force; or insufficient deformation, if the load path does not pass the plastic flow boundary, Figure 5. Therefore, the process limits are the boundary conditions governing the successful outcome during tube hydroforming operations.

The two principal forming phases during high-pressure tube hydroforming are forming and calibration. Under a given loading path, which develops both sufficient axial force to provide adequate sealing and sufficient internal pressure to achieve plastic deformation, the component enters the forming phase where most of the tube deformation takes place. This forming region where the tube blank can be successfully formed, is known as the `feasible working region' [37]. After the majority of deformation has been achieved, component calibration is necessary to ensure that the component retains its shape. During deformation, the tube will increase in yield strength and on removing the internal pressure load-case, elastic recovery may cause the component to deflect from its desired shape, i.e. springback, described later in section 2.3. To decrease the effects of this physical phenomenon, the pressure is dramatically increased above the necessary minimum pressures required to achieve the component corner radii [39].

For a loading path that is not within the feasible working region, component failure occurs due to instability. As previously described these take place either due to; wrinkling instability, due to an excessive an axial load or axial end feed; or `necking' instability, causing the tube to undergo excessive thinning or bursting due to an excessive internal pressure.

- ***Wrinkling***

Dohmann and Hartl state that in the intake region of the hydroform tool wrinkling is unavoidable, although it may be possible to remove or reduce later in the process. Wrinkling may also take place at the centre of the component from excessively high axial forces in combination with insufficient internal pressure, Figure 5. Susceptibility to wrinkling or section collapse during the hydroforming of body-in-white structures is all the more likely due to the large D/t ratio (i.e. > 60) of tubular blanks involved, having much lower buckling strength.

It has been recommended that for tube hydroformed components the initial tube periphery should be some 3-5% smaller than the component cross-sections [38]. If not the tube metal will pinch during hydroform or pre-form tool closure or suffer significant

sectional collapse resulting in possible permanent wrinkles in the body of the component. This would potentially inhibit the final component geometry from being formed and from an aesthetic perspective, the wrinkles or folds may be present on the final component or leave visible markings. Sectional collapse or severe wrinkles may reduce the overall forming envelope of the component by restricting the magnitude of axial force or prevent metal flow causing a localisation of strain at critical features, potentially leading to splitting of the component. The generic features of automotive structural components, are that they possess complex sections and complex changes of section, which potentially inhibit high axial loading to be effective during hydroforming, due to wrinkling susceptibility and frictional effects. The susceptibility to wrinkling or sectional collapse is magnified for large section changes.

- ***Bursting***

A number of different mathematical expressions may be used for predicting bursting or fracture of tubular blanks due to loading by internal pressure. According to Dohmann et al [39] the bursting pressure of a tube may be predicted by:

$$Pi_B = (2t_0 \,.\, \sigma_{TS})/(D_0 - t_0) \qquad \text{Equation 1}$$

Where Pi_B is the bursting pressure, σ_{TS} is the material tensile strength, and D_0 & t_0 are the initial diameter and wall thickness values, respectively. However, this relationship may be inaccurate depending upon the forming conditions and may not be suitable for actual automotive components. Additionally, by ignoring the influence of plane strain deformation, the influence of anisotropy, and any pre-strains resulting from additional pre-process forming operations, discussed in further detail in section 2.3, further inaccuracies in the formulation is likely to arise. The prediction of bursting may be evaluated from the metals forming limit curve (FLC), i.e. the pressure at which the tube fails may be predicted from the point at which the material deformation exceeds the forming limit. The bursting process limit or boundary is presented schematically in Figure 5.

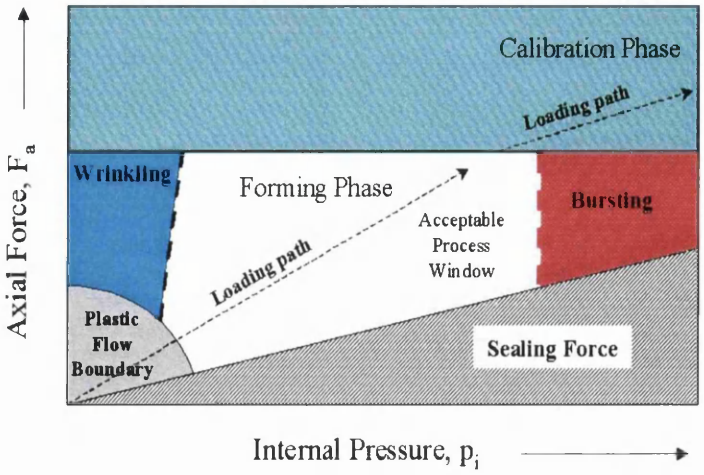

Figure 5: Schematic illustration of tube hydroforming process diagram, showing process boundaries (limits) and forming phases.

To define the hydroforming process diagram or forming window for tube blanks manufactured from strip products requires the inclusion of expressions which also account for the material's normal anisotropy, which is not included in work by Dohmann & Hartl [39]. This is an important phenomenon needing consideration, as it may have implications relating to the process parameters for producing automotive hydroform B-I-W structures.

The recommended average component expansion of 3-5% for complex components also reduces the risk of component bursting/splitting, as the global level of component stretch is considerably lower than the typical strip steel total elongation, Figure 1.

- ***Plastic Flow Boundary***

To consider a component to have formed, the tube must be subjected to sufficient loading, by internal pressure and axial loading, to cause the tube blank to yield. The

beginning of plastic flow or deformation provides an additional boundary or process limit, Figure 5. A crude calculation of the yield pressure may be made in a similar manner as for the bursting pressure. However, like the bursting pressure estimation, this does not account for stress-state, anisotropy or the influence of the die tooling.

- ***Minimum Sealing Force***

In addition to failure of the part, by buckling or bursting, insufficient sealing force, Figure 5, may also result in inadequate component pressurisation and subsequent wrinkling failures.

Under the most basic considerations, the minimum sealing force can be determined from the following expression:

$$F_{a\,(min)} = P_i \,.\, A_i \qquad \text{Equation 2}$$

with

$$A_i = (\pi D_i^2 / 4) \qquad \text{Equation 3}$$

Where P_i = applied internal pressure, D_i = internal diameter of tube, and A_i = internal area of tube end. However, the condition of the tube ends and seal design may also play a significant part in the suitable process conditions to achieve sealing. Indeed, if the tube end quality was too poor, e.g. oval, then it is likely that designated process conditions would not be achieved. Likewise, if the tube end seal quality was poor, or was of an inappropriate design, then a sound seal may not be achievable.

Therefore, to successfully produce a tube hydroformed component, the process conditions must be closely controlled in order to achieve a suitable loading path through the Feasible Working Region. The die and tooling design also play a significant role in achieving a successful part.

Dependent upon component design, a level of tube end feed can be administered from one or both ends of the tube blank. Under such circumstances, the process is sensitive to both axial force/displacement and internal pressure. Theoretical laws have been

established for these boundaries based upon radial expansion of rotationally symmetric tubular blanks, in the absence of die tooling. Therefore, the validity of these laws becomes reduced for practical automotive components, hydroformed inside die tools.

Calibration

During the calibration phase, a reduction in wall thickness is almost always inevitable. For automotive applications this particular aspect of tube hydroforming has significant implications, particularly on impact performance where component corners may be required to absorb high levels of energy. Therefore, thinning of the component corners may lead to lower impact capabilities.

The actual production process for the manufacture of a tube hydroformed component will greatly depend upon the intended application and more importantly the component geometry.

2.2.4 Reported Benefits of Tube Hydroforming

Many benefits may be realised by substituting structural members, conventionally made from spot welded sheet steel pressings, with single piece, steel tube hydroforms. Many of the benefits of using tube hydroforming technology, documented on production automotive components, are detailed in the following sections.

- ***Integration of Parts***

By using tube hydroforming to manufacture a structural component, a single component may replace as many as six individual pressed and spot welded parts [40]. According to Bruggeman [41], tube hydroforming offers a high degree of package space efficiency as a direct result of part integration, which is one of the principal reasons for the high number of hydroformed component applications that have been implemented by General Motors (GM). Figure 6 illustrates an A-Pillar prototype hydroform that which would replace a minimum of 3 pressed parts under a conventional design aside of any performance or dimensional enhancement that the integration may yield.

According to Hannibal and Dieffenbach [42], the true cost benefits of tube hydroforming a component are likely to be realised when a hydroform replaces two or more pressed assemblies. Consequently, the greater the number of component parts integrated, the better the cost position would be for a tube hydroform. The analysis by Hannibal et al assumed that equipment investment would be necessary for the production of the pressed components. In reality it may be possible that these components could be produced on existing presses, thereby only imposing new tooling cost for the draw dies. In contrast, for a tube hydroform it could be feasible to consider that an existing press, of sufficient capacity, could be utilised but it would require the necessary modifications to ensure that it was suitable. Therefore, as a minimum, there would be the additional cost of these press modifications.

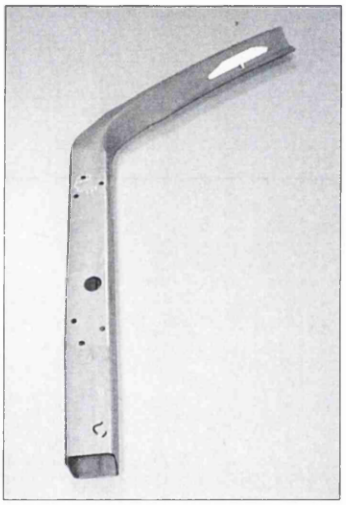

Figure 6: Hydroformed A-pillar prototype component produced from ERW steel tube

Integrating parts also increases the level of part functionality, thereby improving the efficiency of the structure. Part integration could also lead to improved dimensional characteristics, through elimination of tolerances stack issues but this is also likely to be design driven.

- ***Improved Performance***

Stiffness

The utilisation of closed-section tube hydroforms in a body structure, means that substantial gains in terms of torsional stiffness can be achieved [43]. This was found to be largely due to the 'continuous' closed-sections that a tube provides. Mason [40] reported that significant improvements, in terms of torsional strength & stiffness coupled with bending strength, may be met through the substitution of a conventional component with a tube hydroform. The bending stiffness of a tube hydroform was not found to improve significantly, which may be explained by the fact that the component testing was performed on like-for-like structures, i.e. having the same characteristic sectional geometry. In practice it is unlikely that a hydroformed component would have the same sectional geometry as a pressed assembly due design constraints and the manufacturing techniques used to produce and join the hydroforms of a body structure. Improvements in component stiffness are also likely due to the reduced par count. Therefore, in theory, integrating a higher numbers of component parts, should lead to a significantly stiffer vehicle structure.

Impact and Fatigue

Schulz [44] stated that due to the tube hydroforming process, the resulting strain hardening produced a stronger component, having improved crash performance. As the tube hydroforming process is used for many structural components this may be a key characteristic which may be utilised to good effect. However, whilst the strain hardening may improve impact performance, it may not be beneficial for component durability (fatigue) for some BIW applications. According to Boyles et al [45] the results of biaxial pre-strain tests, followed by low cycle fatigue loading, result in a reduction in fatigue life. It is not yet known if this form of deformation provides a suitable representations of the affects of tube hydroforming and, therefore, whether these results are truly representative of BIW components.

Component Strength

The additional work hardening that the original strip steel receives, from ERW tube manufacture and again during component pre-processing and finally hydroforming has been found to significantly increase the component yield strength [45]. Consequently, the computer aided design evaluation, which uses the yield strength of the strip steel, is likely to be subject to substantial error. It is still to be determined whether or not the strain hardening and therefore increase in strength may be considered as useful strength. However, the principal requirement for higher yield strength in structural components is when they are subjected to impact conditions, where the peak load is influenced by the yield strength. Higher peak load values are related directly to higher yield strength values.

- ***Weight Reduction***

The 1998 Vauxhall/Opel Astra model subframe [44] achieved a weight reduction of 30% over its predecessor. Substantial weight reductions have also been reported in the use of tube hydroforming for 1994 Dodge Ram pick-up truck [46]. In this instance, two hydroformed tubes were fabricated into a radiator support, allowing a weight reduction of 3.6kg. During the concept phase of ULSAB, Porsche Engineering Services stated that through the use of tube hydroforming technology, in the form of a Hydroform Intensive Body Structure (HIBS), a 40% weight saving could be achieved. In 1997 Volvo Car Corporation presented results of a study aimed at reducing the weight in the body structure of the Volvo 850 replacement [47].

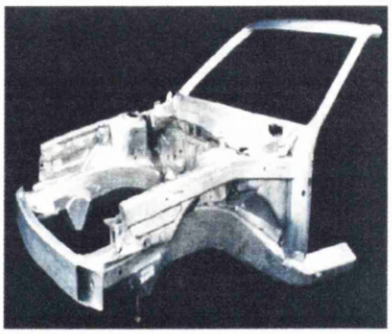

Figure 7: Volvo Hydroform Intensive (aluminium) Front End Structure

The results were part of a continued study aimed at achieving a 50% weight reduction of the front-end structure. By utilising aluminium extrusions, in conjunction with hydroforming technology, Volvo achieved this target weight reduction [48], see Figure 7.

In Volvo's study it was concluded that in attempt to utilise steel tube hydroforms with the same design, only a 10% weight reduction was possible. The reduction in weight was inhibited due to manufacturing restrictions that were not anticipated, due to attempts at pre-bending and hydroforming ultra thin walled (<0.8mm) steel tube.

However, in 1999 Rover Group Ltd published results from the Freelander HIBS project, Figure 8, which failed to deliver a 20% weight reduction target [43]. Unforeseen manufacturing limitations of steel tube hydroforms, coupled with assembly issues prevented attainment of the target weight.

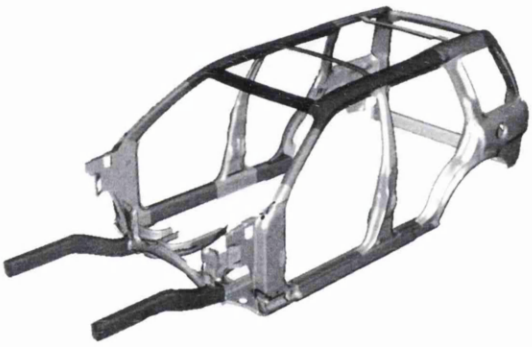

Figure 8: Rover Group's Freelander Hydroform Intensive Body Structure (HIBS)

Interestingly, in the case of the Volvo 850 replacement and Freelander HIBS, holistic design was not implemented. Additionally, in each case, designs that acknowledged the manufacturing limitations of steel tube hydroforming were not employed. As the manufacturing limitations were not anticipated or predicted adequately at the design stage, certain components could not to be manufactured successfully. Interestingly, if it were possible to overcome some of these manufacturing limitations, it may have been possible to reduce vehicle body mass.

- ***Improved Component Accuracy***

According to Leitloff et al [49], tube hydroforms display a high degree of dimensional repeatability. For a wide range of components, the variation in cross section may be as little as 0.1 to 0.2mm and 0.15 to 0.35mm in terms of form-line deviation. Despite this high level of repeatability, the reproducibility of the component from CAD data is considerably poorer. Many factors may be attributed to the comparatively poor reproducibility, including tool manufacture, tube manufacture, pre-bending and pre-forming operations. In addition, variations may result from elastic tool deflections during hydroforming, as a result of the high pressures used.

- ***Reduced Lead Time***

Largely due to the part integration potential of tube hydroforms, a significant decrease in prototype and manufacturing lead-time can be accomplished. According to Payne [50], when using the Vari-form (PSH) process, low cost kirksite or mild steel may be used for prototype tooling. This form of tooling is considerably quicker and cheaper to manufacture. Modifications are also easier at this stage of development and therefore less costly. The final die steel production tools may be used in the 'soft' condition to test the initial production series components, allowing for cost effective remedial action to be carried out as necessary. Finally, the production tools are hardened through heat treatment, in the knowledge that the components can be successfully formed.

For the IHP process, the situation is much different and 'hard' tools are necessary for prototyping. However, although the component may be complex, the prototype and production hydroformed components are only reliant on the manufacture and successful implementation of one suit of die tools, whilst pressed assemblies require all part tools to be developed.

- ***Reduced Costs***

A reduction in costs may arise from a wide range of sources, including design, development, administration and production costs. The following cost reductions have

been identified with the introduction of tube hydroforming technology in place of pressed steel assemblies.

Reduced Tooling Investment Costs

It is claimed that the high investment costs for production tooling are reduced, due to the nature of tube hydroforming and due to the integration of components. The reduction in tooling costs are a consequence of the simplification in the manufacture of die tooling, in going from pressing tools (punch, blank-holder, and die) to hydroform dies, and also from the reduction in the number of die sets to produce the component. According to Prelog et al [51], a reduction in the tooling investment costs of the order of 35% was achieved for rear frame rails and cross members that were produced for GM.

Reduced Material Costs

Through improved metal utilization, material costs may be reduced. This is possible as a tube blank is supplied to the hydroform press or bending machine already cut-to-length. In the case of pressed components, substantial scrap losses may be incurred during blanking and trimming operations. As each part of a multi-piece pressed assembly would require blanking and trimming, substantial improvements in material utilization may be obtained. Despite the higher cost of steel tube compared with strip steel, it is possible to reduce material costs simply through improved metal utilization.

In addition to the aforementioned cost reduction opportunities that tube hydroforming may offer, further opportunities may be realized in the form of:

- Reduced direct labour costs
- Lower logistical planning and associated costs

2.2.5 Steel Tube Manufacture

Steel tube or pipe may be manufactured by a number of processes and produced in either seamless or welded form. For structural members, Electric Resistance Welding is

currently being used and for B-I-W components suitable methods of tube fabrication are still being sought.

- ***Seamless Tube***

The production route for seamless steel tube is by hot forging. Production of tube by this process is typically carried out in three stages [52]. Firstly, a heated bloom is pierced into a hollow bloom by one of a number of techniques, but usually by rotary piercing or press piercing. The bloom is then stretch reduced into tube. To improve the surface and dimensional quality the tubular profile is further reduced in thickness by means of cold drawing. Ultimately, to possess adequate elongation for any forming operations the seamless tube requires annealing or normalising. Typically, seamless tube metal is 30-50% more expensive than ERW tube. Further limitations include the available range of seamless tube D/t ratios. The typical upper D/t limit is 30 and in the UK, the supply of tube with diameters of over 63.5mm is not readily available. The dimensional tolerances on thickness are also generally wider for seamless tube (±10%), which does not lend itself to a high quality product required for B-I-W applications.

- ***Welded Tube [53,54]***

There are principally two conventional main routes for the manufacture of tubes from sheet steel. These include continuous and discontinuous methods, which are described later and have been specifically developed to meet a specialised market segment of tube hydroforming market.

Of the two key production routes, the continuous tube mills are greatly more and typically operate at speeds between 30 and 240 m/minute [60]. The process initiates with slit strip coil. The slit coil material is fed into an accumulator and then through roll forming tools, having a particular flower pattern/sequence. The pattern or sequence is devised to gradually develop the slit coil to an almost closed circular hollow section. The high frequency electric resistance heating is then utilised to ensure the abutting edges of a longitudinal joint reach the appropriate welding temperature. These heated edges of the slit coil are subsequently squeezed together to form the butt weld. Following welding, the

tubes are rapidly cooled, straightened and sized as necessary by passing through a series of dies. A schematic diagram of the overall process is shown in Figure 9.

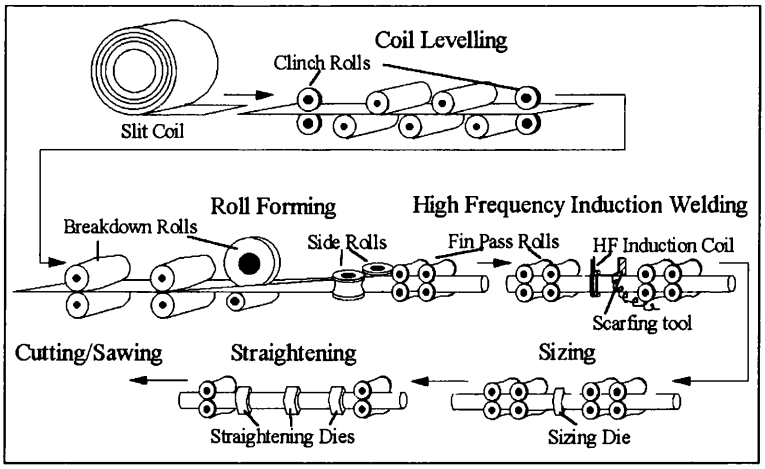

Figure 9: Schematic illustration of ERW tube manufacture

Tubular products manufactured using this welding technique are commonly known as ERW (Electric Resistance Welded) tube. During ERW tube manufacture, electric current flow and welding metallurgy are intimately linked. Ordinarily, the current for resistance heating follows the path of the solid steel around the inside of the tube, from one electrode to the other, as this is the path of least inductive reactance. This is termed `skin effect'. This, however, does not provide the most efficient heating for welding and therefore the use of proximity conductors or impeders is made, which manipulate the current flow, ensuring that it becomes focussed on the slit coil surface edges to be joined. The impeder improves welding efficiencies of tube by as much as 25 percent. This is achieved by diverting the flow of current, from the internal surface of the tube to along the slit coil edges of the vee, in the developing tube.

There are two main types of power unit for high frequency (HF) welding. These are: solid-state inverters and vacuum oscillators. The most efficient and commonly used welding units used are the solid-state inverters. High frequency welding is a high speed, and usually, a high volume production process. One of the main benefits of this process is that the weld quality is not particularly sensitive to the presence of air and is fairly

tolerant to surface oxides and contamination, requiring minimal slit coil edge preparation. Therefore, there is no requirement for inert shielding gases, unless particularly reactive metals are being welded. The main disadvantage is that as it is a continuous automated process, and therefore stops or starts will result in discontinuities in the weld, leading to poor weld quality and potentially high levels of scrap tubing. There are two main process forms of HF welding, those using Induction Coils and those using Electrical Resistance Contacts.

RSEW-HF

RSEW-HF is the designation for high frequency welding using electrical resistance contacts, which ride on either side of the work-piece V-opening ahead of the squeeze rolls. The electrodes are of a sliding type, as only a light pressure is necessary to develop high amperage current to produce satisfactory welds.

RSEW-I

RSEW-I is the designation for high frequency welding using an induction coil. This process uses an induction coil to magnetically induce the current into the tube, generating sufficient heating to weld and is the dominant process used for produced ERW tube.

For both of the processes, the copper conductors carry the power to the coil or electrical contacts, and are cooled by water. To minimize impedance loses the conductors must be closely spaced and of minimum length.

In both types of process the heated surfaces are mechanically pressed together by squeeze rolls, causing the edges of the metal to upset [53,54]. The residual oxides are squeezed out along with the molten metal, leaving flash on both the inside and outside surfaces of the tube. The outer part of the flash is always removed. The process of removing the welding flash is termed `finning', due to the shape of the flash. Tube supplied in the condition with the internal upset flash removed are commonly termed 'fin-cut'. This tube condition is a pre-requisite for hydroforming, as with the fin still present difficulties in

tube end sealing are likely to be encountered and tube pre-bending operations, involving internal mandrels, would be unfeasible for production intent parts. The internal fin may be removed at the tube mill, although this additional operation usually incurs an additional cost. The butt-welding process hot-works the metal in a very local region, providing it with good strength and toughness characteristics. Therefore, the overall weld area and heat effected zone are narrow. As the butt-welded area is hot-worked, no cast microstructures are present as with fusion welding processes, therefore providing a more robust weld.

In the RSEW-HW process, tube surface damage takes place due to the contact between the electrode sliders and the slit coil, which also increases the maintenance costs. However, this is not the case when using an induction coil, as there is no physical contact between the work-piece and the induction coil, which makes it a suitable process for manufacturing tube from coated steel grades.

In the UK, in addition to the dimensional checks performed, a wider range of quality checks may be carried out for ERW tube, including eddy current testing [55], low pressure leak tightness and other destructive mechanical tests [56,57]. Rigorous quality inspections, laid-down by the customer, may also be performed on-line for ERW in an economical and productive manner. Eddy current testing is usually performed on-line and tube not meeting these requirements can easily be sorted and scrapped. Periodic checks during production are performed to ensure that the correct tube wall and minimum weld thickness are achieved. Additionally, two forms of mechanical test are performed. These are tube flattening and flare tests [58].

- ***Other Tube Manufacturing Methods***

CTA Tube

To achieve higher output and further cost savings, Voest-Alpine Industrieanlagenbau (VAI) have developed the CTA (Cost Saving, Time reducing, Availability increasing) technology for welded tube production [59]. The CTA tube production lines utilise the computer-controlled, motorized adjustment of the roll-forming tools [60]. CTA

technology allows production of a wide range of tube and pipe diameters using the same production tooling. Additionally, the standard CTA tube mill facilitates production of much higher D/t ratio tubes, having outside diameters of 127mm with a wall thickness of 1.5mm [60].

Stainless Steel Tube

For continuous production of stainless steel tube, the Electric Resistance Welding is not suitable, instead TIG welding is used to achieve the continuous seam weld. Consequently, the processing of stainless steel tube is slower, having a welding speed of between 1 and 5m/min, depending upon metal thickness [61]. Consequently, in addition to the already expensive substrate metal, the processing costs will consequently lead to an even more expensive tube product. TIG welding is not the only continuous means of producing stainless steel tube. Stainless steel tube may also be laser welded. The upper limit for the laser welding speed is approximately 15m/min [61], but the line speed would depend upon the stainless steel grade and slit coil thickness.

New Automotive Tube Manufacturing Technology

Due to the D/t range limitations of ERW and other production tube, new tube manufacturing technologies have been developed specifically to meet the specific requirements of automotive tube hydroformed components for B-I-W applications.

These methods have included specialised short tube mills, or alternative tube forming methods, in combination with laser welding techniques [62] to primarily manufacture steel tube for automotive markets. In September 2000, Corus the multi-metals supplier announced their tube making capability. Their production process, jointly developed by Hoogovens and Soudronic, shaped a tube blank by a series of press-brake operations, which developed an open, almost circular section from a given length sheet steel blank. The pre-formed tubular section was then passed through a series of steel rolls, followed by laser butt-welding [63]. The process has been adopted by Corus on the merger of Hoogovens with British Steel, with the purchase of a production machine from Soudronic in February 2000. An Engineering Doctorate programme commenced in October 1999 to

perform a detailed study of the Corus tubular blank process, with the aim of identifying the hydroforming capability of the tube blanks produced using this method and the influence of the fabrication variables.

Thyssen-Krupp Stahl presented their capability to produce prototype tube blanks at their Application Technology Centre [64], using a similar process to the Soudronic process. The Thyssen-Krupp facility was claimed to have the capability of producing tubes of 3m in length, with diameters in the range of 60-160mm and wall thickness values in the range of 0.6-2.5mm, thereby meeting most potential hydroforming B-I-W requirements [64].

Whilst the new tube manufacturing methods have emerged, the production methods are considerably slower than conventional tube mill technology and consequently command a higher premium than conventional tube.

Whilst an ERW tube mill may operate at speeds of between 30 and 240m/minute, laser welding speeds are usually in the range of 3m and 15m/minute. In the production of steel tube blanks, these speeds would of course largely depend on the sheet thickness and steel grade being welded. Although the new tube manufacturing methods are considerably slower than ERW production speeds based upon welding speed, the process cycle time for the laser welding operation may not be the slowest element. In the case of the press brake method used by Corus, the slowest element may indeed be number of pressing operations required to develop the sheet blank trip into a circular section, which would be governed by D/t ratio and potentially yield strength. The larger the D/t ratio, the greater the number of pressings that would be required to produce the section, as would be the case for steels with increased yield strength. Consequently, the overall cost of such a product would increase due to increased processing time.

2.2.6 Pre-bending – Process, Tooling and Limitations

For many structural steel hydroformed components, pre-bending is a necessary pre-process operation, required to develop the general component geometry. An outline of the rotary draw bending process for a tube blank is shown in Figure 10. The process starts with loading a tube blank into the bending tools and is positively clamped into position. The pressure (reaction) die is then located and the bending die rotated to develop the bend. Inside of the tube, the internal mandrel supports the tube from sectional collapse and wrinkling tendencies.

Figure 10: Outline of rotary draw-bending process for tubular blanks

The main bending tools components that are used for rotary draw-bending are highlighted in Figure 11 a & b. Tube bending operation, in particular rotary draw-bending, has been used for many other automotive and non-automotive applications but has been an essential operation in the production of many tube hydroformed components.

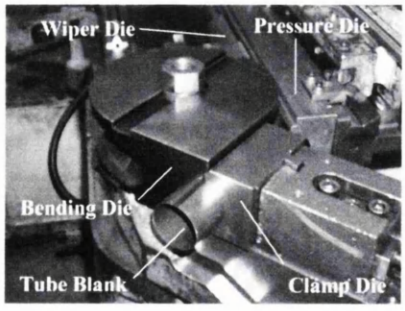

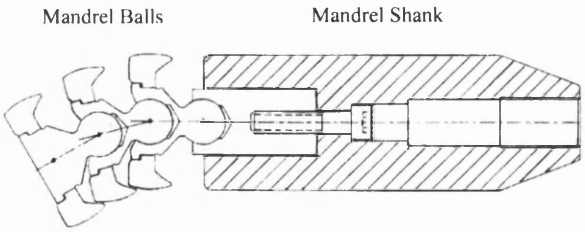

(b) Internal Mandrel

Figure 11: (a) Photograph of CNC Rotary draw bending tools and (b) internal mandrel

Like many forming operations, tube bending has limitations. In simple terms, tube bending has a forming window, characterised by boundaries of a tendency to split and a tendency to wrinkle or collapse. These tendencies are a function of the tube diameter-to-thickness ratio (D/t) and the tube bend radius (R). The tighter the bend radius, the greater the compression, and therefore wrinkling tendency, at the inside of the bend and the greater the level of stretch at the outside of the bend. The larger the D/t, for a given bend radius, the greater the tendency to wrinkle. Therefore, for large D/t ratio tube a greater requirement to provide internal support to the tube exists during the pre-bending operation in order to minimise the risk of wrinkling. The support is achieved by placing a mandrel inside of the tube. For more difficult bends, i.e. small centre-line radius bends on tubes with high D/t ratio, pre-bending tools which have internal mandrel tools and multiple balls are favoured, see Figure 11b. The number of balls and the spacing between balls (pitch) are be increased and reduced, respectively, in order to achieve a more difficult bend configuration [65].

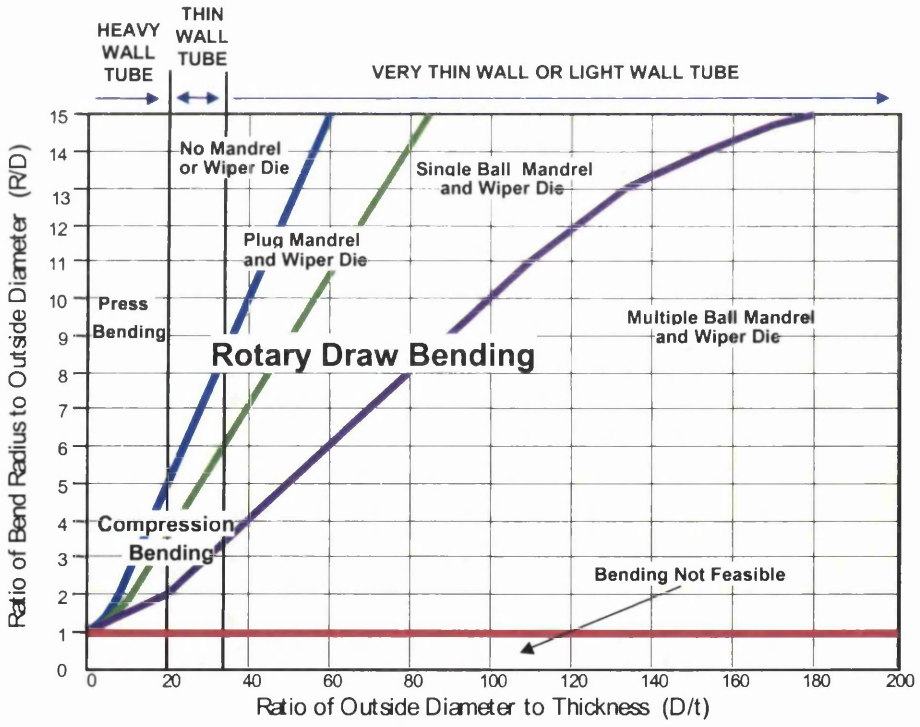

Figure 12: Limitations of pre-bending tooling and process *(According to Kervick and Springborn [66])*

A wiper die, as shown in Figure 11a, also assists with material flow by preventing material build-up behind the bending die, which would otherwise encourage wrinkling.

As a result of the different requirements of differing component geometry, different tool configurations are necessary, each having their own unique feasibility window. According to Kervick and Springborn [66] tube bending below a bend radius of 1D was not feasible, for the full range of D/t ratios, Figure 12. However, from the Freelander HIBS project, Edgar et al [67] found that this was not the case. The minimum tube pre-bend radius was significantly more than 1D for D/t ratios of above 30, as shown in Figure 13. The project found that the tube hydroforms studied tended to wrinkle when higher D/t ratio tubes we used in conjunction with tight pre-bend radii. The wrinkles developed during pre-bending could not be removed during the subsequent hydroforming operations.

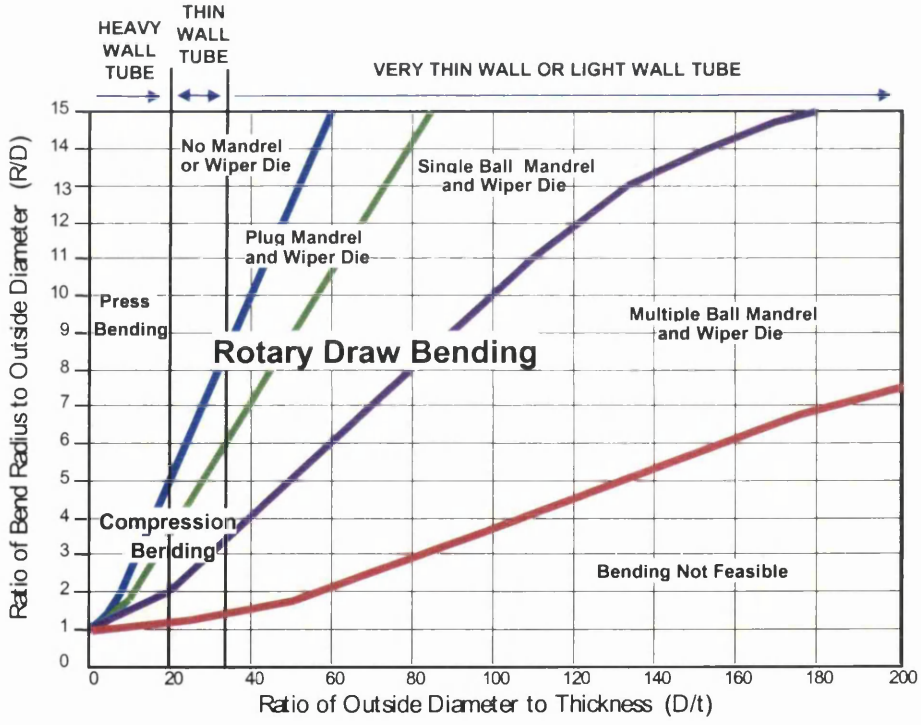

Figure 13: Limitations of pre-bending tooling and process *(According to Edgar et al. [67])*

The observed difference in tube bending feasibility may have related to the difference in the tube metals that were used. The tubes used in the HIBS project are likely to have been more formable, with lower yield strengths. Although similar D/t ratio tubes were considered, the tubes considered by Kervick and Springborn may have been thick walled, i.e. 2.0mm minimum, whilst most of the tubes used in the HIBS project ranged from thin to ultra-thin walled, i.e. 0.7mm-2.0mm thick.

The limitations of pre-bending tubes for tube hydroformed components, in particular light walled, high D/t ratio tubes, is very important, as the feasibility of the pre-bending operation is likely to have a direct influence upon the capability to produce certain B-I-W structural components from strip steel. As pre-bending feasibility is strongly governed by component bend geometry, the manufacturing feasibility of a tube hydroformed component will therefore be strongly dictated by the vehicle architecture.

2.2.7 Pre-forming

Pre-forming operations, other than pre-bending, are conducted to ensure that the tube blank can fit into the hydroform die, in the absence of pinching on tool closure or for other more specific reasons, such as localised expansion. In most cases, pre-forming merely represents closure of the hydroform die tools in automotive hydroforming applications [68]. Some general considerations must be given on how and what the tube blank pre-form geometry should be, in particular how it assists the hydroforming process. This is still a relatively undeveloped area of tube hydroforming manufacture, with very few practical guidelines. This may be a consequence of the large variety of pre-forming operations that may be conducted, from press or crush forming a tube blank to local expansion or reduction, using expanding mandrels or end-swaging equipment. In the PSH process, during die closure, the tube blank is internally pressurised. By doing so, it is claimed that due to lower friction between the die tools and tube blank improve corner radii and component feature definition, thereby dispensing with the need for expensive high-pressure hydroform press equipment [35].

2.2.8 Hydroform Die Tool Design

Whilst a hydroform die tool design must suitable to achieve complete tube filling of the die cavity, other practical considerations must also be considered. In particular, as the hydroforming pressures used are so high, resulting in large normal forces, any resulting thrust forces must be considered in the tool design. Additionally, the press locking forces, in conjunction with the internal normal forces, may apply significant loads and may result in substantial elastic deflections of the die tool. Not only would such abnormal conditions risk shortening the die tool life, but also such distortions may cause component splitting if the die tool split/opening line separates, by opening or twisting [69]. Additional complications may also exist if the component suffers witness lines from tube hydroforming. It is therefore prudent to perform FEA to identify the tool stresses to determine the tool design suitability [68], in addition to the FEA of the forming processes of the component. The other restrictions to the tooling design for hydroformed components, and therefore on the possible component design, have already been mentioned, with respect to component perimeter. However, due to the complexity of the components, it is important to utilise FEA to determine component feasibility. The cost for a late change in the design of a component within a complex vehicle body system, due to feasibility issues, is exceptionally high. The reason being is that manufacturing assembly studies, CAE structural performance studies and cost studies all need to be performed again to validate a new design. Therefore, the implementation of KBE [67] techniques are essential for delivering a cost effective design solution for a component, for B-I-W structures.

2.2.9 Limitations of the Tube Hydroforming Manufacturing Route

Cycle time

Due to the nature of the tube hydroforming process, the cycle time is significantly longer than for sheet steel pressings, with hydroforming process cycle times typically in the range of 10-40 seconds [70]. Differences in process time may also depend upon product specific factors, such as the external component corner radii and numbers and sizes of holes to be pierced during the hydroforming process. The typical elements of a tube

hydroforming production cycle are shown in Figure 14. The data was based upon information from three different German hydroform press manufacturers, Anton Bauer, Schuler SMG and Siempelkamp Pressen Systems (SPS) [71, 72 & 73].

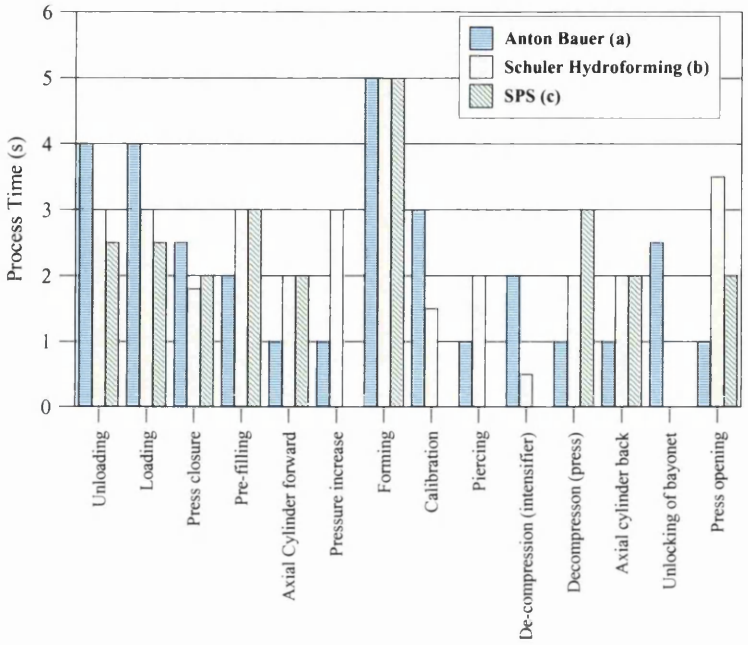

Figure 14: Example of typical hydroforming process operations and cycle times for; (a) Structural component data, using Anton Bauer 35,000kN press [71], (b) Engine cradle data, for a Schuler 35,000kN press [72] and (c) SPS 50,000kN press data (1999) [72].

Figure 14 illustrates state-of-art tube hydroforming cycle time capability based upon data from the latest model presses of the main hydroforming press manufacturers. However, the data refers to different components, which may influence individual process cycle times such as loading or unloading or pre-filling for example. The cycle time for Anton Bauer Hyproloc model press, having a clamping force of 60,000kN, was based upon a 70mm x 2.5mm x 1.5m structural component. The Schuler cycle time data related to the production of the Vauxhall / Opel Astra engine cradle, over twice the length of the component produced by Anton Bauer [44]. The SPS hydroform press data refered only to the general (1999) 50,000kN, model capability.

The cycle times, shown in Figure 14, were for individual events within one complete hydroforming process cycle, although a number of these take place simultaneously. The total estimated cycle times for the Anton Bauer, Schuler and SPS hydroform press equipment were 27.5, 27 and 23 seconds, respectively. The SPS process cycle time, although the lowest, did not include hole piercing and ignored pressure increase and calibration times. The typical press closure and opening times are now of the order of 3 seconds, having significantly reduced [73]. For SPS the tube filling time has also seen a major reduction, from approximately 8 seconds to 2-3 seconds. According to Bieling [71], duration owing to part handling is governed by the part geometry, weight, travel and the handling system used. The hydroforming process time is dependent upon the part geometry, part volume and degree of deformation. However, nothing is mentioned of the material influence, which dictates the magnitude of pressure required [34]. The machine functions are dictated purely by the machine specification, configuration and programming.

Despite the fact that tube hydroforming has a substantially longer process cycle time than pressing, high volume production of vehicle parts may still be achieved but to do this may require significantly higher levels of equipment investment and costs associated with design and development of the components. In assuming a hydroform cycle time of 27.5 seconds for the Schuler press, operating at 85% efficiency, more than 2,500 Vauxhall Astra hydroformed engine cradle components are produced per day. This is based upon the quoted production operation running on a 5 days per week, 3 shifts per day basis [74]. Depending upon the number of pre-bends required, the cycle time of the pre-bending operation may actually be longer than the total hydroforming cycle. In the case of the Vauxhall / Opel Astra engine cradle, two tube bending machines are used to feed the hydroforming unit. The production cell for the Mondeo (Mk1) engine cradle required three manually fed Eagle bending machines to supply the tube PSH hydroforming unit with sufficient pre-formed tube blanks.

Assembly

The assembly of a vehicle B-I-W, comprised of tube hydroformed components, is one of the largest inhibitors to wide-scale implementation of tube hydroforming technology. Whilst resistance spot welding (RSW) provides a robust means of fabricating pressed steel parts, it is not fully compatible with tube hydroformed components, due to welding gun access. An alternative approach for joining sheet to tube hydroforms and hydroform to hydroform may be achieved with the use of Single sided spot welding (SSSW) technology [75]. However, this technology remains relatively undeveloped and has many limitations. These restrictions are largely due to hydroform sectional design and thickness (sectional stiffness). The other alternative joining method for volume production is the application of laser welding. However, the questionable 'up-time' and required accuracy of assembly fixtures means that this method may not be suitable in all instances.

At GM, a combination of metal inert gas welding (MIG), RSW and SSSW were used for joining a hydroformed roof rail to a pressed body side [41]. For the '98 Seville, under similar body construction, the use structural adhesive was used in place of a large number of SSSWs for joining its pressed steel body side panel to the hydroformed roof rail. This would indicate that GM found difficulties in the application of SSSW for joining the hydroform components. It may also suggest that GM were reviewing uncommon joining techniques in the body shop to aid performance.

According to Gleave [76] there are essentially two modes of failure displayed by the SSSW process. These failure modes are mechanical and hot collapse. Consequently, the degree of difficulty in achieving a successful SSSW is considerably higher than for a RSW. The mechanical collapse is influenced by the sectional properties of the tube hydroform. This is because the section is subjected to a concentrated load to one face of the component during SSSW, instead of through two or three overlapping sheets, as in the case of a pressed assembly. Consequently, sectional stiffness, thickness and initial and final yield strength all influence susceptibility to the collapse failure mode [76].

From a manufacturing viewpoint, the issue of joining hydroformed components together to produce a space-frame structure is particularly complex and may result in poor or very complex joint configurations. The joining methods would require MIG or laser welding to join the hydroforms. Special joint conditions would also be necessary to cope with the individual needs of the welding methods. For instance laser welding requires precision fit [77] for butt welds, therefore overlap or "tent pole" configurations may be necessary but are difficult to achieve [77]. The welded joint may also have implications for weight efficiency, durability and cost, as a result of the different requirements of the joint.

Manufacturing Issues

In the production of the tube hydroformed components a wide range of manufacturing issues may inhibit the successful production or quality of a tube hydroformed component. As already discussed, the influence of the higher D/t ratios, in combination with light or ultra light wall tube, necessary for the production of B-I-W hydroforms is almost certain to have a major influence upon the successful manufacture of such components. Some of the following may cause major manufacturing problems or component rejects:

- Tube manufacture (potential limitations of tube production and influence on metal properties)
- Pre-bending (bend geometry limits, internal & external scoring and clamp or bending die marks)
- Pre-forming (pinching and unrecoverable folds or wrinkles)
- Hydroforming (tube end sealing, wrinkling & splitting limitations,, die witness lines, springback)

2.2.10 Innovations in Tube Hydroforming

To address the many current limitations of tube hydroforming technology, international research programmes have been implemented which include new concepts of press design and tooling to reduce cycle time. These include:

- Short Stroke Design - short stroke cylinder beneath bolster plate [72]
- Use of double ram SPS press variant & double lock Bauer Press variant [78, 71]
- Use of improved part loading and tube fluid filling mechanics [78]

The hydroform press companies are studying friction in tube hydroforming in collaborative programmes with steel suppliers.

Independently or in collaboration with automotive partners, the steel companies have been evaluating steel selection, tube manufacturing technology, process & component design, joining and performance characteristics. For the steel companies the aim is to develop or increase their market share in the hydroforming segment of the automotive business sector and to present themselves as innovators and technology providers.

2.2.11 Reported Applications

The principal applications of tube hydroforming technology in the automotive industry have included exhaust components, engine cradles (sub-frames), instrument panel beams and frame rails. These components have found a greater level of implementation compared with structural body components, largely as a result of B-I-W assembly issues. These components are essentially 'bolt-on' modules having minimal impact upon the design of other component/ component systems.

In Europe, the use of tube hydroforming for volume steel component production has included the following:

- Vauxall/Opel Astra Mk4 (Engine Cradle)
- Vauxall/Opel Vectra Mk1(Engine Cradle)
- Rover 75 (Engine Cradle)
- Mondeo Mk1(Engine Cradle)
- VW & Audi A- platform 4WD Models (Rear Axle Components)
- Rover-BMW Mini (Subframe)
- Daimler-Chrysler (Exhaust components)

Despite the inhibitors to utilise this technology for B-I-W components, GM, in the US have become leaders in the field of tube hydroforming technology in the automotive industry, through the introduction of the first, structurally integrated, steel hydroformed

body component in volume production. The integrated component was the Roof Rail & A-pillar reinforcement of the 1997 Buick Park Avenue [79]. In 1997, GM also unveiled the use of tube hydroforming for two lower structural frame rails, and a roof bow used in the 1997 Corvette. At GM this has been followed up with the use of a roof rail in the 1998 Seville [41]. Further tube hydroformed component applications were planned for GM's sport utility vehicles.

2.2.12 Steels used for Tube Hydroforming

Due to the large number of subframe components that are produced using this technology, a very limited range of steels have been utilised. The mamterial cost is an important element of the overall component cost. Therefore, the dominant steel grade that has been utilised for tube hydroforming has been hot rolled mild steel, usually 2mm thick or greater. This was the case for the Vauxhall/Opel Astra engine cradle, which requires additions of Boron in order to maintain formability of the tube following ERW production [80]. However, the majority of sub-frames and chassis applications that have entered production in the UK have been manufactured from HSLA steel tube, with yield strengths in the range 300 to 400MPa yield strength [80]. From reported European automotive research, a range of grades have been examined for B-I-W applications which have included galvanised high strength cold rolled steels by Volvo, for the 850 replacement study [47]. In the Freelander HIBS project, a wide range of formable cold rolled mild steel grades were reviewed but also hot rolled mild steel and hot rolled high strength steels, such as carbon manganese CMn250 & 350 for front side-member components [45].

2.3 Formability and the Influence of Metal Properties

2.3.1 Introduction

The formability of a material may be defined as its capability to take on and retain a desired shape, as a result of permanent plastic deformation.

Sheet metal formability can be influenced by many factors, including intrinsic properties, thickness, tool geometry and tribological factors. What governs the intrinsic properties of

a sheet metal and how they are determined is described in this chapter. Like pressing of sheet metals, tube hydroforming is a cold forming process, therefore only the behaviour and properties of material under ambient temperature conditions have been considered within this thesis.

2.3.2 Tensile Behaviour

The most direct and simple means of determining a metals response to elongation, under the most basic of stress states, is through (uni-axial) tensile testing the metal. During a tensile test on a material, the test machine will impose a fixed elongation rate at which it pulls the shoulders of a test-piece apart. Before commencing the test, the thickness and width are accurately measured. During the test the load developed in elongating the metal is recorded. The corresponding thickness and extension or elongation is also recorded. For steels, where the plastic strain ratio (see later) determination is necessary, the test-piece width is also measured during the test, up to the point of uniform elongation.

The tensile test is destructive and usually performed so that it will result in failure (fracture) of the test-piece. After the test or throughout the duration of the test, the recorded data is converted into engineering stress and engineering (%) strain often referred to as percentage elongation. To calculate the engineering stress, the instantaneous load is divided by the original cross sectional area (width x thickness) of the test-piece. The percent engineering strain or elongation, a dimensionless value, is calculated in the following manner:

$$e\,(\%) = 100.\,(l_{inst} - l_0) / l_0 \qquad \text{Equation 4}$$

where l_0 = original thickness length, and l_{inst} = instantaneous or current thickness length. As mentioned in section 2.2, the properties of steel are determined by their processing conditions and chemistry and also by subsequent forming operations. The processing and chemistry of strip steel governs its yield and tensile strength, elongation and plastic strain ratio (anisotropy parameter). From the recorded data, the information for that particular test direction can be determined.

- ***Yield Strength***

The yield strength of a metal defines its limit of proportional loading [81], i.e. the beginning of permanent plastic deformation. During a tensile test, conventional cold and hot rolled steels exhibit a distinct yield point, which followed by a drop in tensile load for an elongation range typically between 0.2% and 8%. The point just before the drop in load is observed, is known as the upper yield point [82]. In the region of lowered tensile load, which follows the upper yield point, Lueders Bands or stretcher strain marks develop on the surface of the material. The development of Lueders Bands is associated with a discontinuous yield phenomenon, observed in the lower tensile load regime. For certain automotive applications, the appearance of such a 'defect' on a panel surface is unacceptable, particularly for exterior 'A'-class or some visible inner parts. The phenomenon may also cause problems with material flow during press forming, resulting in failures.

As cold-rolled grades are dominantly used for the exterior skin panels or deep drawn interior components, the removal of Lhders Bands is necessary and is performed by temper rolling [83]. The temper rolling process induces a small degree of plastic strain, typically less than 1%, which satisfactorily removes their occurrence but is claimed to have minimal effect on the mechanical characteristics and forming performance of the steel. In removing the defined yield point, the stress-strain curve becomes continuous, thus removing the defined yield point. In order that a consistent yield point may be characterised for steel and other metals exhibiting a continuous stress-strain curve, an offset method is used. In performing the offset method, the elastic modulus line is mathematically 'offset' by a given elongation value. Typically, 0.2% elongation is used as the offset value. The value of stress at the point at which the offset line intercepts the stress-strain curve is the proof stress. For 0.2% offset, the proof stress is defined as the 0.2% proof stress.

- ***Tensile Strength***

The tensile strength of a metal is defined by the maximum tensile stress that it can withstand, which is calculated from the maximum load developed during the tensile test.

In terms of the material elongation, the point of maximum load corresponds to the limit of uniform elongation. When the maximum load is reached the reduction in test-piece width becomes non-uniform and a diffuse neck (or waist) develops in the test-piece. With further increases in strain the load drops dramatically. A local, through thickness, neck develops inside of the diffuse neck, ultimately with the test ending with fracture which corresponds to the total elongation of the material.

From data measured during the tensile test, the yield, or proof stress, tensile strength, uniform elongation and total elongation can be determined. From the measurements made, further information on the metals intrinsic properties can also be made.

- ***Plastic Strain Ratio (r-value)***

The plastic strain ratio or r-value is a measure of a sheet metals anisotropy and for a given test direction it is defined as the ratio of true width strain to true thickness strain, given by:

$$r = \varepsilon_w / \varepsilon_t \qquad \text{Equation 5}$$

The r-value is often termed the Lankford coefficient, after Lankford developed the concept of the plastic strain ratio. The r-value is a measure of the resistance to thinning (or thickening) [84]. For a steel with a high r-value, e.g. 2.5, the resistance to thinning is greater than for one of a lower r-value, e.g. 1.0. The reason for this behaviour relates to the difference in yield strength through the thickness of the sheet metal compared with the yield strength in the plane of the sheet (Normal Anisotropy). An estimate of the average r-value is given by the r-bar value determined from the following:

$$\bar{r} = (r_0 + 2.r_{45} + r_{90}) /4 \qquad \text{Equation 6}$$

where r_0 and r_{90} are determined from the sheet rolling and transverse directions, respectively, whilst r_{45} is determined at 45° to these directions. A high r-value, under certain forming conditions, will allow a considerably greater depth of draw, i.e. a greater panel depth, when pressing sheet metal and thus it can be a very beneficial property.

A measure of the magnitude in variation of Planar Anisotropy in a sheet metal can be given by the delta r-value. This formability indicator can provide indications of the likelihood of 'earring' type defects, which are associated with sheet metals having high values of Δr and deep draw applications. General a low Δr is desirable to reduce earring defects. The Δr value may also provide an indicator to define the optimal orientation for a blank to be cut from a coil. This variation in r-value for sheet metal is calculated from given by the following expression:

$$\Delta r = (r_0 - 2.r_{45} + r_{90}) /2 \qquad \text{Equation 7}$$

- ***Strain-hardening exponent (n-value)***

The strain-hardening exponent or n-value is a mathematical value defining the capability of the metal to strengthen during straining. The n-value can be determined from the true stress-strain data. The true stress is calculated by the following:

$$\sigma = S. (1+e) \qquad \text{Equation 8}$$

where σ = true stress and S = engineering stress. The true strain may be calculated from:

$$\varepsilon = \ln (1+e) \qquad \text{Equation 9}$$

where ε = true strain and ln = natural logarithm. The true stress-strain curve is assumed to follow a logarithmic power law according to Hollomon [85]:

$$\sigma = K.\varepsilon^n \qquad \text{Equation 10}$$

where n = strain hardening exponent. The curve roughly follows a parabolic shape. If the stress-strain curve is plotted as a straight-line, i.e. on a log-log scale, the n-value can be determined from the slope of the line, Figure 15. In addition, the strength coefficient or K value can be established from this plot at the value of stress corresponding to ln (ε) = 1. For strip steels the n-value is usually determined from a specific elongation range, e.g. 10-15% elongation. However, it is uncertain whether utilising the n-value corresponding to an elongation range provides an accurate representation of the actual n-value and that a more precise value may be determined through an alternative method. A typical n-value for strip steel is between 0.15 and 0.25, depending upon strength and grade. Stainless steels are more commonly found to possess n-values in the order of 0.3 – 0.5.

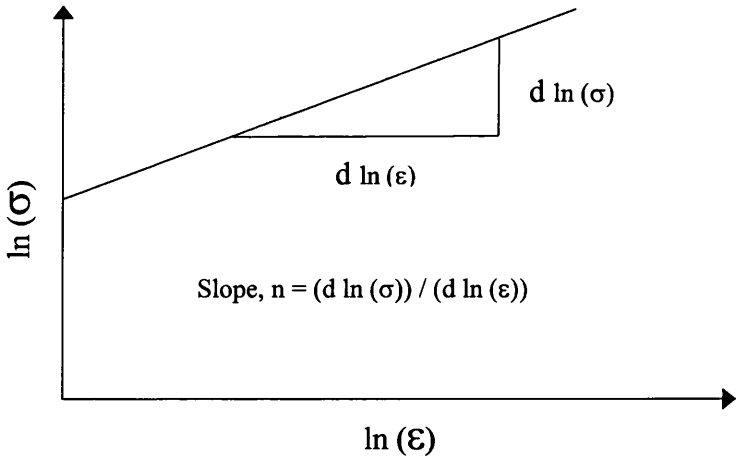

Figure 15: Schematic illustration of n-value (strain-hardening exponent) determination

Sheet metals that exhibit higher n-values are able to stretch comparatively more in the absence of diffuse and local necking than with lower n-values. If the sheet metal were

partially cold-worked, it would suffer a loss in the work-hardening capability and would possess a lower n-value if tensile tested again, which is an important factor when considering the potential forming influences of tube manufacture.

Another mathematical description of the hardening curve, suitable for steel experiencing large plastic deformations, is Swift's (Krupkowsky) hardening curve [86]:

$$\sigma = K(\varepsilon_0 + \varepsilon_p)^n \qquad \text{Equation 11}$$

This expression defines the yield point more closely than Hollomon's power law, particularly for metals that have received prior cold work.

- ***Tensile Instability***

For a ductile metal, such as sheet steel, necking usually begins at maximum load under tensile testing. During plastic deformation, the level-of strain hardening is opposed by the progressive decrease in cross section of the metal, up to the point of maximum load.

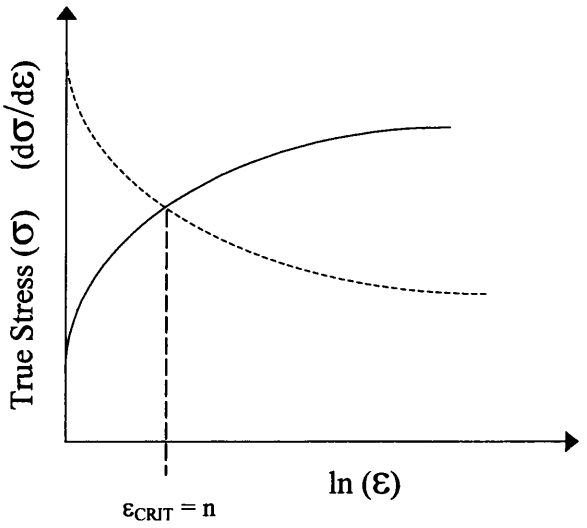

Figure 16: Schematic illustration of critical strain (n) value determination

However, when the maximum load has been exceeded, the decrease in cross section becomes larger than the increase in load carrying capability of the metal. Just prior to the onset of necking there is a point of no change in load.

According to Backofen [87], there are a number of different methods to identify or characterising the point of instability for a metal being subjected to tensile stresses, Figure 16 & Figure 17. From Figure 16, the critical true strain value coincides with the uniform elongation value and an accurate representation of the n-value for strip steels.

Another well-known method for determining the critical true strain, or diffuse instability strain, is achieved using Considiere's construction, Figure 17. The construction requires that at tangent be drawn from a base point, having an engineering strain value of 1 to the left of the origin. The tangent point defines the instability strain, e_{crit}.

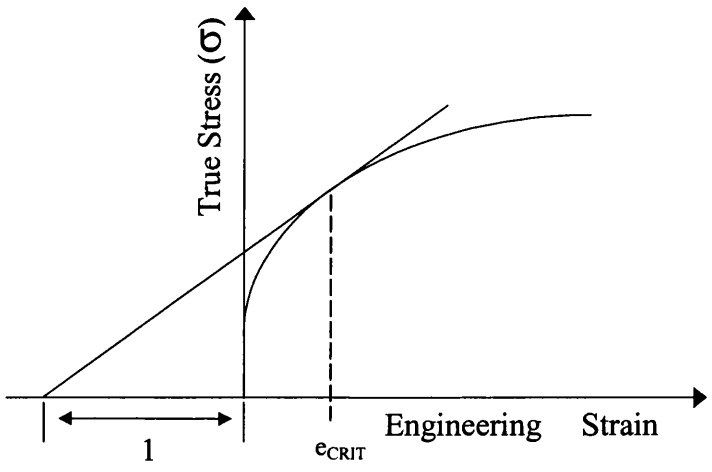

Figure 17: Schematic illustration of Considieres construction

Diffuse instability, Figure 18, is said to occur when the maximum true strain equates to the following:

$$\varepsilon_1 = n.\ 1 \qquad \text{Equation 12}$$

In this expression ε_1 = the maximum principal true strain. During tensile deformation a second form of instability occurs termed local necking, prior to fracture, refer to Figure 18. Under loading conditions of uniaxial tensile stress, localised necking for sheet metal theoretically takes place when the maximum principal true strain equates to the following [88]:

$$\varepsilon_1 = n.\ 2 \qquad \text{Equation 13}$$

The point of tensile instability for a sheet metal has great relevance for a tubular metal, when subjected to loading by internal pressure, as the critical strain may be modified, depending upon the stress-state.

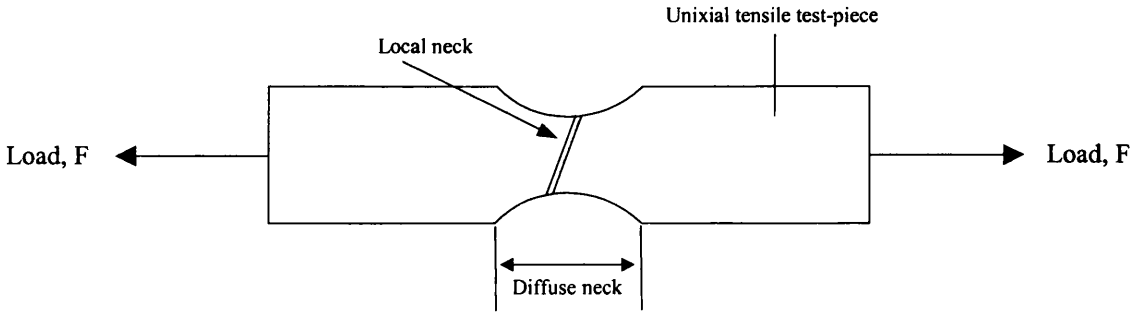

Figure 18: Schematic illustration of uniaxial tensile necking behaviour

In the case of a tubular metal, subjected to loading by internal pressure (closed ends condition), the maximum true strain at instability is [89]:

$$\varepsilon_1 = n.\ 0.5 \qquad \text{Equation 14}$$

If a tube is hydroformed in a 'free-forming manner', in the absence of die wall contact, and the tube reaches the critical true strain value, the tube will be subject to tensile instability. According to Marciniak [90], diffuse instability for a tube takes place in the form of a local bulge within the length of the tube, Figure 19. The length of the diffuse neck or bulge is of a similar scale to the tube diameter. This form of instability is latter followed by the tube undergoing local necking, parallel to the tube length, followed ultimately by bursting/splitting.

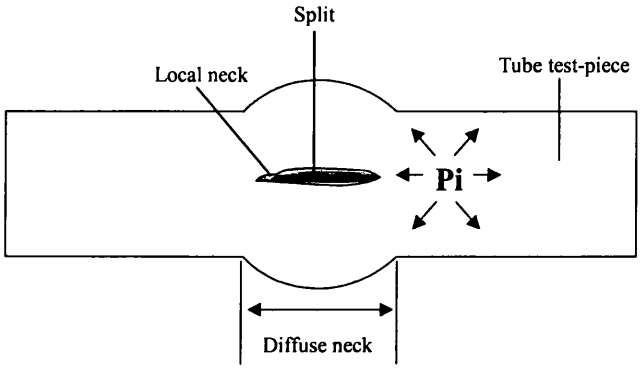

Figure 19: Schematic illustration of tube necking behaviour *(subjected to internal pressure, Pi)*

- ***Yield Criteria***

Predictions of yield phenomena for complex states of stress are postulated by mathematical expressions called yield criteria. These describe the combinations of stresses required to cause a material to yield. In the context of this thesis only the condition of plane stress is considered to prevail, i.e. no triaxial stresses, as the thesis is primarily concerned with sheet metal phenomenon and the deformation of thin walled tube under internal pressure, where conditions of plane stress are found [91]. These assumptions are upheld in the absence of tooling. However, the influence of high contact (normal) pressure between the tube wall and the die, as a result of high internal pressures, may cause deviations from this general assumption.

Under plane stress conditions, the most widely used yield criteria for sheet steel forming is that of von Miss'. Under plane stress conditions ($\sigma_3 = 0$) von Miss'' yield criterion may also be expressed as:

$$[\sigma_1^2 + \sigma_2^2 + (\sigma_1 - \sigma_2)^2] = 2\sigma_Y^2 \qquad \text{Equation 15}$$

The criterion is termed quadratic due its quadratic expression. In stress space the formula describes an ellipse, which is termed a yield ellipse. Within the perimeter of the yield ellipse, elastic conditions are predicted to prevail. Outside of it, plastic conditions are assumed to exist [92].

The effective or equivalent uni-axial yield stress, may be expressed as follows:

$$\sigma_e = (1/\sqrt{2}).[\sigma_1^2 + \sigma_2^2 + (\sigma_1 - \sigma_2)^2]^{1/2} \qquad \text{Equation 16}$$

For uniaxial tensile load conditions, under conditions of isotropic hardening, the effective stress σ_e is directly equivalent to the tensile stress. In terms of the developed plastic strain, due to strain hardening, the effective strain may be derived from the following expression:

$$d\varepsilon_e = (\sqrt{2}/3).[d\varepsilon_1^2 + d\varepsilon_2^2 + (d\varepsilon_1 - d\varepsilon_2)^2]^{1/2} \qquad \text{Equation 17}$$

This expression reduces to $d\varepsilon_e = d\varepsilon_1$ for pure tension. The von Miss' criterion assumes a condition of isotropy, i.e. the metal will yield uniformly under all combined stress-states, Figure 20. When a sheet metal is subjected to loading under a combined stress state, for example a stress ratio = 0.5 (i.e. plane strain) the equivalent yielding point is some 15% greater than the uniaxial case [93]. This assumption of a sheet metals yielding is a close approximation for isotropic metals, i.e. those with an r-bar value of unity.

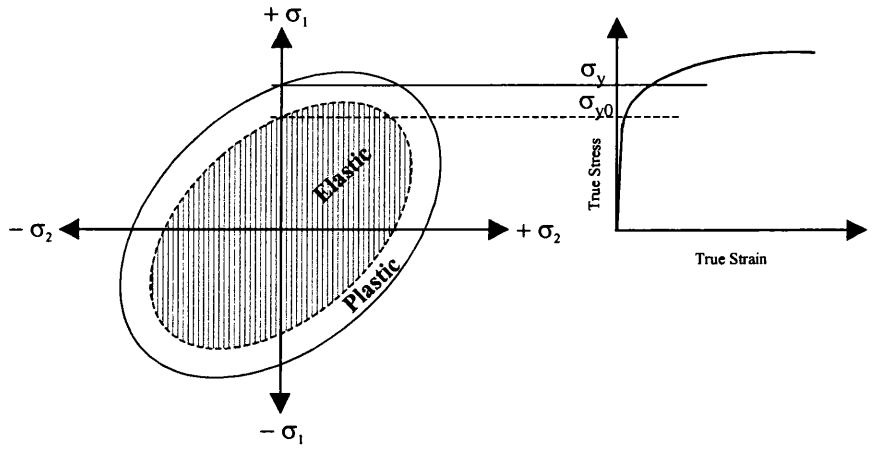

Figure 20: Schematic illustration of yield ellipse showing elastic and plastic deformation

However, this is not the case for metals exhibiting high degrees of anisotropy. The effect of normal anisotropy on the yield ellipse is to distort the ellipse, Figure 21.

For a sheet metal with an r-bar value = 2, that is subjected to a stress ratio = 0.5 (plane strain), the yielding point is some 30% greater in plane strain than for uniaxial tension [94].

An adaptation of the von Miss' criteria, accounting for anisotropy, was made by Hill [95]. Hill's (1948) quadratic yield criterion, with respect to the rolling direction (y), is given by the expression:

$$\sigma_y^{\,2} = [1/(F+H)].[\ F\sigma_y^{\,2} + G\sigma_x^{\,2} + H(\sigma_y - \sigma_x)^2]^{1/2} \qquad \text{Equation 18}$$

In this expression F, G, H are Hill's anisotropy parameters and σ_y and σ_x are the instantaneous yield stresses for the rolling and transverse sheet metal directions.

The parameters F, G and H relate to the plastic strain ratios and initial rolling direction yield strength (σ_o) as follows:

$$G/H = 1/r_0 , \quad F/H = 1/r_{90} \quad \text{and} \quad G + H = (\sigma_o)^{-1/2}$$

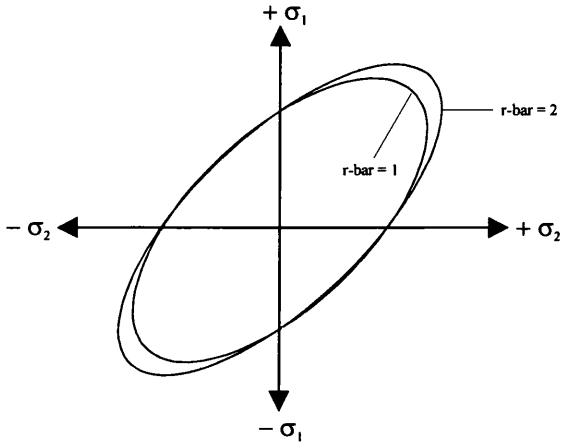

Figure 21: Schematic of yield ellipse showing influence of average plastic strain ratio

2.3.3 Forming Modes (Forming Limit Diagram)

In the production of a metallic component a number of forming modes or deformation modes may be experienced, see Figure 22 [96], depending upon the ratio of major to minor strain experienced. The range of deformation modes that are possible, without the component splitting or wrinkling, are best illustrated by the Forming Limit Diagram (FLD) after Keeler [97] and Goodwin [98], Figure 22. Under conditions of positive major and minor strain, the mode is one of biaxial tension, or a stretch-stretch mode. Where the minor strain is zero and the major strain is positive, this mode is considered pure stretch or plane strain. Under a drawing mode of deformation, a level of negative minor strain is experienced, as found in a tensile test, i.e. the test-piece width reduces. The uniaxial tensile test is characterised by having a (strain) ratio of true major to true minor strain of –2.

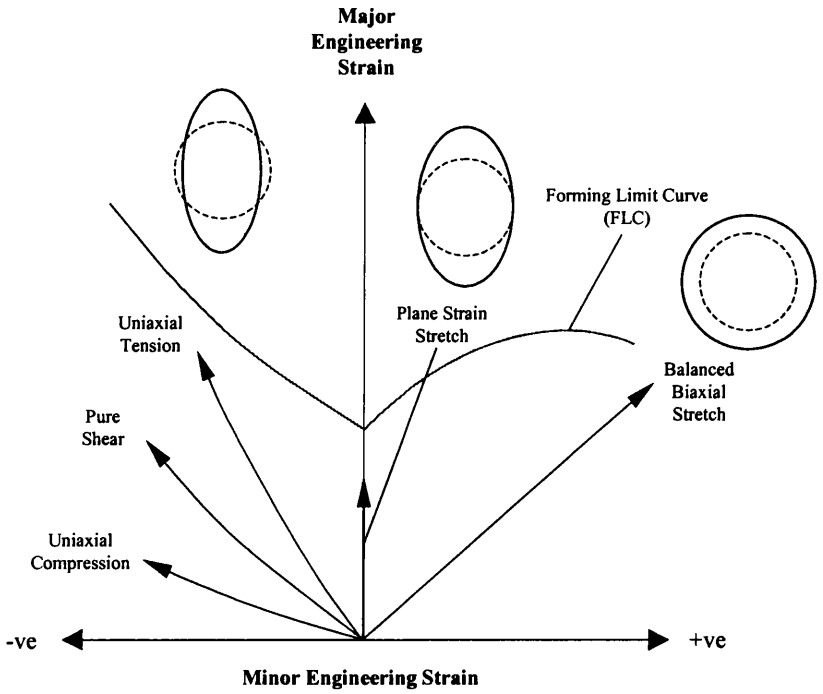

Figure 22: Schematic illustration of Forming Limit Diagram (FLD) showing different forming modes and forming limit curve (FLC)

When material is subjected to a strain ratio of –1.0 (pure shear), it does not thin or thicken but retains a constant thickness. Below this strain ratio, a sheet metal usually thickens or develops wrinkles due to the high level of compressive strain. At a strain ratio of –0.5, the metal experiences uniaxial compression.

The following factors are likely to influence whether or not wrinkles appear in sheet steel panel wrinkles after pressing [99]:

- Magnitude of negative minor strains or stresses
- Part geometry
- Degree of material support from tooling
- Material thickness
- Material properties
- Tooling Clearances

Some of these influencing factors may also hold true for tube hydroforming. Wrinkling type defects are undesirable in a component, from an aesthetic and usually a performance perspective, and should be designed out wherever possible.

As already mentioned, under plane strain forming conditions no minor strain, positive or negative, is experienced. Consequently, for every percent major strain the metal thins to the same degree, and hence the lowest point on the Forming Limit Diagram (FLD) is that of plane strain, usually termed FLD_0. The deformation modes that are displayed by a component, relate to a number of factors including, the intrinsic properties of the material, thickness, tool geometry, surface characteristics of the material & tooling, interaction with the lubricant and press parameters, e.g. Blank-holder load & punch speed.

The FLD concept allows the component strains to be displayed against the sheet metal Forming Limit Curve (FLC) for a particular strain ratio, whatever the particular forming conditions. The FLC describes the limiting strain value that can be formed achieved, in the absence of necking.

- ***Experimental Determination of the FLC***

To determine the FLC experimentally, several test methods involving strip metal are used. In principal, the metal is deformed to fracture or just prior to fracture, i.e. necking. The strip sample dimensions used vary, depending on test technique. To enable the surface strain measurement, the principal method that has been used is circle grid analysis [100]. This method of grid circle analysis has been used for samples to establish the forming limit curve but also on pressed components to evaluate press forming severity, die tryout, trial steel products and coatings and lubricants [101].

In using the circle grid method, it has been recommended that grids with an array of circles having diameters of the order of 2mm. The aim of this was to achieve optimal accuracy [102].

Usually, unique sample widths provide unique (different strain ratio) data points from which to construct the FLC. Traditionally, a mixture of tensile test samples, hydraulic bulge and punch-stretch tests were used obtain full range FLC data [103]. More recently, the Nakazima [104] or similar tests are employed, although independent research laboratories may use their own standards. The principal of the Nakazima test was to produce different strain modes by changing the test sample width, whilst using the same equipment and tooling to perform the test. Narrower samples produced greater levels of negative strain, similar to those found with tensile tests, whilst wider samples would develop strain with more positive minor strains due to increased material restraint. A similar technique was used by Hecker and involved punch-stretching test samples of different widths [105].

- ***Empirical FLC Relationship***

In the mid 1970s, Keeler and Brasier [106] proposed that the minimum engineering FLC point, FLD_0, corresponding to plain strain deformation, may be predicted from the following relationship:

$$FLD_0 = (23.3 + 360t)(n/0.21) \qquad \text{Equation 19}$$

In the expression, t is the material thickness in inches and n is the n-value. Furthermore, the recommended maximum n-value to be used in the above expression was not to exceed a value of 0.21. Keeler and Brasier also suggested that for the left-hand of the FLC, the major strain component would correspond to the sum of the true strain FLC_0 value and a component of pure shear, proportional to the minor strain. For the right-hand side of the FLC, it was suggested that it corresponded to Keeler's 'standard' shaped curve, generated by stretch-forming.

Keeler and Brasier stated that the FLC describes the critical strain-state at the onset of visual localised thinning in sheet metal and is usually drawn as a best-fit to test data points. According to Backofen, between plane strain (stress ratio = 0.5) and balanced biaxial deformation (stress ratio =1.0), i.e. on the right-hand side of the FLC, no visual

local necking may be observed [107]. Therefore, it would seem that test data obtained for this side of the FLC may be prone to error.

Based upon the Keeler and Brazier relationship, the ability of a sheet metal to stretch is governed by the n-value and also its thickness. For drawing deformations, a high r-value is an important property as this enables a deeper draw due to the greater resistance to thinning and thickening, preventing it from tearing but also resisting the development of wrinkles. In sheet metal pressings, drawing conditions are controlled by the magnitude of blank-holder force, applied to flange region of the blank. With a very high blank-holder force, the metal from the flange can be prevented from moving therefore inhibiting draw and promoting stretching conditions. In contrast with a much lower blank-holder force, a larger degree of draw is likely, although at too low a blank-holder force wrinkling of the flange area may result.

In 1997, a working group of the Beneleux Deep Drawing Research Group (BDDRG) performed a study into practical testing to determine FLC's [108]. The aim of the study was to identify factors that controlled the accuracy and reproduceability of the FLD tests performed on metallic metals. One of the aims of the study was help with recommending an accurate & reproducible FLC methodology for metallic metals, as the current ISO standard's guidelines [109] for producing FLC's were 'too fuzzy'[108].

In the study four independent laboratories performed an FLC using the same sheet steel. The laboratories used their own techniques to produce the FLCs. The variables between the laboratories that were observed included the following:

- Punch Diameter (75mm –160mm)
- Lubrication (polymer foil & grease, polymer foils, and a range of drawing oils)
- Grid Shape & Size (1mm –2.5mm)
- Grid Application Method (Electochemical etching, printing and Photosensitive resin)
- Grid Measuring Method (Home-made camera system / CAMSYS)
- Strain Determination (manual or algorithm smoother)

From this study, Monfort concluded that a wide range of scatter in test results was found between laboratories, which could be attributable to many different factors. These factors included; different measuring equipment, different means of determining the failure (necking) strain, different means of applying the circle grid, and the different grid sizes used.

The study also demonstrated that a scatter of 5-10% true strain was observed for the plane strain region. Partly, due to the significant variation in test results between the laboratories, the complexity of the problem remains unresolved and as yet no real improvement in the FLC test standardisation has been made. Despite this fact, the FLD concept has continued to be used as the principal means to evaluate the success of a pressed sheet metal component.

Since the FLC techniques have been widely applied to sheet metal forming, these approaches may be equally applicable for the analysis of simple tube hydroforms, where plane stress conditions prevail. In the production of a pressed component, many forming conditions may be observed, such as drawing, stretching, bending and flanging. Although the FLC is said to be valid for linear strain paths only [110], it is often "loosely" used for components subjected to multi-stage forming operations, e.g. draw, flange & re-strike, which therefore this increases the opportunity to use this technique for evaluation of tube hydroformed components.

From results of unpublished internal research [111,112], performed at British Steel's Welsh Technology Centre, it was found that the strain path associated with an individual grid circle on a Nakazima strip was non-linear. For all Nakazima strip widths, the strain paths were found to be bilinear or even trilinear. The initial strain path developed a major strain of approximately 10%, which was slightly biaxial, exhibiting a positive minor strain of 5 to 10%. This biaxial strain appeared to be independent of the hemispherical punch size (50mm or a 100mm) used in the tests. The second path would dominate most of the remaining strain mode. Ultimately, the strain paths exhibiting a final path close to

plane strain and ended with necking. Despite such effects, the FLC in whatever form is still widely for sheet metal pressing evaluation, particularly under trouble-shooting circumstances and before press tools for the production of new parts are "bought-off". However, more emphasis is now placed upon using the FLC in FEA during the design and development of automotive components.

Many of the forming conditions experienced by sheet metal pressings may also be found in the manufacture of a tube hydroform, in particular:

- Bending (tube-making, pre-forming)
- Stretching (tube-making, pre-bending, pre-forming, hydroforming)
- Drawing (pre-bending, pre-forming, hydroforming)
- Compression (tube-making, pre-bending, pre-forming, hydroforming)

- ***Failure Prediction Under Complex Strain Path Conditions***

In cases when complex strain histories are involved, then alternative failure criterion may be more suitable, i.e. when the strain path during forming is no longer linear or has multiple paths. Under such circumstances the Forming Limit Stress Curve (FLSC) could be manipulated to produce the new 'pre-strained' FLC. This would be applicable when a discrete region of the component has been subjected to a given magnitude of pre-strain, such as the outside of a bent tube. This was suggested by Darlington et. al. [113], who demonstrated that for decreasing tube centre-line bend radii, the original FLC would decrease proportionally.

Other researchers [114,115] have also suggested that this may be suitable for hydroforming. Despite the capability to use this criterion for non-linear strain paths it was claimed that the stress-based failure criteria was prone to error. It was stated that the safe forming region is much narrower in stress space and that variations in tensile properties ('noise' [110]) would strongly influence the accuracy of this technique.

- ***Bending & Springback***

The springback of a component is associated with the relaxation or recovery of elastic strains or stresses steels, Figure 23. Commonly, with sheet formed components a degree of springback may be associated with all forming operations. However, components which are produced from high strength sheet metals, such as high strength steels, or low modulus metals, such as aluminium, pose significantly greater potential for springback problems over traditional low carbon due to greater levels of elastic recovery.

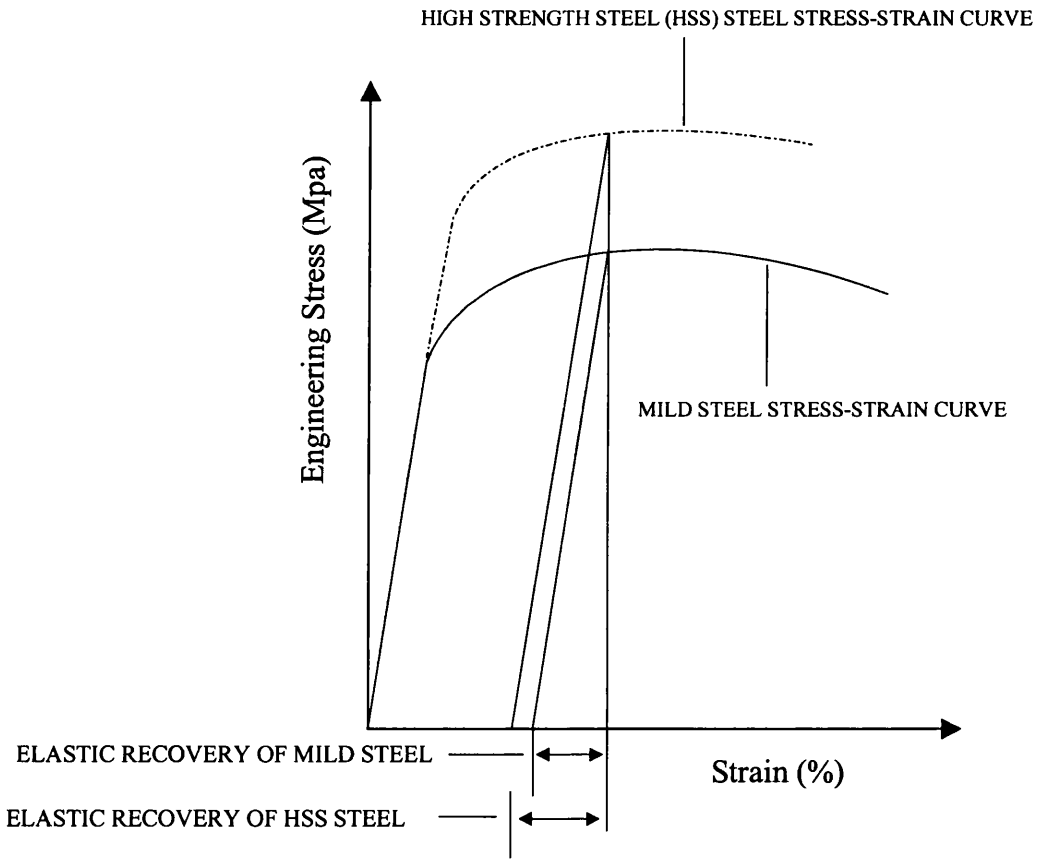

Figure 23: Schematic illustration of Springback (elastic recovery) for strip steel

Springback may also be found in the production of hydroformed components, although it has been claimed that, due to the effects of calibration, the tendency is lower [116]. Two main operations when springback phenomenon is likely to have a significant impact, other than following the hydroforming process, are pre-bending and pre-forming stages.

During tube bending operations, springback always takes place and is accounted for by over or under bending the tube. Continual monitoring of the tube material batch being bent is necessary to allow for any changes in the mechanical properties, namely yield strength, that may influence the final pre-bend geometry [117]. The pre-forming of a component may also strongly be influenced by springback as it usually a press forming process required to reshape the tube blank, so that can fit inside the hydroforming die cavity. However, in the case of pre-forming using hydroform die tools, as opposed to separate pre-form tooling, the issue of springback is of considerably less significance. Springback may also take place after hydroforming, relating to shallow, sweeping component geometry, in which case the component cannot develop sufficient strain along the shallow surface to maintain the die shape [118].

2.4 Influence of Friction and Lubrication in Tube Hydroforming

2.4.1 Introduction

Friction may be defined as the resistance to slip or motion, when two surfaces are in contact with one another. According to Coulomb [119], the friction coefficient is independent of:

- Area of contact between the sliding surfaces
- Sliding velocity
- Applied load

The following relationship is thus said to relate the normal force and the frictional resistive force between the two sliding entities:

$$F_R = \mu.N \qquad \text{Equation 20}$$

where F_R = frictional force, μ = coefficient of friction and N = normal force. Amonton [120] suggested that the two sliding entities possessed a real area of contact, A_r , and that the frictional force was related to the shear stress, τ , required to plough and rupture

through surface asperity junctions. Therefore, according to Amonton, the frictional force was considered to follow relationship:

$$F_R = A_r . \tau. \qquad \text{Equation 21}$$

However, for light loads equation 21 simplifies to equation 20, as the real area of contact is dependent upon the applied normal force and the surface flow stress required to support this normal load. The phenomenon of friction is further complicated by the introduction of a lubricant and therefore relates to number of variables.

The variables that have been considered to influence metallic friction include [33]:

- Micro-surface of the work-piece (or of the coating of the work-piece)
- Micro-surface of the die (or die's coating)
- Lubricant type & quantity
- Relative velocity between work-piece and die
- Normal pressure between die and work-piece
- Die geometry
- Temperature of die, work-piece, and lubricant

Further, the instantaneous work-piece geometry may also influence friction, as it may modify the stress system and thus the normal load transmitted to the surfaces. To this end, friction plays an important role in metal forming, as the work-piece and die tooling are largely in intimate contact during deformation. Consequently, friction has a significant influence on the flow of material over a die surface and subsequently will influence its strain distribution.

2.4.2 Micro-surface Characteristics

The surface topography of a metal work-piece plays a significant role in the frictional behaviour in a forming process [121, 122]. The micro-surface of a metal may be defined by a number of measurements of key characteristics, including: macro-waviness,

roughness and peak count. The properties of the surface asperities are also a measure of the surface condition and frictional behaviour that a material may display. The surface asperities are typically defined by the following characteristics:

- Peak height (Rp)
- Valley height/depth (Rv)
- Total height (valley to peak) (Rt or Rz – previously Ry)
- Peak density

These surface characteristics are measured with reference to a centre-line. The most commonly measured characteristic or parameter is the arithmetic mean surface roughness, largely due to the ease with which this parameters is measured. The roughness value refers to the sum of the surface asperity peaks and valleys (troughs). The valleys are below the reference centre-line and are negative in their summation, whilst the peaks are positive. The average roughness value is determined for a specified sampling length. A more mathematically robust description of the surface roughness of a sheet metal is given by the Rq value, where the Rq value is the Root Mean Square (r.m.s) roughness value [123]. Another recognised surface parameter, which provides a more robust characterisation of the surface is the total height parameter, Rz (formerly Ry). The total profile height of the sampling length is given by Rz, whilst Rt is the total profile height for the evaluation length [123]. The difference between sampling and evaluation length is that one evaluation length may contain one or more sampling lengths. There are two further height parameters and these are Rp and Rv, which are the peak profile height and asperity depth, respectively, [123. Emmens [124] found that for sliding surfaces under comparatively light loads, similar to those found in some deep drawing applications, the friction coefficient is proportional to the square of the peak profile height Rp. The reason was believed to stem from the fact that this parameter was important in the microscopic flow of the lubricant over the surface. For cold rolled strip the surface roughness must be controlled to meet the customer requirements. Under "normal" conditions, the cold rolled strip should be supplied with mean surface roughness in the range $0.6\mu m \ll Ra \gg 1.9\mu m$, although tighter specifications are possible and a smooth finish can be supplied which has an $Ra \ll 0.6$ [125].

The asperity size and indeed shape on a metallic surface can play an important role in enabling lubricant to remain on the surface and therefore may be very beneficial. However, cold rolled strip steel with an excessive surface roughness value may reduce the finish quality of a paint application, particularly for exposed panels [126]. Additionally, the macro-waviness can also have a significant influence upon the appearance of a painted surface.

The micro-surface characteristics alone do not provide a means of predicting the frictional behaviour. More importantly it is how the surface characteristics, within a tribological system behave, i.e. in conjunction with a given lubricant, tool micro-surface properties, sliding motion and surface pressures.

2.4.3 Lubrication

The principal method to reduce friction between a die and a work-piece is by the application of a lubricant to one or both of the sliding surfaces. Lubricants can generally be categorised as follows [127]:

- Fluid-film lubricants
- Solid lubricants
- Extreme Pressure (EP) lubricants

These categories outline available lubricants. However, some cross over does exist, in particular between solid and EP lubricants.

- ***Fluid-film Lubricant***

When a liquid lubricant, such a mineral oil, is applied to the surface of a work-piece and brought into contact with a die, the fluid acts as a film between the two entities. Depending upon the film thickness, the lubricant may separate the entities entirely or only partially. Depending upon the lubricant quantity and applied pressure, and therefore film thickness, the frictional behaviour may be very different. The properties or behaviour of a lubricant, in terms of the form of lubrication provided may be categorised

according to the Stribeck diagram [128], Figure 24. In principal, Stribeck related the coefficient of friction and film thickness to the lubricant viscosity, the relative velocity (between the two sliding entities) and the contact pressure applied to these entities (work-piece and die).

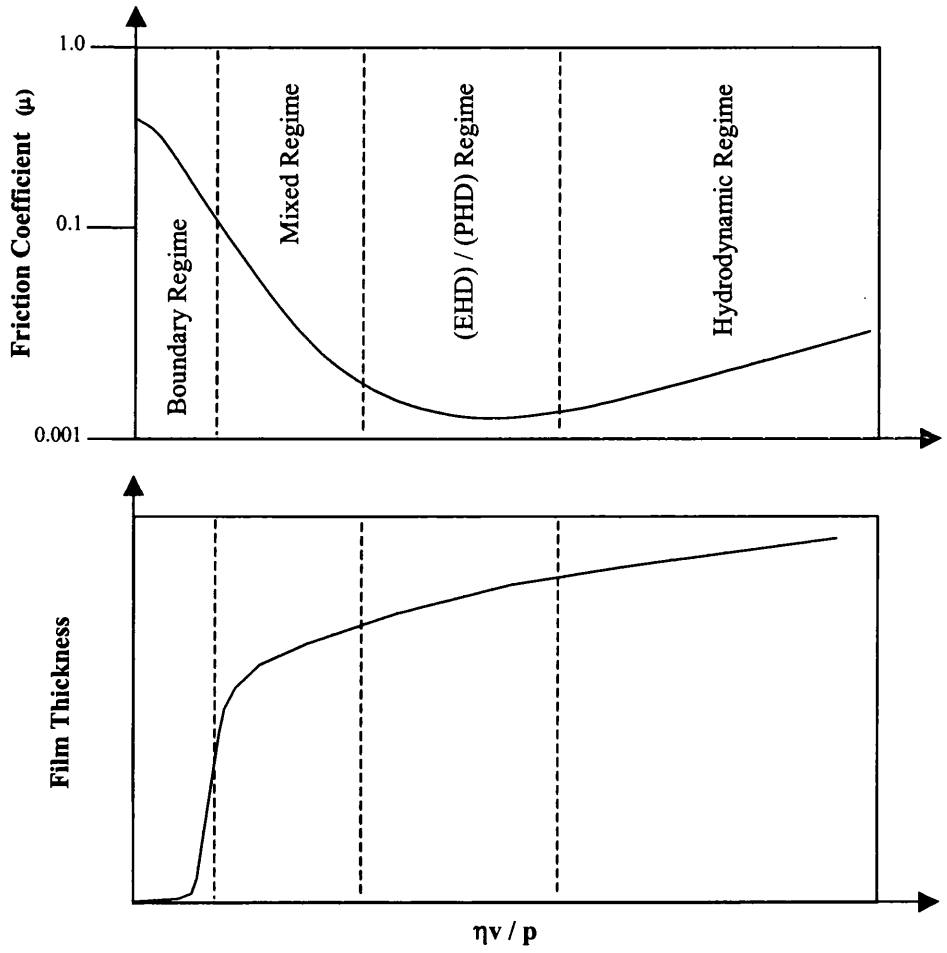

Figure 24: Schematic illustration of the Stribeck diagram

According to Stribeck, fluid film lubricants may fall into one of the following regimes:

- Dry (Static)
- Boundary
- Mixed
- Elasto-hydrodynamic (EHD) or Plasto-hydrodynamic (PHD)
- Hydrodynamic

The Stribeck curve was further developed by Schipper [129], who proposed the following expression, accounting for the surface roughness in conjunction with a fluid-film lubricant:

$$L = (\eta.v) / (p.Ra) \qquad \text{Equation 22}$$

where L is a dimensionless value, η is the dynamic viscosity, p is the mean contact pressure and Ra is the mean surface roughness.

2.4.4 Determination of Friction Coefficient

From a simple strip-draw test, for example a double flat clamp die test (Figure 25), the friction coefficient may be determined as follows [130]:

$$\mu = F_T / 2F_N \qquad \text{Equation 23}$$

In this expression, F_T = the traction force (required to pull the strip between the clamped dies) and F_N = clamping force of the dies. In a simple test like this, a steel strip is pulled for a set distance, in order to provide a representative average velocity. Tests such as these may have clamping forces and traction velocity modified to provide information on the influence of clamping pressure and sliding velocity and how these variables influence the behaviour of the lubricant tested and its interaction with the surface characteristics of a given strip steel.

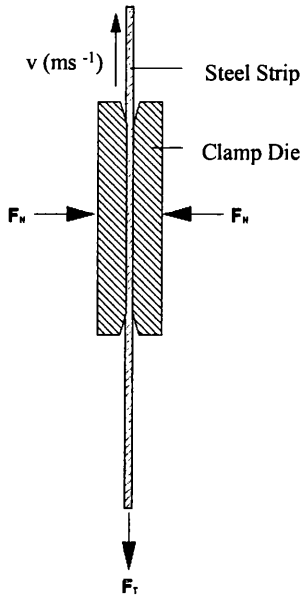

Figure 25: Schematic illustration of strip friction test

2.4.5 Friction and Lubrication in Tube Hydroforming

The influence of friction in sheet metal forming is complex. Consequently, in FEA of sheet metal pressing, friction behaviour is often assumed to follow Coulomb's Law. This constant global friction coefficient, applied to an entire panel, is widely used. The value of 0.15 is a commonly value for the friction coefficient in the absence of experimental data [131 & 132]. The actual value of friction during the hydroforming process is not known and simple strip tests may not represent the frictional behaviour accurately. As contact pressure in fluid-film lubrication has an influence on the resultant friction coefficient, then in all probability, tube hydroforming frictional behaviour is likely to differ from those of sheet metal pressing, as a result of the higher contact pressures. For the simple strip test, the dynamic friction coefficient remains essentially constant as the clamping load increases. In contrast, during tube hydroforming the internal pressure increases during forming to stretch and finally calibrate the component. Therefore, the applied Normal load and hence the frictional force increase.

In 1976 Limb et al [133] found that different lubricants had a profound influence on the hydroforming of a T-piece. The effectiveness of the lubricants studied was ranked by means of the "T" (or branch) height that could be achieved. From the experimental hydroforming trials of the "T"-piece, it was found that PTFE sheet performed the best, for all of the different metallic tube materials tested, namely Copper, Steel, Aluminium and 70/30 Brass. The spray form of PTFE was also found to perform well.

A number of recent experimental investigations have been performed in an attempt to simulate the hydroforming conditions and to study frictional behaviour of certain substrate metal surfaces and lubricants. By simplification of the hydroform tool geometry and process conditions, the friction coefficient may be determined. In test results reported by Eichhorn [134], the friction coefficient found in the hydroforming tests was considerably lower than the values obtained from sheet strip tests. This phenomenon was identified as being independent of the lubricant used and related to the hydroforming process conditions. This illustrates the importance of understanding friction phenomenon in tube hydroforming and whilst tests performed on strip steel may give indicators of the frictional behaviour, due to the interaction between micro-surface and lubricant, it may not provide absolute friction values for use in mathematical modelling of the tube hydroforming process.

From (Equation 23), the frictional force is directly proportional to the contact normal force, F_N. In the case of a tube of diameter D, of a length L, the normal force is directly proportional to the internal pressure (p_i) applied to the tube [135] as shown in following expression:

$$F_N = p_i \, . \, \pi DL \qquad \text{Equation 24}$$

From (Equation 23) and (Equation 24) it can be seen that the friction coefficient for such conditions may be determined when the frictional force opposing motion is known from the following expression [135]:

$$\mu = F_R / (p_i \,.\, \pi DL) \qquad \text{Equation 25}$$

In June 2000, selected dissertation results were presented at the ERC / NSM International conference on tube hydroforming [135]. The results were from a simplified analysis of friction in tube hydroforming by Prior, as described above. The test was devised to simulate friction in the 'guide zone' of a hydroformed component using a straight length of tube. By pushing one end of the tube forward, using the end seal (punch), and using a controlled reverse of the other end seal, the tube was made to slide within the die, whilst applying internal fluid pressure, which forced it against the die wall. Under this controlled action, travel velocities of between 3mm and 18mm/s was simulated. Although this end seal velocity was at the low end of the capability of many commercially available machines, which may achieve travels speeds of 99mm/s or more, it may still be representative of some hydroforming processes. In particular those requiring only small magnitudes of axial end feed at substantially lower feed rates.

The hydroforming friction tests were performed on tube manufactured from hot and cold rolled stainless steel (grade 321) material. The measured profile height of the surface texture (Rz) for the cold-rolled stainless steel was 4-9μm. For the hot-rolled material the Rz value was considerably higher, between 20 and 25μm. The friction tests were conducted using three different lubricants; an oil-based lubricant, a polymer-dispersion (supplied by Fuchs Lubritech) and a molybdenum disulphide (Mo_2S) laquer. The later two lubricants were applied as films (5μm thick) to the steel substrate surfaces, significantly thinner than the total profile height of the hot-rolled tubes tested. The key results of the research programme are presented in the following sections.

Influence of Internal Pressure

The tests were aimed at identifying the influence of applied internal pressure and were performed using a sliding velocity of 3mm/s. The test results demonstrated that by increasing the internal pressure up to 1500Bar, the friction coefficient decreased for all of the lubricants evaluated. The friction coefficient for the oil, dropped from 0.07 to approximately 0.03, whilst the tests results using the Mo_2S lubricant exhibited a drop in friction from 0.04 to 0.01. The polymer-dispersion, however, displayed an almost constant low value of friction coefficient dropping from just under 0.018 to 0.008. In the case of the oil lubricant the reason for the reduction in friction coefficient may have been due to the fact that increasing normal pressure would cause an increase in the shearing forces experienced by the lubricant. This would have caused the lubrication regime changed from a boundary to a mixed regime. The Mo_2S experienced less of an effect compared to the oil-based lubricant. This was believed to be due its mechanism of lubrication, involving shearing. The Mo_2S lubricant may have become more compacted with the higher normal load, and therefore more efficient. This, in turn, may have accounted for a reduction in the friction coefficient. In the case of the polymer-dispersion, the lubricant was likely to behave similar to graphite, in that weak bonds between the polymer chains would slide easily over one another under a shear load. However, a significant increase in the normal load would cause a significant increase in the shear load, thereby decreasing the sliding efficiency caused by damage to the polymer chains.

Influence of Sliding Velocity

At an internal pressure of 1000Bar, the sliding velocity was found to have very little influence upon the measured friction coefficient, for the entire range of sliding velocities utilised. In the case of the oil lubricant, the friction coefficient was observed to decrease from approximately 0.05 down to 0.03 over a sliding velocity range 3-15mm/s. This behaviour was suggested to have been caused by an increase in shear strain exerted on the oil lubricant. As a consequence, this resulted in a shift of the lubrication regime toward a more mixed regime, from the initial boundary regime. However, from the tests using the Mo_2S and polymer-dispersion lubricants, the coefficient of friction increased

slightly with increasing sliding velocity, for the range 3-15mm/s. This fact may have been attributed to a lack of film thickness or poor film adhesion.

Influence of Micro-Surface on Lubrication

The test performed upon the hot and cold-rolled stainless steel tube exhibited strongly different friction coefficients for the full range of sliding velocities when using the oil lubricant. The metals were found to exhibit increasing friction coefficient values with increasing end seal displacement (0-75mm), with values of between 0.025 and 0.038 for the cold-rolled and between 0.038 and 0.045 for the hot-rolled. However, in the case of the Mo_2S laquer, the friction coefficient did not display significant increases, typically 0.01 to 0.021 for the hot and cold rolled tube metals.

In summary, whilst an average global friction coefficient of approximately 0.15 may be suitable for FEA of the pressing of sheet metal components, the frictional investigations discussed in the previous pages illustrates that this may not be a suitable value for FEA of the tube hydroforming process. However, under circumstances of many unknown parameters (e.g. lubricant type, surface parameters and processing conditions) and their interactions, coupled with the influence of more complex geometry, it will be important to generate approximate values (or ranges) suitable for simulation of the tube hydroforming process.

2.5 Finite Element Analysis (FEA)

2.5.1 Introduction

Finite element analysis (FEA) is the application of the finite element method, to obtain approximate numerical solutions to boundary value problems [136]. In deriving a solution for numerical problems, the finite element method reduces the infinite number of degrees of freedom of a body to a finite number. This is achieved by a discretisation process which sub-divides a domain (body) into sub-domains, known as finite elements.

The unknown variables of the problem are calculated based upon the load case applied to the boundary points (nodes) of the elements [137].

2.5.2 Implementation of FEA for Tube Hydroform Design & Development

Sheet metal forming simulation has become routine practice in assisting with evaluation of component design feasibility and process development. The key purpose for utilising FEA to calculate the sheet metal forming process is to achieve a reduction in the component development lead-time, enabling production tooling to be manufactured earlier and with less risk. For tube hydroforming, substantial development of the commercial codes has been made in order to achieve a similar FE capability offered to simulate the sheet metal forming process. Engel, of Schuler Hydro-Forming, demonstrated the that one of the direct benefits of simulating the tube hydroforming process was a 5 day reduction over the minimum 10 day component prototype development period [138].

Currently, there is little experience and knowledge of tube hydroforming technology, compared with sheet metal pressing due to the complexity of the forming operations involved. These operations may include pre-bending, pre-forming and ultimately tube hydroforming, which individually are complex operations. Additionally, complications include the lack of specific design approaches and methods of utilising FEA for evaluation of the tube hydroforming process, which for pressed steel parts are already available.

One of the many benefits of FEA is that it can solve multiple complex equations, providing fast and accurate predictions of a forming process. Consequently, FEA is tremendously beneficial to hydroform press and die manufactures, but also to the vehicle manufacturers and their suppliers. For example, simulation of the tube hydroforming process eliminates the necessity for crude and cumbersome hand calculations to predict strain from estimated cross-sectional elongation values. Therefore, FEA provides manufacturers with significantly higher levels of confidence to be able to decide on

whether or not a part can be manufactured. Subsequently, the risks, in terms of delays and costs, for a product, system or full vehicle development programme are reduced.

By utilising FEA at the design & development stages of a tube hydroformed component, the following benefits may be realised:

- Reduction in lead-time
- Component feasibility statement/s
- Optimisation of component geometry & performance
- Greater levels of component development
- Greater levels of process optimisation (e.g. internal pressure, axial feed or axial force)
- Optimisation of tooling geometry and tolling process configurations
- Cost reduction (prototyping duration and tooling)
- Improved component quality (repeatability & reproducibility)
- Reduced levels of component rejects
- Reduced design and development risks

2.5.3 Requirements for Simulation of the Tube Hydroforming Process

To be able to model the full tube hydroforming process there are several basic requirements beyond the mandatory requirements for FEA. These are the following:

- Accurate representation of the tooling for :
    - Pre-bending (internal mandrel, clamp die, pressure die and bending die)
    - Pre-forming (other than hydroform die tools)
    - Hydroforming (main die tools and axial ram configurations)
- Capability of simulating full process conditions (displacements, forces and pressures)
- Accurate description of metal properties and characteristics & failure
- Accurate contact definition between the tube and tooling and between tube and itself
- Accurate representation of mult-istage forming

2.5.4 Commercial FE Codes suitable for Analysis of Tube Hydroforming

To conduct FEA of the tube hydroforming process a wide range of commercial codes are available. The main commercially available forming analysis codes used internationally by the automotive industry, are the following:

- Pam-Stamp™ (Explicit)
- Optris (Explicit)
- LS-Dyna (Explicit)
- Auto-form (Implicit)
- ABAQUS (Explicit)

Implicit versus Explicit Finite Element Method

- ***Implicit Method***

The metal forming process is considered as an incremental static problem when using the implicit finite method [139].

The equation representing a discrete system (problem) may be expressed as follows [140]:

$$[K] . [u] = [F] \qquad \text{Equation 26}$$

Where **[K]** = the stiffness matrix, **[u]** = the nodal displacement vector, and **[F]** = nodal force vector. The stiffness matrix, K, represents an array of coefficients that relate to the unknown field variables, u, and F represents the initial boundary conditions. Equation 25 is solved using an iterative procedure, such as the Newton-Raphson Method. In each of the iterations, the stiffness matrix must be computed. Consequently, this is numerically expensive. However, fewer increments may be necessary to achieve a solution. This may also be a drawback as analysis using this method may experience difficulties in accurately describing permanently changing boundary conditions [141]. A key advantage of the implicit analysis is that mesh refinement has no or little impact on the calculation time [141].

- ***Explicit Method***

Metal forming analysis, performed using the explicit finite element method, treats the problem as a dynamic one. A generalised equation for describing a problem when using the explicit method, is as follows [139]:

$$M(d^2u/dt^2)+ C\,(du/dt) + F(t,u) = P(t,u) \qquad \text{Equation 27}$$

Where M is the mass matrix, C is the damping matrix, u is the nodal displacement vector, F is the vector of internal nodal forces and P is the vector of external forces. Commonly, the solution to the calculation is achieved using the central differences time integration technique [142]. The solution of the problem, defined by the explicit method , may be simplified by means of the diagonal mass matrix [139].

The principal drawback of the explicit method is that time increment (time step) must remain smaller than the critical time step for the solution to remain numerically stable [143]. The critical time step is governed by the characteristic length of the smallest element of the deforming work-piece and the speed of elastic wave propagation through it. Therefore for the solution to be numerically stable the following must be satisfied [143]:

$$\Delta t \leq \Delta t_{CRIT} = L \,.\, \sqrt{(\rho/E)} \qquad \text{Equation 28}$$

and

$$L \,.\, \sqrt{(\rho/E)} = L/C \qquad \text{Equation 29}$$

In the above expression, Δt is the time step, Δt_{CRIT} is the critical time step, L is the length of the smallest element, ρ is the density of the metal, E is the elastic modulus and C is the velocity of an elastic wave through the metal.

- ***Pam-Stamp™***

The commercial code Pam-Stamp™ is a dedicated software package for the simulation of metal forming, originally developed for sheet metal pressing by ESI Group (Engineering Systems International). The code uses a dynamic explicit solver (Pam-Stamp) to perform the calculations [143]. The pre and post processors (Generis and Pam-View [143]) make up the complete software package providing a user-friendly interface to set-up hydroforming and press-forming simulation models and to view the results of the analysis, respectively.

Pam-Stamp™ has been rigorously tested and used by many of the major vehicle manufacturers, including BMW AG, VW- Audi AG, General Motors (GM) Hyundai and Renault, all of whom have found benefits, particularly in terms of reducing lead-times.

Pam-Stamp™ can be used to simulate pre-bending, pre-forming and tube hydroforming, in addition to the sheet hydroforming process. In the 2000 software release, an automatic tube bending model generator was introduced, reducing the need for the user to develop the individual bending tool surfaces and corresponding meshes [144]. In this latest software version, the material models and contact algorithms have also been improved, specifically for hydroforming analysis [145].

A degree of user freedom exists when using Pam-Stamp™ software, as the user may define the stress-strain and FLC representation. However, until 2000, a limited number of means of describing metal yielding were available. Hills 1948 and 1990 yield criteria were been the dominant forms for representing yield criteria, with or without the influence of plastic strain ratios or r-bar [146]. However, in the 2000 Pam-Stamp software release, the capability to incorporate kinematic yield functions was implemented [145]. Whilst potentially providing more accurate results, the availability of this data input requires significantly more outlay in terms of practical test requirements (at cost) to identify the necessary parameters. The friction model in Pam-Stamp, like many other forming analysis codes, has largely been limited to Coulomb's (Amonton's) Law until the latest version 2000.

- ***Optris***

Optris was originally developed by Dynamic Software and at the beginning of year 2000, Optris was bought-out by ESI [147]. Oprtis was specifically developed for press-forming simulation and like Pam-Stamp and LS-Dyna it made use of the explicit time integration scheme. As a result of its high accuracy and acclaimed user-friendly graphical interface, Optris was used by many of the major OEMs including:

- PSA (Peugot-Citreon Group)
- Renault
- Daimler-Benz
- Fiat
- Ford (Europe)

Early in 1999, Optris developed the capability to perform simulation of tube bending, therefore providing the ability to conduct full process simulation for a tube hydroformed.

- ***LS-Dyna***

As with Pam-Stamp™ and Optris, the code LS-Dyna 3D, developed by Livermore Software Technology Incorporated, used a dynamic explicit time scheme [148]. Therefore, the capabilities and limitations of LS-Dyna were much the same as Pam-Stamp and Optris. LS-Dyna was used dominantly by OEMs in the USA, relating to the codes Californian origin. The principal OEMs users of LS-Dyna were GM, Ford and Chrysler. LS-Dyna's users extended to a wide range of automotive 1st tier and steel suppliers, which included National and US steel. Additionally, Siempelkamp Pressen Systeme used LS-Dyna for hydroforming research and component development purposes.

- ***Autoform***

The software code Autoform uses the implicit time integration scheme and ws supplied by Autoform Engineering GmbH [149]. As Autoform used the implicit calculation

method, considerably faster calculation times were possible, as fewer time steps are calculated in analysis. Autoform, like Pam-Stamp™ and Optris, was originally developed for sheet metal forming. However, due to the growing requirements to develop software to simulate the tube and sheet hydroforming processes, additional Autoform modules were created specifically for the hydroforming market.

Whilst Autoform provided a "full process" simulation capability, the pre-bending simulation was a simplified analysis of the actual operation and was calculated using the approximation of a one-step analysis approach, as described later in this section [150]. Therefore, the results of the Autoform pre-bending analysis could lead to significant approximations and ultimately could influence the accuracy of the final hydroforming predictions. Whilst Autoform can be used for forming analysis was not developed for structural analysis. However, it was possible to use results of the forming analysis mapped into structural analysis model, using a neutral file format.

2.5.5 Reported use of FEA for Tube Hydroforming Process Simulation

- ***FEA of the Hydroforming Process***

In 1997 Fiat's research centre published results of a series of validation tests using Pam-Stamp™ software [151]. The tests were performed to study capabilities of the FEA codeto simulate tube and sheet hydroforming. Amongst the tests were basic hydraulic bulge tests of steel tube and sheet material, using simple die geometry. The simulation results presented showed excellent agreement with the experimental trials, although the examples were limited. The main results presented were the principal strain profiles of the test samples versus those predicted by the software. However, no details of the process conditions were provided. In addition to the experimental tests, example applications of the software for hydroformed components were also given, illustrating capability of the software to provide solutions to complex tube hydroforming conditions.

One of the examples illustrated was of a tube hydroformed Y-piece, requiring substantial axial end feed in combination with a controlled pressure cycle. The example showed that

despite the difficult component geometry, the software could be used to identify the optimal hydroforming processing conditions, thereby leading to a substantial reduction in the prototype development phase, when compared with practical trial and error methods.

Since the early reported use of FEA for the tube hydroforming process, an extensive number of technical publications have now been published detailing various aspects of the hydroforming process and FEA code capability. Many of the publications have been made after the commencement this thesis, which illustrated the level of international interest in tube hydroforming in the automotive industry. As a result of the dates of the publications, it is possible to speculate that a significant amount of this interest in tube hydroforming technology was due to the steel consortium project, ULSAB.

- ***FEA used in Hydroforming Research & Development***

As part of an American programme to develop a better understanding of the mechanics of the tube hydroforming process, the Auto/Steel partnership performed a series of hydroforming trials using different experimental hydroform die tools. The hydroforming trials were all simulated. One of the objectives was to identify the current state-of-the-art in terms of simulation capability of one of the preferred commercial software packages, used by the American automotive industry. The package used for the simulations of the trials was LS-DYNA. Some of the findings from the programme were published at the SAE International Congress and Exposition in 1998.

In one of the studies, experimental trials were performed using a die with a rectangular expansion at its centre [152]. The remainder of the tooling was tubular. The objective of the study was to establish whether or not the empirical FLC would provide a suitable failure criterion for tube hydroforming. This would enable the simulation software to predict the splitting of tube blanks being hydroformed into components. However, despite the results of the trials illustrating that the FLC would be suitable only one tube material, with a single diameter and thickness was evaluated. The tube material was a draw quality, hot rolled steel, manufactured into 50.8mm x 1.89mm tube. The change in perimeter between tube and rectangular tool would develop a 37.0% expansion. The

simulation utilised the tube parent properties only, ignoring the weld-line, and hydroforming was performed assuming a global friction coefficient of 0.1 for all of the simulations, although the lubricant used in the experimental trials was not detailed or documented to have any relationship from any friction tests or studies. No direct correlation was made between the experimental trials and the simulations. Despite this, the simulations identified that a rapid localised of strain would take place at the logarithmic thickness strain, $-\varepsilon_t = n$ (strain hardening exponent). The simulations, like the experimental trials using this type of die geometry, illustrated that the predominant forming modes for this form of tube hydroforming would be somewhere between plain strain and a drawing deformation, dependent upon the degree of axial end feed.

In the published results of the second study [153], comparisons between experimental trials and simulations were made. The tube material used in the study was of the same grade. However, the die tooling possessed a circular expansion at the component centre, instead of a rectangular expansion. An axial feed of 17mm (0.33D) was used at each tube end for the experimental trials and was replicated in the simulations. A pressure curve, achieving a maximum internal pressure of 400Bar was applied to the tube blanks, within a time period of 10 seconds. An identical pressure curve was adopted in the simulations. In the simulations, an attempt to model the weld-line was made. However, the results of the simulations were found to considerably over estimate the thickness strain magnitude in elements adjacent the weld-line, with the model predicting failure. In the absence of the weld-line, the simulation results predicted a similar thickness distribution (using a friction coefficient of 0.05) to that of the experimental tests. In general the experimental thickness strains were found to be moderately less (approx. 0.1mm) than those predicted by the LS-DYNA simulations.

In addition to the correlation between experimental data & simulation that were performed, results of parametric simulations were used to study the influence of tube blank length and friction coefficient. The results indicated that as the tube length decreased an increase in negative minor strain would take place, i.e. the material in the expansion region would be subjected to less thinning.

In June 2000, Nippon Steel Corporation's research laboratories conducted experiments and Pam-Stamp™ simulations of T-piece tube hydroforming in an attempt to identify key the characteristics of the forming process [154]. The study involved examining the influence of metal anisotropy and its interaction with the process. Additionally, the influence of thickness and strength were also studied but not reported. To evaluate the forming performance, hydroforming indexes were used as benchmarks. The two benchmarks used to evaluate the T-piece were T (or branch) height and expansion ratio. Both of these were calculated at the point at which the material was considered to reach a critical thinning value (0.2). From a performance perspective, this thinning level may be judged as suitable. However, no uniform elongation or n-value was provided with which to judge if this would be a suitable limit for all metals, as increasing thickness and n-value increase the allowable thickness strain (thinning) before failure. The expansion ratio was simply the ratio of T height to initial diameter at the critical thinning value. The results of the simulations indicated that an optimal orientation of anisotropy for T-piece hydroforming could be achieved if the tube was to have the highest r-value oriented in line with the tube's longitudinal axis. Whilst, the anisotropy parameters didn't match those found in typical mild strip steels, the simulations provided information which could have been used to develop new strip steel products or to assist with development of new tube manufacturing techniques to allow the hydroforming process to benefit from the sheet orientation used.

In comparing the experimental results with the simulations, good correlation was obtained between the strain and thickness profiles presented for both strength of steel tubes studied.

In June 2000 Usinor Research and Development also published results of hydroforming research aimed at identifying a failure criterion for FEA and a means of characterising tube performance [155]. The research study made use of a research hydroform tool, which caused expansion of tube material to cause failure by splitting/necking. No details of the tool geometry were given. However, the hydroforming tool had the capability to modify strain mode by utilising different levels of controlled axial end feed of the tube. In

the study, tubes of the same diameter but with different wall thickness' were tested. The results of the practical tests indicated that the expansion capability of the tubes was significantly influenced by tube D/t ratio, despite the limited range of tubes tested. This implication suggests that the tube manufacturing process would influence the degree of formability of the tube metal. For the smaller tube (D/t ratio of 13.4) a lower expansion level was achieved. The paper claimed that the expansion of the smaller D/t ratio tube could be more closely approximated by the tube instability limit. For the larger D/t ratios (42.2) the expansions achieved closely replicated Cayssail's FLC. This illustrated that Cayssail's FLC may not make a suitable failure criterion in FEA of the tube hydroforming process. The authors suggest that some of the discrepancy between FLC and experimental results were due to the use of longitudinal properties and not the more usual transverse properties used to define Cayssail's numerical FLC. However, it is unlikely that the direction of test properties used had such a significant difference as displayed between FLC and the experimental results that were presented. Nevertheless, the FEA performed to simulate the experimental tests was found to correlate well in terms of strain distribution around the tube circumference, in particular when the weld characteristics of the tube were integrated into the model, unlike the results from the Auto/Steel partnership.

- ***Application of FEA to Full Component Simulation***

In 1999 Volkswagen AG presented results of hydroforming simulation [156], used as an aid in component development and process optimisation of a number of suspension components. The hydroformed components were from the rear axle of the VW 4motion Golf and Audi TT roadster vehicle models. Pam-Stamp™ was used for the simulating the process of each tube hydroformed part. A number of complex tube hydroforming operations, were illustrated. Analysis of the hydroforming process for the bush bearing of the rear axle component was also presented. Forming of the rear axle incorporated pre-bending, pre-forming and hydroforming. Additionally, a further operation that was conducted in the hydroform press was the production of the shoulder for bush bearings. The forming of the bush bearing was complex and involved locally bulging the tube outward, on one side, followed by inverting the tube back on itself until it came into

contact with the other side by using an integral punch. The simulation replicated the physical forming bush bearing operation accurately. Results of the material optimisation to produce the track control arm were also presented. Two different diameters (30mm and 34mm) were examined, each at two different thickness', 2.0mm and 2.3mm, respectively. The steel tube material studied was hot rolled mild steel. Despite full process simulation being presented, explicit full details of the pre-bending operation were not provided. However, Darlington et al [157], demonstrated that Pam-Stamp™ could be used to model the pre-bending process and how it could be used to optimise the process in terms of internal mandrel positioning.

Budd company, a major tier one supplier in the US, published details of how they used Pam-Stamp™ software to optimise process and develop tooling for tube hydroforming a frame rail component [158]. The numerical simulations provided a virtual die try-out of the tooling, material and processing conditions, which would have otherwise been costly in terms of time and money. It was also recognised that, in the absence of simulation, fewer tooling alternatives would have been examined in prototyping, potentially inhibiting an optimal solution from being found. Through implementation of the software, various pre-form shapes were reviewed to provide an optimal starting point for the hydroforming process. The optimal pre-form geometry was latter successfully used in the prototype phase. This example clearly illustrates that FEA is an enabling technology for the successful implementation of tube hydroforming.

- ***FEA, Tube Hydroforming into Performance***

Recent developments in the use of FEA for the tube hydroforming have illustrated that it is necessary to have a better understanding of the process to be achieve accurate process simulations. Furthermore, only when suitably accurate solutions of the hydroforming process are achieved can the forming analysis be reliably carried forward into the performance crash or fatigue performance analysis of the component / assembly. From a collaborative project between Ove Arup & Partners and Tower Automotive, it was unveiled that the inclusion of the forming analysis had a very strong influence upon the crash analysis results for a side frame rail component [159]. The influence of the forming

characteristics played a significant role in modifying the predicted mode of crash failure. Without the full effect of forming, a mixed mode of failure was observed. The modes included bending and crushing, although the bending mode was far more dominant. However, in the analysis incorporating the forming effects, the more efficient crushing mode was observed, with little or no bending. This clearly illustrates that not only is the forming analysis important, from a feasibility viewpoint but also from a passive safety and structural performance perspective. However, limited confidence in tube hydroforming process simulations has meant that this form of component evaluation is rarely utilised, thereby inhibiting more widespread deployment of tube hydroforming technology.

2.5.6 New Trends and Developments in Hydroformed Component Analysis

- ***One-Step Solvers***

The number of commercially available one-step solvers has dramatically increased over the last few years. The one-step solvers provided an excellent opportunity to deliver an engineering statement of component feasibility very rapidly, with forming analysis calculations typically taking a few minutes compared with several hours using explicit FEA codes. Therefore, one-step codes have developed as valuable tool in the design process, initially for steel or aluminium pressed part feasibility. The use of one-step codes removed much of the approximations used to evaluate a component's design.

One-step solvers simplify the pressing process by only considering the initial and final part states. Any steps in between these states are neglected in the calculations. Therefore, the simplification, minimises the calculation of the process to just one step and utilises the implicit time integration scheme for this. Although different one-step methods may be used, the traditional one-step approach is the inverse method. This method considers the final, deformed component (3D) geometry, as the starting reference point of the analysis. The 3D component geometry is meshed, and this mesh is projected into a flat 2D plane. The 2D mesh approximately resembles the physical blank shape required to stamp the component geometry. The one-step solver is therefore an efficient codes to simplify the

forming operation, whilst incorporating the material's strain hardening curve, anisotropy and failure criteria. The outputs predicted by one-step analysis include: material thinning, thickness, forming severity (proximity to FLC and likelihood of wrinkling) and effective stresses and strains.

Part of the simplification of the calculation is that contact and friction are usually not considered in the algorithm, although a simplification of frictional effects may be superimposed. This is likely to change in the future, through incorporation of increased levels of input detail with FEA code refinement.

Application of One-Step for Tube Hydroforming Process Simulation

Although historically one-step solvers have been introduced to speed up the process of die design and component feasibility for sheet pressing, they have been utilised very little in the analysis of hydroformed component feasibility and significant code development has been required to enable this. In 1998 Karima et. al [160], demonstrated the capability of FTi's one-step solver to perform one-step analysis of the pre-bending process and various other simplistic component shapes. Although the components were rather small, the analysis was performed to illustrate that simple analysis, including an examination of the influence of end feed could be calculated.

However, the accuracy of one-step analyses to date has been limited, particularly as there has not been any inclusion of friction behaviour. Despite the inaccuracies, due to limited data input, trends could be identified using the one-step analysis method

More recently, one-step solvers were tested to evaluate multiple stage forming, such as pre-bending, pre-forming and hydroforming. The code N-Step™ was presented by Hora et al. [161] who claimed that it was possible to analyse multiple stage, tube hydroforming process operations.

- ***Planning Tools and Knowledge Based Engineering***

A number of engineering design aids or tools have emerged that will change the way in which tube hydroformed components are designed and developed. Hora et al [161] described how, dedicated planning tools, rapid one-step solvers and specific control algorithms to automatically adjust process parameters, in addition to incremental analysis, will provide a complete package which may enable optimal component development and production of future hydroformed components.

In November 1999 the Design Team at Corus Automotive Engineering unveiled ICAD, the Knowledge Based Engineering (KBE) system, which was developed as a design aid for tube hydroforming [67]. The KBE system, feeds and filters information between CAD (computer aided design) & CAE (computer aided engineering) to optimise component geometry, based upon a set of input engineering design rules, which consider both manufacturing guidelines and material data. The aim of the hydroforming KBE system is to provide a statement of manufacturing feasibility for hydroformed components within a very small time-scale. Manufacturing feasibility is governed by section analysis, which evaluates section elongation along an entire component and properties, such as bending and torsional stiffness, aspect ratio and skew. The component sections can therefore be modified accordingly or a different tube diameter reviewed, for example. The KBE system also provided indicators of pre-bend feasibility, driven by guidelines and estimated bend radii, initial tube diameter and wall thickness from the CAD model.

It is claimed that KBE can deliver details of tube diameter, length, estimates of forming and piercing pressures and an initial estimate of the hydroform press capacity require to manufacture the component, all within one hour of importing the component CAD data. Under conventional circumstances, this would have taken more than 8 hours [162].

By performing this early evaluation of the component design, modifications can easily be filtered back through to CAD, which in turn can be used to update the component CAE performance analysis. Importantly, it can also be used to focus the one-step and incremental hydroforming analysis, providing a more feasible and optimal component

solution in a considerably shorter period of time, thereby reducing component risk and cost.

2.6 Review of Literature Summary

Whilst tube hydroforming technology received significant levels of interest from vehicle manufacturers and suppliers alike, due to its proven and potential benefits, the process had major areas which still required significant research and development. These major areas of research, included forming processes, joining technologies & joint designs and component performance, which were necessary to enable greater levels of implementation of tube hydroforming technology for the B-I-W. In order that a better understanding could be achieved in all areas, an improved knowledge of the fundamental material forming behaviour during the hydroforming process needed to be established. Developing an improved knowledge of the tube hydroforming process was a key aspiration of this thesis.

The changes in mechanical properties to strip steel due resulting from tube manufacture are unknown for many steel products. Consequently, the principal means of evaluating failure, the forming limit (FLC), also becomes an unknown. This fact is further exacerbated by the potential influence of a complex array of forming operations, such as pre-bending, that may be required to produce a automotive tube hydroformed component.

To enable greater levels of tube hydroforming technology deployment in the automotive industry, significant levels of development in the commercially available FE codes were identified as pre-requisite to enable accurate forming. These key aspects are essential, as greater levels of reliance are placed upon FE simulation techniques as an aid in establishing shelf-engineered, design and manufacturing solutions for different automotive technologies.

Consequently, this explains the reason for the large number of recent tube hydroforming FE publications, which have not conclusively illustrated the capability to predict the tube

hydroforming process under a wide variety of forming conditions or indeed a wide range of steel grades. The reason for the discrepancies between experimental results and the simulations may have related to the process assumptions, the techniques or material descriptions used. The differences may also have been due to the lack of actual tube hydroforming process data or limitations with the FE codes themselves. To achieve more reliable tube hydroforming FE process models, accurate information with regard to tube material, friction behaviour and the material forming limit need to be determined, in conjunction with actual process parameters. By doing so, this will help to identify FE code and other limitations and assist in it's development.

2.7 Conclusions from Review of Literature

1. A very limited knowledge base exists on the influence of ERW tube manufacture upon strip steel products, including material properties, surface characteristics and consequently a limited knowledge base exists for tube hydroforming behaviour of many steel tube products.

2. An of area of significant importance, requiring further research for tube hydroforming, was identified as the determination of a suitable failure criterion for predicting necking or splitting steel tube during the hydroforming process.

3. Finite Element Analysis (FEA) has been highlighted as an important tool for the design and development of tube hydroformed components but requires exploration to identify limitations of its capability to predict the behaviour of a wide range of steel tube products under different hydroforming process conditions.

3.0 Definition of Research Project

The following Engineering Doctorate Research Project, in conjunction with 26 weeks of taught courses, commenced during October 1996. The following sections, 3.1 and 3.2 outline the project descriptor and provided the basis for the literature review and an outline background as to why the project work undertaken.

3.1 General Project Objective

The general project objective was to examine the behaviour of sheet steel under tube hydroforming conditions and to determine the influence of the initial properties upon the process. Within the scope of the project, a model to predict the hydroforming process was to be developed. Before such a model could be achieved a number of key areas, highlighted in the literature review, required research to build toward the process model. By developing this understanding of the tube hydroforming process, the forming limitations could be identified and potentially overcome by product design, process development or through improved strip steel products or tube manufacturing processes.

3.2 Project Description

The project was commenced to develop an improved understanding of the tube hydroforming process, which due to many manufacturing limitations, has not been implementation for the production of structural B-I-W components.

To achieve the project objective several aims were identified from the literature review and are presented in section 3.3.

3.3 Project Aims

Coil and Tube Material Characterisation

General Aim: *To establish the basic material dimensions and formability parameters necessary to identify the influence of tube manufacture and to provide robust data for the development of an accurate mathematical model of the process and input for FEA.*

Material Dimensions

Aim: *To identify the current ERW tube manufacturing capability to supply tube blanks of accurate and consistent dimensions for tube hydroforming.*

Coil & Tube Mechanical Property Data

Aim: *To determine the key intrinsic material parameters from simple small-scale tests, in accordance with industry norms and best practices.*

Experimental & Analytical Forming Limit Curves and Alternative Failure Criteria

Aim: *To experimentally determine the forming limit curve for each steel grade studied and to verify selected analytical forming limit curve models, including the development of new models, which may be utilised for the evaluation of a hydroformed component design and process conditions.*

Surface Texture

Aim: *To determine the physical surface characteristics of the strip steels and steel tube materials used in the project to identify any changes from coil to tube, which may highlight potential surface texture or and or lubricant developments required for tube blanks for hydroforming.*

Small Scale Evaluation of Dry Film lubricants using MSD tests

Aim: *To identify the influence of various dry film lubricants on forming behaviour and potential suitability for tube hydroforming.*

Experimental Tube Hydroforming Trials

Aim: *To determine the key material parameters which influence the tube hydroforming process and to validate the analytical and FE models developed*

FEA of the Tube Hydroforming Process

Aim: *To establish the state-of-the-art in FEA capabilities in order to identify guidelines for improving tube hydroforming process modeling.*

4.0 Material and Experimental Procedure

4.1 Material

Three conventional strip steels grades were selected in the research project, in addition to a forming grade of stainless steel. All of the tube material for the research project was produced via traditional, continuous, high volume production methods. The conventional strip steels were produced by British Steel Strip Products and manufactured into tube at UK tube mills. The stainless steel material was obtained from an Avesta owned tube mill. The steels were selected on the basis of their current use for many automotive applications and to provide a wide cross section of behavioural characteristics during tube hydroforming. The tube materials studied in this research programme were:

- Cold-rolled mild steel (FeP04) ERW tube (70mm diameter, 1.2mm wall thickness)
- Hot-rolled mild steel (FeP10) ERW tube (70mm diameter, 2.1mm wall thickness)
- Hot-rolled HSLA (XF300) ERW tube (70mm diameter, 2.1mm wall thickness)
- Stainless Steel (grade 304) TIG welded tube (70mm diameter, 1.5mm wall thickness)

The FeP04 and 304 stainless steel tube materials studied were of D/t ratios that could be utilised for some B-I-W applications. These materials were representative of steel tube which could be utilised for potential future hydroforming B-I-W applications.

The hot rolled mild steel and HSLA steel tube materials were representative of materials currently used for sub-frame and chassis hydroformed components.

During the course of the research programme, a significant level of difficulty was encountered in attempting to obtain suitable quality tube material. This fact was made more complex with the added requirement of coil / sheet material from the same parent coil as the tube. This difficulty was partly attributed to the UK availability of suitable automotive steel grades having tube dimensions representative of B-I-W structural components.

A European Coal and Steel Community (ECSC) research project, studying the performance of tube hydroforms, ran concurrently with this thesis. Consequently, a suitable quantity of one material used for the ECSC project was available for this thesis, namely the FeP04 tube and parent coil. Subsequently, the availability of this material influenced the hydroforming tool design and selection of the other materials. The acquisition of this material for this thesis was achieved through close liaison with the research staff at the Welsh Technology Centre, who had responsibility for the direct acquisition of the coil and tube material from the tube mill. For the hot rolled ERW tube, acquisition of this material was made through close co-operation with the quality manager of Phoenix Steel Tube, Ray Barrow. Due to Phoenix Steel Tube's monthly tube rolling schedules for the XF300 steel grade, arrangements were set to obtain this material (coil and tube for characterisation) in February 2000.

A suitable hot rolled mild steel coil, for comparison with the hot rolled HSLA material, was obtained internally through BSSP links with the Midlands based BSD (British Steel Distribution) centres. The coil required slitting prior to dispatch to the tube mill. Through careful arrangement, between the distribution centre and Phoenix Steel Tube, the coil was dispatched for rolling alongside the 70 x 2.1mm (RMS 229) Opel Vectra engine cradle tubing. The arrangement with Phoenix Steel Tube was made all the more difficult, as this plant was due for closure during May 2000, with the majority of the tube mill equipment being transferred to other Tyco Tube Mills in the UK, namely Newmann-Tipper Tubes and Tyco's Oldbury plant.

To obtain sufficient samples of the slit coil material, corresponding to the hot rolled steel tubes, it was necessary to visit the tube mills during the tube production runs. This was difficult to time as a result of the continually changing tube rolling schedules.

- **Hot Rolled Mild Steel (FeP10)**

The hot rolled mild steel was selected for comparison with the HSLA steel in terms of tube hydroforming behaviour. The slit coil of the hot rolled mild steel was a small edge slit weighing approximately 2.2tonnes and its parent coil was processed at British Steel's

Port Talbot works and subsequently delivered to BSD Wombourne for slitting. The slit coil was then transported to the Phoenix Steel Tube mill, Oldbury, West Midlands. Coil samples were obtained from the middle of the slit coil only, ensuring sufficient metal for strip characterisation tests but also ensuring sufficient coil was available for tube production for the hydroforming trials. The sample of slit coil metal was obtained by stopping the tube mill during production and shearing a series of 3m lengths from the slit coil. The coil was then rejoined, using the MIG welding unit, and the tube mill restarted. The stopping, followed by restarting of the tube mill incurred tube scrap losses as a result of poor welding quality. Therefore, to stop more than once during this production would have significantly reduced the number of "good" quality tube lengths produced for the experimental hydroforming trials. Following rough cutting on-line, the tube material was collected and stored ready for cutting to length. The tube material was then cut to length, de-burred, bundled and dispatched to the WTC, following receipt of payment.

- **High Strength Low Alloy Steel (HSLA)**

As with the hot rolled mild steel, the HSLA steel tube was manufactured from a slit coil. In this instance, the coil was produced at British Steel's Llanwern works. The samples that were used in the investigations were performed on the single slit coil only and not the parent coil. From a 20tonne HSLA coil, a 2.5tonne slit coil was processed at BSD Wombourne, for subsequent tube production at Phoenix Steel Tube mill, Oldbury West Midlands. Due the increased coil size a greater quantity of tube could be produced, and therefore samples from the coil front (nose), middle (mid-coil) and back (tail) were obtained. Again, as with the hot rolled mild steel, obtaining samples was achieved by stopping the tube mill during production and shearing the necessary samples from the slit coil, before rejoining the coil, using the MIG welding unit, and restarting the tube mill. As in the case of the Hot rolled mild steel (FeP10) tube, the HSLA tube was rough cut on-line during tube production and subsequently collected and stored ready for cutting to length. The tube material was then cut to length, de-burred, bundled and dispatched to the WTC, following receipt of payment.

The Phoenix Steel Tube mill that was utilised to process the FeP10 and HSLA slit coils into tube was run at an average line speed of 200m/min.

- **Cold Rolled Mild Steel FePO4**

For the FeP04 grade steel, random samples were taken from a full width coil blank for analysis. The blank was one of 75 cut to a length of 2.5m from the front end of a 12.5tonne coil. The blank cutting and coil slitting was performed at the British Steel Distribution Centre (BSD) Wednesfield site. For tube making, the remaining coil was slit into 5 individual coils, each having a width of 218mm. No samples were obtained from the individual slit coils prior to rolling of the tube, only from the original full width blanks. The 5 slit coils were transported from BSD Wednesfield to the Glynwed, Newman-Tipper Tubes mill at Wednesbury, West Midlands for tube production. The tubes in this instance were processed at an average line speed of 120m/min.

Supplementary to the samples that were taken at random from the coil, additional samples were taken from the rolling (longitudinal) direction and the coil rolling transverse direction at designated intervals across the entire 1227.5mm blank width. These samples would serve to illustrate the variation in the parent coil properties and thickness before processing into tube metal and therefore potential variation in properties and thickness.

The hot rolled tube materials rolled at Phoenix Steel Tube were subject to Eddy current tests, performed in accordance with BS 3889 Pt 2a. The FeP04 tube was not subjected to Eddy current testing. Instead mechanical test techniques were utilised to evaluate weld-quality. No welding quality issues were found manufacturing the FeP04 mild steel tube, at what was above the conventional / normal tube product D/t range available at UK tube mills.

- **Stainless Steel 304(1.4301)**

It was not possible to obtain the parent coil material matching stainless steel 304 tube. However, the tube material was put through a normalising heat treatment which could

have annihilated the effects of tube manufacture, in terms of mechanical properties. Therefore, obtaining the parent coil was of considerably less importance than the conventional low carbon steels. The stainless steel tube was obtained from the Avesta Sandvick tube mill.

4.2 Determination of Original Coil Properties & Characteristics

For each of the steels that were studied, it was important to perform full characterisation of the parent coil material, including verifying the original thickness, establishing the tensile mechanical properties & chemistry, and quantifying the original surface texture.

The significance of determining the material characteristics was that any potential changes in material behaviour, due to the tube manufacturing process, could be determined. This could ultimately provide information on how the material would b expected to behave during the tube hydroforming process. More importantly it may be used to devise improved strip steel products and or tube manufacturing processes. The coil material data could also be used to highlight the potential short falls and risks associated in FEA simulation of the tube hydroforming process when assuming sheet data to represent tube data.

4.2.1 Verification of Coil Thickness

The original coil thickness is of major importance in the tube hydroforming process as component strain is achieved by loading or stressing the tube blank, unlike sheet metal pressings, which are strained resulting in stresses. Therefore, physical coil thickness and its uniformity can have a considerable influence upon the final component quality. If the in-going coil thickness variation was high this could lead to a greater number of tube hydroform component rejections. Obtaining information on the original coil thickness also aids in determining the process effects of tube manufacture. For each coil metal studied, thickness measurements were performed to determine coil variation across the full or slit coil width. To measure the thickness of the coil a flat nosed digital Mituyo digital micrometer (accuracy +/- 0.001mm) was used. For the FeP10 and HSLA slit coils,

three measurements were made at marked intervals to calculate the average thickness cross coil (measured averages and standard deviations are presented in the results).

The selected measurement points of the slit coil materials corresponded with the location around the circumference of the tube, with reference to the weld-line. For the HSLA steel, three coil samples from the front, middle and back positions were measured. For the FeP10 steel only the middle coil sample was measured and for the FeP04 grade of steel, thickness distributions were determined across the entire blank / coil width for two separate 2.5m length blanks.

4.2.2 Chemical Composition

For each of the steels studied, the chemical analysis was established by taking samples of the steels and sending these for analysis at Port Talbot Works BOS plant laboratories. The steel samples that were supplied to the plant laboratory consisted of a $25mm^2$ section and nibblings of each of the steels. For the HSLA steel, chemical analysis was performed on samples taken from the front, middle (mid) and back of coil positions, in addition to the 'ladle analysis' that was performed during steel production. This enabled an evaluation of the consistency of the chemistry through the coil and subsequent tube product.

4.2.3 Tensile Properties

To determine the original intrinsic mechanical properties of each steels studied in this thesis, standard tensile testing in accordance with BSEN 1002: Part1:1990 was performed. By adopting a standard tensile test, the mechanical properties of the sheet coil metals studied were assessed against known standards or typical values. Additionally, a standard tensile test would provide data on potential variability in the parent or original slit coil metal and set a base-line to study any changes that may occur due to tube manufacture. To determine the coil tensile mechanical properties, tensile tests on 80mm gauge-length tensile test-pieces were performed to determine the stress-strain relationship. To establish the planar anisotropy of each metal, rectangular coupons for

test-piece machining were therefore obtained from the 0°, 45° and 90° directions of each steel coil material.

The 80mm gauge-length test-pieces were machined by the Welsh Technology Centre's Workshop from 240mmx 40mm rectangular coupons that were supplied. tensile test-pieces were then tested to failure using WTC's Zwick 1474 tensile testing machine.

For the FeP10 and HSLA steels, longitudinal coupons were sectioned from across the entire width of each slit coil and for the FeP04 steel, across the entire coil width. For the longitudinal direction a minimum of two repeat tests were performed and three where sufficient sample material allowed.

As mentioned previously, tensile tests were also performed for the 45° and transverse (90°) directions. For the 45° orientation, only three repeat tests were performed, which ensured that the planar anisotropy of the steel was determined, without excessive wastage of the slit coil material. For an ERW tube blank, the longitudinal direction is the same as the rolling direction of the sheet coil. The 45° direction is also of less significance for tube hydroforming of such metal, compared with the stress-strain characteristics for the 0° and 90° directions. This is because the 0° and 90° directions are those which may coincide with the major strain direction, during bending and hydroforming of the ERW tube, respectively.

For the FeP10 and HSLA slit coil materials, a minimum of 10 repeat tensile tests were performed for the 90° direction. As the width of the slit coil was only 218mm, the shoulders of the transverse tensile test-pieces were significantly reduced from the 240mm standard length, thereby having a reduced clamping area. However, it was ensured that the shoulder radius and gauge-length geometry were unaffected during machining and that no slippage took place during testing. Therefore, the 90° tensile test results for the slit coil materials remained unaffected.

After each sample had been accurately machined to size, the original width and thickness of the thickness length were measured. The average measurements were then entered into the Zwick machine's tensile test programme. The cross-head speed of the Zwick tensile test machine was pre-set to deliver a strain rate of 0.001/sec up to an elongation range covering the 0.2% proof / yield stress. This was necessary to ensure that sufficient data was captured to accurately determine the proof stress/yield value. From the 0.2% proof / yield stress range up to fracture of the test-piece, a nominal strain rate of 0.01/sec was employed. During the tensile test, the load, extension, thickness and width were continuously recorded by the Zwick facility. From this data the programme determined the yield or 0.2% proof stress, the uniform and total elongation values, and the plastic strain ratio and strain-hardening exponent, at pre-designated elongation values. The strain-hardening exponent was calculated for the elongation ranges of 5-10%, 10-15% and 10-20%. The strain hardening exponent values were calculated from the slope of the log true stress versus log true strain data at the designated elongation ranges. The plastic strain ratio values were calculated automatically by the Zwick machine for elongation values of 5, 10, 15 and 20%. The test-piece width measurement ceased when the tensile strength was reached during the test as the r-values determined would become invalid.

4.2.4 Surface Texture

Surface texture analysis was performed using digital Tallyscan apparatus at the WTC. The analyses were performed on both coil and tube materials to quantify the surface texture parameters and to determine if any changes in texture had taken place as a result of tube manufacture. The data obtained was from 2D and 3D surface measurements. In the case of the coil blanks, the upper and lower surfaces were measured, with the lower surface of the FeP04 Coil relating to the outer surface of the tube and the upper surface to the internal surface of the tube. In the case of the FeP10 and HSLA steels, the outer most surface of the coil represented the outermost surface of the tube.

4.2.5 Forming Limit Curves

- ***Determination of Experimental Forming Limit Curves (FLCs)***

A modified Erichsen cupping test, employing the Nakazima strip method [163], was used to determine the forming limit curve of each of the original steel coil materials. The test method involved pressing a number of steel strips with varying width (28mm-110mm) to failure, using a hemispherical punch, see schematic in Figure 26. The strips were clamped in position between two die plates, each 165mm in diameter. The die plates incorporated a single 5mm draw-bead in the lower (blank-holder) die plate. The test was used to establish the forming limit curve for the coil transverse direction to correlate with the major strain direction during tube hydroforming.

Strip Preparation

Each strip was guillotined to a length of 165mm, and a selected width. The strip edges were then deburred using a hand deburring tool. For the narrow (28mm-40mm) FeP10 and HSLA strips, the edges were ground smooth to prevent edge cracking at high strains, due to sheared edge effects. Strain levels from the FLC test which were limited by the influence of edge effects would not be representative of a component. The deburred, strips were subsequently cleaned thoroughly and degreased using acetone prior to electrochemically etching. The purpose of applying the circle grid using an electrochemical etching technique, prior to pressing, was to enable measurement of the surface strains after testing, in order to determine the FLC. The nominal diameter of the grid circles in their initial, non-deformed state was 2.35mm, although these were measured prior to testing for improve accuracy.

FLC test

A 50mm diameter tool steel punch was used in the FLC tests, which was set at a constant travel speed of 1mm/s following application of the blank-holder load. In order to ensure appropriate material restraint during pressing, the upper and lower die plates were clamped together, under a constant hydraulic blank-holder load, the die plates also integrated a full draw bead ring. The tooling arrangement used to determine the FLCs from the sheet steels is illustrated in Figure 26.

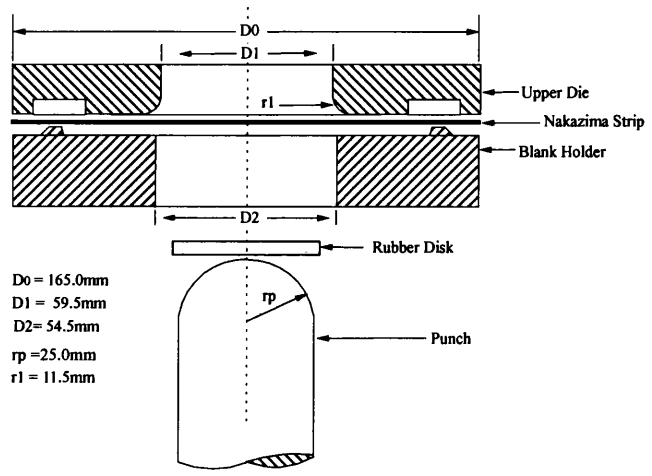

Figure 26: Schematic illustration of tooling used for FLC test

The blank-holder load, in conjunction with the draw-bead, provided a suitable degree of material restraint, thereby preventing movement / draw of the flange material. For the FeP04 steel, a blank-holder load of 110kN was used. For the FeP10 and HSLA steels a blank-holder load of 125kN was used, allowing for the increase in material hickness and strength.

For all of the strips tested, 30mm diameter disks of natural white rubber (grade 295C) were positioned between the steel punch and steel strips, to provide lubrication. The rubber disks were used to promote fracture at the pole / top of the deformed strip, instead of at the strip side-walls, tangential to the punch nose. No additional lubrication was incorporated in any of the FLC tests.

Circle Strain Analysis

The technique used to determine the forming limit curve was performed in accordance with BSSP's operating procedure [164] which was based upon a closest circle approach method, using visual discrimination of the deformed circles. The circles selected for measurement were those that were not fractured or necked but were just outside of the necked zone. The circle strain analysis was performed in accordance with BSSP

operating procedure [165]. A Microvision 2000 camera system, fitted with an optical lens was used to determine the original grid circle and deformed grid circle diameters. The diameter of each of the deformed circles on the tested strips and tensile test-pieces were measured. On obtaining the measurements of the deformed circles, Figure 27, the engineering major (e_1) and minor (e_2) strains were calculated according to equation 30:

$$e_{1,2}\,(\%) = 100 \times (d_{1,2}-d_0) / d_0 \qquad \text{Equation 30}$$

In equation 29, d_0 represents the initial diameter and $d_{1,2}$ was the final diameter with respect to the major and minor orientations that were measured. The major strain during the tests was perpendicular to the width of the Nakazima strip and the minor strain was parallel to the width. The strains were calculated and the FLC data plotted on a forming limit diagram, FLD. From the test data, separate best-fit curves were derived for the left-hand and right-hand side of the FLC. For the left-hand side R^2 values of 0.963, 0.97 and 0.989 were obtained for the FeP04, FeP10 and HSLA data, respectively. For the right-hand side curves the correlation was poorer with R^2 values of 0.901, 0.965 and 0.941 for the FeP04, FeP10 and HSLA data, respectively.

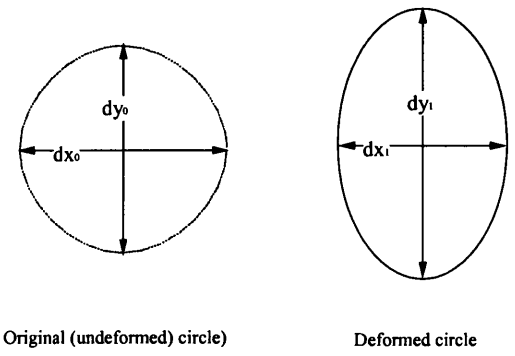

Figure 27: Schematic illustration of circle strain analysis

To supplement the Nakazima strips tested and analysed using the above method, pre-gridded tensile test-pieces were also tested to failure and analysed.

- ***Analytical Forming Limits Curves (FLCs)***

Whilst the experimental method described provided a means of determining the forming limit of the coil materials it did not provide an indication of the limiting strain available to the tube materials for hydroforming. It was therefore necessary to evaluate a range of analytical forming limit curves, including empirical and theoretical curves. The experimental coil FLCs would provide a means of assessing the capability of the analytical FLC models to predict necking for the tube hydroforming process.

In 1978 Sauer et al [166] proposed a that the FLC could be determined from the following theoretical expression:

$$\varepsilon_e = [\, 2n \,.\, \sqrt{(1 - \alpha_n + \alpha_n^2)} / (1+\alpha_n) \,] - \varepsilon_0 \qquad \text{Equation 31}$$

In the above expression ε_e is the effective strain, α_n is the stress ratio at the point of necking, and ε_0 is the pre-strain. By solving the expression for the principal strains, the FLC can be determined. This analytical model also allows the incorporation of pre-strains, which potentially enables the incorporate of tube manufacturing or pre-bending influences. The initial limitation of this failure criterion was that the pre-strains could either be complex or unknown and that a constant stress ratio in the tube material may not be developed during hydroforming. The Sauer FLC model was calculated based upon the intrinsic material properties, determined from the tensile tests.

The FLC model examined by Bleck et al [167] was the Swift-Hill model. In this model, the FLC was considered to compose of two curves joined at the plane strain intercept. For the left-hand side of the FLC the major and minor strains could be determined from the equations (1) & (2) respectively:

$$\varepsilon_1 = n\,[(1+ (1 - \alpha)r) / (1+ \alpha)] \qquad \text{Equation 32}$$

$$\varepsilon_2 = n\,[(\alpha - (1 - \alpha)r) / (1+ \alpha)] \qquad \text{Equation 33}$$

The Swift-Hill model incorporated anisotropy into the FLC model in the form of the material's r-value. However, unlike the Sauer model it did not incorporate 2n only n. Therefore, the Swift-Hill model in this form would be anticipated to only predict diffuse necking and not local necking and consequently would not provide sufficient accuracy. In 2000 Asnafi [168] proposed the following theoretical expression to determine the forming limit curve. Unlike the two previous models, the Asnafi model incorporated the strain ratio, not the stress ratio. Asnafi claimed that by using the major strain at fracture, the FLC could be determined from the following equation:

$$\varepsilon_1 = 2n\,[4/3\,.\,(1 + \beta + \beta^2)]^{-1/2} \qquad \text{Equation 34}$$

In the above expression β represents the strain ratio. In addition to these theoretical approaches to determine the FLC, the empirical model described in section 2.3 was also determined for each coil and tube material. The n-value used in all of the analytical models that were considered was the terminal n-value, n_t, i.e. the true strain equivalent to the steel's uniform elongation value.

In order to distinguish the accuracy of the analytical FLC models, test data was generated for comparative purposes. The test data included data obtained from gridded tensile test-pieces and Nakazima strips tested to failure. The strains measured were different from those used to generate the FLC for each steel sheet material. Under these circumstances the difference was in the selection / visual discrimination of the deformed circles. To be able to evaluate the capability of the FLCs, their ability to delineate between 'safe' strain and 'necked' strain was important. The visual reference by which this data was selected is schematically illustrated in Figure 28. The safe circles that were measured from the tensile test-pieces or Nakazima strips were usually one grid circle away from the local neck or at least one coil thickness away from the neck. This method provided a simple means of verifying the analytical coil FLC models but also the analytical tube FLC's with the tube hydroforming strain data from the experimental trials.

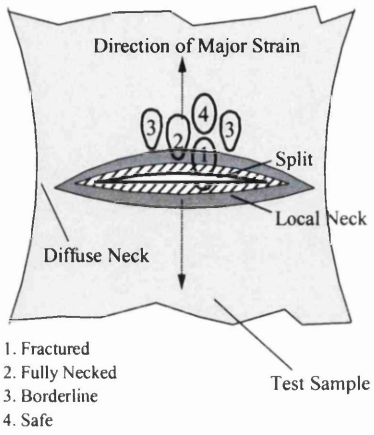

Figure 28: Visual discrimination used to delineate between necked and safe strains

4.3 Determination of Tube Properties & Tube Manufacturing Effects

4.3.1 Introduction

A number of mechanical quality tests were performed on the steel tubes studied during the research project. These included the previously mentioned tube flattening and end flaring tests, in addition to the mandatory thickness and diameter checks. The hot rolled and stainless steel tube used during the research project was of a quality necessary to meet automotive hydroforming requirements. The FeP04 tube was a non-standard tube and had no current application and was rolled specifically for the ECSC tube hydroforming research project.

4.3.2 Verification of Tube Dimensions

For each tube metal, both the thickness and diameter were measured around the tube circumference at 15° intervals from the weld line, (Figure 29), using a ball micrometer and Vernier thickness, respectively. In each instance three separate samples of each tube material were measured. The samples were sectioned from the 6m tube lengths obtained from the tube mill during rolling. Three repeat measurements were made on the samples, which were sectioned at intervals of 3m. This would also provide an indication of the

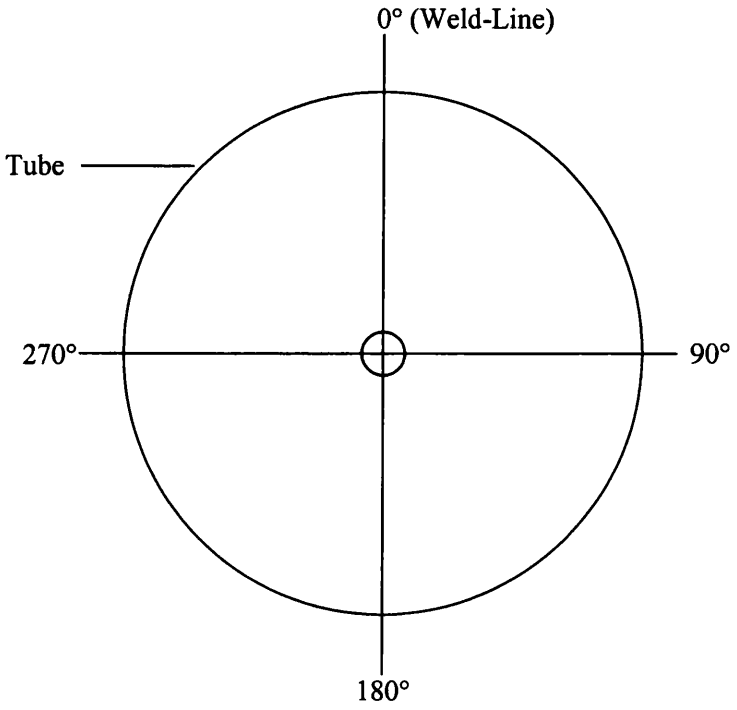

Figure 29: Convention used for samples measurements of tube material sections.

potential variation expected between tube blanks. (Average and SD quoted for tube thickness measurements).

4.3.3 Chemical Composition

For each steel tube material obtained with coil metal, the chemical analyses were performed on the coil metal. However, in the case of the stainless steel metal, chemical analysis was performed on samples taken from tube material as no coil material was obtained.

4.3.4 Tensile Properties

- ***80mm Gauge Length Tensile Tests***

For the tube material, longitudinal (0°) tensile tests were performed on coupons sectioned from three specific locations around the tube, namely from 90°, 180° and 270° positions from the tube weld-line (0°), refer to Figure 29. The aims of the 80mm gauge length tube tensile tests were to establish an accurate description of each steel tube's average stress-strain characteristics, in order to establish tube manufacturing influences and for material data input into the Finite Element simulations and the analytical FLC models.

- ***10mm Gauge Length Tensile Tests***

In addition to the 80mm thickness length tensile tests, miniature tensile test-pieces having a 10mm gauge length were tested from coupons cut at 15° intervals from around the tube circumference, with respect to the weld-line (0°). These tests would establish the variation in properties of the tube material and would identify any localised tube manufacturing effects. The mini-tensile tests were conducted on the FeP04, HSLA and Stainless steel tubes only. The cross-head speed of the Z010 test facility was set to 6.5mm/min, which delivered a strain rate of 0.01/sec.

- ***Weld Property Determination***

To establish the weld properties of the tube materials, the use of miniature tensile testing was also employed. The 5mm nominal width of the miniature test-pieces meant that within the test-piece width, both parent and weld metal were present. Therefore, the test properties could only be representative of 5mm of the actual tube material, displaying a combined or composite weld and parent material behaviour. This fact needed consideration when incorporating the results data into the tube hydroforming FE models. The miniature tensile tests were performed in triplicate and the results reported are the average of the three tests.

4.3.5 Analytical Forming Limits Curves (FLCs)

As for the coil materials, analytical tube FLCs were generated for tube material studied. For the tube materials, the FLC models were based upon mechanical property data

obtained from the longitudinal tensile tests. The n-value used in the FLC models was the terminal n-value n_t to ensure consistency between coil and tube material. As with analytical coil FLCs, test data from obtained from tube tensile test-pieces on safe and necked strains was used for the evaluation of the FLC models.

4.4 Small Scale Evaluation of Lubricants on Forming

4.4.1 Introduction

In order to establish the relative performance of the lubricants to be used in the tube hydroforming trials, a simple (small-scale) sheet metal cupping test, called the modified stretch-draw test was utilised. The cupping test would provide detailed information of the effects on percentage draw, fracture height and the influence upon strain distribution. This test could therefore provide indications of how a lubricant would most likely perform under tube hydroforming conditions, illustrating the degree of restraint upon tube end-feed, strain distribution and influence of strain path and FLD process signature. The test would not indicate the influences of the tube material properties or influences from the interaction with the lubricant when tube hydroforming.

4.4.2 Procedure

The MSD test was developed at the Welsh Technology Centre to evaluate the effect of surface interactions on forming behaviour. Historically, the use of this test has included evaluation of lubricants, zinc coated steels, tool surface treatments and has been used for comparing the performance of low cost tooling [169] for sheet metal forming. The MSD test combined both stretching and a drawing deformation, the ratio of which is controlled through an applied clamping force from blank-holder die plates. The tooling comprises of a 50mm punch, with an upper forming die and a blank-holder, shown in Figure 30. A circular sheet blank was used in this test, having a 117mm diameter. After blanking out the circular samples, they were de-burred, degreased and thoroughly cleaned. During the test the circular sample was placed centrally on the blank-holder. The blank-holder was then raised up to the sample, whilst the upper die remained fixed, clamping the sample between both die plates under a designated clamping load. For a set of samples the blank-holder load is increased from 10kN upwards until no or very little sign of draw was

observed. The percentage draw was determined from the final (average) diameter of the circular samples.

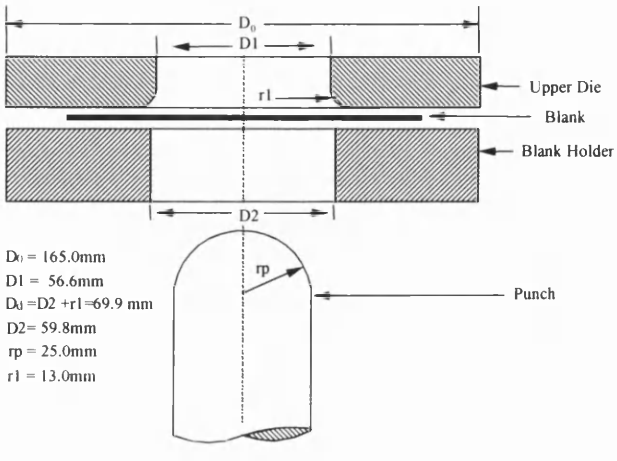

Figure 30: Schematic illustration of MSD (Modified Stretch-Draw) tooling

- ***Gridding***

Each clean MSD sample was electrochemically etched with a grid of 2.35mm diameter circles, as in the case of the Nakazima strips used for FLC determination. This was vital for determining the strain distribution measurements of the deformed samples following testing. Measurements to determine the strain distribution were performed for each material and lubricant combination, for the samples subjected to blank-holder loads in the range of 60-82kN. This method was different to that used by Cartwright [169], who measured the strain distributions of samples that displayed 10% draw.

- ***Application of lubricant***

Three dry film lubricants were used in the MSD tests, in addition to an unlubricated 'control' condition. Application of the lubricant involved fully coating both sides of the circular samples. The Molykote (321R) Mo_2S dry film lubricant was applied to the blanks using a spray canister. The spray lubricant was applied ensuring a liberal coverage, whilst attempting to achieve a coating that was as uniform as possible. The spayed sample was then allowed to dry for 30mins. A similar method was adopted for the samples lubricated

using the Molykote PTFE spray coating, although it was much more difficult to judge the uniformity of the coating due to its transparent nature. The Hydrodraw lubricant on the other hand was applied by means of a sponge. In this case only two coats were applied, with intervals of 5mins to allow the lubricant to dry between coats.

For each combination of lubricant and material, a minimum of eight MSD samples were tested to illustrate the performance under different blank-holder regimes. Sets of samples of each steel grade were tested unlubricated as a 'control'.

4.5 Experimental Tube Hydroforming Trials

4.5.1 Background : Anton Bauer Hyprotec Hyron 1800 Press

The Anton Bauer high-pressure hydroform press facility, which was located at the Welsh Technology Centre, and used in the experimental tube hydroforming trials is shown in Figure 31.

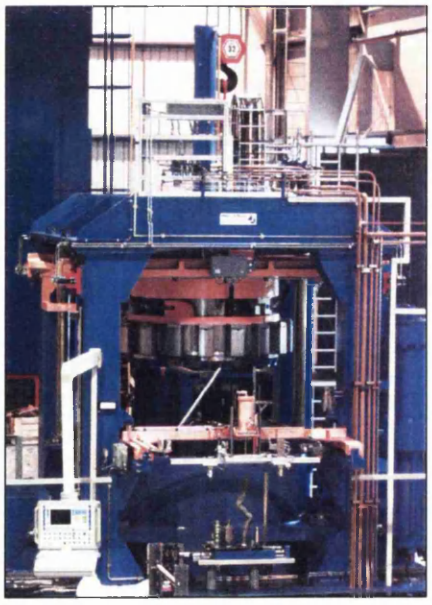

Figure 31: Anton Bauer - Hyprotec Hyron (1800) hydroform press.

The Anton Bauer high-pressure hydroform press facility in the Welsh Technology Centre (WTC) was commissioned at the end of July 1997. The installation, unlike hydraulic press derivatives, required no pit to be excavated, although reinforcement of the concrete floor was necessary to sustain its 35 tonne press. The Anton Bauer press was the first high-pressure tube hydroforming press installed in the United Kingdom, specifically for research purposes. The machine was capable of developing a maximum internal pressure of 4,100Bar, and delivering 2,500kN compressive force at each of the two axial rams.

Due to the unique mechanical locking mechanism, 88,000kN of locking force could be achieved. According to the Anton Bauer specification, the hydroform press could hydroform tubes having a diameter of up to 100mm and up to 4mm in wall thickness. The key limitation of the of the WTC hydroform press was the fact that the axial ram positioning was directly opposed, although this could be offset by 150mm if necessary.

Figure 32: Photograph illustrating lower die tooling configuration, including position of right hand docking head and tube end seal, inside of the hydroform press.

4.5.2 Hydroform Tool Change Over & Fitting

- ***Docking-Head Removal***

The fitting of the newly manufactured research die tool segments for this thesis required complete removal of the die-shoe pair from inside of the Anton Bauer press. Before the die-shoes could be removed the axial rams (docking heads) and tube end seals required removal from inside of the press, refer to Figure 32.

- ***Positioning and use of the Die Changeover Table***

Further to the docking head removal and to assist with die shoe removal from the press, a dedicated die changeover table was positioned at one side of the press by using the CTC's 35tonne crane, interlocking the table track on the change-over table and the tack on the press. The changeover table was secured to the press with locating pins. Before the die shoes could be removed, the upper die safety pin was removed, disconnecting the die shoe from the moving upper turret. Using the press control console, the press was closed and the two die shoes were coupled together, by inserting two I-sections connecting the upper and lower die shoes. The lower die was then remotely unlocked from the press base and lifted upwards.

The motorised changeover table was then positioned beneath the coupled die-shoes. The die-shoes were then slowly lowered onto the table and the moving table then retracted from inside of the press. Once the table was in the home position, safety-locking pins were used to secure the tables position and the I-sections were removed. The upper die shoe was then lifted off the lower die shoe and positioned onto suitable blocks before uncoupling the inner die tooling. The upper die tooling was then stripped of the unnecessary tooling, with the new tool segments being fitted into the relevant positions and fixed in place by bolts and steel dowel pins. The lower die shoe was also lowered from the changeover table o the suitable blocks. The die tooling could be accessed without uncoupling it from the die shoe. The die shoe was then stripped of the unnecessary dies and the lower segment blocks were positioned and bolted into the lower die base plate. Two drilled bars were positioned and bolted into the base plate, either side of the lower die segments, in order to locate and fix the side tools. The side tools were

appropriately positioned and keyed in to place with steel dowel pins and then bolted. When the die shoes were back in position, a safety bolt was inserted, coupling the die set upper and die shoe to upper turret.

Refitting of the docking heads, before the trials were commenced, was the reverse of the removal operation.

4.5.3 Tube Hydroforming Process Trials

Initial Trials

Initial trials were performed to evaluate the behaviour of the tube blanks in the hydroform die tools, die tool set-up and to determine suitable machine process settings. However, a number issues were discovered with the segmented tooling configuration, in addition to the requirement for a suitable high performance lubricant to achieve the goals set out in the programme.

Main Trials

An upper limit of 1000Bar was set for the main hydroforming trials, due to issues with the tooling witness lines at pressures exceeding this. To study the effects that particular feed rates had on the component strain profiles and strain paths, linear displacement-pressure gradients were utilised. This also simplified the processing conditions for the FEA modelling and correlation between FEA models and experimental results.

Three principal axial end feed rates were used in the main tube hydroforming trials. These were 0.2mm/s (or 0.04mm/Bar), 0.625mm/s (or 0.0125mm/Bar) and 1.25mm/s (or 0.025mm/Bar), i.e. a feed rate that would achieve 4mm, 12.5mm and 25mm tube end displacement (respectively) on achieving the maximum pressure of 1000Bar. A pressure gradient of 50Bar/s was maintained throughout the hydroforming trials. For all of the main trials, only Hydrodraw 625 was used as a lubricant.

For each end feed rate, the influence of increasing internal pressure was studied by hydroforming separate steel tubes (for each grade) using 100Bar increments.

Subsequently, the necessary circle strain analysis and corner radius measurements were performed on the tubes, hydroformed to different pressures for each respective end-feed.

4.5.4 Design & Manufacture of Tailored Welded Tube (TWT)

Based upon the available materials and the CTC laser welding facility, a TWT was designed which would serve to illustrate a means of optimising tube blank forming characteristics and also to investigate FE analysis capability to simulate TWT configurations. The TWT would also serve to illustrate the engineering capabilities and multi-material opportunities available to material suppliers and OEMs.

- ***TWT Design***

Based upon the high level of thinning experienced by the conventional steel tube during the initial experimental hydroforming trials and the strong contrast in behaviour between the FeP04 and stainless steel 304, it was that a symmetric three-piece TWT, having a stainless steel centre-piece, would be manufactured. The component was designed to produce a TWT configuration that would utilise the FeP04 tube at both ends of the stainless steel tube.

The hydroforming process was tailored to the TWT configuration. The laser-butt weld regions of the TWT were selected to be in 'non-critical' locations before and after the tube hydroforming process, i.e. they would not enter the expansion region, refer to Figure 33.

The selection of the butt weld position and process design was due to the fact that at low feed rates the conventional FeP04 steel tubes were prone to splitting in the expansion zone. However, in strong contrast, the stainless steel tube did not.

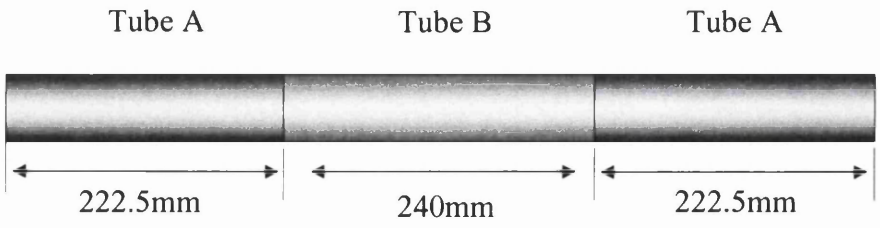

Figure 33: Schematic illustration of Tailored Welded Tube (TWT) configuration studied (Tube A = FeP04 70x1.2mm and Tube B = Stainless Steel 304 70x1.5mm)

- ***Manufacture of TWT (FeP04:SS(304):FeP04)***

A three-piece TWT was successfully manufactured using a rotary manipulator in conjunction with the 5kW $C0_2$ Laser Ecosse laser welding facility at the CTC. The TWT assembly was prepared, according to dimensions given in Figure 33. IN the manufacture of the TWT, initially two tubes of the three-piece assembly were jigged together, i.e. one FeP04 tube with a stainless 304 tube. The two tubes were subsequently laser butt-welded

The laser welding was achieved by fixing the position of the laser welding head and rotating the tube assembly in the rotary manipulator. The other FeP04 tube was then jigged to the welded pair and welded in the same manner to produce the final desired TWT configuration (Figure 34). During welding, an approximate laser power of 3.8kW was developed at the work-piece, using a focal length of 250mm and 25Lpm of helium shielding gas. The speed of the rotary manipulator that was used was 15rpm, achieving an equivalent linear laser welding speed of 3.2m/min. In each instance, the laser welds were examined visually using a microscope camera to ensure defect free welds. Figure 34 shows the component tube sub-assembly, TWT and the hydroformed TWT.

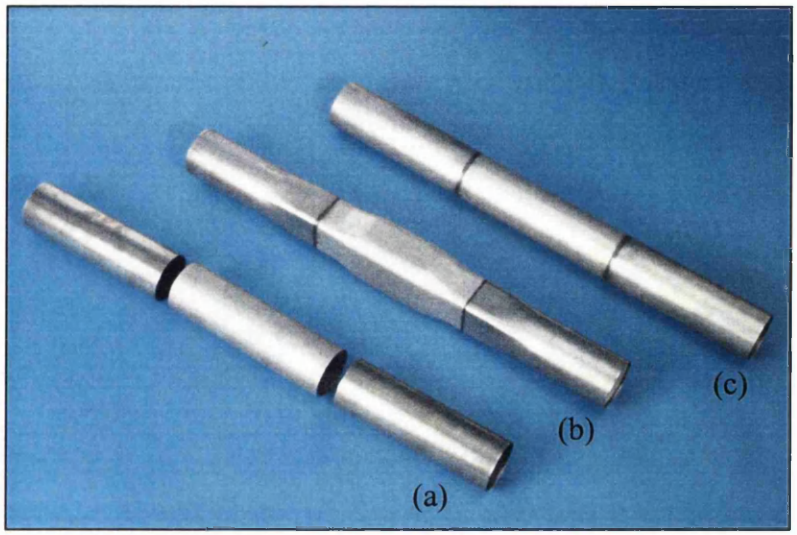

Figure 34: Photograph of FeP04 (70x1.5mm) : SS 304 (70x1.5mm) : FeP04 (70x1.2mm) Tailored Welded Tube (TWT) (a) sub-assembly, (b) Hydroformed TWT (c) TWT

4.5.5 Tube Preparation

Each tube required thorough cleaning to remove the dirt & oil from the tube mill and tube saw cutting swarf that production tubes possessed. The cleaning involved thorough degreasing of the tubes, inside and out. Further to this, examination of the tubes was performed to avoid any using any tubes with undesirable cut end conditions or dents, due to transportation. Dimensional checks were also performed to ensure that the tubes met the required specifications, in terms of allowable length and diameter and thickness.

After cleaning, the tubes were electrochemical etched with the same circle grid used for the sheet Nakazima, tensile test-pieces and MSD samples. After gridding the tubes that were not lubricated using the PTFE or Hydrodraw 625 dry film lubricants, the tubes were coated lightly with mill oil, to prevent corrosion.

The tubes lubricated with dry film coatings were positioned on end. The PTFE spray was applied as with the MSD samples and allowed to go off for at least 30 minutes. Sponge application of the dry film lubricant, Hydrodraw 625, was also used for tubes. Two

coatings were applied, the second applied 10 minutes after the first. A minimum of 20 minutes was allowed to elapse before hydroforming the tubes, to ensure that the Hydrodraw lubricant had dried sufficiently, thereby ensuring satisfactory performance.

4.5.6 Circle Strain Analysis

Circle strain analysis (CSA) was performed as described in section 4.25 and circles conforming to either safe, borderline and necked data, Figure 28, were measured to establish suitable FLD data. This in turn was used to evaluate the analytical tube FLC models. Strain profiles were measured along the length of the tubes to determine the effects of the hydroforming processing conditions. The strain profiles were measured (end-to-end) across both the 70mm and 80mm faces, LA and LB respectively. In the case of the profiles that were made across 70mm faces, the face measured did not possess the weld line. Further to these, strain profiles were obtained from the centre of the expansion zone of the tube hydroforms, at section A-A. Details of sections LA, LB and A-A are illustrated in section 5.9, FE Model Verification.

4.5.7 Corner Radius Measurement

Supplementary to the CSA, corner radius measurements were performed at section A-A on the Hydrodraw 625 lubricated SS 304 hydroforms. These hydroforms were selected as these tubes were free from wrinkling, or necking/splitting defects for the entire range of processing conditions studied, and would therefore provide more suitable samples for accurate corner radius measurement. The corner radii were measured using a standard set of radius gauges, for corner radii of between 5mm and 13.5mm. For radii between 13.5mm and 35mm machined radius gauges, supplied by WTC's workshop were used. Each corner radius was measured in triplicate and an average calculated to compare with the FEA model data.

5.0 FEA of the Tube Hydroforming Process

5.1 Introduction

As mentioned, the use of commercial FEA codes has increased significantly in the automotive industry to reduce lead-time to manufacture and ultimately lead-time to market. However, only within the last four years have significant developments been made for the simulations of tube hydroformed components. Until only very recently, between 1998 and 2000, a limited number of commercially available codes were capable of full process tube hydroforming simulation, including pre-bending, pre-forming and hydroforming. The though process capability was not available during the ULSAB programme and simplified models of the hydroforming process were used instead. Vehicle manufacturers, Tier one, material and contracted hydroform press/tooling suppliers were still developing their full process simulation capability, with many of them illustrating the state-of-art at the 'International Conference on Hydroforming', Fellbach, Germany in October 1999.

FEA may be used in the concept of a new component design, by means of feasibility studies, but also for component development and optimisation. Examples of component optimisation may include forming analysis to determine thickness reduction potential, which may involve examining the potential of changing a steel grade from a lower strength to a higher strength grade, or analysis of a component with modified geometry to improve performance. FEA may also be used for optimisation and include studies to review: the tube blank geometry, i.e. length, thickness and in particular starting diameter, the grade of material, friction and lubrication effects, pre-bending geometry, pre-forming sequences and hydroforming process characteristics.

In conducting the FEA of the tube hydroforming trials in the programme of research in this Thesis, the dedicated commercial forming simulation code Pam-stamp^{TM} was used. The selection of Pam-stamp^{TM} was made on the basis that the code was globally accepted by the automotive industry and was dedicated for metal forming simulation. Therefore,

the results of the FEA would be of benefit to and have credibility within the automotive industry.

5.2 Input Variables

The code Pam-stamp™ is capable of solving non-linear dynamic problems using an explicit time integration scheme and allows the complete field of measurable variables, relevant to tube hydroforming process, to be incorporated into the forming simulation. The software package is highly menu driven and therefore the input parameters of the tube hydroforming process such as: friction & contact, internal pressure, die tool movements, application of axial force or end feed and the intrinsic metal properties, to be easily input and modelled.

The experimental hydroforming trials were devised such that a simple FE model of the process could easily be developed. In the experimental trials, the tube hydroforming process consisted of tool closure, followed by a hydroforming stage using specified process parameters. These stages were replicated in the Fe models. The generation and development of the full set of FE models, is described in the following sections.

5.3 Model Generation

The first stage in modeling the experimental tube hydroforming trials was the creation of a 3D surface representation of the working surfaces of the hydroforming die tooling and the tube blanks. The surfaces of the hydroform tool segments were created using the commercial pre processor and mesh generator package Hypermesh®. The decision to use Hypermesh® to generate the model surfaces was made on the basis that the die tool surface geometry was simplistic and did not require the use of a dedicated CAD package.

The tooling geometry consisted of three principal sections, with transitions between each of these sections. The principal sections of the tool geometry included: two 70mm diameter (tube guide regions); a 70mm x 80mm rectangular expansion zone, located at the centre of the tool segments; and two 60mm x 60mm box sections, located either side of the expansion zone. To produce the surface geometry of the tools, simple line

geometry was created for these sections. For the straight sections the Hypermesh® 'drag line' command [170] was used to produce continuous sections of the required length. For the transitional sections the command 'spline' was used. This produced the surface connection between the straight sections. Through these manipulations of these commands, all of the die surfaces of the component were generated. The tool surface geometry that was developed in Hypermesh® is shown in Figure 35.

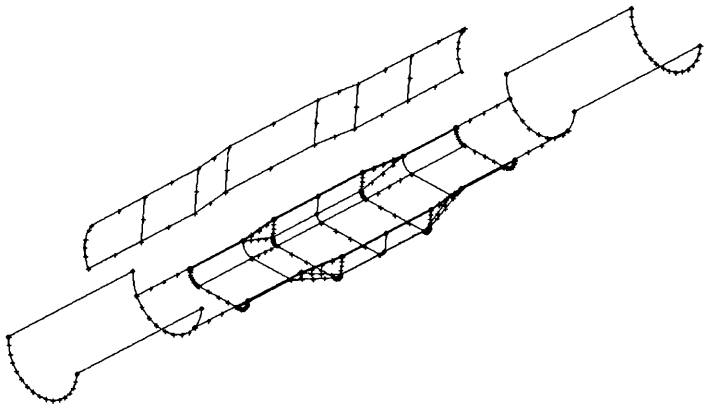

Figure 35: Hydroform die tool 'working' surfaces for side and lower tool sets.

- ***Tool Surface Mesh***

The tooling surfaces generated were meshed with a distribution of elements that was selected on the basis of providing a good representation of the tool geometry, particularly for the component corner radii, whilst maintaining element quality. Great care was taken in selecting the number of elements for individual sections of the tool surfaces in order that simple connection between adjacent meshed surfaces was possible. The majority of elements used for the tooling were quadrilateral, accompanied by a small number of triangular elements, where appropriate, which was necessary to avoid large distortions of the quadrilateral elements. Otherwise these would adversely affect the accuracy and stability of the resultant calculations. After the surfaces were meshed, the individual surface meshes required connection between surfaces for each of the tools created. In connecting the surface meshes, the unconnected edges of the surface meshes of the tools

were highlighted. The edges were deleted and connection between adjacent nodes was made using the 'equivalence node' command.

As the tooling was axisymmetric, it was only necessary to create one quarter of the upper/lower tool, and one half of the side tool. These were then reflected about their planes of symmetry, to create a full set of meshed surfaces for the upper, lower and side tools. The number of elements generated for the full side tool and full lower/upper tool was 500 and 2634, respectively. Therefore the total elements used in to the full FE model were 6268.

- ***Tube Blank Mesh***

Once the hydroform tooling geometry was fully meshed, the surface and then the elements representing the tube blank were generated. Unlike the tool meshes, the mesh for the different tube materials were generated on the mid-thickness surface of the tube (Figure 36).

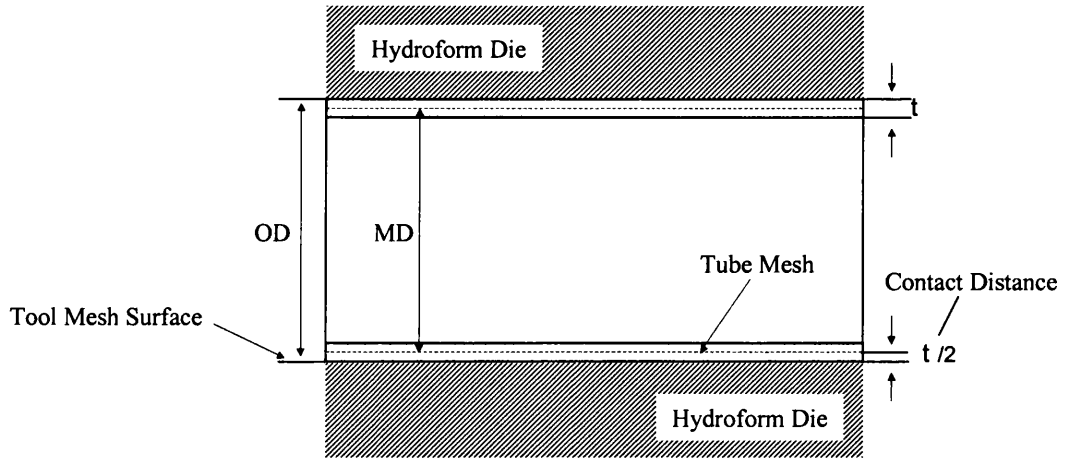

Key : -
Average Tube Outside Diameter = OD
Tube Mesh Diameter = MD = OD - t
Average Tube Thickness = t

Figure 36: Schematic illustration of tube blank and hydroform die tool FE meshes

Therefore, for each tube with a different thickness, a circle having the tube outside diameter, less the tube wall thickness was created. In the case of the austenitic stainless steel and the HR mild steel tube metal a uniform tube mesh was developed, with the weld-lines being ignored. However, for the cold rolled (FeP04) mild steel and the HSLA steel, the tube mesh geometry was developed to incorporate the weld properties as determined from practical tests. The properties to be incorporated were from 5mm width, miniature tensile test results. Therefore, the weld zone was considered to be 5mm wide with the remaining metal belonging to the parent metal.

After creating a circle around a reference point, the line of the circle for one edge of the tube was then generated into the tube surface by using the 'drag line' command. The distance the circle was dragged was the nominal tube length used in the experimental hydroforming trials, i.e. 685mm.

Once the surface was generated, the number to elements represent the tube blank mesh was defined. The tube surface was discretised into quadrilateral elements, 3mm wide by 5mm long. The width of elements in the tube blank mesh element aligned with the tube circumference and the 5mm spacing aligned with along the tube length. This ensured that the elements were as square as possible, whilst achieving reasonable computation times as the element number and size was not too large or too small, respectively. The number of elements used to represent the models having tube blanks that did not incorporate welds was 9590. For the models with tube blanks integrating a weld-line, 10001 elements were used to represent the blank parent material, whilst 685 were used to represent the weld-line.

The completed hydroform tooling and tube blank meshes were exported in a format compatible with the Pam-Stamp™ pre processor Generis ™. The total number of elements used for the models having tube blanks incorporating and not incorporating the tube weld-line are 16269 and 15858, respectively. The file export format from Hypermesh® that was used was Nastran. The meshed hydroform tool surfaces and tube blank (incorporating weld-line) are shown in Figure 37.

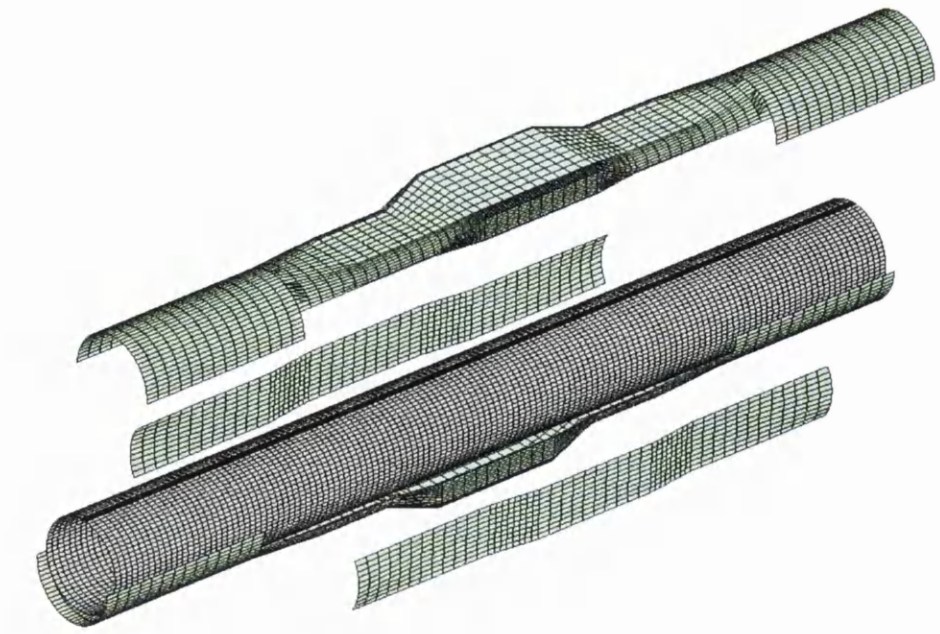

Figure 37: Tube* and hydroforming tooling meshes used in FE models (*weld integrated)

5.4 Pre-Processing

5.4.1 Importing Mesh File of Hydroform Tooling and Tube Blank

- ***Positioning of Tube Blank and Tooling***

The Nastran export file, containing the hydroform tool and tube blank meshes, was imported into Pam-stamp ™ - Generis ™. In order to perform the necessary simulations, the tools and tube blank were firstly oriented to align the component axis favourably and also to position the tools in the open position, with the tube blank located on the surface of the lower die tool. The tube was created so that it was parallel to the z-axis, the upper and lower tooling would move in the y-axis and the side tools would move in the x-axis. In order to position the tube and tool meshes appropriately, the side tools were displaced 5.5mm in the x-axis, outwards from their closed (home) position. In practice, the side tools were at distance of 7.5mm away from the closed position. The reason for the reduction in distance outward from home was purely to reduce calculation times, related to the side tools travelling in free space, before contact with the tube blank. The tube blank itself required a translation of +5mm in the y-axis to place it correctly on the

bottom of the lower die surface and the upper tool mesh required a translation of +10mm in the y-axis to avoid direct contact or penetration of the tube blank mesh. In practice, during die closure, the side tools were pushed over the lower die tool set, under the action of an array of large aluminium bronze wedge structures. This was closely followed by the closure and mating of the upper die set with the lower die set and side tools. These tool movements were replicated in the FEA models.

- ***Checking of Finite Element Meshes***

Before proceeding with assigning mechanical properties, boundary conditions and loads to the tube blank and tool meshes, the quality of the meshes were checked in Generis™ for skew, warping and aspect ratio. Additionally, the element normal orientations were examined. If the orientation of these were incorrect, then adjustment was made to ensure that they all faced in the correct direction. The normal orientations used were all outward, for the tube blank, and all inward toward the tube blank, for the hydroform tool surfaces. A number of element quality checks were performed in Hypermesh® prior to model mesh export. The checks that were made in Generis™ were necessary to ensure that the file had imported correctly. After completing the mesh checks, labels were assigned to each mesh to identify the tube blank, and each of the tools.

- ***Assigning Material Properties***

Once the meshes of the model had been positioned appropriately, checked and labelled, the material properties were assigned. For the tool meshes, the metal was considered to be rigid and was modelled using Pam-stamp™ material type 100 [174]. For the tube blank, an existing (elastic-plastic) material model, type 107, was used to describe the material behaviour [174]. The material model 107 provided the capability to incorporate anisotropy in addition to elastic-plastic behaviour in the forming analysis. In using material model 107, it was assumed that the tube material would behave according to Hill's 1948 yield criteria and that hardening would take place in an isotropic manner.

The material stress-strain data, used in the FEA models, based upon the small-scale tensile test results, is given in Table 1. To be able to recommend the most suitable material description for simulating the hydroforming process, different means of assigning the intrinsic material properties to the model were examined. In particular, the validity of utilising coil properties, the influence of different anisotropy models and the influence of selected strain hardening input were all investigated. The influence of the different material input descriptions is discussed later in section 5.5.

Material Grade & Form	**Orientation to rolling direction**	**Rel (MPa)**	**Rp 0.2% (MPa)**	**Rm (MPa)**	**K (MPa)**	**ε_0**	**'n_T'**	**'r3' (15%)**	**'r4' (20%)**	**Gauge (mm)**
FeP04 Coil	***0°***	-	171.6	319.2	***553.29***	***0.0046***	***0.218***		***1.96***	***1.186***
FeP04Coil	45°	-	182.3	329.0			0.215		***1.45***	1.189
FeP04 Coil	90°	-	174.7	312.0			0.205		***2.41***	1.179
FeP04 Tube	***0°***	-	***213.7***	***302.8***	***517.62***	***0.0145***	***0.209***	-	-	***1.185***
FeP04 Tube Weld	***0°***	-	***396.5***	***455.4***	***611.35***	***0.0061***	***0.085***	-	-	***1.185***
FeP10 Coil	***0°***	252.5	-	362.0	***608.07***	***0.0118***	***0.198***		***0.90***	***2.027***
FeP10 Coil	45°	250.8	-	352.0			0.190		***1.10***	2.022
FeP10 Coil	90°	262.7	-	354.4			0.193		***1.00***	2.022
FeP10 Tube	***0°***	-	295.8	366.0	***540.07***	***0.0087***	***0.127***	-	-	***2.045***
HSLA Coil	***0°***	361.1	-	438.6	***721.08***	***0.0238***	***0.185***	***0.62***		***2.087***
HSLA Coil	45°	379.1	-	434.7			0.190	***0.97***		2.093
HSLA Coil	90°	391.4	-	449.0			0.175	***0.79***		2.096
HSLA Tube	***0°***	-	372.0	444.8	***697.26***	***0.0187***	***0.158***	-	-	***2.157***
HSLA Tube Weld	***0°***	-	504.5	542.5	***651.7***	***0.0032 2***	***0.045***	-	-	***2.157***
SS-304 Tube (1.4301)	***0°***	-	273.1	614.9	***1243.78***	***0.0112***	***0.395***	-	-	***1.486***

Table 1: FEA tube hydroforming process model, thickness and Krupkowsky (Swift) parameters (indicated by bold italic).

For each of the different tube blank materials, the elastic modulus, Poisson's ratio, density, wall thickness, plastic stress-strain curve and anisotropy parameters were entered. The majority of these data were derived from the mechanical tensile tests performed in this research programme. The others were obtained from textbooks giving standard values. The elastic (Young's) Modulus, Poisson's ratio and steel density were assumed to be constant values of 210GPa [171], 0.3 [171] and 7850kg/m^3 [172], respectively. Other parameters were kept at default settings recommended by the code vendors. For the plastic stress-strain curve, the Krupkowsky formulation was applied. This formulation is an approximation to the true stress-true strain curve of actual test data. The principal reason for adopting this formulation is that it provides a plastic stress-strain curve beyond the value of uniform elongation. Whereas the actual test data, converted into true plastic stress-strain format, incorporates the curve drop with increasing strain, when the strain value has exceeded uniform elongation. This is unlike either the Holloman or Krupkowsky formulations, in which for a given strain increase there is a subsequent increase in stress. The Krupkowsky parameters used to describe the weld zones for the HSLA and FeP04 tube materials are also given in Table 1.

The tube hydroforming process models generated, all used the sheet material plastic strain ratios (or Lankford coefficients) to describe anisotropy for both the sheet and the tube. The influence of changing the anisotropy model description was also examined (section 4.7.5). The sheet anisotropy should also be relevant for the tube models, as the plastic strain ratio changes very little after 10-15 percent elongation during the tensile test. The difference between sheet and tube anisotropy at this magnitude of strain would be small and therefore the effect would be negligible.

All of the Krupkowsky input parameters for the tube materials studied, are given in Table 1 and are highlighted in bold-italic.

- ***Contact & Friction***

During, the development of the FE models for assessing the initial tool design schemes, only the penalty contact algorithms were available. However, this algorithm was found to

be deficient for tube hydroforming, due to mesh penetrations and an alternative contact algorithm used. The contact algorithm used to represent the experimental hydroforming process trials was the Lagrangian contact model, available in Pam-Stamp versions '98 onwards. The Lagrangian formulation was stated as superior to the Penalty algorithm, and therefore for certain forming applications, such as tube hydroforming, the accuracy of the analyses are improved [173]. The friction model available in the 1998 version of Pam-stamp™ was Coulomb's law, and the values of friction coefficient reviewed in this programme of research were 0.01 to 0.3, with the aim of identifying a suitable representation of a global friction coefficient value in practice.

- ***Application of Boundary Conditions***

The constraints to the movement and degrees of freedom applied to the tool meshes, for the tool closure (pre-forming) were as follows. For the lower tool mesh fully fixed conditions were applied for all rotations and translations. For the side tools, freedom to translate to achieve tool closure was permitted. All other translations and rotations were fixed. For the upper die tool, again only freedom in the direction of travel to achieve tool closure was permitted.

- ***Mesh Refinement***

Mesh refinement is an important attribute in achieving a high degree of FE model accuracy. For hydroforming simulation, mesh refinement has two main functions. Firstly, it improves the surface geometry representation of the formed component. Secondly, it improves the accuracy of the results, in terms of strain and thickness distributions. The refinement of the tube blank mesh was made through a division of the original selected quadrilateral elements into 4 equal, smaller quadrilateral elements. The selection of the tube blank to receive mesh refinement was performed by means of highlighting the entire tube mesh. The initiation of the adaptive meshing was controlled using a critical angle criterion. When a user defined or the default critical angle (7°) between two adjacent elements was reached, then each quad element divided into 4 new elements. For the tube hydroforming trials, the selective refinement "only" option was chosen. This meant that elements were refined only and not de-refined (made coarse). Figure 38 illustrates the

adaptive mesh refinement method used in Pam-Stamp^{TM}. Two levels of adaptive meshing were assigned to the tube mesh for the simulations, i.e. the mesh refinement process was selected to enable refinement of the mesh twice during the entire hydroforming process.

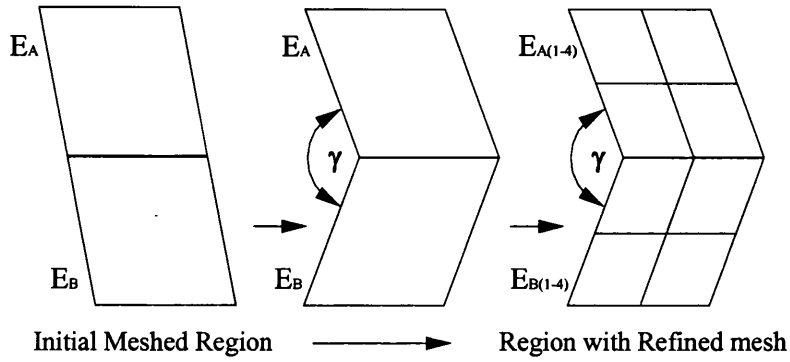

Figure 38: Schematic illustration of automatic mesh refinement at critical angle (γ)

- ***FEA of Pre form Process***

The FEA of the pre-forming process involved simulation of the closure of the hydroform tool meshes, with subsequent partial reshaping of the tube blank, as in the practice. To close the tool meshes prescribed velocity curves were applied to each of the side tool meshes and the upper tool mesh, whilst the lower tool mesh remained fixed, as found in practice. The velocity curve chosen was from the automatic set-up, but provided a realistic motion of the tools, having an acceleration phase as the tool began to move and a deceleration phase as the tool began to slow prior to stopping.

Suitable values of "cruise" tool velocity were calculated and assigned to the required tool meshes, namely the meshes for side and upper tools. The following equation was used to calculate the tool closure time for each tool and also to identify the beginning or start time for the hydroforming pressure cycle. As mentioned previously the action of the tools required complete closure of the side tooling, followed by closure of the upper tool, achieving full tool closure. The velocity curve that was applied to the upper tool mesh commenced at the completion time of the velocity curves of the side tool meshes, i.e.

when the side tool meshes came to rest in the closed position. The velocity curves for the side and upper tooling motion were calculated based upon equation 34 [174]:

$$v = (10/9) \,.\, (z/T) \qquad \text{Equation 34}$$

In this expression z = (tool or node) displacement (mm), T = total time (ms) and v = 'tool cruise velocity'.

The velocity curves prescribed to the tools required an orientation for their direction of travel. For the side tools, the direction of travel was in the x-axis, with a positive or negative scale factor being applied, dependent upon the specific direction necessary to obtain closure. The velocity curve applied to the upper tool was in the y-axis, with a scale factor of –1 to produce a downward closure of the tool. The velocity curves applied to the side tools and upper tool are shown in Figure 39.

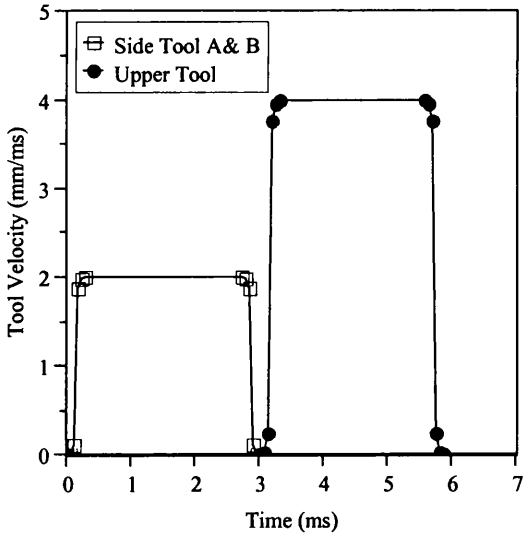

Figure 39: Velocity curves used in FE models for tool closure (pre-forming)

During closure of the tool meshes, the tube blank was firstly pre-formed under the action of the side tools. The pre-form was finally completed by closure of the upper die, which

pushed the tube into the die cavity, again modifying the tube geometry before hydroforming.

- ***Hydroform Process Parameters***

To model the hydroforming process in Pam-Stamp™ required the use of the fluid cell function, which was a unique facility, specifically developed to enable analysis of tube and sheet hydroforming processes

Fluid Cell

The fluid cell represented the internal fluid medium within the tube blank in the analyses performed. The volume of the fluid was defined by selection of the internal surface of complete tube blank mesh, which ensured that the entire tube was pressurized from the inside. The variation in internal fluid cell volume induces a pressure load on the elements of the fluid cell (tube blank). The pressure was a function of the fluid cell volume change, the bulk modulus of the artificial fluid medium and the fluid flow rate, which was given by the following equation [174]:

$$P_{i\,MAX} = K_B.(-d(V)/V + Qd(t)/V) \qquad \text{Equation 35}$$

Where K_B is the fluid bulk modulus, d(V) is the change in fluid volume, V is the current volume , Q is the fluid flow rate and $P_{i\,MAX}$ is the maximum internal pressure.

The internal fluid pressure, flow rate curves, together with the fluid bulk modulus were user defined in the Fluid Cell menu. The fluid volume and volume change were calculated by the code Pam-Stamp™.

The imposed flow rate in all of the FE models was set to ensure that the assigned pressure curve was always achieved. A linear pressure increase was used in all cases, ramping up to 1000 Bar to follow the simplified experimental process parameters. The pressure gradient was set at 50Bar /ms to deliver the same pressure gradient developed in the experimental trials. Therefore, the FE model would accelerate the process by a factor of

1000. The bulk modulus value used in the models was the value for water, 2.05GPa [175] and assumed constant in all analyses.

Axial (Tube) End Feed or Displacement

The analyses of the tube hydroforming process also involved prescribing an applied axial displacement or tube 'end feed' to each of the ends of the tube blank. To apply an axial displacement to the tube ends, the nodes at end of the tube meshes were grouped together. The group of nodes was then constrained to move in the direction of axial displacement, namely the z-axis. To specify an applied axial displacement a velocity curve, as used for the movement of the tool meshes, was applied to an individual node from the group of nodes. The velocity used in each case was determined from equation 35, based upon the completion time of the pressure cycle and the magnitude of the displacement required. The direction of displacement was controlled by specifying the orientation, i.e. +(z-axis) or –(z-axis).

5.5 Comparison of Material Input Methods

In establishing an accurate model of the hydroforming process for each tube material, specific assumptions were made, where necessary, with regard to the material input data. The key input parameters that describe a material's behaviour, which may be modified, and therefore may significantly influence the outcome of the FEA calculations, are:

- Material stress-strain curve description (controls strain-hardening and material flow)
- Anisotropy description (influences resistance to thinning)

- ***Influence of Material Strain-Hardening Description***

As a range of different forms of strain-hardening curves may be used to model the plastic behaviour of a tube and a recognised best approach method is necessary. The various input methods for Pam-Stamp™, including Krupkowsky, Hollomon and a table of data points [174], all based upon the tensile data.

Two different descriptions of the true stress-strain behaviour were examined in this thesis. The first description was the Krupkowsky (Swift) curve approximation. This curve was used to represent all of the low-carbon steel tubes and the approximations were judged to be reasonably accurate. Further, the material properties for each coil material was used in separate series of tube hydroforming models, with the aim of determining the affects of utilising material in a more formable condition, without the influence of tube manufacture. These simulations would also serve to illustrate the affects of assuming sheet properties during an early component design phase, in the absence of tube data or a suitable tube material database.

In the case of the SS 304 tube metal, the converted tensile test data was found deviate strongly from the Krupkowsky curve approximation. Therefore, it was deemed necessary to compare both material descriptions using the converted experimental tensile test data and the Krupkowsky curve fit method. The direct influence of the different material descriptions was observed and all remaining analyses were performed utilising the converted experimental tensile-test data.

- ***Influence of Metal Anisotropy***

In terms of examining the influence of material anisotropy, the FeP04 cold rolled steel tube possessed the greatest degree of planar and normal anisotropy. Therefore, this material was selected to numerically study of influence of tube material anisotropy. In the study, a comparison of assigning r-bar, compared with using Lankford coefficients for a series of different levels of axial end feed. Therefore these analyses were performed, to illustrate the influence that may be anticipated if the anisotropy were to vary within the steel coil or new tube blank making technology would allow a different orientations to its longitudinal axis.

The following anisotropy models were studied using the type 107 material model:

- Lankford Coefficients (plastic strain ratios)
- r-bar (average plastic strain ratio)

To illustrate the influence of selecting the most accurate material description to represent the forming behaviour during tube hydroforming, the above anisotropy models were examined under two different hydroforming conditions, namely equivalent tube end feed rates of 0.0125mm/Bar and 0.025mm/Bar.

5.6 Comparison of Friction Effects

- ***Influence of Friction Coefficient***

The influence of friction was studied by means of modifying a global Coulomb friction coefficient, which was applied to each individual friction pair, e.g.. Side Tool A and tube blank. The values of friction coefficient, used in the analyses of the main tube hydroforming trials, were between 0.01 and 0.15, where a n approximate value of 0.15 is conventionally used for simulations representing press-forming of sheet steel.

5.7 Tube Hydroforming Process Models

The aim of the tube hydroforming process models was to evaluate the influence of the material properties on the outcome of the hydroformed component in terms of developed strain and developed component corner radii to be able to make an assessment of the state-of-the-art in tube hydroforming simulation. The FE models developed illustrated the influence of processing conditions and could indicate the optimal forming conditions. As no process data acquisition software was available on Anton Bauer hydroform press, only screen traces, it was decided that the experimental process conditions would be displacement controlled, as opposed to force controlled. This would enable better matching of FE to the experimental tube hydroforming conditions, providing opportunity to generate more accurate correlation. Confirmation of the displacements was possible by measuring the final components, which would not be possible under a force controlled process regime.

5.8 Development of Tailored Welded Tube (TWT) Hydroform Models

A model of the Tailored Welded Tube (TWT) configuration was developed for the metal combination manufactured and described earlier in this thesis. The combination of

materials and tube thickness necessitated the development of a modelling technique, which would account for the step of the different wall thickness of the tube materials on the inside surface of the TWT. The decision as to where the butt weld-line would be positioned, with respect to the hydroform die cavity, was made on the basis of locating the welds in non-critical regions, to prevent failure in the butt weld. The model developed ignored the mechanical properties of all the tube welds. The reasoning behind this was, at the design stage it would be likely that little or no data would be available for the weld properties between the dissimilar tube materials and/or dissimilar thickness'. The TWT model developed was based upon the minimum material data that would be likely to be available at the early design phase of a component. This data included stress-strain data from the FeP04 and SS 304 tube models, coupled with assumed frictional conditions and the intended experimental processing conditions. This work content also provided the opportunity to simulate a complex component design using well defined material & process conditions prior to manufacture of the TWT and the experimental proving trails. This tube configuration also provided a strong statement of Pam-Stamp™'s capability to simulate complex component systems and tube configurations.

In the development of the TWT models, the selection of the method for modeling the joint between the tube materials was a key issue to resolve. For pressing simulations of tailored welded blanks (TWBs) using Pam-Stamp™, a wide range of methods to model the butt-weld joint. However, for tubular components these models used to represent the joint required investigation.

- ***Spot Weld and Rigid Body Models***

This method involved joining the adjacent tube blanks by means of spot welds [174], having a rigid link between the edge nodes of each tube blank mesh. The rigid bodies model assigned boundary conditions between the adjoining nodes of the adjacent tubes materials. These methods did not allow for the incorporation of weld properties. During the study these two methods of modelling the weld-line, in the absence of weld-properties, were examined but were found to not to be compatible with tube the hydroforming process model.

- ***Equivalenced Node Method***

An additional method for modelling the TWT was to use "equivalenced nodes", which could be used with or without incorporating the weld-line. In this method, the tube blank meshes were created so that the adjoining edge nodes of the two different tubes merge together at a local point and one of two options were available.

One "equivalenced node" method, used by Dry [176] for modelling of sheet laser tailored welded blanks (LWTBs), ensured that the blank meshes were aligned with the each sheet mid thickness on the same plane. The difference in thickness of the blanks was achieved by modifying the contact description, artificially accounting for this condition.

However, the thickness offset could translate into differences between modelled and measured strain and also differences between modelled and measured component radii, although these would be small. The equivalence method that was used for modelling the TWT hydroforms in this thesis allowed for a small sloping step between the tube blank meshes. The particular TWT configuration modelled in this Thesis had five zones in total. Three of these zones related to the parent tube materials. The remaining two zones represented the two steps belonging to the welds between the tubes. Figure 40 illustrates the FEA set-up for only one half of the full model TWT configuration, including a laser butt-weld region, (Zone 3) and the adjacent tube meshes, Zones 1 and 2. To ensure that the step was kept as small as possible, in addition to ensuring that the smallest element size did not fall below 1mm, the length of the step used was 5mm long. Within this 5mm length, the tube was discretised using 5 elements to represent this length. Additionally, the discretised region could be assigned appropriate laser weld properties. Although 5 elements were used to describe the length of Zone 3, the number of elements around the circumference of the tube was manipulated to match the other two zones, therefore ensuring coherency between meshes. The final aspect ratio for the elements in Zone 3 was therefore 3:1 (perimeter:length). The TWT model was comprised of two FeP04 tubes, each joined to the opposite end of a stainless steel tube, as produced experimentally. The height of the step of Zone 3, between the FeP04 meshed blank and

the stainless steel meshed blank was 0.301mm and deemed insignificant to generate problems with the TWT simulations.

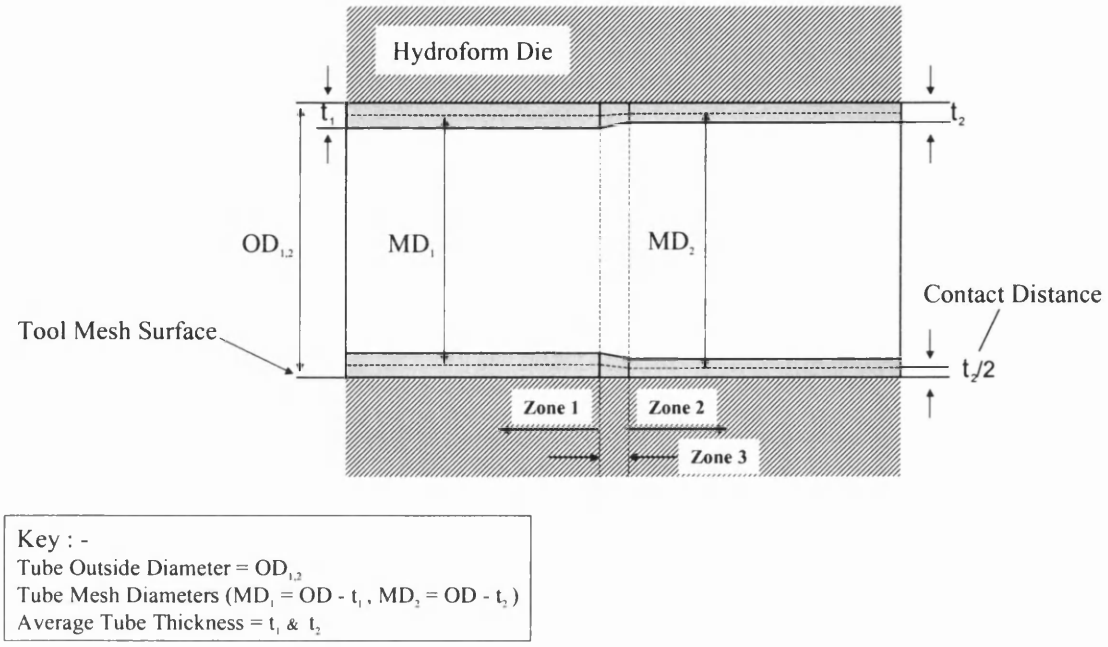

Figure 40: Schematic illustration of TWT and hydroform die tooling FE meshes

The properties used in the model of the TWT relate to the respective material input parameters used for the FeP04 tube and the SS (304) tube given in Table 1.

In all the FE analyses of the TWT hydroforming process, the experimental process parameters were artificially accelerated by a magnitude of 1000, i.e. 50Bar/s experimentally became 50Bar/ms in the models.

5.9 Model Verification

5.9.1 Strain Profile Measurements

The principal means of model verification was to examine and measure the strain pre-defined paths and at key sections along the component. Strain analysis was selected as the principal comparative means of verifying the hydroform models, as thickness comparisons would be influenced by the wall thickness variation of production tube material. The selected strain profiles that were used for comparing the FE models with

the experimental tube hydroforms were along the component length, section LA (through 70mm face) and LB (through 80mm face) and at the centre of the hydroformed tube at section A-A, see Figure 41.

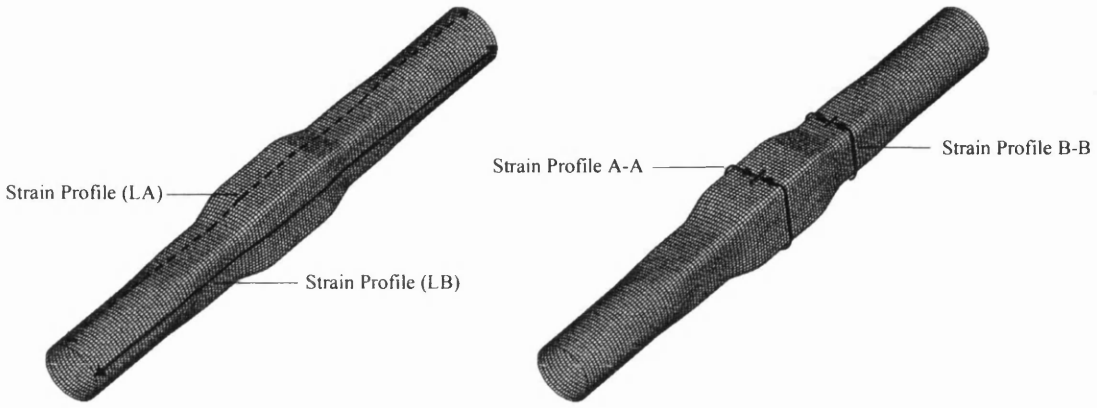

Figure 41: Strain profiles measured for verification of FE models with experimental data

The model data was then compared directly with the measurements of the experimental hydroforms. The strain data was also obtained from the pre form, at section B-B.

5.9.2 Corner Radius Measurements

In addition to the strain profiles, external corner radius measurements were performed on a limited number of suitable FE models, due to the influences of wrinkling and catastrophic necking/splitting. In the models that corner radius measurements were possible, namely the SS 304 FEA models, correlation was made directly with the experimental measurements. The method used to measure the corner radii of the FE hydroform model was achieved by manipulating the radius measurement feature that was available in Pam-Stamp version 2000. The corner radii of all four component corners were measured by selecting the last tube node having contact between the tube hydroform and the die walls either side of the radius, see Figure 42.

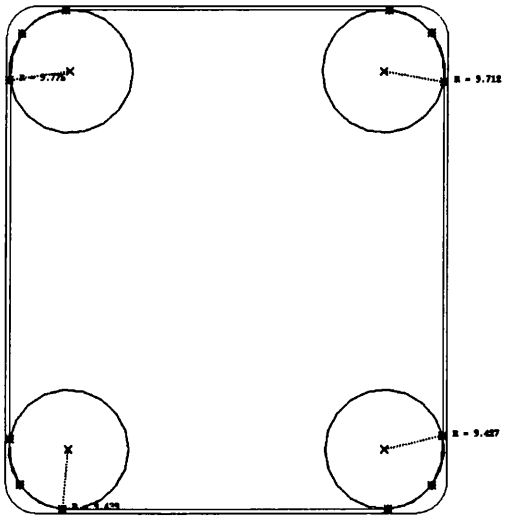

Figure 42: Example of FE model corner radius measurement

The radius measurements were recorded and the average of the four radius measurements was then calculated for direct comparison with the experimental average value, based upon a specific internal pressure and feed rate.

The corner radius measurements were only performed with the models that utilised adaptive meshing in order to ensure an accurate representation of the corner radius.

5.9.3 Thinning Analysis

A further useful means of evaluating the effects of the hydroforming process was to examine the thinning level with reference to a thinning limit, which could be used with basic tensile test data. It was therefore possible to observe the influence of the model parameters on the degree of thinning anticipated, and what conditions would be likely to produce a successful component. The thinning limit of each of the materials used was based upon the Empirical FLC equation [106], for the FeP04, FeP10 and HSLA and SS (304) steels. The thinning limit calculated was based upon the FLD_0 value, see Equation

37. As only the left-hand side of the FLD was under consideration, due to die geometry, friction and processing conditions, the thinning limit remains essentially constant from zero minor strain and for increasing values of negative minor strain. Under different conditions, e.g. when positive minor strain exists, the technique becomes invalid and a separate thinning limit would be required.

The calculated thinning limit for each steel sheet and tube material was based upon the following empirical approximation [177]:

$$e_t = [1/((e_1 + 1).(e_2 + 1))] - 1 \qquad \text{Equation 36}$$

In the above expression e_t = engineering thickness strain, e_1 = engineering major strain and e_2 = engineering minor strain. The thinning limits are determined by replacing the engineering major strain e_1 with the FLD_0 value in equation 36. The thinning limits for the tube materials and the converted 10% safe limits are presented in Table 4, against the analytical FLC models. The likelihood of failure prediction by local necking of the tube hydroform was easily by executed comparing the maximum thinning value of the FE model with the calculated thinning limit, based upon the analytical FLC models. The tube hydroform FE models under the different processing conditions, frictional values and material models were evaluated by determining the maximum thinning value at 100Bar pressure intervals, up to the maximum forming pressure of 1000Bar.

All of the tube hydroforming FEA models were prepared using Pam-Stamp™ Generis™ and the solver Pam-Stamp™. Viewing of the results was engaged through Pam-View™. The tube hydroforming analyses were subsequently run using a Silicon Graphics Indigo2 (R10000) workstation and an Origin 2000 server, based at the British Steel Strip Products, Customer Technical Centre, Port Talbot.

6.0 Results

The results of the experimental programme are presented in this chapter. Firstly, all coil characterisation performed is presented in section 6.1. The tube material characterisation is presented in section 6.2. Following the material characterisation, the performance & resultant forming behaviour of the steels using the selected dry film lubricants is presented in section 6.3. Section 6.4 details the results of the experimental hydroforming and section 6.5 describes the findings of the FE models developed.

6.1 Determination of Original Coil Properties & Characteristics

6.1.1 Coil Thickness

FeP04

The cold-rolled, extra deep draw quality, mild steel exhibited a strong thickness variation across the coil width. The average thickness was found to vary between 1.139mm, at one edge, and 1.158mm at the other, with the greatest thickness value of 1.185mm, measured at the coil centre, see Figure 43.

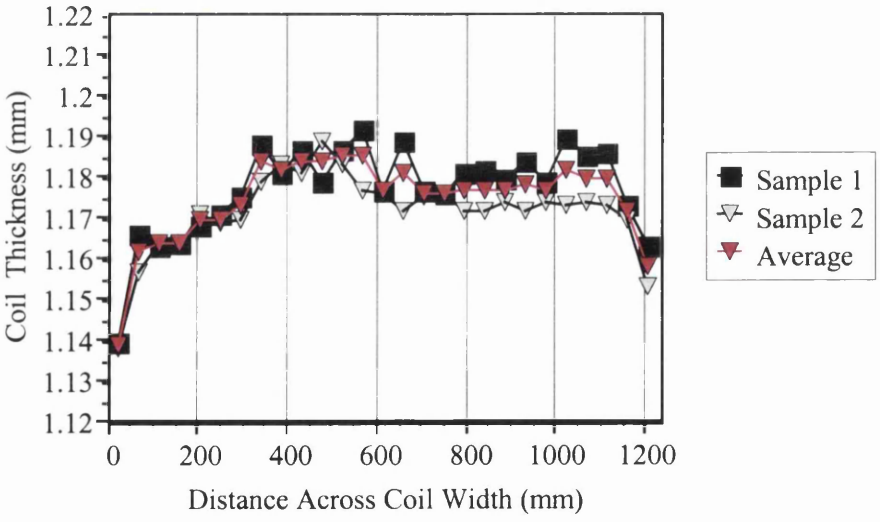

Figure 43: Cross-coil thickness profile for FeP04 coil material

A strong drop-off in thickness, at approximately 20mm from the coil edges was observed for the FeP04 coil material. The measurements illustrated a variation in average coil thickness of 4.1%.

FeP10

The hot-rolled, draw quality mild steel, was found to have a 3% variation in average thickness across the (218mm) slit coil width, with 1.98mm at one edge and 2.04mm at the other. The coil thickness measurements determined a clear increase in thickness from one edge to the other. Figure 44, illustrates the coil edge effect identified. The variation in thickness was lower than for the FeP04 coil, although the sample measurements related to a considerably narrower width. Additionally, the FeP10 thickness measurements were made at the mid-coil position, where the thickness is likely to be more consistent. (Average thickness = 2.017mm. The standard deviation for thickness measurements made on the mid coil samples = 0.013).

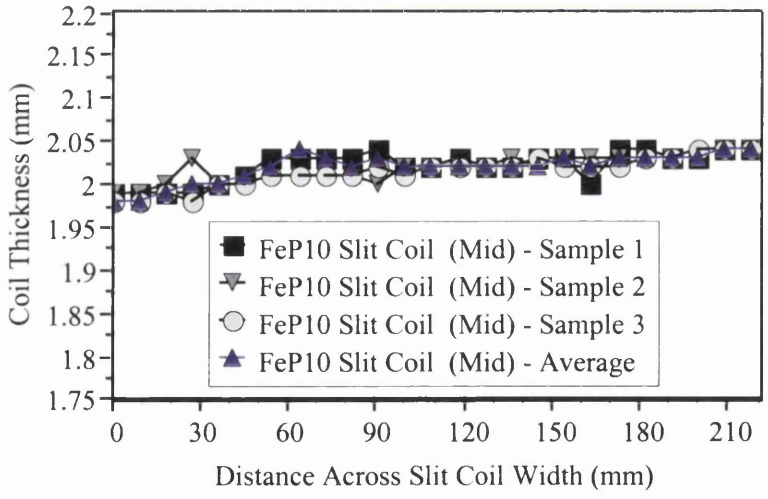

Figure 44: Cross-coil thickness profile for FeP10 slit coil material

HSLA (XF300)

The maximum difference in average thickness, for the slit coil (front), was found to be 1.95%, with the measured average thickness at one edge being 2.307mm and 2.352mm at the other, Figure 45.

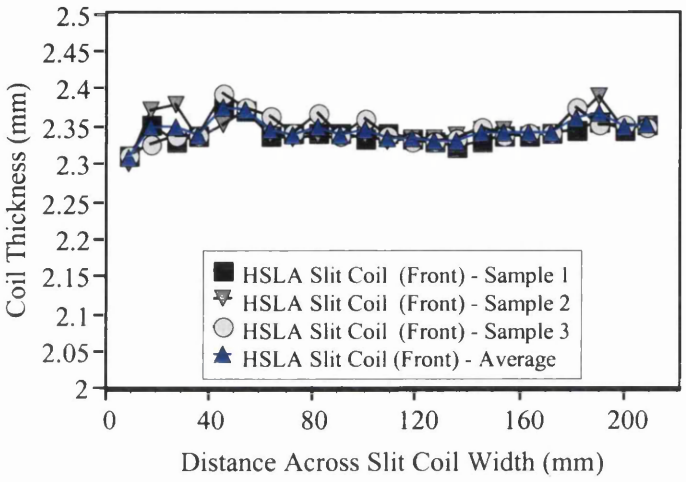

Figure 45: Cross-coil thickness profile for HSLA slit coil (Front) material

The measured average thickness for the (middle) slit coil metal was found to be 2.103mm at one edge and 2.059mm at the other, Figure. 46.

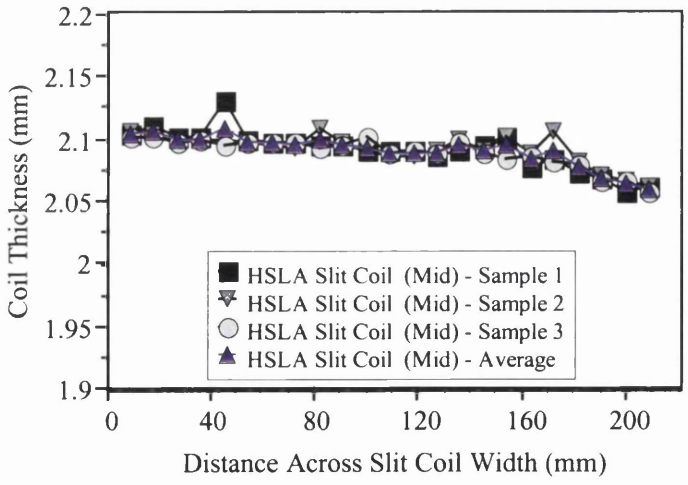

Figure 46: Cross-coil thickness profile for HSLA slit coil (Mid) material

As with the FeP10 slit coil thickness measurements, the thickness was found to vary almost linearly (increase/decrease) from one edge to the other. The maximum variation in average thickness, across the width of the slit coil (mid.), was found to be 2.1%.

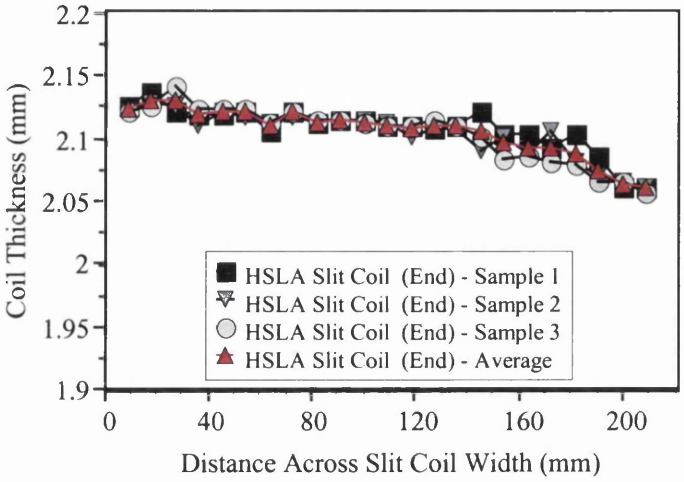

Figure 47: Cross-coil thickness profile for HSLA slit coil (End) material

The end of slit coil exhibited a similar thickness range and profile to that of the mid slit coil material measured, with an average thickness at one edge of 2.123mm and 2.060mm at the other, Figure 47. A variation of 11.4% was found between the average thickness, for the front and the end of coil material. The average thickness for the front, mid and end samples is 2.344mm, 2.09mm, 2.105mm, respectively. Standard deviation found from the thickness measurements made for the front, mid and end of coil = 0.017, 0.013 and 0.019, respectively). Figure 48 shows the BSSP thickness trace for the HSLA (pre-slit). The thickness measurements made correlate well with the thickness trace obtained.

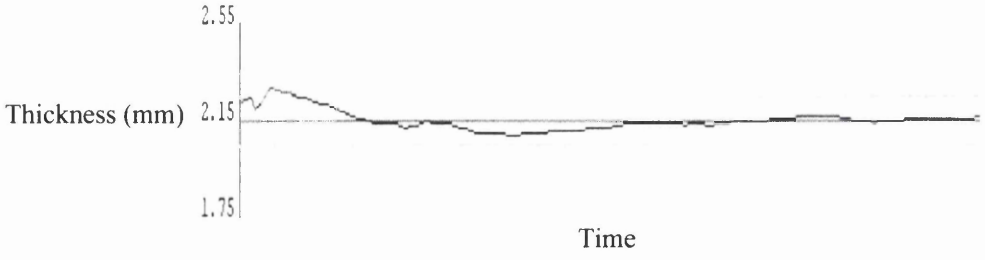

Figure 48: British Steel Strip Products thickness trace for HSLA coil

6.1.2 Chemical Composition

The results of the chemical analyses, given in Table 2, are described below:

	Element																
Material	C	Si	Mn	P	S	Ni	Cu	Sn	N	Al	Cr	Mo	Nb	Ti	V	Co	B
FeP04 Coil	0.039	0.005	0.247	0.017	0.017	-	0.021	-	0.0044	0.035	0.012	-	0.001	0.008	0.001	-	-
FeP10 Coil	0.029	0.002	0.204	0.015	0.011	0.017	0.005	0.001	0.0043	0.042	0.052	0.01	-	0.002	-	-	-
Stainless Steel Tube	0.036	0.42	1.58	-	0.01	7.7	0.33	-	0.0466	-	16.4	0.36	-	-	-	-	-
HSLA Ladle Analysis	0.047	0.004	0.38	0.011	0.005	0.047	0.027	0.004	0.0027	0.031	0.052	0.013	0.015	0.001	0.001	0.001	0.0002
HSLA Slit Coil (Front)	0.048	0.067	0.77	0.028	0.006	-	0.015	-	0.0026	0.037	0.015	-	<0.01	<0./01	-	-	-
HSLA Slit Coil (Mid)	0.048	0.063	0.77	0.024	0.006	-	0.007	-	0.0028	0.028	0.016	-	<0.01	<0.01	-	-	-
HSLA Slit Coil (End)	0.048	0.082	0.77	0.028	0.006	-	0.007	-	0.0027	0.033	0.018	-	<0.01	<0/01	-	-	-

Table 2: Chemical composition of steels studied in programme

FeP04

The chemistry of the FeP04 steel grade was found to be below the specified maximum chemical composition limits [178] of carbon (0.08% max), phosphorus (0.045%max), sulphur (0.045%max), manganese (0.6% max). Therefore, the grade studied was of a suitable chemistry to be considered to be 'clean' and was in line with the specification of a fully killed, extra deep draw quality steel for cold forming applications.

FeP10

The FeP10 steel was also found to conform to the specified maximum chemical composition limits for draw quality mild, hot rolled steels [179]. As anticipated, the chemical composition was found to be very similar to that of the FeP04 material.

HSLA

With the HSLA steel, details of the ladle analysis chemistry was obtained from the British Steel Intranet site along with the other coil processing details and coil dimensions, including width and thickness. Supplementary to this data, through coil chemical analysis was obtained for the front, middle and back of coil, through tests performed at the BOS plant laboratory, Port Talbot Works, South Wales. In general, the HSLA steel was found

to have chemistry inside of the specified compositional tolerances [179]. However, the level of phosphorus was found to be 0.028 (wt %) for the front and back of coil samples, which was just over the maximum allowable level of 0.025 (wt %). In contrast, the ladle analysis was found to yield 0.011 (wt %) phosphorus. The results of the ladle analysis generally indicated that the steel was cleaner than the results of the analysis of the slit coil samples. Although the carbon levels were found to be nearly identical, the manganese levels measured from the slit coil samples (0.77 wt %) were found to be just over double of the ladle analysis (0.38 wt %).

6.1.3 Tensile Mechanical Properties

The average mechanical properties determined from the steel coil metal, based upon 80mm gauge length tensile tests, are presented in Table 3 and described below.

Material and Form	RD	Rel (MPa)	Rp 0.2% (MPa)	Y/Ult (%)	Rm (MPa)	Ag (%)	A (%)	n1 (5-10%)	n2 (10-15%)	n3 (10-20%)	r2 (10%)	r3 (15%)	r4 (20%)
FeP04 Coil	0°	-	171.6	53.8	319.2	24.4	41.4	0.238	0.218	0.214	2.01	2.00	1.96
FeP04 Coil	45°	-	182.3	55.4	329.0	24.0	39.3	0.229	0.207	0.201	1.48	1.46	1.45
FeP04 Coil	90°	-	174.7	56.0	312.0	22.7	39.4	0.233	0.209	0.204	2.48	2.44	2.41
FeP04 Tube	0°	-	213.7	70.6	302.8	23.2	40.5	0.181	0.185	0.188	-	-	-
FeP10 Slit Coil	0°	252.5	-	69.8	362.0	21.8	36.0	0.205	0.191	0.182	0.88	0.89	0.90
FeP10 Slit Coil	45°	250.8	-	71.2	352.0	20.9	37.8	0.201	0.185	0.182	0.98	0.99	1.10
FeP10 Slit Coil	90°	262.7	-	74.1	354.4	21.3	32.8	0.219	0.188	0.184	0.94	0.97	1.00
FeP10 Tube	0°	-	295.8	80.8	366.0	13.6	29.4	0.100	0.016	-	-	-	-
HSLA Slit Coil	0°	361.1	-	82.3	438.6	20.6	30.8	0.194	0.179	0.178	0.60	0.62	0.60
HSLA Slit Coil	45°	379.1	-	87.2	434.7	21.0	33.8	0.154	0.175	0.175	0.90	0.97	1.01
HSLA Slit Coil	90°	391.4	-	87.2	449.0	19.1	28.7	0.164	0.172	-	0.76	0.79	-
HSLA Tube	0°	-	372.0	83.6	444.8	17.1	28.5	0.131	0.144	-	-	-	-
SS 304 Tube	0°	-	273.1	44.4	614.9	48.5	51.8	0.282	0.361	0.338	-	-	-

Table 3: Mechanical properties of steel coil and tube materials studied

- ***FeP04***

Supplementary to the thickness measurements performed across the coil width, mechanical tensile tests were also performed for each of the materials.

Longitudinal

The 0.2% proof strength of the FeP04 coil material was found to vary between 178.7MPa at one edge and 157.0MPa at other, Figure 49. Similarly, the tensile strength was also found to be higher at the same edge (327.05 MPa) compared with the other (300.5MPa).

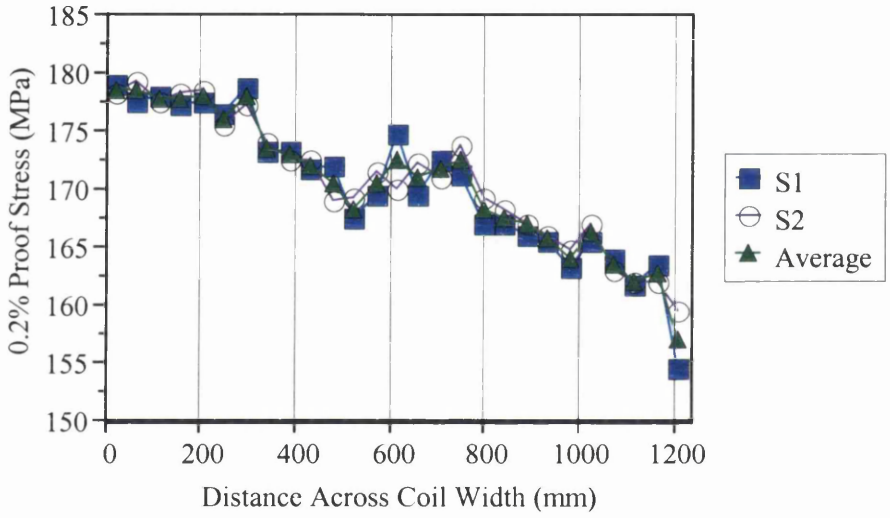

Figure 49: FeP04 cross-coil variation in (longitudinal) 0.2% proof strength

The uniform elongation at the stronger coil edge was found to display a lower value of elongation, 23.5% compared with 24.55% at other edge. A similar trend was observed in terms of the total elongation, illustrating poor cross-coil consistency. In addition to the observed variation in the values of uniform and total elongation, the strain-hardening exponent displayed a similar pattern, 0.211 for one edge versus 0.22 for the other, Figure

50. The anisotropy parameter or r-value for the longitudinal test direction was found to vary by more than 13% across the coil width, from 1.82 to 2.03 at the other edge.

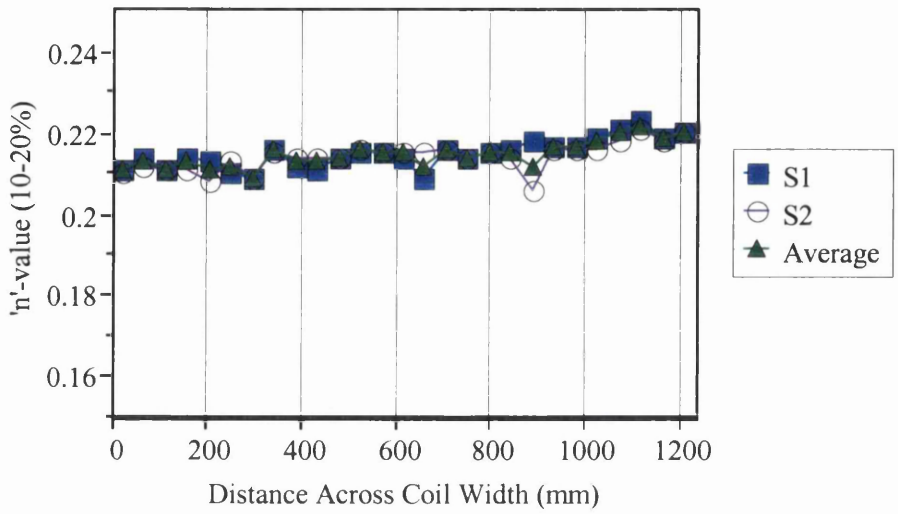

Figure 50: FeP04 cross-coil variation in (longitudinal) n-value (10-20%)

Transverse

For the transverse tensile tests, similar results to the longitudinal tensile tests were obtained. One coil edge was found to have the highest proof and tensile strength, 178.5 and 316.0 MPa respectively, compared with the other edge having 167.8 and 302.0 MPa respectively. However, the uniform and total elongation values were found to be approximately the same. The transverse r-value displayed only minor differences between edges, 2.3 for the one and 2.38 for the other. However, at the centre of the coil a value of 2.54 was obtained.

The variation in properties between 0°, 45° and 90° were found to be very small, with the exception of the r-value. The difference between the mechanical properties for the rolling direction and the 45° direction were found to be less than 6%. Between the rolling and the transverse direction the properties were found to differ by a maximum of 7%, which was attributable to the uniform elongation values, consequently a similar difference was displayed by the terminal n-value, n_T. From the r-values determined from the coil, the

material was found to be strongly anisotropic in nature, having average r-values of 1.96, 1.45 and 2.41 for the 0°, 45° and 90° orientations to the rolling direction, respectively.

FeP10

Longitudinal

The hot rolled mild steel, exhibited upper and lower yield point phenomena. A lower yield point value of 255.1 MPa was obtained for one edge of the slit coil whilst a value of 261.1 MPa, was obtained for the other. A minimum value 245.3 MPa was obtained 153mm across the slit coil width, displayed in Figure 51.

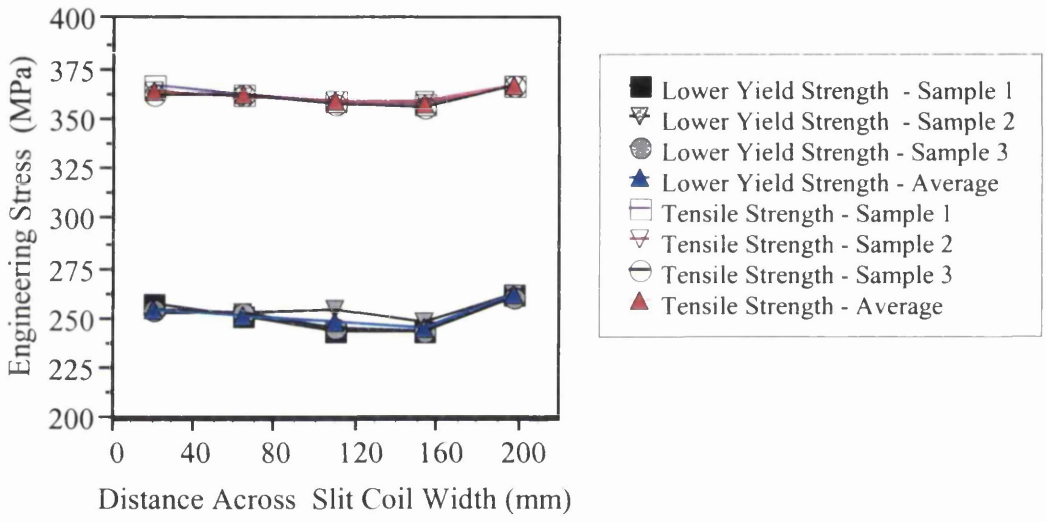

Figure 51: FeP10 cross slit coil variation in (longitudinal) lower yield and tensile strength

As with the yield values, only small differences in tensile strength were displayed across the coil. Like the lower yield point, a similar drop at 153mm across the slit coil was also observed for the tensile strength.

Little variation in uniform or total elongation was observed for the coil, with no more than 1% elongation difference in average uniform elongation and no more than 2% elongation for the total elongation. The low variation once again may be explained by the position the sample coil was obtained from, i.e. mid coil.

As in the case for the cold rolled mild steel, the difference in properties between 0°, 45° and 90° for the FeP10 coil were also typically below 5%, with the exception of the total elongation values. The results for transverse test direction displayed an average total elongation value 9% lower than the corresponding value for the rolling direction. The r-values for the FeP10 slit coil were all close to a value of unity, giving rise to an r-bar of 1.03.

HSLA

Longitudinal

For the HSLA steel an average lower yield value of 362.7 MPa was obtained for the one edge, whilst an average value of 346.1 MPa was found at the other. For the front, middle and rear coil positions similar lower yield and tensile strength profiles were displayed, Figure 52. The tensile strength possessed a very similar profile to the yield strength and did not vary more than 15 MPa with the slit coil.

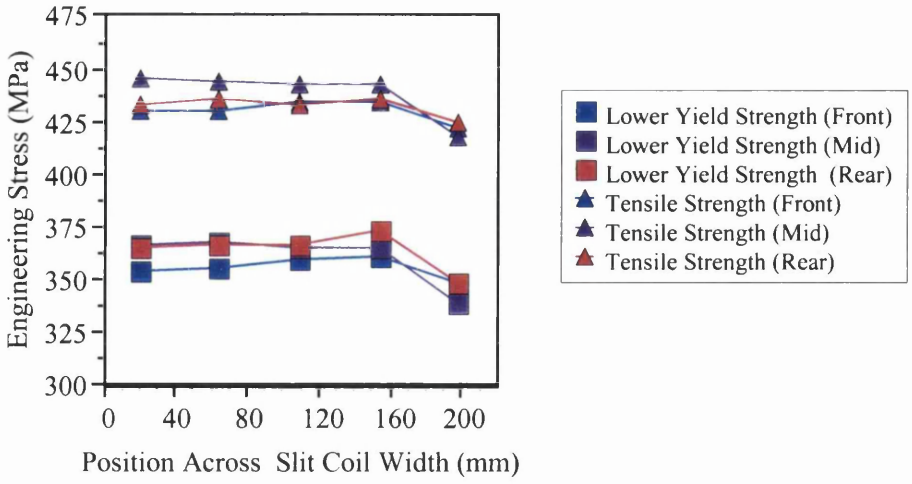

Figure 52: HSLA cross-coil variation in (longitudinal) lower yield and tensile strength for Front, Mid and End of slit coil samples

One edge of the slit coil, which displayed higher yield and tensile strength, also displayed the lowest average uniform and total elongation, Figure 53.

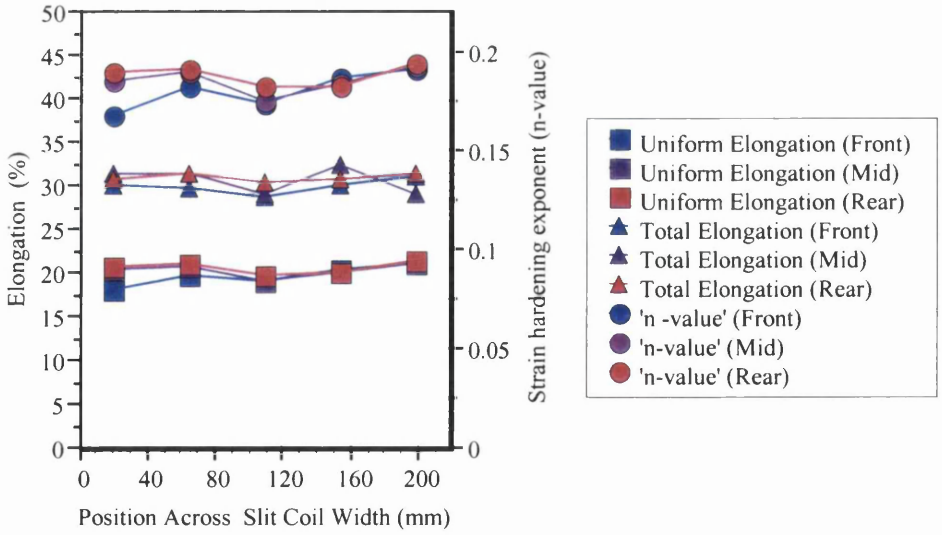

Figure 53: HSLA cross-coil variation in (longitudinal) n-value, uniform and total elongation values for Front, Mid and End of slit coil samples

The variation in properties between the rolling and the 45° direction was found to be less than 5%. The maximum difference was found in the lower yield strength values obtained. The difference in properties between the rolling and transverse directions was far more prominent. In general, the transverse direction was found to display lower formability, having lower uniform and total elongation values, 1.5% and 2.1% elongation lower respectively. In addition to the lower elongation value, the transverse metal also displayed higher yield and tensile strength values, 391.4MPa and 449.0MPa compared with 361.1 and 438.6MPa, respectively. The HSLA steel was also found to be less isotropic than the mild steel FeP10, with an r-bar of 0.85 compared with 1.03 for FeP10.

6.1.4 Surface Texture Analysis

The results of the surface texture analysis performed on the coil materials are presented in Figures 54 and 55, for average 3D and (2D) extracted profiles, respectively.

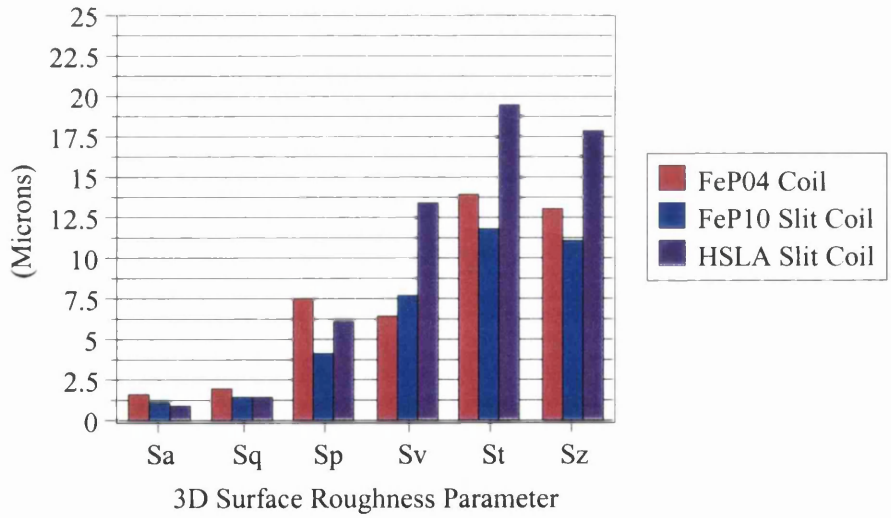

Figure 54: Comparison of averaged 3D surface coil texture parameters of materials *(Sa = mean surface roughness, Sq = rms roughness, Sp = peak height, Sv = valley depth, Sz = profile height for sample length, St = profile height for evaluation length).*

The 3D results are denoted by the prefix S and the 2D results by the prefix R. The 2D texture analysis results presented are average results based upon the average of 3 (2D) extracted profiles per sample.

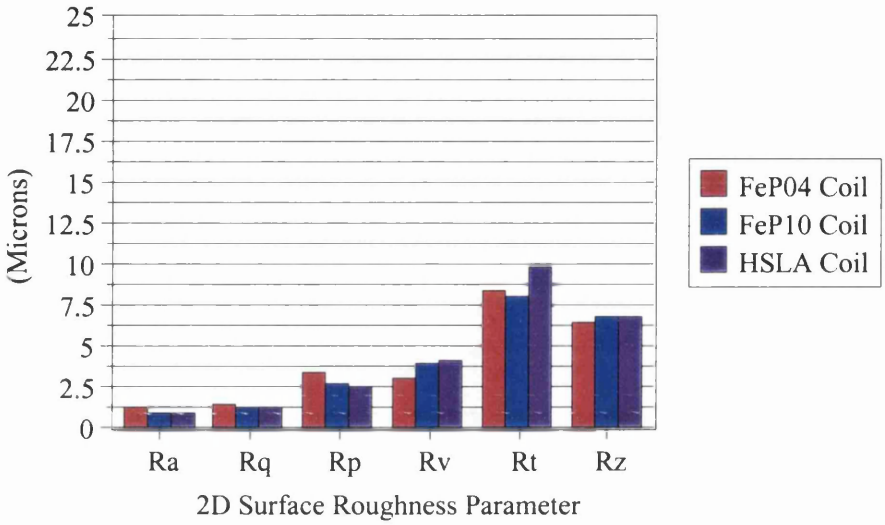

Figure 55: Comparison of average 2D surface texture parameters of coil materials studied. *(Ra = mean surface roughness, Rq = rms roughness, Rp = peak height, Rv = valley depth, Rz = profile height for sample length, Rt = profile height for evaluation length).*

From average data presented in Figures 54 and 55, it can be seen that whilst the two different measurement forms provide values of different magnitude, the principal surface roughness characteristics of Ra and Sa were comparable. In both instances, the FeP04 steel possessed the highest roughness values in terms of both average roughness (Ra = 1.32μm, Sa = 1.74μm) and root mean square roughness (Rq = 1.57μm, Sq = 2.07μm) for the given profiles and areas measured, respectively. In each case, the HSLA coil was found to possess the lowest roughness values, although only marginally lower, (Ra) 0.05μm & (Sa) 0.06μm, respectively than the FeP10 coil.

The texture results for asperity average peak height, valley depth and total height, were found not to be entirely the same between the average of the 2D extracted profiles and the 3D measurements. The 3D results indicate a significantly higher total height (sample and

evaluation length) in comparison with the other coil materials, whilst the 2D analysis do not support this trend, having a more uniform set of values for the total height.

For the average of the 2D profiles the material exhibiting the greatest peak height was found to be FeP04 (3.38μm) compared with 2.77 μm and 2.6 μm for the FeP10 and HSLA steels respectively. Whilst the FeP04 coil material possessed the largest peak height, it was also found to have the shallowest 2D valley depth (3.08μm). This compared with 4.01μm and 4.21μm for the FeP10 and HSLA coil materials, respectively. In terms of the 2D total profile height Rz, little separated the FeP10 and HSLA coil metals with values of 6.68μm and 6.81μm respectively. The FeP04 coil material displayed a slightly lower Rz value of 6.46 μm.

6.1.5 Sheet Forming Limit Curves (FLC)

The forming limit curves determined from the small scale Nakazima tests are shown in Figures 6.10 through 6.12 for the FeP04, FeP10 and HSLA steel, respectively. The results are presented against the Empirical FLC and the theoretical Swift-Hill, Asnafi and Sauer FLC models. The results of the experimental FLC tests are also presented alongside strain data from necked tensile test and Nakazima strips, Figures 56a, 57a and 58a, and safe tensile test and Nakazima data, Figures 56b, 57b, and 58b, respectively.

The FeP04 experimental FLC was found to be some 15% major strain higher than the Empirical curve at the plane strain position, whilst the position of FLD_0 was found to be located at 7.5% minor strain. At 20% negative minor strain, two FLC the curves were separated by 10% major strain. The experimental data, shown in Figure 56a, strongly exhibited a non-zero plane strain intercept. The right-hand side of the experimental FLC was found to be some 7% major strain higher than the Empirical FLC.

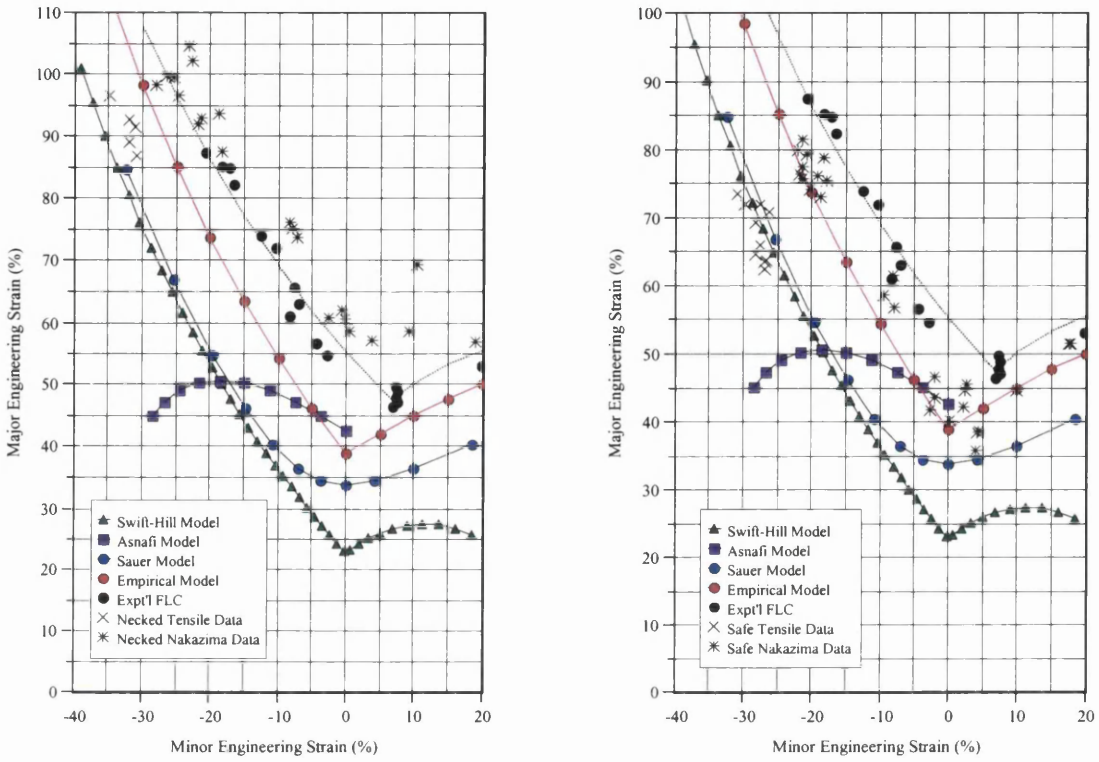

(a) (b)

Figure 56: FeP04 analytical FLC models compared with (a) necked tensile and Nakazima test data and (b) with safe tensile and Nakazima test data

From comparison of the analytical curves with the experimental FLCs presented in Figures 56 to 58, the Empirical FLC showed the closest correlation with the experimental FLC, Nakazima data and tensile data. The Swift-Hill and Sauer FLC models underestimated the experimental forming limit of the materials. The Asnafi FLC curve displayed an inaccurate representation of the FLC shape and poor capability to depict necking or safe strains failure strains.

Despite the plane strain intercept positioning, the experimental FeP04 FLC compared well with the corresponding Empirical FLC, with a maximum difference of 7% major

strain at the plain strain intercept, i.e. zero minor strain. The slope of the right-hand side of the experimental curve was, however, steeper than the Empirical FLC. The FeP04 and FeP10 sheet materials displayed similar experimental forming limit curves, with minimum FLC values of almost 50% in each case, the FeP10 material being moderately higher by 3% major strain. In both cases the left-hand side of the FLC curves displayed slopes which were moderately shallower than the Empirical FLC. Interestingly the degree of draw was also similar, although moderately higher for the FeP04 material as would be expected.

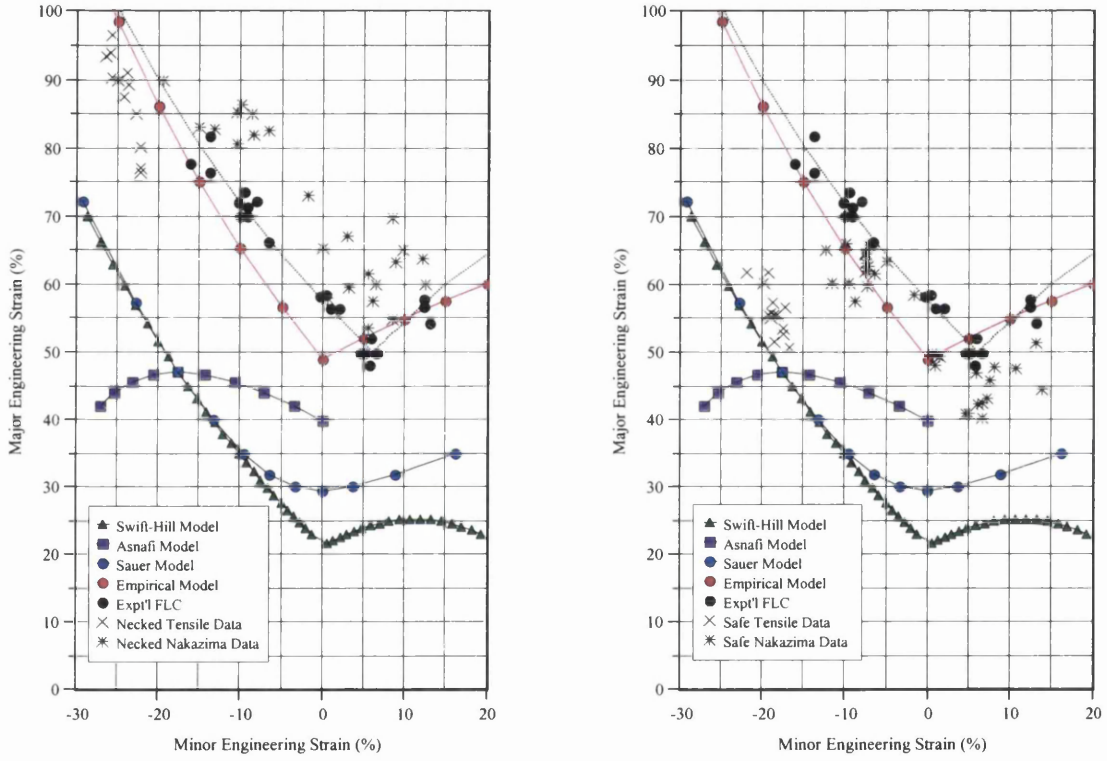

Figure 57: FeP10 analytical FLC models compared with (a) necked tensile and Nakazima test data and (b) with safe tensile and Nakazima test data

Unlike the results of the FeP04 and FeP10 metals, the HSLA steel displayed an FLC below the Empirical FLC, i.e. the Empirical FLC prediction overestimated the forming

limit. The experimental FLC was found to be some 6% major strain lower at the plain strain intercept point and was positioned at 8% minor strain.

Of interest was the difference displayed between the Nakazima and tensile data. For the same magnitude of major strain the tensile data possessed a more negative minor strain (5-10% strain), which reinforces the belief that the FLC test, which made use of a hemispherical punch, caused the data to shift to the right. Also of interest was the fact that the Empirical FLC was found to overestimate the necked tensile data by a small margin, approximately 5-10% major strain.

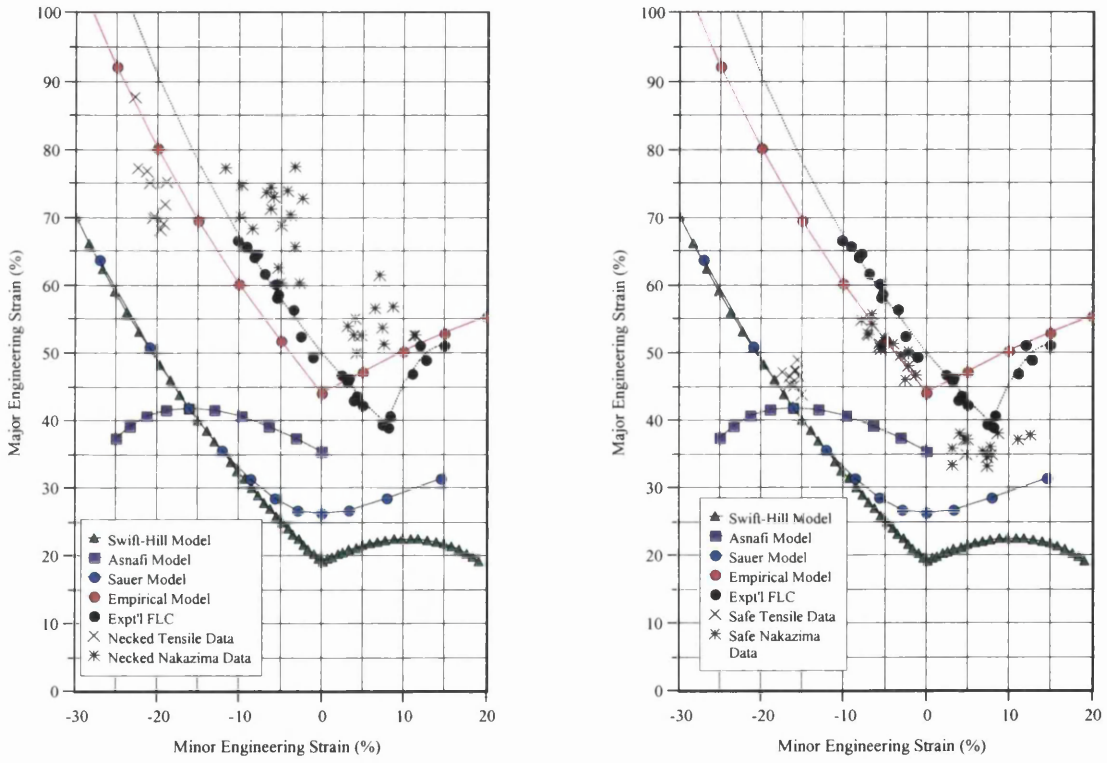

Figure 58: HSLA analytical FLC models compared with (a) necked tensile and Nakazima test data and (b) with safe tensile and Nakazima test data.

In comparison with the theoretical FLC models (Asnafi, Sauer & Swift-Hill), the Empirical model showed the closest correlation with the experimental FLC, Nakazima data and tensile data. The Asnafi FLC model did not correspond well with the experimental data, in particular with reference to the shape of the FLC. The Sauer, like the standard Swift-Hill model, was considerably lower than the experimental data and Empirical FLC for each of the coil metals studied. However, the modified Swift-Hill FLC proposed was found to correlate well with the experimental data and is presented in Figure 59 against the experimental FLC. For the FeP04, FeP10 and HSLA steel coil materials. However, the biaxial curves of the modified Swift-Hill FLCs appeared exaggerated in comparison with the experimentally derived FLCs.

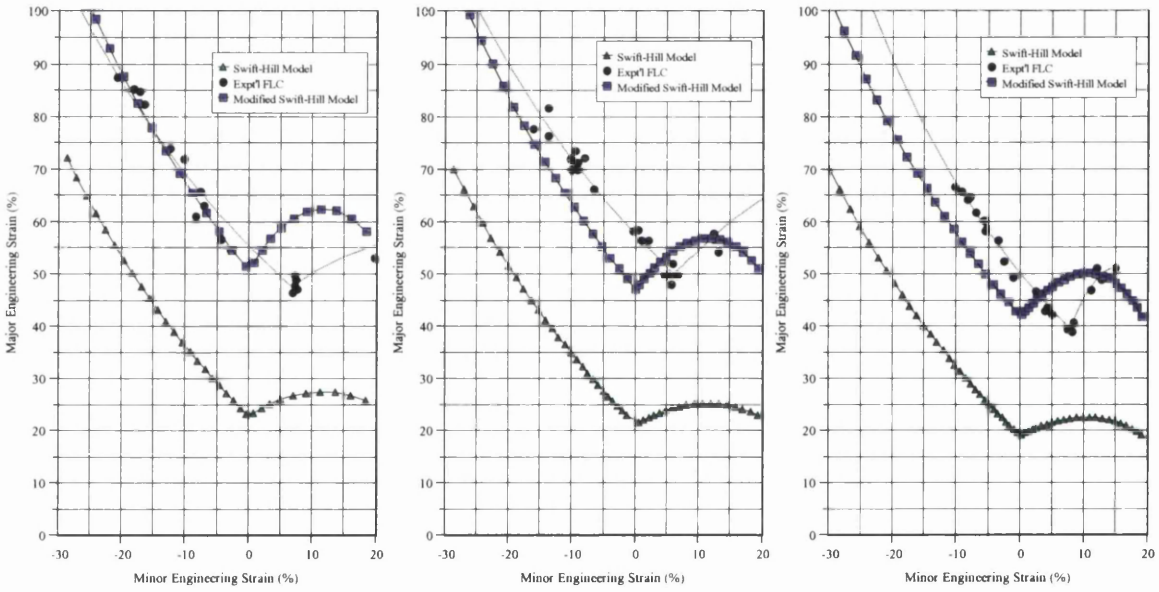

(a) (b) (c)

Figure 59: Comparison of modified Swift-Hill FLC model with experimental data and Swift-Hill FLC model for (a) FeP04 Coil, (b) FeP10 Coil and (c) HSLA Coil

The analytical curve FLD_0 values of the Analytical FLC models studied in this thesis are presented in Table 4.

Material and Form	Orientation to Rolling Direction	Empirical FLD_0	Sauer FLD_0	Asnafi FLD_0	Swift-Hill FLD_0	Modified Swift-Hill FLD_0
FeP04 Coil	0°	40.0	33.7	43.9	24.4	48.8
FeP04 Coil	90°	38.9	33.4	42.6	22.5	44.5
FeP04 Tube	0°	39.9	32.1	43.6	23.0	46.0
FeP10 Coil	0°	48.8	30.2	40.9	21.9	43.8
FeP10 Coil	90°	47.7	29.3	39.7	21.3	42.6
FeP10 Tube	0°	31.7	18.5	24.6	13.3	26.6
HSLA Coil	0°	46.5	28.0	37.8	20.4	40.4
HSLA Coil	90°	44.1	26.3	35.4	19.1	38.2
HSLA Tube	0°	40.5	23.5	31.5	17.1	34.2

Table 4: FLD_0 values for different analytical FLC models reviewed

6.2 Determination of Tube Properties & Characteristics

6.2.1 Tube Wall Thickness

In all instances the measured tube wall thickness values were within the allowed thickness tolerances according BS 6323 Part2, with the exception of the HSLA front of coil tube. The results of the tube wall thickness measurements of the tubes studied in this thesis are presented in Figures 60 to 65 and results of the measurements are detailed as follows:

- ***FeP04***

The minimum tube wall thickness was found at the weld region (1.167mm), being some 0.033mm below the nominal tube wall thickness. The maximum value of tube wall thickness measured was 1.195mm and the average was 1.186mm, ignoring the weld, and 1.185mm including the weld. From Figure 60 it is possible to see that the tube material was thicker either side of the weld. Significant differences in wall thickness at 180° from weld-line were also observed, refer to Figure 60. (Average wall thickness = 1.186mm. Standard deviation of wall thickness measurements = 0.004).

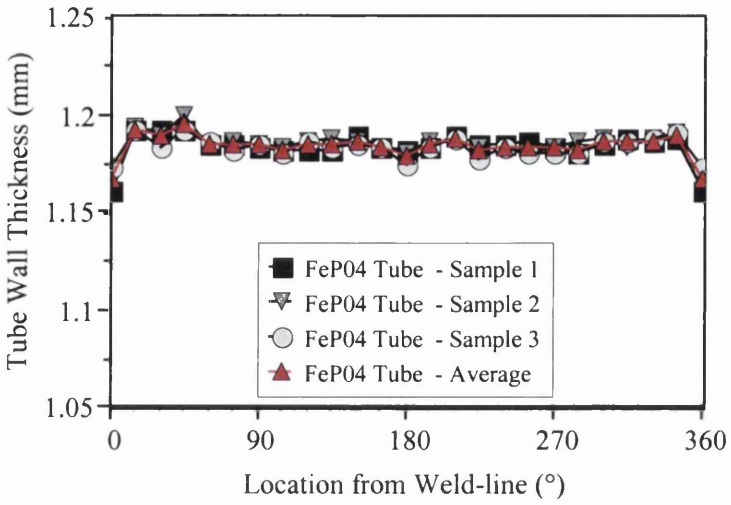

Figure 60: FeP04 tube wall thickness profile

- ***FeP10***

As in the case of the FeP04 tube, the minimum tube wall thickness was found at the weld location (1.888mm), Figure 65. Maximum wall thickness was found to be 2.08mm, at the 345° position from the weld-line.

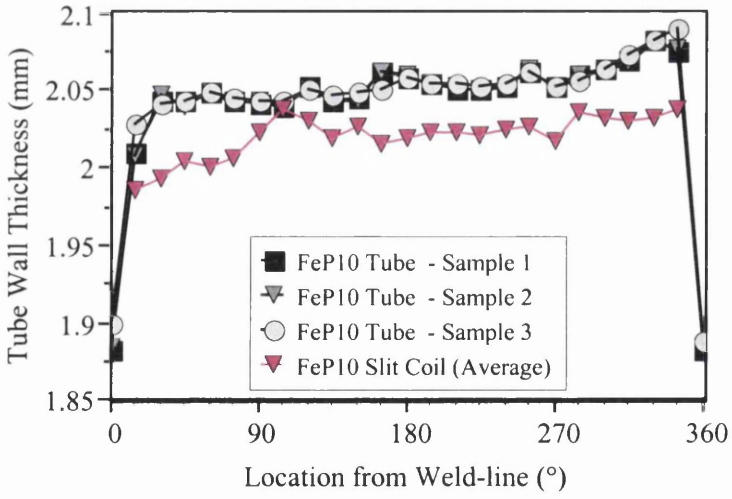

Figure 61: FeP10 tube wall thickness profile

The average tube wall thickness was 2.053mm compared with the average slit coil thickness of 2.019mm. (Average wall thickness = 2.053mm. Standard deviation in wall thickness measurements made = 0.0139).

- ***HSLA (XF300)***

Front of Coil

The results of the thickness measurements for the HSLA front of coil tube, Figure 62, indicated that the thinnest region of the tube was at the weld-line (2.141mm), whilst the maximum wall thickness measured was 2.338mm at 45°. The minimum parent wall thickness was 2.284mm at 240°. The average parent tube wall thickness was 2.306mm compared to the slit coil average of 2.346mm.

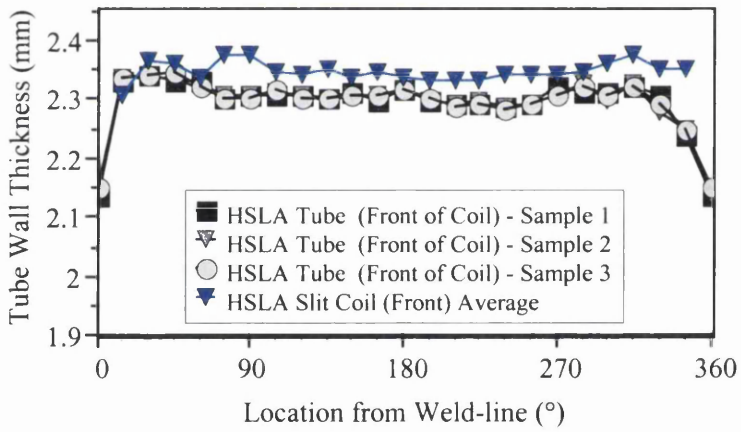

Figure 62: HSLA tube wall thickness profiles (Front of Coil)

Mid Coil

Again, as with the HSLA front of coil tube, the mid-coil tube thickness was found to be lowest for the weld-line (1.978mm), Figure 63. A strong variation in wall thickness distribution was found for the HSLA material, starting at approximately 15° through to 345°. The thickness distribution closely mapped the shape of the coil thickness profile

across its width. From the coil and the tube thickness measurements, the coil material appeared to be thicker than the tube material.

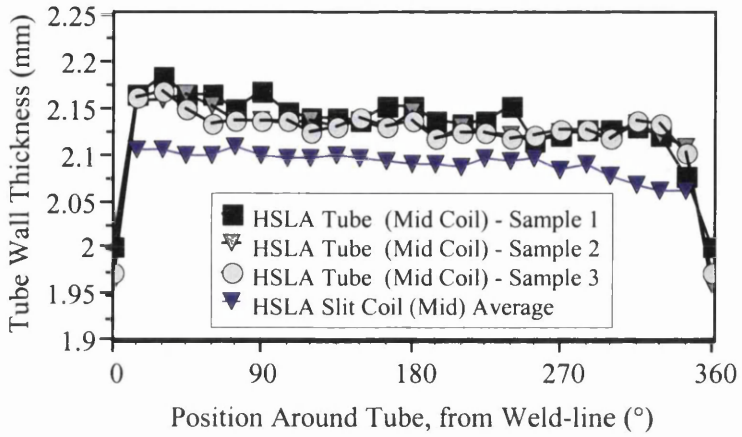

Figure 63: HSLA tube wall thickness profile (Mid Coil)

End of Coil

At the end of coil, the tube wall thickness distribution, Figure 64, also identified the thinnest region of the tube to be the weld (2.002mm), having a similar value to the mid thickness coil tube material. Once again, the same form of decrease in thickness around the tube circumference was found for the end of coil tube, as it was for the mid coil tube. Additionally, as with the mid coil tube the end of coil tube was found to be thicker than the parent coil obtained from the same location. (Average tube wall thickness for HSLA front, mid and end = 2.306mm, 2.134mm, 2.135mm, respectively. Standard deviation in thickness measurements made, for front, mid and end = 0.0204, 0.017 and 0.019, respectively).

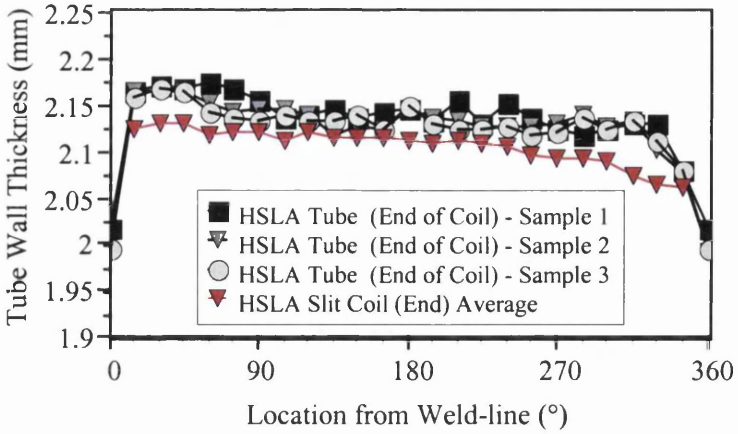

Figure 64: HSLA tube wall thickness profile (End of Coil)

- ***SS (304)***

The stainless steel (304) tube displayed a reasonable uniformity in wall, having an average parent wall thickness of 1.490mm, with the exception of the weld region thickness, Figure 65. Unlike the ERW tube material, the TIG welded stainless steel tube displayed a weld-seam, which was 0.09mm thicker than the parent tube. The measured thickness range of the parent tube was found to fall ±0.018mm either side of the average wall thickness, illustrating the high degree of uniformity.

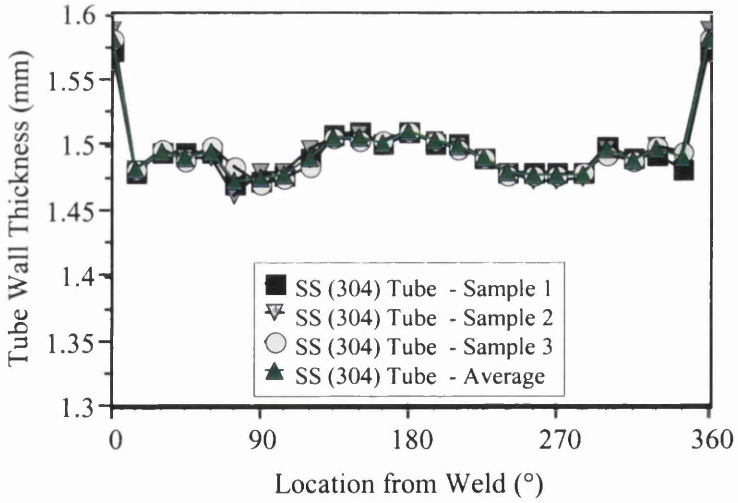

Figure 65: Stainless steel type 304 tube wall thickness profile

6.2.2 Tube Diameter

- ***FeP04***

The diameter and thickness configuration of the FeP04 tube fell outside the coverage of the BS 6323 Part 5 specification, due to the unconventional D/t ratio of the tube. In terms of ERW tube which are typically available, the standard states that tube with diameters in the range 50mm to 70mm and with D/t ratios greater than 40, should have a tolerance of ±0.5mm. According to BS 6323 part 6, under circumstances where the D/t ratio is greater than 33, the tolerance on diameter is usually agreed between the purchaser and the manufacturer. For the FeP04 tube, the maximum measured diameter was 70.31mm at the 105°/285° position and the minimum was 69.94mm at the 0°/180° position, Figure 66. Therefore, the tube diameter conformed to the diameter tolerance of the lower D/t ratio tube providing a statement of the production capability in terms of dimensional quality.

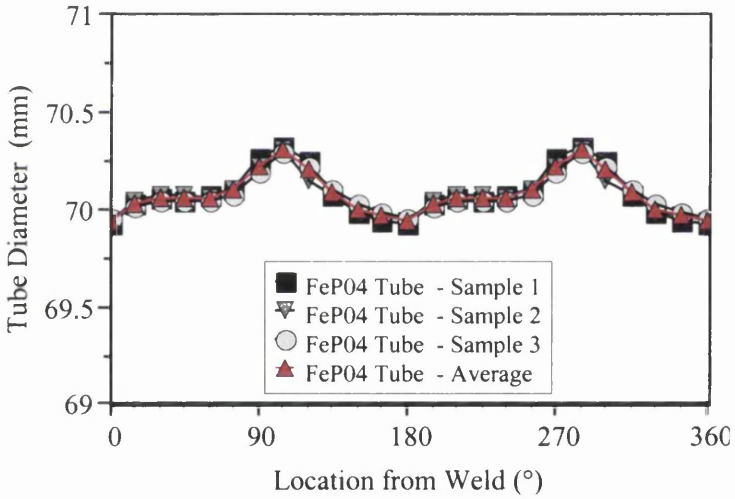

Figure 66: FeP04 tube diameter profile

- ***FeP10***

The variation in tube diameter displayed by the FeP10 tube was substantially less than the FeP04 tube. This was clear from the range between maximum and minimum diameter for the FeP10 tube, which found to be less than half that of the FeP04 tube at 0.018mm (Figure 67). The maximum measured diameter was 70.12mm, 0.19mm less than the FeP04 tube. The minimum diameter was 69.94mm, found at the 90°/270° position.

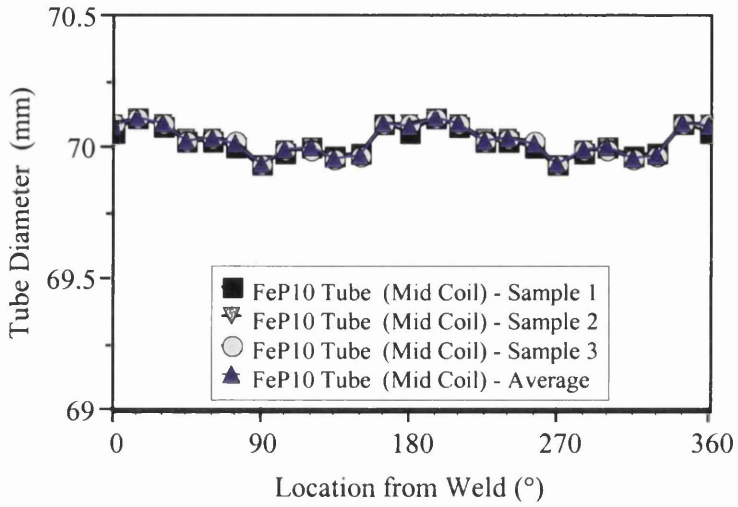

Figure 67: FeP10 tube diameter profile

- ***HSLA***

The results of the HSLA tube diameter measurements are presented in Figures 68-70 and detailed below:

Front of Coil

The maximum tube diameter observed for the front of coil material was 70.35mm, slightly higher than the FeP04 tube. According to BS 6323 Part 6, tubes in the diameter range 50mm to 70mm, with a D/t ratio of up to 33, should have a diameter tolerance of ±0.2mm on the tube mean diameter. This implies a maximum allowable mean diameter of 70.2mm and a minimum allowable mean diameter of 69.98mm. Unlike the FeP04 and FeP10 tube metals, the minimum tube diameter was not less than 70mm with the minimum tube diameter being some 70.02mm, with the average tube diameter at 70.14mm, Figure 68.

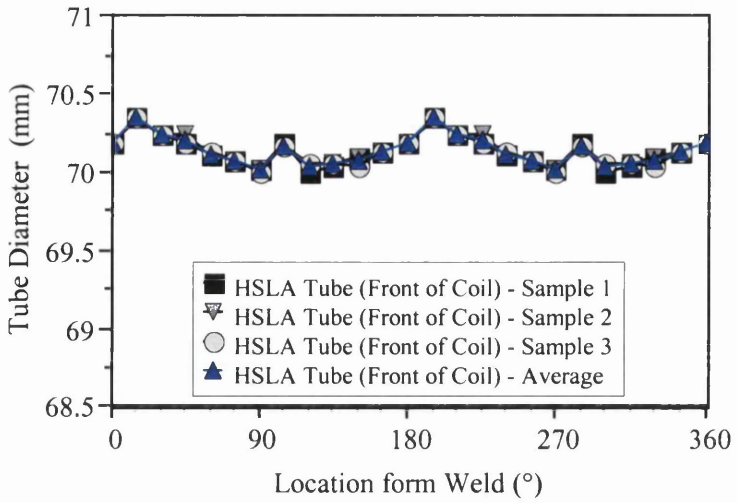

Figure 68: HSLA tube diameter profile (Front of Coil)

Mid Coil

A greater degree of spread in results was observed for the middle of coil than for the front or rear of coil measurements, Figure 69. The minimum average tube diameter in this case was found to fall just below 70mm at 69.97mm. The maximum diameter was 70.22mm. This was slightly over the BS 6323 standard tolerance but the average diameter was below at 70.09mm.

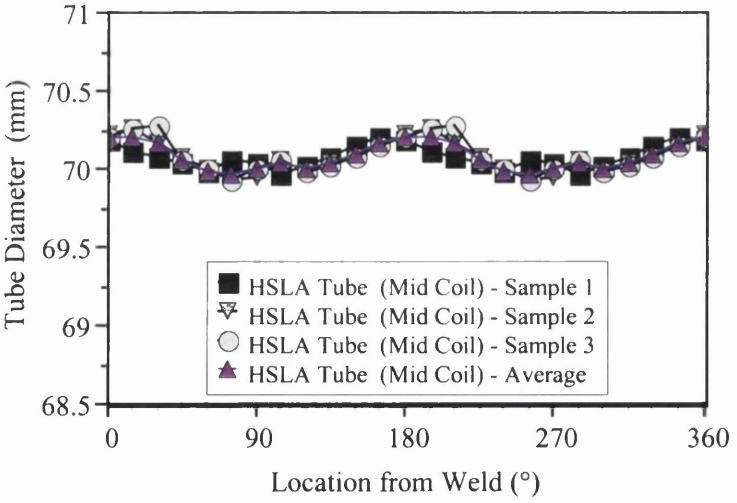

Figure 69: HSLA tube diameter profile (Mid Coil)

End of Coil

As with the front and mid coil measurements, the tube from the end of the coil was found to be inside of the BS 6232 standard tolerance, having a maximum diameter of 70.24mm and an average diameter of 70.10mm, Figure 70. The lowest diameter measurement was 70.01mm at the 120°/300° position.

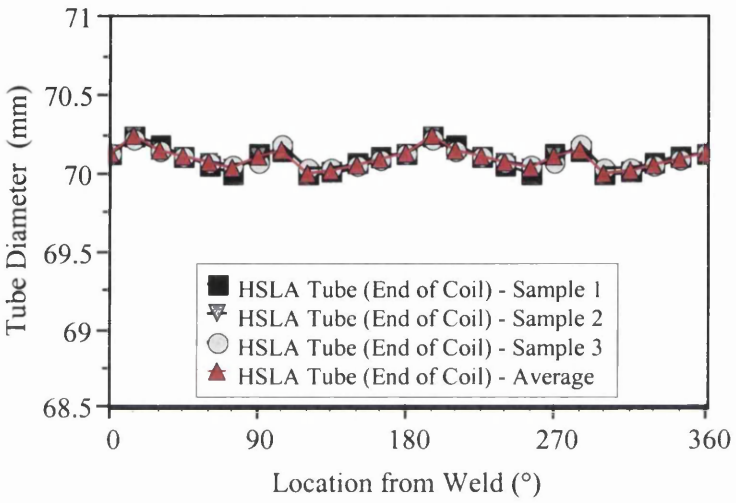

Figure 70: HSLA tube diameter profile (End of Coil)

- ***SS (304)***

The diameter variation of the SS 304 tube is presented in Figure 71. The SS tube displayed a low degree of diameter variation and interestingly the majority of the tube was found to be below 70mm.

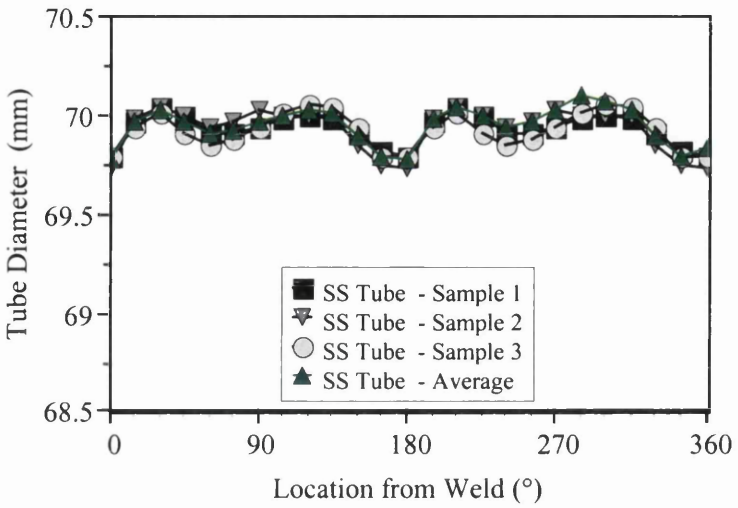

Figure 71: Stainless steel type 304 tube diameter profile

6.2.3 Tube Mechanical Properties

The mechanical properties of the tube metals are compared with the coil data in, **Table 3,** show that: -

- ***FeP04***

In the case of the tube material, the FeP04 was found to have experienced a significant increase in 0.2% proof stress value. The increase was 42.1MPa over the measured sheet coil value average. The measured proof stress was 70MPa higher than the minimum yield value, which is used for design stress calculations. In the absence of a suitable material database or actual test data, the minimum coil proof stress (140MPa) is also used in the Swift (Krupkowsky) formula to describe the true stress-strain behaviour in FE simulations of pressing forming operations. This strong difference between the sheet and tube properties highlighted the need for accurate evaluation of tube intrinsic properties, in order to accurately predict the behaviour of the material in forming or structural performance simulations.

The n-value (n_3) was also found to change significantly, reducing by 12.1% or by 0.026, from 0.214 for the coil to 0.188 for the FeP04 tube. The tensile strength was found to

reduce by 16.4MPa, which is believed to be related to variations in the coil material, rolling and rolling transverse directions and not directly related to the tube manufacturing process. Similar reductions in the uniform and total elongation values were observed, i.e. 1.2% and 0.9% elongation respectively.

- ***FeP10***

The hot rolled mild steel tube displayed continuous stress-strain curves. The mechanical properties were significantly different from the sheet material for the rolling direction. The yield strength was a different type to that observed in the sheet, i.e. it had changed from the discontinuous to continuous yielding due to the work-hardening affect of tube manufacture. Moreover, an increase in measured yield of more than 40MPa was found. In contrast, almost no change in tensile strength (1%) was observed. In addition to the strong changes in yield strength observed, the uniform and total elongation values were substantially lower, 8.3% and 6.6% elongation don on the sheet values. The reduction of almost 30% in uniform elongation also resulted in a significantly reduced terminal n-value, n_T. Due to the strong reduction in uniform elongation, i.e. below 20%, the n-value for the 10-20% elongation range could not calculated.

To obtain a value for the n-value at the higher end of the uniform elongation range, a value of elongation close to, but below the uniform elongation would be required. To directly compare the tube and the sheet would then require the sheet steel to have the n-value calculated over the same strain range. This issue adds strength to the proposition of utilising the terminal n-value, n_T, which only changes with changing uniform elongation.

- ***HSLA***

As in the case of the hot rolled mild steel (FeP10) tube, in terms of yield strength, the HSLA tube displayed continuous yielding behaviour. However, unlike the FeP10 tube material the HSLA tube was found to increase only very slightly (10.9MPa) over its parent slit coil yield strength value. As for the cold and hot rolled mild steel tubes, the HSLA tube showed little change in tensile strength. Similar trends to the other tube materials were observed in terms of reductions in the elongation values, although not as

significant. The uniform and total elongation values suffered a reduction of 3.6% and 2.3% elongation, respectively. The level of reduction in uniform elongation was 17.0.%, compared with 37.7% for FeP10. This compares with a 4.9% reduction in uniform elongation for the FeP04 metal being made in to tube. The change in uniform elongation values illustrates that the reductions anticipated are not directly a function of the diameter and thickness ratio but would appear to relate to the original coil physical properties & chemistry.

6.2.4 Tube Property Variation

From the 10mm thickness miniature tensile tests performed upon the weld and tube parent material samples of the FeP04, HSLA and SS 304 tube metals it was found that weld properties were dependent upon both the material and the welding process used. The variation in parent tube properties also related to the original properties and tube rolling conditions. The findings from the selected tube material studied are decribed in the following section.

- ***FeP04***

The FeP04 tube metal exhibited significant variation in the mechanical properties. The 0.2% proof strength, tensile strength, and uniform and total elongation values around the tube circumference were all strongly affected, Figure 72. The difference between the minimum and maximum measured 0.2% proof strength and tensile strength values was found to be 51.3MPa and the 28.9MPa, with average parent tube values of 207.5MPa and 306.2MPa, respectively. In terms of the parent tube, elongation values showed similarly large variations. The range in values for uniform and total elongation were 4.9% and 13.6%, having average values of 22.4% and 53.1%, respectively. The parent tube 0.2% proof strength appeared to increase at the 15° and 345° positions, i.e. either side of the weld region, whilst the uniform elongation was found to decrease at 345°. The most significant difference was found between the tube weld and the parent tube properties determined. In terms of 0.2% proof and tensile strength the weld was found to be higher

by 189.0MPa and 149.2MPa, whilst in the case of uniform and total elongation values the weld was lower by 13.6% and 21.9%, respectively.

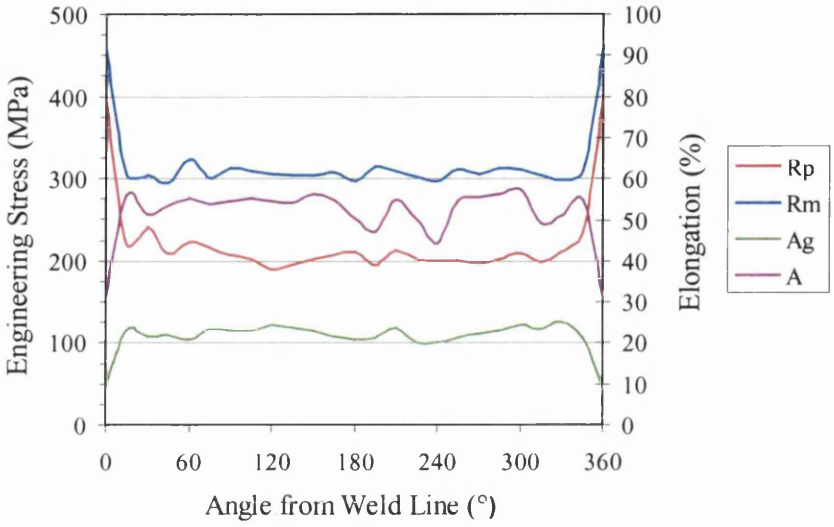

Figure 72: Variation in mechanical properties of FeP04 tube

- ***HSLA***

The HSLA tube material exhibited a close match between front and mid coil test results, despite the differences in material thickness, refer to Figure 73. This illustrates that the variation in properties is directly related to the tube mill set up and processing conditions. The particular tube mill configuration imposes a particular pattern or signature on the tube metal properties. The circumferential variations in mechanical properties displayed by the HSLA parent tube was similar to those of the FeP04 tube material, although differing in magnitudes. The total elongation and 0.2% proof strength values displayed the greatest difference with ranging from 27.6 to 49.8 % elongation. As with the FeP04 tube metal, slight increases in proof strength and decreases in uniform elongation were found with the HSLA tube metal adjacent the weld region, with the weld metal displaying significantly higher strength and reduced ductility to the parent metal. Unlike the FeP04 metal, the HSLA tube metal displayed very little increase in tensile strength, with a total spread of 23.7MPa.

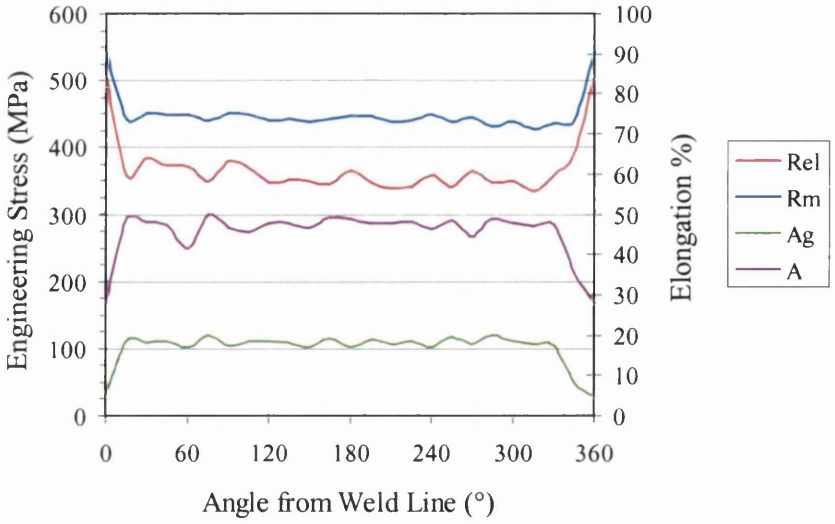

Figure 73: Variation in mechanical properties of HSLA tube (Mid Coil)

- ***SS 304***

From the 10mm thickness length tensile tests performed on the stainless steel 304 tube material at 15° intervals, it was found that the 0.2% proof and tensile strength displayed a reasonable degree of uniformity, Figure 74, when compared with the FEP04 and HSLA ERW tube material results.

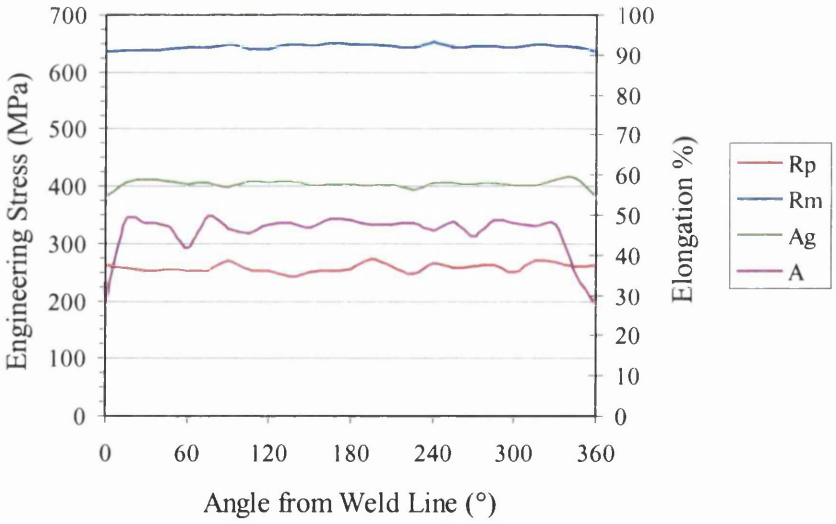

Figure 74: Variation in mechanical properties of Stainless steel tube (304)

Of the two characteristics, the proof strength was found to display the greatest variations, with the lowest measured value of the order of 240MPa, whilst the highest was some 270MPa. The tests also indicate that the weld region displayed almost average tube properties, although it was found to be slightly weaker and would be less formable. The most notable difference was found the in uniform elongation values of the weld and the parent material of the tube. The weld metal displayed a uniform elongation 3.3% (elongation) lower than the parent material average.

6.2.5 Tube Surface Texture Analysis

The 2D texture results for the tube material are presented graphically in Figure 75.

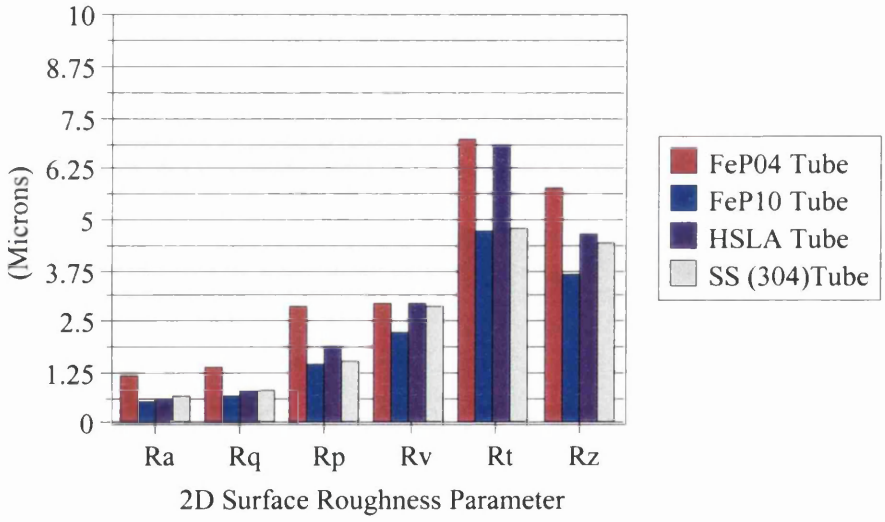

Figure 75: Comparison of average 2D surface texture parameters of tube materials

(Ra = mean surface roughness, Rq = rms roughness, Rp = peak height, Rv = valley depth, Rz = profile height for sample length, Rt = profile height for evaluation length).

On comparing the three tube materials with the parent sheet materials, significant changes in surface roughness, peak height, valley depth and total profile height were observed. The changes in the surface texture characteristics were different for each

material. Figure 76 illustrates a typical representation of the FeP04 coil and tube material 3D mean surface roughness profile, Sa.

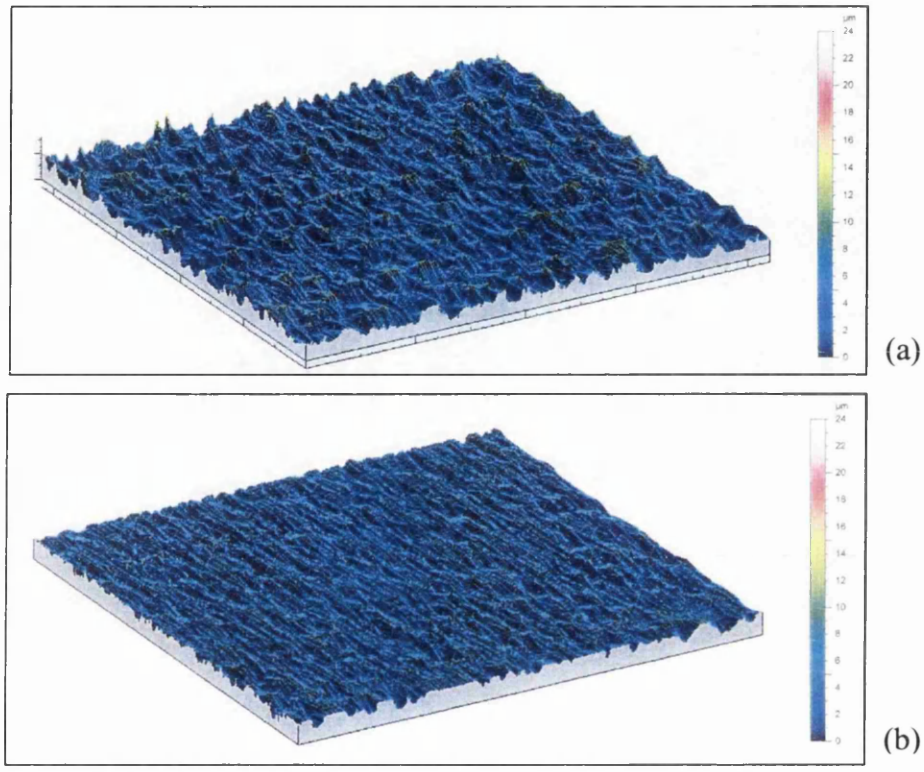

Figure 76: FeP04 3D surface roughness (Sa) representations (a) coil and (b) tube

Table 5 outlines the key 2D surface texture changes based upon the 2D measurements performed on the coil and tube materials.

	Change in Surface Texture Parameter (%)			
Material	**Ra**	**Rp**	**Rv**	**Rt**
FeP04	-12	-16	-4	-17
FeP10	-59	-47	-44	-42
HSLA	-38	-28	-31	-30

Table 5: Changes to coil 2D surface texture parameters after tube manufacture

The FeP04 tube material was found to have the least change in texture between coil and tube. The changes for FeP04 were of the order of 12%, 16%, 4% in Ra, Rp, and Rv respectively.

In contrast, the changes to the coil due to tube manufacture for the FeP10 steel were far more significant. A reduction of 59% in Ra was found, whilst the peak height Rp was reduced by the order of 47%. The reduction in the valley depth was reduced by an almost equivalent value (44%) in comparison with the peak height.

In the case of the HSLA the changes were not as dramatic as those observed with the FeP10 hot rolled grade although a stronger reduction than the FeP04 metal was observed. The reductions included a 38% reduction in Ra, a 28% reduction in Rp and a similar reduction of Rv (31%).

Although the no changes were measurable for the stainless steel tube, the texture results displayed for all of the characteristics were comparable to the FeP10 tube metal.

6.3 Small Scale Evaluation of Lubricants

6.3.1 Percentage Draw Versus Blank-holder Load

The results of percentage draw versus blank-holder load for the MSD test that were performed on the FeP04 coil material samples is shown in Figure 77.

The MSD test samples that utilised the dry film lubricants displayed a significant difference in behaviour to those without lubricant for all three of the coil metals tested. The behaviour displayed for all the metals was generally similar, i.e. the use of the lubricants increased the level of draw demonstrated by the samples, therefore raising the curve of percentage draw versus blank-holder load. The steels in the unlubricated condition all exhibited approximately the same level of draw at the maximum blank-holder load, i.e. between 2.5 and 5.5%.

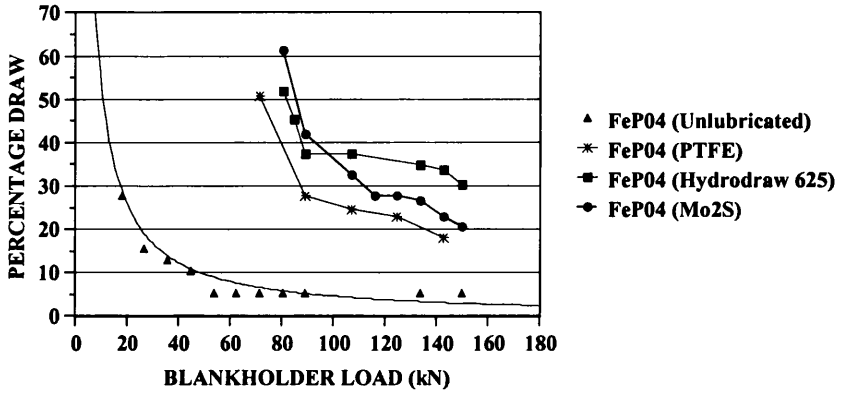

Figure 77: Relationship between blank-holder load and percentage draw in Modified Stretch-Draw (MSD) tests on FeP04 coil using different dry film lubricants

Whilst there was a significant observable difference in behaviour between the different coil materials, there was moderately less difference displayed between the lubricated samples of each material. The lubricant that displayed the highest percentage draw, indicating superior press performance, at the higher blank-holder loads was the dry film lubricant Hydrodraw 625. For the HSLA and FeP10 coil metals the low friction lubricant Mo_2S displayed a percentage draw 4% lower than Hydrodraw 625. However, in strong contrast the FeP04 coil material displayed a more pronounced difference in lubricant performance between the lubricant Mo_2S and Hydrodraw 625. Out of the dry film lubricants used on the FeP04 coil material, the PTFE dry film lubricant provided the worst press performance, achieving 18% draw compared with 30% using Hydrodraw 625, for the highest blank-holder load used.

In the case of the MSD tests performed on the FeP04 coil material, the dry film lubricants not only raised the percentage draw – blank-holder load curve, but also shifted the curve dramatically to the right. For the lubricated FeP04 material, under blank-holder loads of less than 72kN, the samples did not experience fracture when using the dry film lubricant. However, in the unlubricated condition, the samples fractured at blank-holder loads of more than 18kN.

6.3.2 Fracture Height

The results of fracture height versus blank-holder load for the MSD test that were performed on the FeP10 coil material are shown in Figure 78.

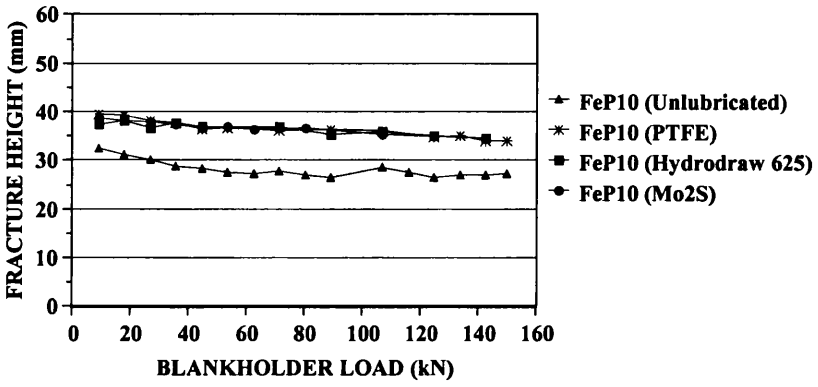

Figure 78: Relationship between blank-holder load and fracture height for FeP10 slit coil in Modified Stretch-Draw (MSD) tests using different dry film lubricants

In the unlubricated condition, the fracture heights observed for all of the steel samples were found to be almost constant for blank-holder loads above 37kN. This minimum fracture height was approximately 27mm compared with the 25mm punch radius, that was used. However, the lubricants increased the fracture height. As in the case with percentage draw, the largest value of fracture height were observed in the tests on steel samples that used the Hydrodraw 625 dry film lubricant. The hot rolled materials displayed less draw and therefore their corresponding fracture heights were lower.

6.3.3 FLD Signatures

The strain profiles measured for a blank-holder loads in the range of 63kN to 81kN. The reason for this was that, firstly it was not possible to measure the strain profiles relating to a percentage draw, as they differed widely. Secondly, under the selected hydroforming conditions, the strain profiles of the experimental hydroforms would be compared on a basis of processing conditions not on the degree of draw. The strain profiles are presented for each metal, illustrating the influence of the lubricants on the FLD signature. The FeP04 metal displayed a significant degree of draw, indicated by the high levels of minor

strain. The high level of minor strain displayed by the FeP04 sample corresponded to the sample flange in the case of the lubricated samples. High levels of negative minor strain were also experienced by the sample in the vicinity of the sample relating to the draw radius, although the measured values of major strain were lower.

In contrast the flange of the unlubricated samples experienced only plane strain deformation, with typically less than 10% major strain deformation. The strain at the crown of the unlubricated sample was also found to exhibit strains closely emulating plane strain. A low level of biaxial strain was noted, despite the fact that the sample was subjected to a lighter blank-holder load. The lubricated samples displayed stronger levels of biaxial deformation, with the most biaxial displayed by the sample lubricated with Hydrodraw 625. Interestingly, the experimental FLC illustrated clearly the failure at the pole of the each of the samples measured, supporting the experimental FLC tests using the Nakazima strips.

Unlike the FeP04 steel, the mild and high strength steels did not display the same form of drawing deformation. Thus, although the flange of the cup sample did 'draw-in' it did not follow the same mode of deformation. The mode of deformation observed in the cup flanges was characteristic of compression, whilst that of the FeP04 sample close to pure shear. The FeP10 and HSLA steels were found to have experienced higher levels of positive minor strain at the crown of the samples for similar and lower blank-holder loads, even for the unlubricated samples. Consequently, the failure points for most of the FLD signatures measured were to the right of the experimental FLCs.

6.4 Design & Manufacture of Tube Hydroforming Research Tooling

6.4.1 Background

In order to achieve the aims set out in the programme objectives in Chapter 3.0, a hydroforming tool design was selected that would have a number of key characteristics in order to establish the following:

- Develop or verify a suitable failure model for tube hydroforming
- Influence of processing conditions on steel behaviour
- Influence of processing conditions upon external component corner radii
- Influence of steel properties on process
- Develop a tube hydroforming process model
- Influence of pre-forming configuration on component geometry

6.4.2 Design Features

To achieve these aims a tooling design was selected with suitable attributes that would allow such investigations. To meet all of the requirements would be difficult and whilst some may be identified others may not.

- ***Global and Local Expansion***

The most important of the aims would be to establish the practical FLC and establish the validity of the analytical tube FLCs for the metals that were studied, something that is not easily established by other forms of experimentation. In doing so a suitable change in the tube perimeter would be required to initiate failure by bursting. However, the minimum component radius would need to be at least 3-3.5 times the tube wall thickness to avoid shear effects. Therefore a 5mm radius was selected as the minimum external component radius, which was compatible with the FeP04 tube, which was the first of the steel tube metals obtained. An estimation of the forming pressure required to deliver the 5mm

component radius was 1500Bar, based upon Bikert's proposed theoretical internal pressure-corner radius relationship [34]. However, to develop a similar corner radius in the HSLA tube would require almost 4000Bar and would be at the upper limit of the Anton Bauer hydroform press capability. Additionally, the estimated sealing forces to maintain this pressure would also exceed the machine capability.

The initial tool sectional design was selected to cause failure when insufficient axial end feed was applied. A perimeter (global) expansion of above the FLD_0 value was considered for the initial design. For typical sheet metals the FLD_0 value would be of the order of 30% or higher. However, no estimation of the local expansion could be made in the absence of an accurate process model.

- ***Design Constraints***

Instead of utilising a square centre section a rectangular section was opted for, as this would also illustrate the influence of component geometry on the strain distribution of the component. However, it was also important to ensure that some contact was maintained between the tool and the tube. Otherwise a free forming mode of deformation would have resulted. This would then have caused the tube to expand to the level of diffuse instability strain, considerably below the FLD_0 value. Subsequently, the tube would be expected to burst and therefore not achieve a high level of component fill. Another reason that at least one length of the tool cavity would have to be 70mm was that minimal, if any pre-strain of the tube in the region of expansion segment was required. This was to ensure that the strain paths would be as linear as possible. By doing so it would be possible to study the influence that pre-strain from a pre-forming operation would have.

The expansion tooling design was also to integrate with the segmented tooling at Welsh Technology Centre, used for European Coal & Steel Community (ECSC) research activities on the influence of tube hydroforming on component performance. The constraints from this tooling would mean that 70mm diameter tube would be required. The ECSC tooling was segmented and devised for producing $60mm^2$ box sections, having 10mm corner radii, for impact and torsion trials. The segments could be modified

to change the length of the box section produced by either selected an arrangement of 3 or 5 segments along the component length. The end segments of the tooling consisted of an upper and lower tool set each. Along the length of these tool segments the tooling incorporated; the tube guide region, a box region and a transition region, linking the two different sections. The change in section between the tube and the $60mm^2$ box section would be approximately 1.3%, although a higher degree of strain may be expected at the component corners. The remaining tool configuration consisted of upper, lower and side tool segments enabling pre-forming within the hydroforming die during tool closure.

It was decided that it would be possible to substitute the set of upper, lower and side tool centre segments with segments from the new tool design. This would place a further requirement on the new tool design. This further requirement would be the necessity to have a transition between the $60mm^2$ box section and the expansion tooling within the length of the tool segment (200mm).

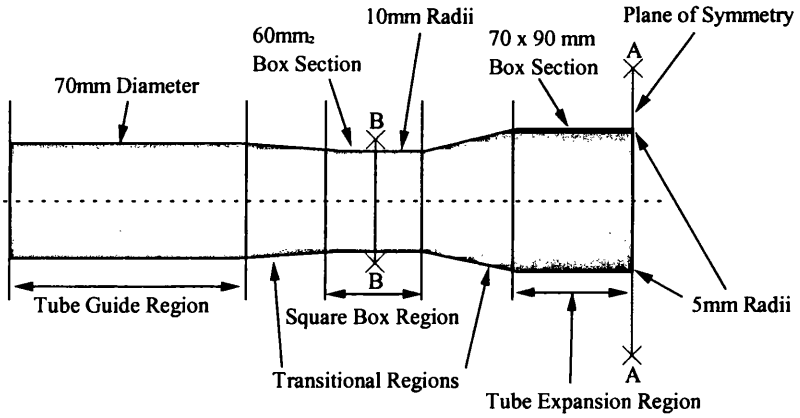

Figure 79: Schematic illustration showing initial concept design for the research tube hydroform tooling (Left-hand side only)

The initial concept design was base upon FeP04 sheet metal properties. Therefore an expansion section of 70mm x 90mm was assumed, having an expansion of 41% just above the FLD_0 value (40%), shown in Figure 79. As this section was considered to be

too severe, an alternative section of 70mm x 80mm was to be considered following the findings from the FEA.

6.4.3 Assessment of Die Design

The initial design was evaluated using the Pam-Stamp FEA software code. The analysis of the initial design was performed for the tool centre segment configuration only and not for the full component tooling. To obtain an initial feasibility statement, the FeP04 tube blank was evaluated by simulating the processing conditions of various linear axial compressive force to pressure relationships. The metal parameters considered were those relating to the tube metal only, i.e. ignoring the weld line. The simulation parameters that were used are given in Chapter 5.0 FEA of the tube hydroforming process.

It was quickly identified that whilst, it may be possible to achieve a component with such a geometry. The process window was found to be very narrow. Moreover, suitable forming conditions would require an applied axial force to be as close as possible to the sealing force. Consequently, this would mean that there would be little scope for modifying process conditions. If the full tooling were to be modelled it would be anticipated that the wrinkling susceptibility could reduce slightly. However, a significant increase in the component thinning would take place, which would be expected to be higher for the sealing force relationship as minimal compressive force is applied.

- ***Initial evaluation of hydroforming tooling***

A decision was therefore taken to analyse the less severe expansion geometry of 70mm x 80mm having 5mm corner radii. Initially, half models of the tube and tooling were created, see Figure 80, in order to speed up analysis times. The aim of this FEA was to establish the suitability of this geometry to provide the necessary data to meet the project aims. Based purely upon constancy of volume the estimated expansion would require 66.25mm of end feed from each tube end to maintain the tube wall thickness, i.e. minimise wall thinning. Offsetting the tube wall thinning, to prevent component splitting, would be difficult as the section was variable and may result in localised thinning not only global thinning. The tube FLC, as described by Darlington et al [113], was used as a

means of predicting component failure in the absence of a known analytical model. By utilising this type of experimental FLC, an underestimate of the actual forming limit of the tube metal was likely and therefore would provide a greater degree of safety.

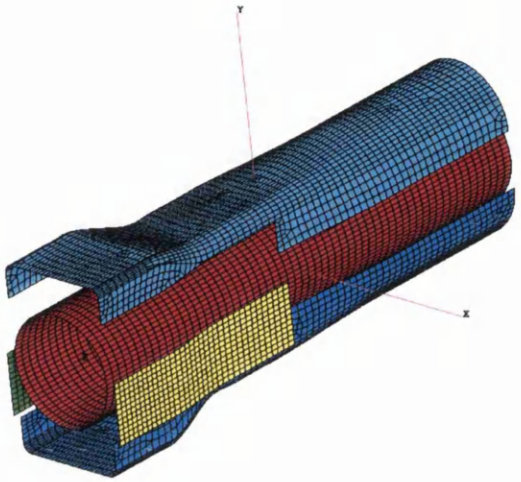

Figure 80: Image of FEA half model for FeP04 tube and hydroforming tooling design

However, as no friction data was available, a sensitivity analysis was performed using FEA. Initially, this was performed using a global coulomb friction coefficient in the range of 0.1 to 0.3, in the knowledge that typically for pressing simulations a global value of 0.15 is used [132]. Liu et al also utilised a friction coefficient value of 0.1 in tube hydroforming analyses in which they claimed the analysis results provided reasonable accuracy [152]. However, it was unknown what a suitable representative value of Coulomb friction coefficient would be in practice and what influence different types of lubricant, fluid or dry film, would have on the forming behaviour. As anticipated, the component geometry was found to be sensitive to friction in the analyses. Modifying the friction coefficient value governed the degree of total end feed during hydroforming before (predicted) failure took place. Figure 81, illustrates the FEA results, in which a friction coefficient of 0.1 and a superimposed axial feed rate of 3.3 mm/s (scaled by 1000), caused (predicted) failure in the tube hydroform. Failure was predicted by the model strains, which exceeding the experimental tube forming limit curve, given in the FLD plot in Figure 81a. The pressure at which the tube FLC was exceeded was 495Bar,

therefore indicating the likely bursting pressure to be 495Bar. This analysis assumed uniform tube properties. In practice the variation in properties and thickness could cause failures at lower pressures, proportional to the FLC-10%. However, depending upon the High levels of strain were experienced in the expanding centre section. Strains exceeding the material uniform elongation were present at the corners of the expansion zone. The FEA predicted failure (necking strains) actually took place in the side wall elements, directly adjacent the corners of the expansion zone, Figure 81b.

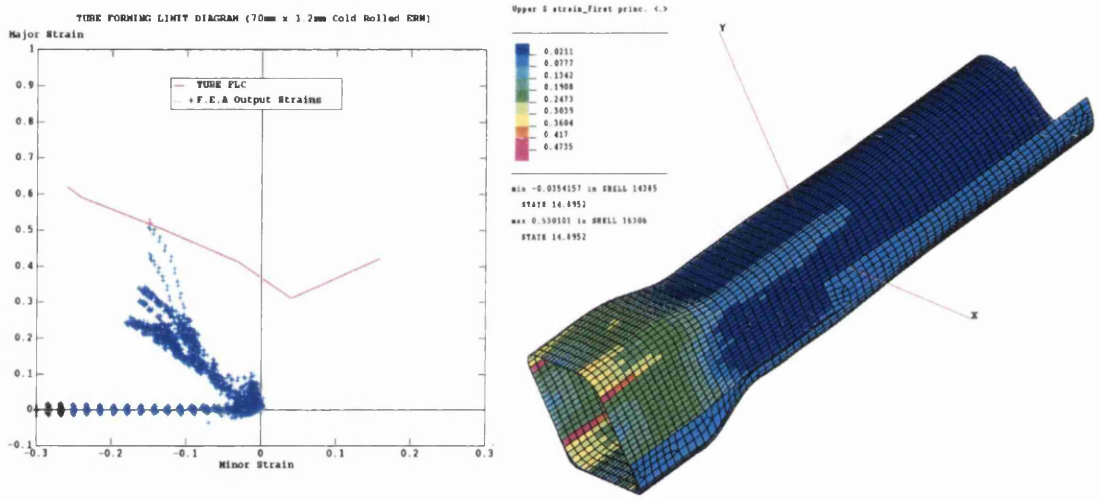

(a) (b)

Figure 81: FEA results indicating necking/splitting at 495Bar internal pressure predicted by experimental tube FLC (Hydroforming process conditions: 0.06625mm/Bar feed rate, FC=0.1), (a) FLD plot of hydroform analysis at 495Bar and (b) Major Strain contour plot.

The high level of compressive strain displayed at the tubes ends / guide region of the hydroform, resulting in wall thickening is shown in the FLD in Figure 81a, characterised by an almost zero value of major strain and high levels of negative minor strain. However, with an increased feed rate of double this value, an improvement in the forming conditions was predicted, with failure taking place above 715Bar, and a substantial improvement in the fill-out of the expansion section of the hydroform. The

friction coefficient increased the degree of compressive minor strain in the tube end, preventing the flow of material into the expansion region of the die cavity.

The model illustrated that failure was likely to take place under the forming conditions specified. In practice, it was considered that it could be possible to modify the forming conditions with the use of low friction lubricants such as Mo_2S or PTFE. Therefore a series of tests were performed to identify suitable lubricants to assist in hydroforming the tube materials. Contact was also made with a lubricant supplier who was developing a hydroforming lubricant.

6.4.4 Design and Manufacture of Hydroform Die Tools

- ***Issue of CAD Drawings and Supplier Nomination***

Based upon the findings of the FE analyses, the tool geometry would enable the key characteristics to be fulfilled, providing FLD data and enabling verification of the FEA models developed. Consequently, committal to the tooling design was made. CAD drawings were prepared by Welsh Technology Centre CAD centre, based upon details from the Anton Bauer tooling drawings of WTC's hydroform tool segments. The new drawings developed were for the central expansion segments, the lower die segment of which is shown in Figure 82.

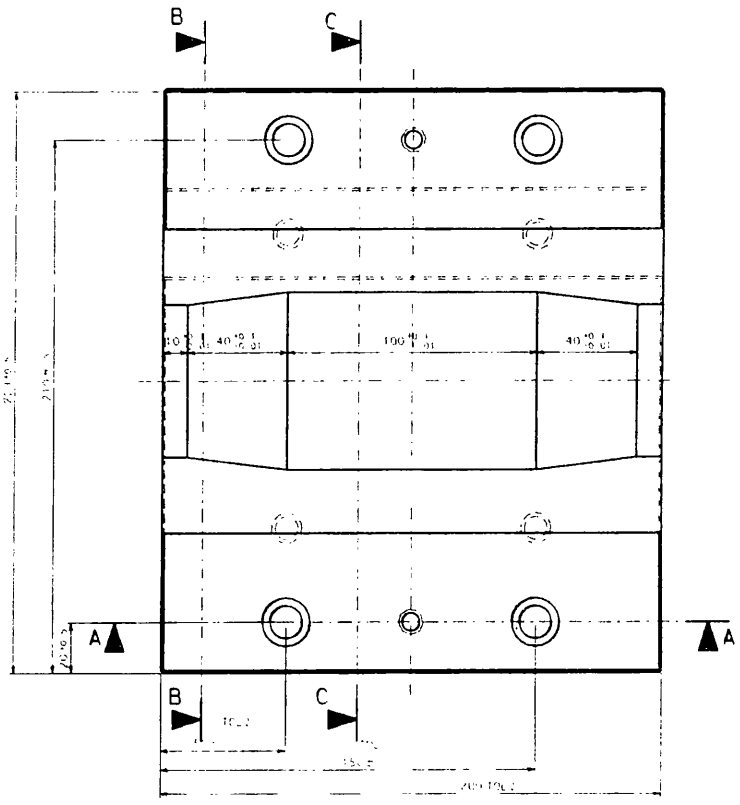

Figure 82: Image of CAD drawing of lower hydroforming die tool (expansion) segment

The additional details of tooling geometry that was used to create the surfaces for the full hydroforming FE models, were obtained from the Anton Bauer tooling drawings. Quotations were obtained from a number of local BSSP approved suppliers. Neath Precision Engineering Ltd (NPE) were selected to manufacture the hydroforming tooling expansion segments on the basis of the lowest quotation, shortest lead-time and previous history.

- ***Tool Material Specification***

The tool material specified for the research tube hydroform die segments was kept consistent with the Anton Bauer tooling. The equivalent tooling specification was BD2 [180] or D2 tool steel. The tooling required a final Rockwell hardness specification of Rc 60, in accordance with the Anton Bauer CAD drawings and die repair section of the operation and maintenance manual [181]. The tooling also placed a further requirement of a polished finish to match the other tooling. In order to achieve this, NPE were

supplied the centre segments of the 60mm^2 box section tooling. This was also to ensure that whilst the drawings were provided as a manufacturing guide, the segments were manufactured to match, ensuring a good fit with the remainder of the segments.

- ***Tool Segment Manufacture***

Specific manufacturing requirements were placed upon NPE due to the nature of requirements for manufacture of the steel die tool metal. This was primarily the requirement of stress-relief annealing after an initial machining operation. The stress relief anneal was performed at a temperature of 650°C for 12hrs, followed by a furnace cool for 24hrs. For the side tools, the general profiles were achieved by electro-spark erosion with a wire filament, ensuring sufficient metal remained to provide the final finish. All of the drilling operations were performed in the 'as annealed' tool condition. The heat treatment process was performed by Bodycote Heat Treatments Limited, using a vacuum furnace and specialised jigging to avoid distortion of the tools. On return of the segments, final milling and grinding operations were performed with the tooling in the hardened and tempered condition to achieve the required final tolerance dimensions and finish.

6.5 Experimental Tube Hydroforming Trials

6.5.1 Initial Trials

During the initial trials, FeP04 tubes that had a light covering of mill oil were hydroformed with increasing levels of end feed to trial the tooling. However, it was quickly discovered that the components were all splitting, even with an axial end feed of 40mm applied at either end of the tube. The reason for the splitting of the tubes was a result of friction, which was preventing tube material flow into to the expansion region. Instead it was being consumed in the tube guide region of the component in the form of thickening. Furthermore, no further end feed was possible as the tube ends were developing sharp fins with increasing end feed, in attempt to form over the (tapered cone) tube end seals, between the seals and the surrounding die tooling. Consequently, this may have resulted in damage to the hydroformer end seals and tooling if pursued. The fins developed due to the type of sealing mechanism used, i.e. tapered cone, but also due to the high frictional effects between the tube and die tools. A similar effect was observed when attempting to hydroform the FeP04 and stainless steel 304 tubing with a PTFE lubricant. Therefore, it was necessary to utilise a higher performance lubricant that would be compatible with the filtration system. The lubricant that was found to be the most suitable was the dry film lubricant Hydrodraw 625, which dried as an almost transparent film suitable making circle strain analysis easier as the lubricant was soluble in water and easier to remove than Mo_2S. The hydroforming trials using Hydrodraw 625 were proceeded by the MSD tests to evaluate its performance.

During the initial trials, additional issues arose, which largely related to the die tool witness lines. The witness lines were due to the tool split lines, which generated witness markings at high pressures as the material attempted to squeeze between the die segments. To minimise the effect of the witness lines caused by the tube metals being squeezed into the dies separating lines aluminium adhesive tape was used to patch over the split lines, between the lower and side tools and the upper and side tools. This method was found to be effective at pressures up to approximately 1000Bar, above which

significant tool deflection, either from elastic deformation or tool movement, would cause the witness lines to initiate splitting of the tube blanks. This issue was exacerbated, as the split lines were perpendicular to the direction of major strain, i.e. the witness lines would be parallel to any potential crack and may cause crack initiation.

6.5.2 Tube Hydroforming Process Trials

The main tube hydroforming trials therefore had a number of constraints imposed on them. Further to the frictional and witness line effects, the hydroforming process conditions required simplification due to the fact that the Anton Bauer press did not posses any data acquisition facility, only a visual screen trace. The simplification was important as the FE models of the process could be developed based upon minimal information, i.e. a simple pressure gradient, maximum pressure and defined axial force to pressure gradient or axial end feed rate. As there was no acquisition processing controlled by axial end feed (displacement) was opted for as the tube length, and therefore the axial feed, could be checked after hydroforming.

From the initial tests performed on the tube metal without lubricant or lubricated with PTFE, it was not possible to form the expansion section. Thus all of the tube blanks used exhibited necking or fracture, FeP04 and SS 304.

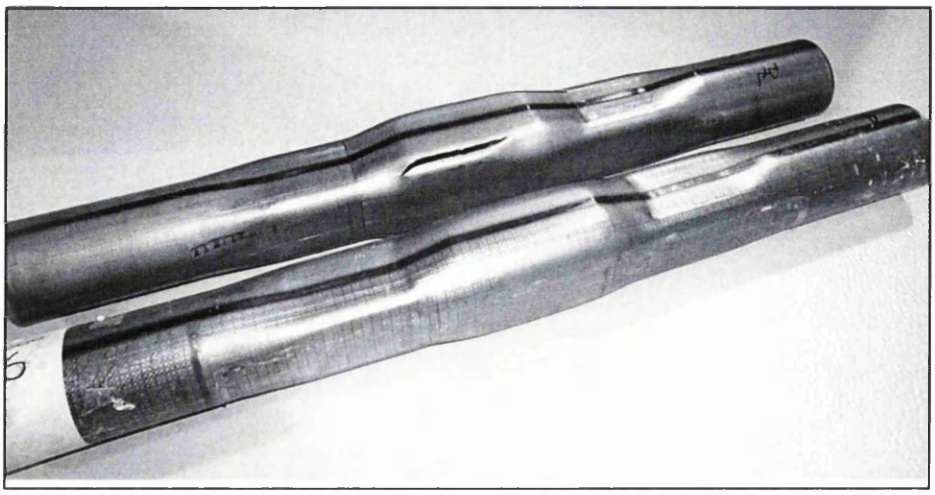

Figure 83: Photograph illustrating influence of lubricant on component thinning. Hydroformed FeP04 tube displaying split was unlubricated (Failure pressure 460Bar, 0.2mm/s feed rate or 0.004mm/Bar feed rate). Hydroformed FeP04 tube not displaying split was lubricated with Hydrodraw 625 (Max. forming pressure 700Bar, 0.2mm/s feed rate or 0.004mm/Bar).

The influence that the low friction lubricant Hydrodraw 625 had is illustrated by Figure 83. An unlubricated FeP04 tube, using an axial end feed rate of 0.004mm/Bar, burst at 460Bar. Whilst the FeP04 tube, lubricated with Hydrodraw 625, did not display a split or signs of necking at 700Bar, even though an axial end feed rate lower by factor of 10 was used. However, under this low feed rate a greater variation in burst pressures was found for the lubricated FeP04 tube. The failure pressure ranged from 680Bar to 790Bar. Figure 84 shows a FeP04 tube which was formed up to a maximum pressure of 760Bar and suffered catastrophic failure from bursting/splitting.

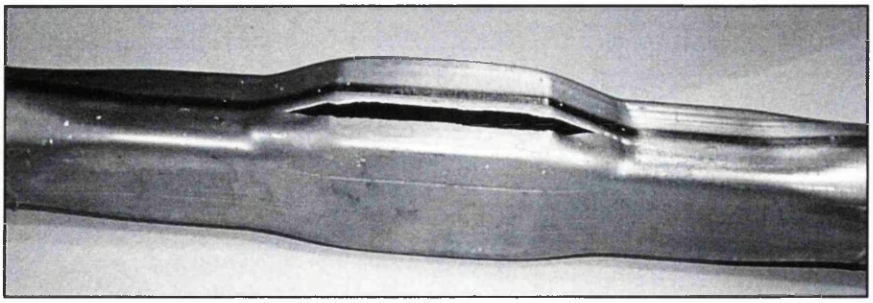

Figure 84: Photograph showing lubricated FeP04 tube, which burst at 760Bar (0.2mm/s or 0.004mm/Bar feed rate)

The influence of the process parameters used had a significant influence upon the strain distributions and ultimately governed the ability to fabricate the component, i.e. successfully formed or failed by splitting (bursting) or wrinkling.

The degree of difference in the response to the hydroforming conditions used varied between the steels. In general, it was found that by increasing the feed rate the success of forming increased. This may be seen from Figure 85, in which the FeP04 component formed safely, exhibiting a higher degree of corner and feature fill out at the higher pressures in combination with the 0.025mm/Bar feed rate. However, the actual response of the tube material and thickness would dictate whether or not the component would form successfully

The HSLA tube failed to achieve a suitable geometry, as deep wrinkles were still present in the component. For the same conditions, the extra deep draw quality FeP04 tube filled the corner radii of the component. Thus, between the three components, a marked difference in the sharpness of the expansion zone features (radii) exists.

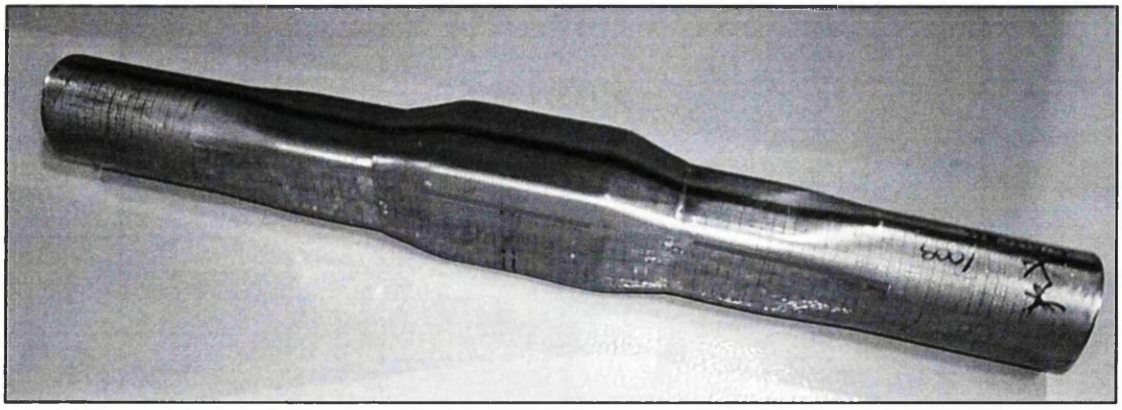

Figure 85: Photograph illustrating high degree of corner and feature fill out displayed by the FeP04 component formed with an internal pressure of 1000Bar and a feed rate of 1.25mm/ms or 0.025mm/Bar (Lubricant : Hydrodraw 625) .

- ***0.2mm/s (0.004mm/Bar) Feed Rate***

The FeP04, FeP10 and HSLA tube materials, lubricated with Hydrodraw 625, all experienced failure due to necking/fracture as a result of insufficient metal feeding of metal into the expansion region. For the FeP04 metal the failure pressures were all of the order of 750-800Bar, with necking taking place on the top face of the component, usually occurring between the corner radius and the weld line. The failures that took place were found to generally coincide with roll-forming lines or markings that were present on the tube metal. No failures took place in the weld-line, confirming the weld integrity. In the case of the HSLA and FeP10 tubes, necking developed in the expansion section of the component on the centre of the faces having the longest sides (80mm).

Under this specified feed rate, the bursting pressures for the FeP10 tubes were found to be of the order 550 to 650Bar and for the HSLA tubes the bursting or local necking pressures were found to be of the order 750 to 900Bar. In strong contrast to the other tube materials, the stainless steel tube metal did not fail by necking or fracture when a feed rate of 0.004mm/Bar was used. However, the level of thinning associated with these forming conditions was consequently high (>15% at 700Bar), based upon the ratio of

major to minor strain. Therefore, it would be unlikely to be suitable for a structural component in terms of component durability and crash performance as a result of thinning. Additionally, a degree of the work hardening capability may have been expended in this large deformation.

Under the constant feed rate condition of 0.004mm/Bar, difficulties were observed in achieving a continuous ramp up of the pressure curve and in each cycle a drop in pressure was experienced. This fact lead to difficulties in obtaining the desired maximum pressure. Whilst only a very small level of end feed was used (0.004mm/Bar), the magnitude of negative minor strain was still considerable, of the order of 10 %. This fact may account for a rapid reduction in the sealing capability, as the tube would have effectively been drawn in to the die cavity and therefore temporarily come off the end seals, thus resulting in a pressure drop. In the case of the stainless steel tube, difficulties were found in obtaining the maximum pressure of 1000Bar, and maximum pressures of between 930Bar and 970Bar were achieved. Consequently, this would have an influence upon the development of the corner radii.

This case illustrates the difficulty of utilising a constant feed rate for a component with a complex geometry and the requirement of dedicated processing conditions to account for the behaviour of the metal, friction and tool geometry combination.

The fabricated TWTs that were produced were capable of being formed to a pressure of 700Bar without thinning excessively, i.e. below 20.

- ***0.625mm/s (0.0125mm/Bar)Feed Rate***

Under this feed rate condition the FeP04 tube was found to be on the borderline to failure. Whilst not displaying necking or fracture the surface texture of the components were found to be exhibit strong similarities to a necked region. Unlike the FeP04 tube metal, the HSLA steel did not form successfully and failed at pressures between 800 and 900Bar, Figure 86. However, it was noted that, in using this feed rate fewer difficulties

were experienced in achieving the desired pressure cycle than when a feed rate of 0.2mm/s (0.004mm/Bar).

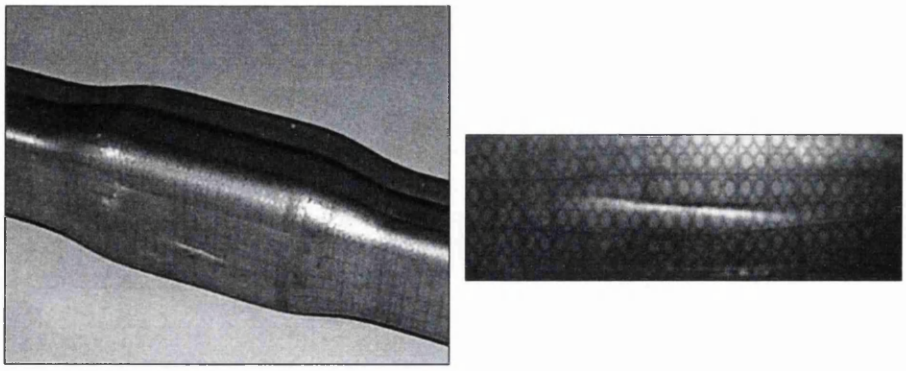

Figure 86: Images of HSLA hydroform displaying necking in side wall (900Bar).

- ***1.25mm/s (0.025mm/Bar) Feed Rate***

With this feed rate, none of the tubes tested failed due to necking or splitting. However, the HSLA tube metal experienced 'body' wrinkling, i.e. wrinkling in the body of the component not just at the component ends/ guide region. From examination of the HSLA tubes tested the wrinkles developed at approximately 500Bar. The wrinkles were perpendicular the direction of metal feeding as would be expected. With increasing pressure, the wrinkles were minimised although not removed, even at 1000Bar. Although the corner radii were not completely filled under these forming conditions the majority of the component detail was filled. The wrinkles or folds partly prevented the filling out of the corners in the case of the HSLA. The stainless steel tube metal also did not fill the corners at this pressure. However, the FeP04 tube metal did fill the corner radii on the tubes top face. Interestingly, as with the other tube metals the corner radii around the component were not equal, with the corner radii of the top face being considerably smaller than the lower face.

6.5.3 Experimental Strain Profiles

Due to the almost symmetrical nature of the experimental tube hydroform geometry, the components formed showed little difference between the measured strain profiles LA and LB, as illustrated by Figure 87.

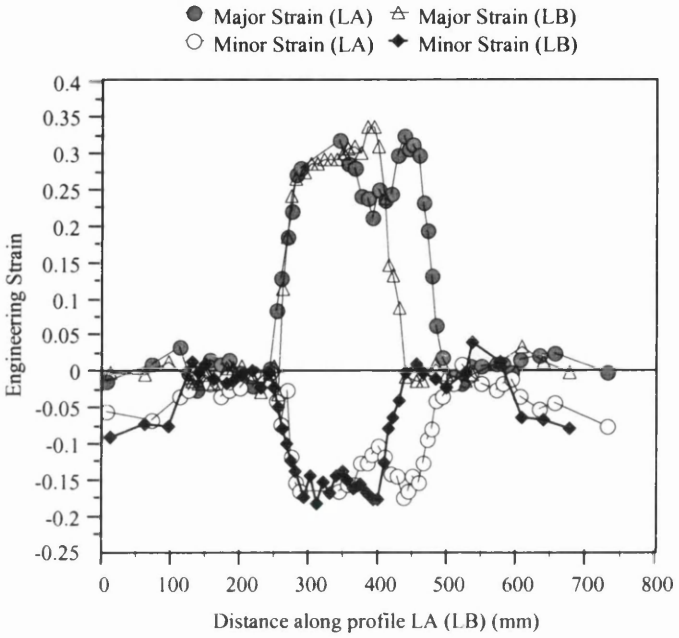

Figure 87: Comparison of experimental strain profile LA and LB for FeP04 hydroform (1000Bar, 1.25mm/s (0.025mm/Bar) feed rate).

The principal difference that was demonstrated was that the longer length of line, corresponding to LA, across the expansion region, introduced a greater average level of strain than for profile LB. However, as anticipated the highest strain belonged to LB as the profile length corresponded to the widest face of the rectangular expansion section.

The different processing conditions caused differences in the forming behaviour of the tube blanks for each metal and between metals. With increasing internal pressure the metals displayed an increase in the magnitude of strain displayed, particularly at the expansion region. The most notable difference in behaviour was observed for the 70 x 2.0mm HSLA tube, which displayed very different forming characteristics and therefore

component geometry for the different feed rates. From the major and minor strain plots of the experimental tube hydroforms (Figure 88) the major strain profiles displayed by the tubes were not equal or closely matched by the level of developed minor strain.

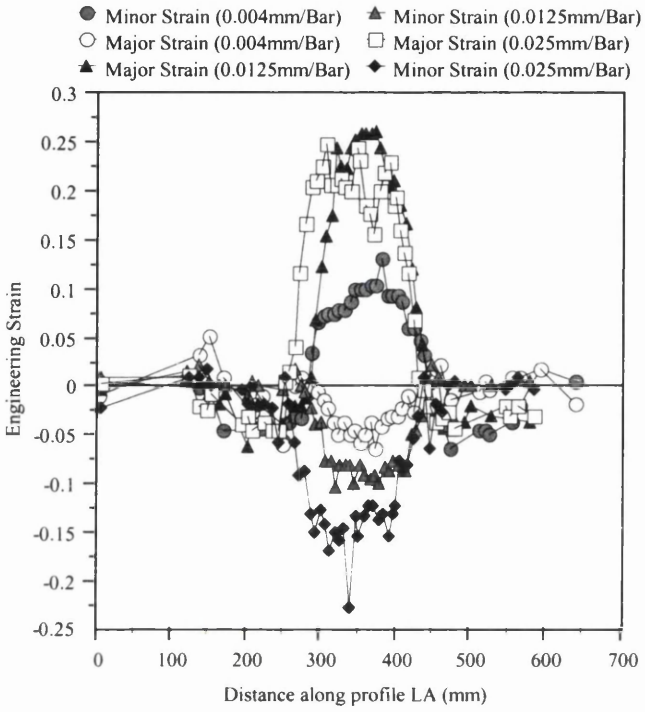

Figure 88: Comparison of experimental strain profiles (LA) for HSLA experimental hydroforms formed at a maximum internal pressure of 500Bar using different feed rates.

This lack of balance between the two strain profiles illustrates the high thinning tendency for the tube hydroformed using a 0.625mm/s (0.125mm/Bar) feed. However, under a 1.25mm/s (0.025mm/Bar) feed rate the major strain and minor strain distributions were found to be considerably non-uniform, as a result of the component wrinkling. Under the 0.2mm/s (0.004mm/Bar) feed rate, the level of major that was determined for the profile LA was considerably lower than that of the intermediate and high feed rate of 0.625mm/s (0.0125mm/Bar) and 1.25mm/s (0.025mm/Bar), respectively. The maximum major strain value achieved was below 15% for the 0.2mm/s (0.004mmBar) feed rate compared to

26% and 25% for the 0.625mm/s (0.0125mm/Bar) and 1.25mm/s (0.025mm/Bar) feed rates, respectively.

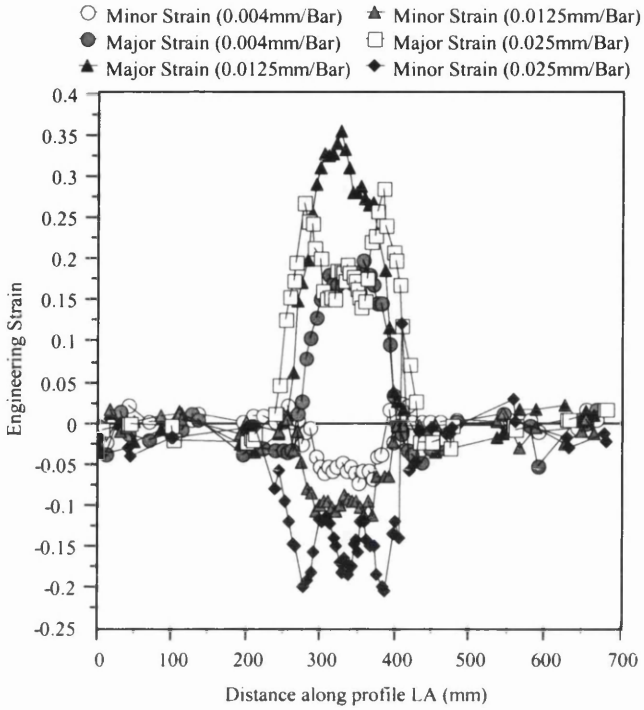

Figure 89: Comparison of experimental strain profiles (LA) for HSLA experimental hydroforms formed at a maximum internal pressure of 700Bar using different feed rates.

On increasing the pressure to 700Bar the profiles change dramatically, see Figure 89. The maximum strain for the component subjected to a feed rate of 0.625mm/s (0.0125mm/Bar) was some 35%, approximately a 10% increase, coupled with less than 1% increase in the corresponding negative minor strain. However, the profile displayed for the 1.25mm/s (0.025mm/Bar) feed rate was found to have almost equal levels of major and negative minor strain indicating significantly lower levels of component thinning. In contrast, the magnitude of the major strain of the tube having a feed rate of 0.2mm/s (0.004mm/Bar), was found to be equal to the level of strain at the centre of the 1.25mm/s (0.025mm/Bar) feed rate component, whilst experiencing less than 7% negative minor strain. This also indicated the high level of component thinning. Whilst the processing conditions caused the degree of difference in profile LA, as described,

there was also a similarly strong difference in the component geometry as might be expected from the strain profiles, see Figure 90.

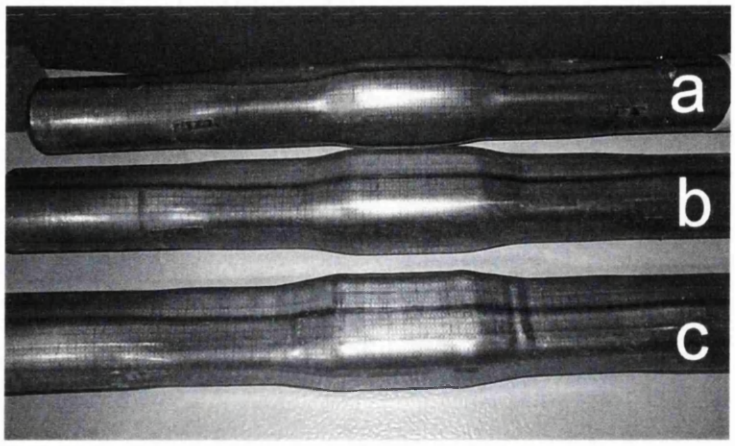

Figure 90: Photograph illustrating the influence on HSLA component geometry as a result of different axial end feeding rate, (a) 0.2mm/s (0.004mm/Bar), (b) 0.625mm/s (0.0125mm/Bar) and (c) 1.25mm/s (0.025mm/Bar), at a maximum pressure of 700Bar.

6.5.4 Analytical Tube FLCs

The strain (profile) data and safe, borderline and failure data measured from the research hydroforms (successful and failed components), supplemented by data from gridded tube tensiles, are presented against the analytical tube FLC models in Figures 91 & 92 .

These figures correspond to the FeP04, FeP10, HSLA and SS 304 tube materials, respectively. These figures illustrate the calculated analytical FLC models corresponding to the FeP04, FeP10, HSLA and 304 stainless steel tube materials.

The calculated FLD0 values are shown in Table 4.

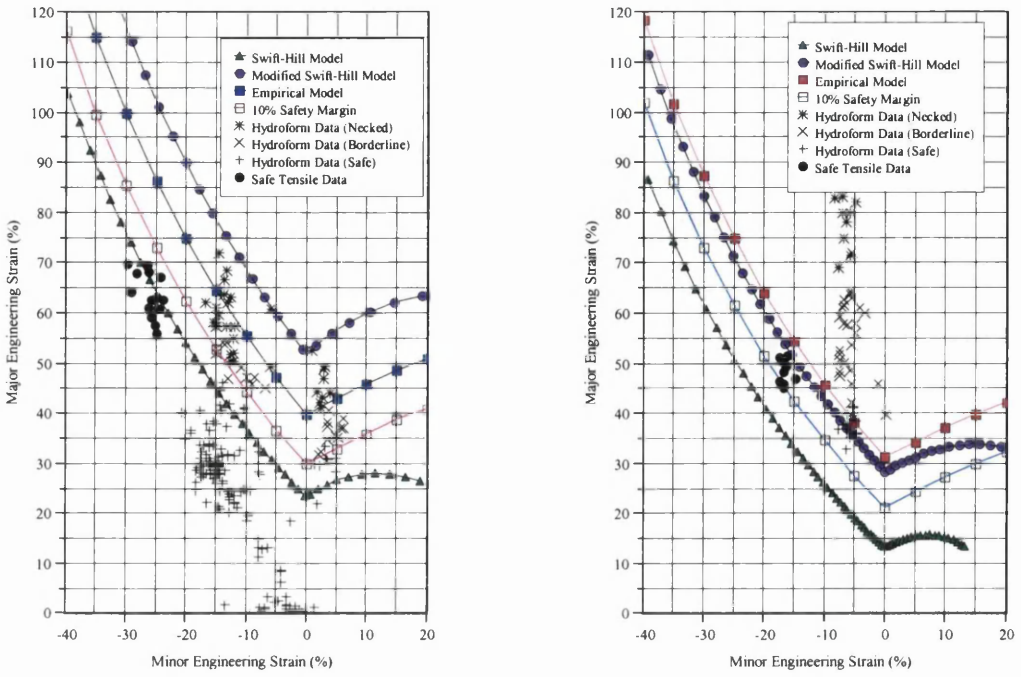

Figure 91: Experimental tube hydroform Forming Limit Diagram (FLD) data versus analytical tube FLCs for (a) FeP04 and (b) FeP10.

FeP04 Tube FLC

The FeP04 tube Forming Limit Diagram (FLD) data showed best correlation with Empirical FLC. The majority of 'borderline' and necked data points fell between the Empirical FLC and its 10% safety margin. This indicated that the Empirical formulation would provide a suitable failure criterion for this tube material. The Swift-Hill FLC appeared to demonstrate the ability to predict a transition in behaviour from 'safe' and 'borderline' or necked. The Modified Swift-Hill FLC was found to overestimate the necked strain levels, which may have related to this formulation's incorporation of the material anisotropy, which in this instance was strongly anisotropic.

FeP10 Tube FLC

The Empirical FLC of the FeP10 tube material did not satisfactorily capture the transition between 'safe' and 'borderline' strains. All of the 'borderline' and necked data was found to be above Swift-Hill and Empirical FLCs. The Swift-Hill FLC underestimated the

FeP10 tube material's 'safe' level of strain based upon the tube hydroform and tensile test sample data.

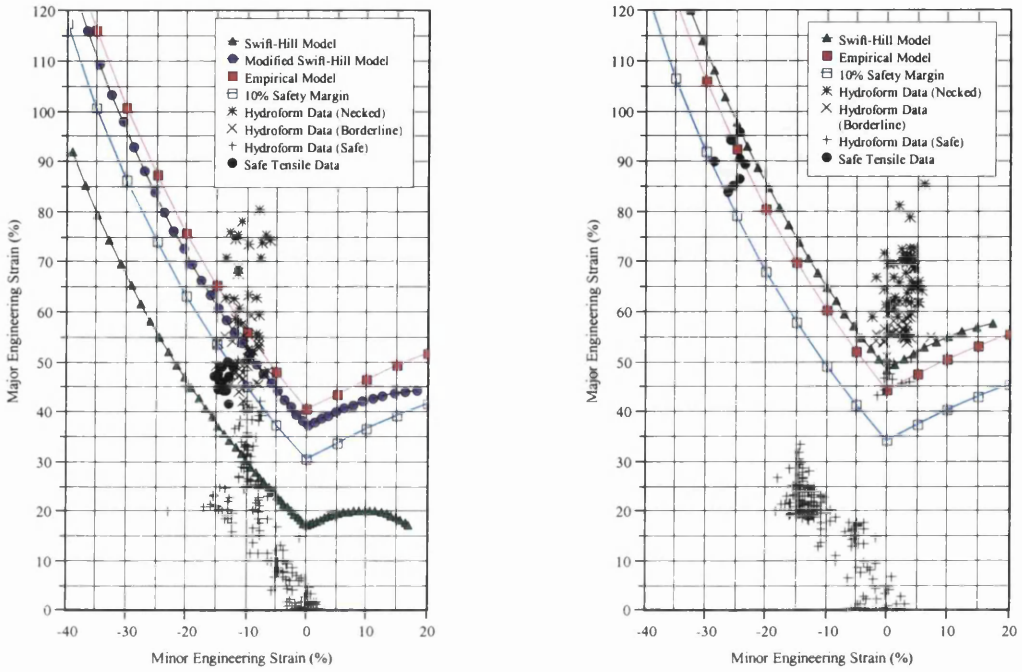

(a) (b)

Figure 92: Experimental tube hydroform Forming Limit Diagram (FLD) data versus analytical tube FLCs for (a) HSLA and (b) Stainless Steel (304).

HSLA Tube FLC

The Modified Swift-Hill FLC and Empirical demonstrated the ability to capture the onset of necking with good precision. The Empirical FLC (10%) safety margin provided suitably accurate delineation between the 'safe' and 'borderline' strain data for both tensile test and tube hydroform samples. This indicated that the Empirical FLC would provide a suitable criterion for evaluating tube hydroformed components manufactured from this material.

SS 304 Tube FLC

The Swift-Hill representation of the 304 stainless steel tube FLC displayed reasonable correlation to the strain data. More importantly the Empirical displayed a strong capability to predict the difference between the 'safe' and 'necked' data. However, 'borderline' data was considered necked by the Empirical FLC on the basis that it did not fall between the 10% safety margin and the FLC.

6.6 Finite Element Analysis of the Tube Hydroforming Process

The results of the analyses from the models developed for the different steels, studied in this research programme, are described in the following sections.

6.6.1 Pre-form Analyses

Selected results of the pre-forms that were simulated are presented in the following section. The section cut representations of section A-A, and B-B during various degrees of tool closure, are shown in Figures 93a & 93b. It was found that, for this particular tooling arrangement and geometry, friction coefficient had a negligible influence on either component thinning or developed surface strain.

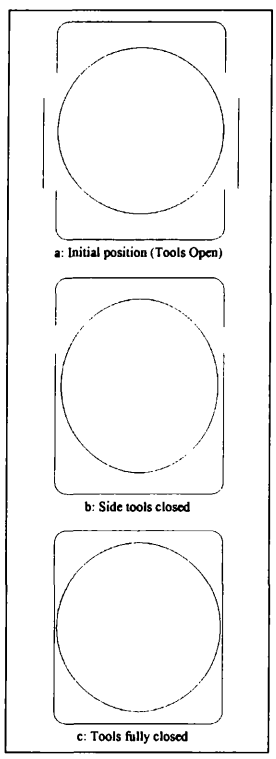

(a)

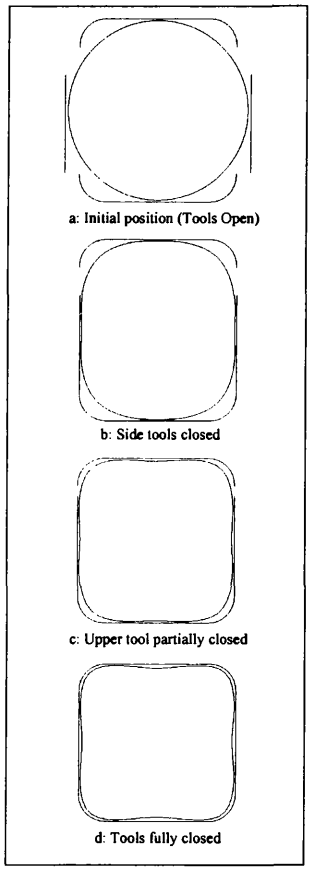

(b)

Figure 93: Example of section cuts through tooling and FeP04 tube at various stages of tooling closure (pre-forming), (a) Section A-A and (b) Section B-B.

Likewise, the tube wall thickness had little influence on the thinning level of the pre-form. However, the influence of initial tube wall thickness was found to increase the level of predicted peak major strain found at the component corner regions, shown in Figure 94. The results illustrate that with increasing initial wall thickness the strain experienced at the component corner increases. The results also indicate a distinct difference in behaviour between the stainless steel tube and the other steel tubes, i.e. the surface strains were all significantly lower.

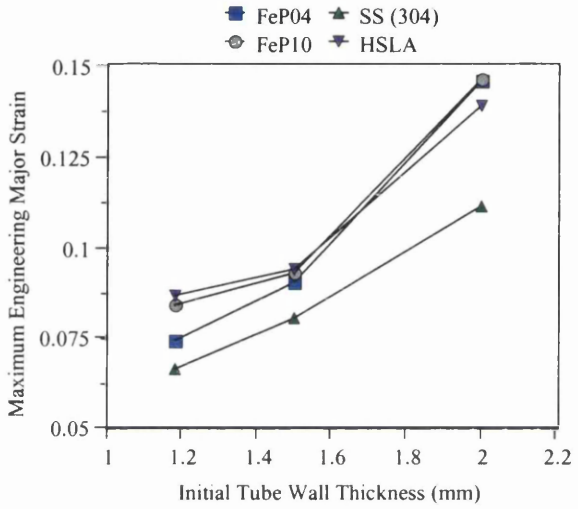

Figure 94: FEA results illustrating influence of initial tube wall thickness on predicted peak major strain after pre-forming (tool closure).

The comparison between the FE model predictions and the experimental measurements for the pre-form peak surface strains measured at section B-B is shown in Table 6.

Tube Material	Predicted Major Strain (%)	Measured Major Strain (%)
FeP04	6.83	6.02
FeP10	12.94	9.53
HSLA	13.87	9.41
Stainless Steel (304)	7.81	7.59

Table 6: Comparison between experimental measurements and FEA predicted values for peak surface strains after tool closure (pre-forming).

The surface strain measurements of the FeP04 and SS 304 pre-forms illustrated good correlation. However, the correlation for the two hot rolled steels was not as accurate, with differences of the order of 3.5% strain and above. For all of the tube metals, the peak surface strain of the FE models was found to be greater than measured experimentally.

6.6.2 Comparison of Material Inputs Methods

- ***Anisotropy Model***

For the FeP04 tube, under the two different hydroforming process conditions, the tube hydroforming model using r-bar was found to develop slightly greater levels of major strain than the model using Lankford coefficients. Consequently the r-bar model displayed a moderately higher degree of thinning, Figure 95. The actual difference in thinning between the models using the different anisotropy models was small, approximately 1-2 % thinning, for the pressure range of 200 and 1000Bar.

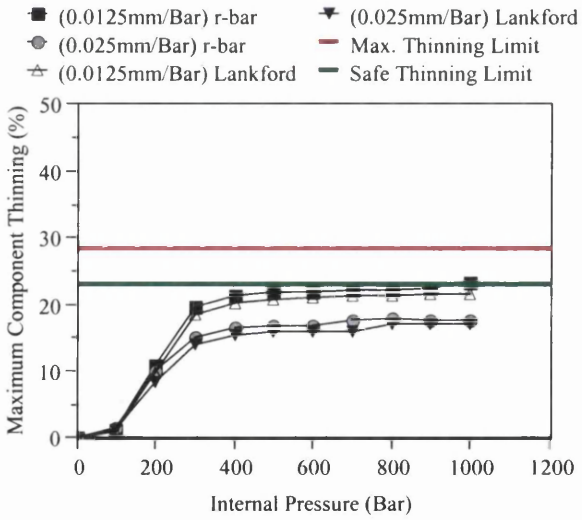

Figure 95: FEA results illustrating influence of different anisotropy models on predicted thinning of FeP04 tube using various equivalent axial feed rates (Model FC=0.1).

For the process conditions using a feed rate of 0.0125mm/bar both models displayed strong levels of thinning. The r-bar model was predicted to just exceed the safe thinning limit on reaching 1000Bar, whilst the thinning level for the Lankford model was found

fall inside the safe limit. For a 1.25mm/s (0.025mm/Bar) feed rate, the thinning levels for both anisotropy models were predicted to be inside the safe limit.

- ***Sheet versus Tube Material***

The analyses of forming the FeP04 component, assuming full sheet properties, was found to predict failure for the all three processing conditions simulated, i.e. feed rates of 0.2mm/s (0.004mm/Bar), 0.625mm/s (0.0125mm/Bar) and 1.25mm/s (0.025mm/Bar), respectively, Figure 96. The cause of failure in each case was due to early unrecoverable wrinkling between 200 and 400Bar, which inhibited tube metal flow into the die cavity. Ultimately, with increasing pressure, the sharp metal folds that developed were not removed and the components did not fill out and thus subsequently split.

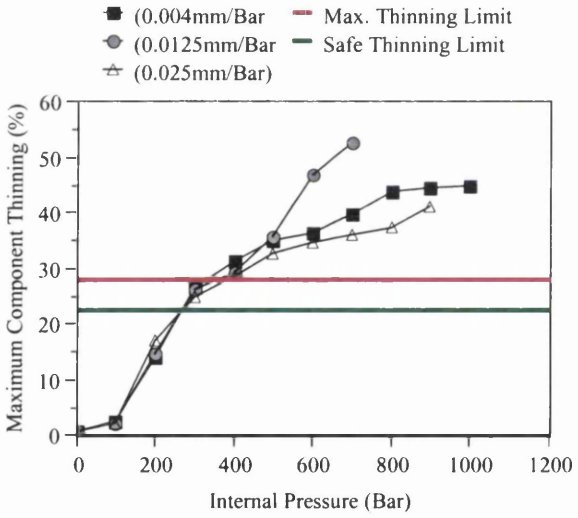

Figure 96: FEA results illustrating influence of using FeP04 sheet mechanical properties on predicted thinning of FeP04 tube using various axial feed rates (Model FC=0.1).

In the analyses of the FeP10 component, assuming sheet metal properties, only under the processing conditions of 0.004mm/Bar was the component predicted to have severe thinning (23.5%) but was still not predicted fail or go beyond the safe thinning limit. In each other processing condition, namely, 0.625mm/s (0.0125mm/Bar) and 1.25mm/s

(0.025mm/Bar), the component was predicted to form with a thinning level considerably below the safe thinning limit, Figure 97. For the component formed with a feed rate of 1.25mm/s (0.025mm/Bar), the predicted level of thinning was as low as 11.8% at a pressure of 1000Bar.

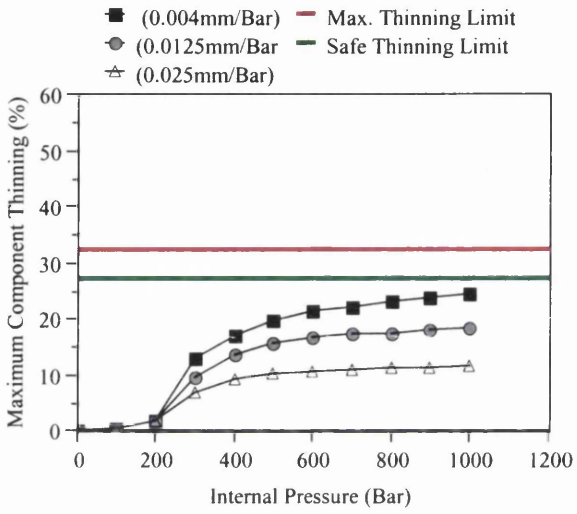

Figure 97: FEA results illustrating influence of using FeP10 sheet mechanical properties on predicted thinning of FeP10 tube using various axial feed rates (Model FC=0.1).

From the analyses performed on the HSLA component, using sheet properties, the component was predicted to undergo excessive thinning and split for the two processing conditions of 0.2mm/s (0.004mm/Bar) and 0.625mm/s (0.0125mm/Bar). However, the results predicted when using a feed rate of 1.25mm/s (0.025mm/Bar) illustrated that a component would only thin moderately (8.5% thinning) and was free from wrinkles or folds in the centre expansion section of the component, Figure 98.

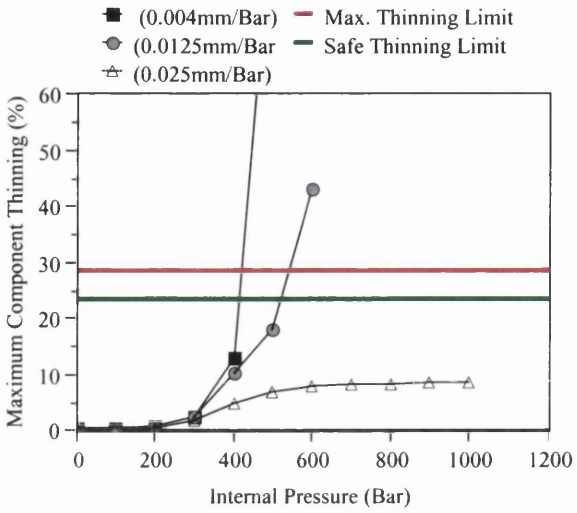

Figure 98: FEA results illustrating influence of using HSLA sheet mechanical properties on predicted thinning of HSLA tube using various axial feed rates (Model FC=0.1).

- ***Experimental versus Krupkowsky Hardening Curve***

The two different strain hardening curves for the stainless steel tube are illustrated in Figure 99 (a) and the predicted thinning of the stainless steel tube using the two different curves is illustrated in Figure 99 (b).

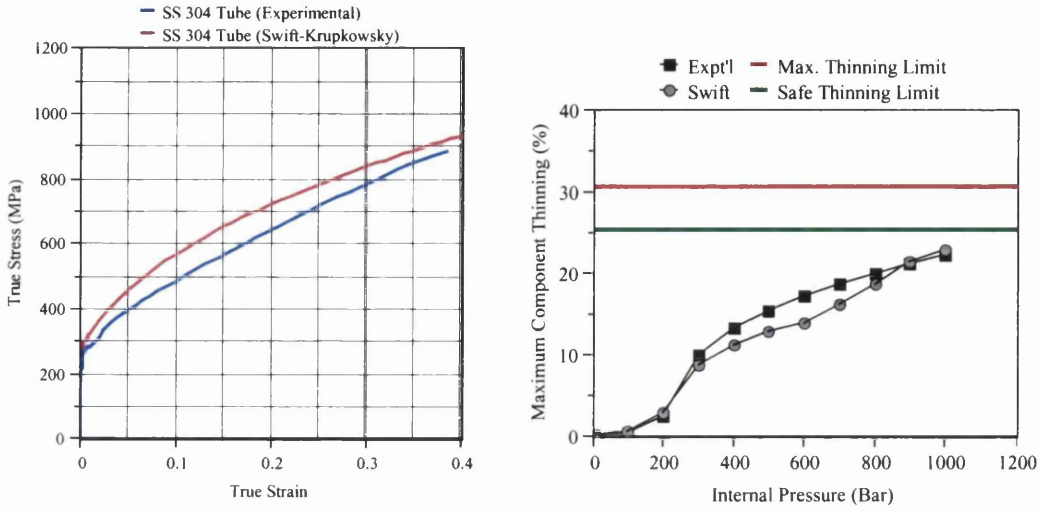

(a) (b)

Figure 99: (a) Comparison of 304 stainless steel tube material strain-hardening curves and (b) Comparison of strain-hardening curves on predicted thinning.

The FEA results show that the difference in the hardening curves translated to a maximum difference of 3.4% thinning between the models, which was found at the middle of pressure cycle. Above this pressure the thinning values converged. In both instances at 1000Bar, the metal was predicted to form with thinning levels below the safe limit.

6.6.3 Tube Hydroforming Process Models

- ***Thinning Analyses***

The predicted thinning of the FeP04, FeP10 and HSLA tube hydroform models for feed rates of 0.625mm/ms (0.0125mm/Bar) and 1.25mm/ms (0.025mm/Bar) are shown in Figures 100 through 104. In the case of the stainless steel 304 tube hydroform models, the predicted thinning levels using the feed rates of 0.004mm/Bar, 0.0125mm/Bar and 0.025mm/Bar, are shown in Figures 103a-c. The results of the thinning analyses for the TWT models, using a feed rate of 0.004mm/Bar are illustrated in Figure 104. In principal with the increasing internal pressure, the maximum wall thinning of the tube hydroform increased and was associated with the expansion zone. The tube end feed offset the level

of thinning in most cases, with the offset being governed by both feed rate and friction coefficient. Interestingly a critical level of thinning was reached for most models under the low-pressure level of between 200 and 400Bar, which was then capped or continued again depending on friction, feed rate and the metal properties.

One of the key findings was that substantial differences in the predicted behaviour were observed between the FE models based upon the coil properties and those models that were based upon tube properties.

FeP04

Unexpectedly, the FeP04 coil and tube, whilst only possessing slight differences for most of the metal properties, a significant difference was found between the sheet and tube FE models. The FE model using sheet properties developed wrinkling in the expansion region of the hydroform at low pressures, between 200 and 400Bar. This ultimately inhibited the flow of metal supplied by end feeding, resulting in splitting for each of the feed rates used. However, the FE model using the tube properties was not found to wrinkle, and increasing the feed rate was found to reduce the level of thinning. The metal property that was most strongly different between the sheet and the tube metal was the 0.2% proof strength, i.e. values of 171.6MPa and 213.7MPa were used for the sheet and tube, respectively.

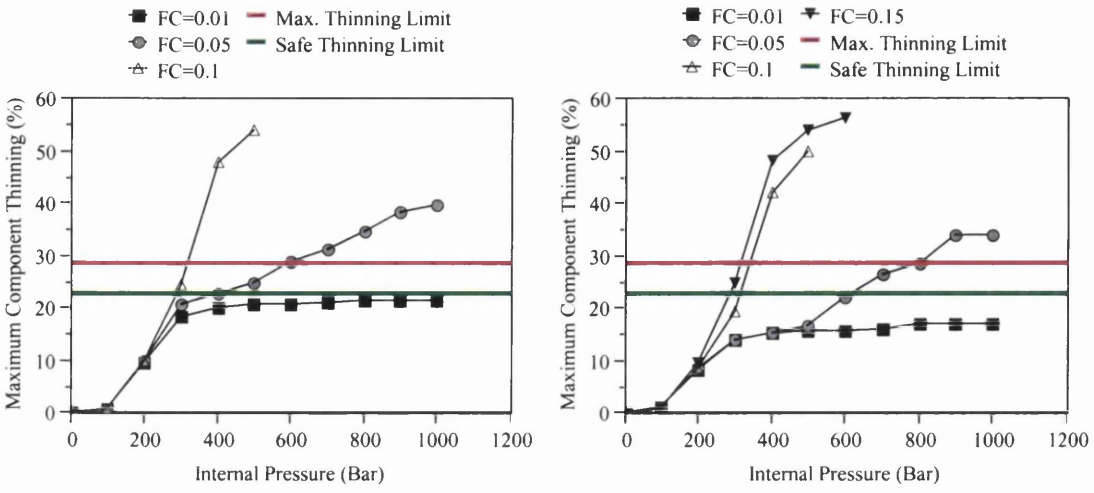

(a) (b)

Figure 100: FEA results illustrating combined influence of internal pressure and friction upon FeP04 component thinning using an axial feed rate of (a) 0.625mm/ms (0.0125mm/Bar) and (b) 1.25mm/ms (0.025mm/Bar) and tube mechanical properties in the FE model.

FeP10

The FeP10 FE model, using tube properties, did not perform as well as the model using sheet properties, and was predicted to fail or thin excessively under all hydroforming conditions considered, with the exception of the highest feed rate and lowest friction coefficient. The model utilising sheet properties was predicted to form, without excessive thinning, splitting or wrinkling for all three feed rates, which was contradictory to the experimental hydroform trials in which the metal failed by splitting.

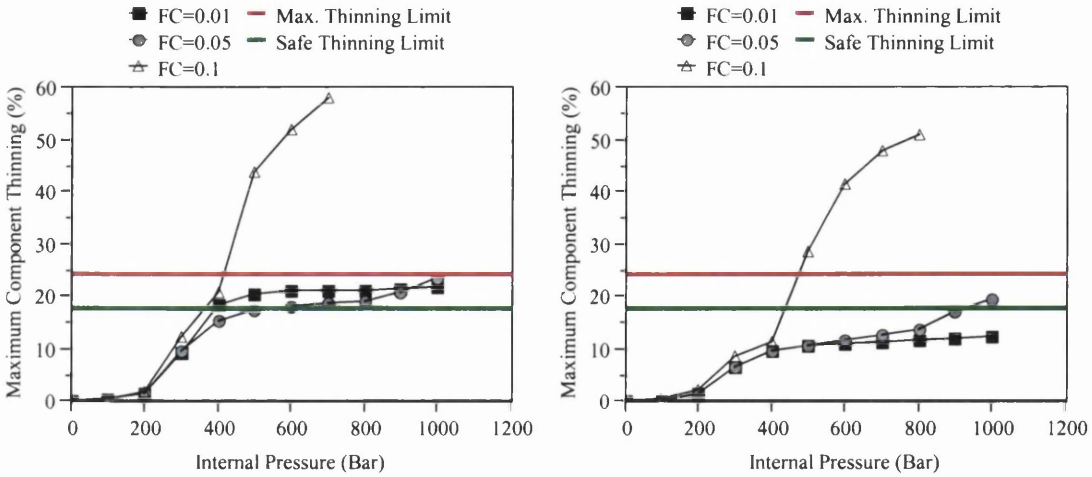

Figure 101: FEA results illustrating combined influence of internal pressure and friction upon FeP10 tube thinning using an axial feed rate of (a) 0.625mm/ms (0.0125mm/Bar) and (b) 1.25mm/ms (0.025mm/Bar) and tube mechanical properties in the FE model.

HSLA

Interestingly, the HSLA tube FE model was found to be prone to wrinkling in the expansion zone of the component using the higher feed rate of 1.25mm/ms (0.025mm/Bar), with the folds/undulations developing as low as 400Bar. Some degree of wrinkle removal was found as the pressure increased and forced the tube against the die walls but not all of the folds were removed from the hydroform, as found experimentally. This was in contrast to the FE model results obtained when using the HSLA sheet properties, Figure 98.

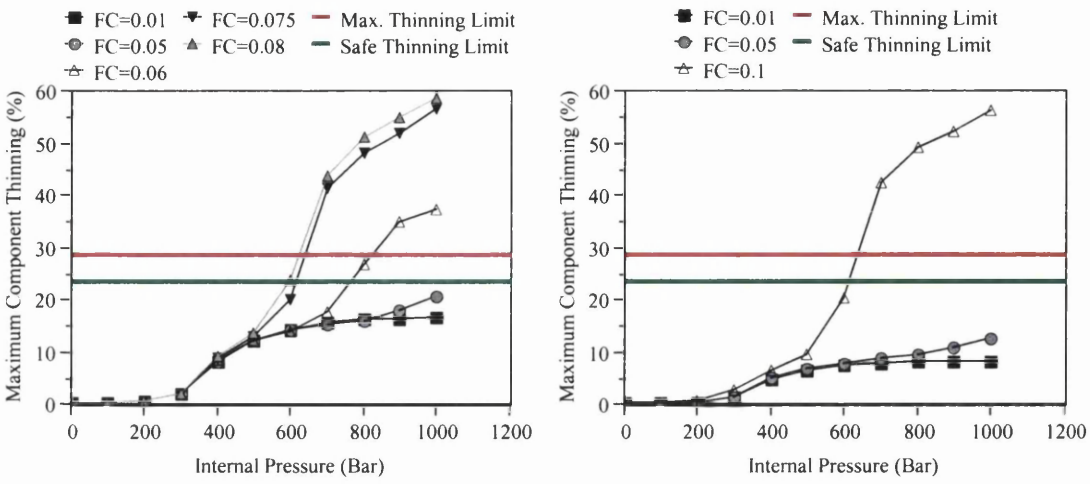

Figure 102: FEA results illustrating combined influence of internal pressure and friction upon HSLA tube thinning using an axial feed rate of (a) 0.625mm/ms (0.0125mm/Bar) and (b) 1.25mm/ms (0.025mm/Bar) and tube mechanical properties in the FE model.

SS 304 (1.4301)

The stainless steel, unsurprising was the only tube metal that was not found to display excessive thinning at the lower feed rate levels when utilising the lowest friction coefficient. Also, the thinning behaviour of the stainless steel tube metal was far more strongly influenced by the friction coefficient when the higher feed rates were used than the other tube metals. At the higher feed rates, a low level of thinning was anticipated with the lowest friction coefficient. However, with increasing friction coefficient increased the level of thinning dramatically, resulting in a wide variation in the predicted thinning between the lowest and highest friction coefficient used. This behaviour was unlike the other tube metals.

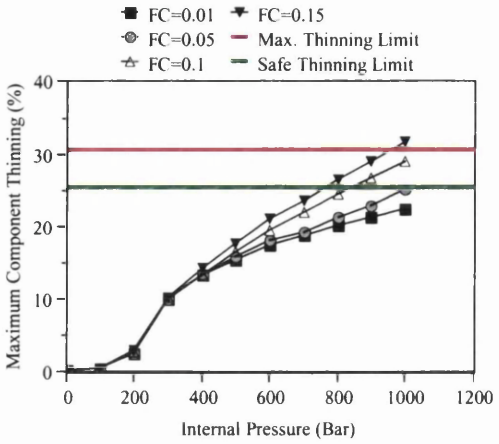

(a)

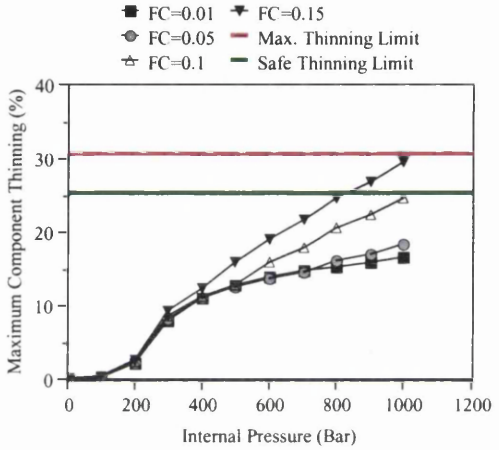

(b)

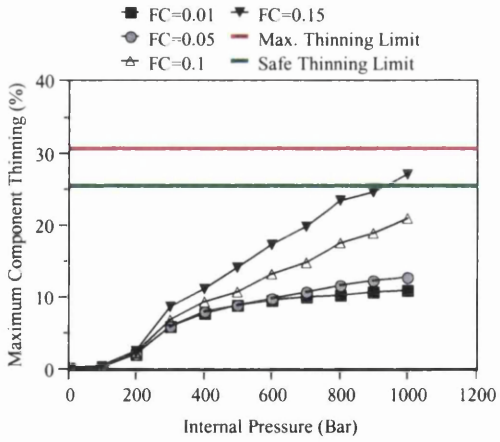

(c)

Figure 103: FEA results illustrating combined influence of internal pressure and friction upon HSLA tube thinning using an axial feed rate of (a) 0.2mm/ms (0.004mm/Bar) (b) of 0.625mm/ms (0.0125mm/Bar) and (b) 1.25mm/ms (0.025mm/Bar) based on tube properties.

TWT

In general the TWT model was found to experience a very similar thinning trend to the stainless steel tube. As with the stainless steel tube model, excessive wall thinning of the TWT would be avoided if a sufficiently low friction coefficient, of the order of 0.025 or, could be achieved.

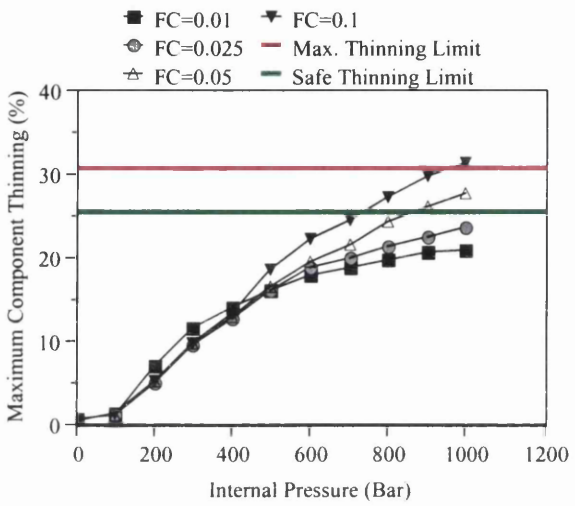

Figure 104: FEA results illustrating combined influence of internal pressure and friction on the thinning of the TWT (FeP04:SS 304:FeP04) for an axial feed rate of 0.2mm/ms (0.004mm/ Bar) based upon tube properties.

Major Strain Contour Plots

An example of the major strain contour plots for the FeP04 tube model are shown in Figure 105 at various stages of the hydroform process cycle, with an feed rate of 1.25mm/ms (0.025mm/Bar).

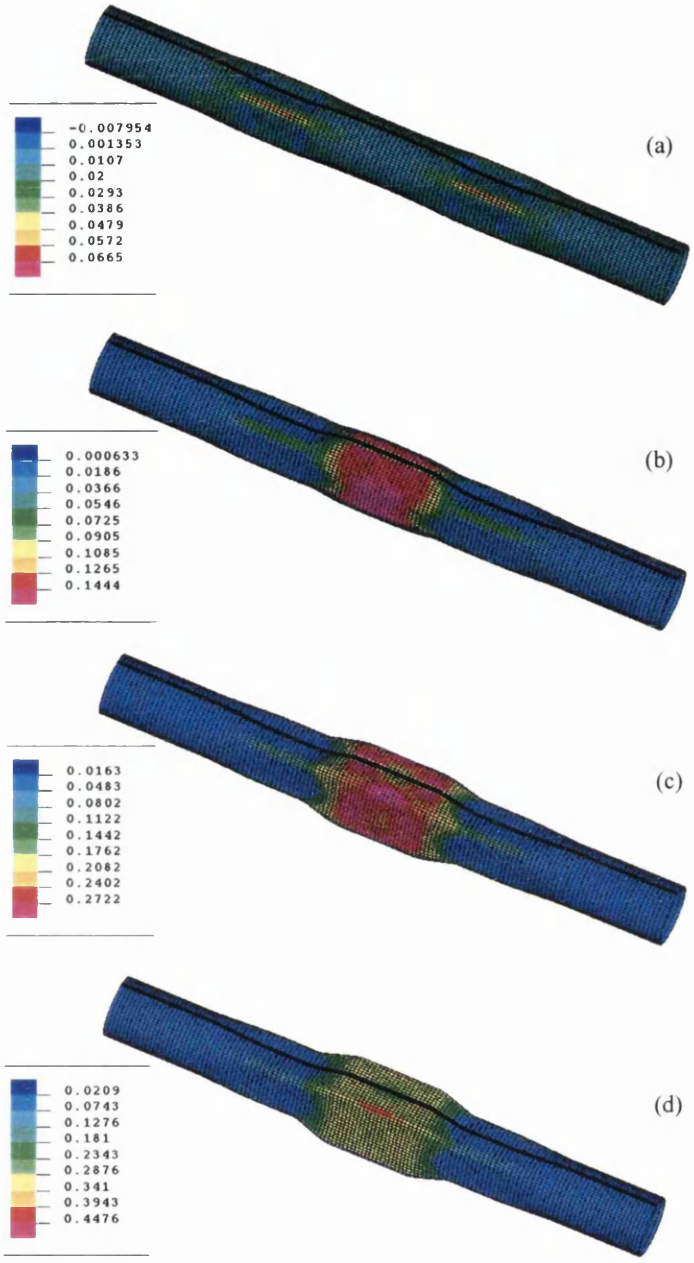

Figure 105: FEA major strain contour plots for FeP04 tube at various internal pressures using a 0.025mm/Bar feed rate (a) Pre-form (0Bar), (b) 200Bar, (c) 400Bar and (d) 1000Bar, model incorporated tube mechanical properties and FC=0.01.

- ***Strain Path & FLCs***

To illustrate the influence of the feed rate and friction on the hydroforming process for the FeP04 tube models, the critical strain path relating to the element at the centre of the corner radius at section A-A was obtained for the process cycle forming to 1000Bar.

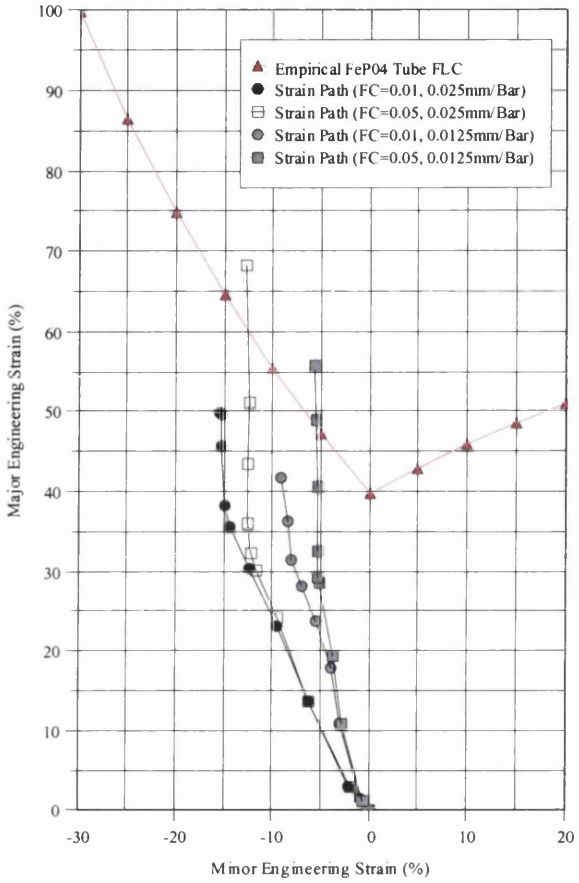

Figure 106: FEA results illustrating the influence of friction coefficient and feed rate on strain path of an element at the centre of an upper corner radius at section A-A for the FeP04 tube model (1000Bar).

The influence of the two different feed rates of 0.625mm/ms (0.0125mm/Bar) and 1.25mm/ms (0.025mm/Bar) are plotted against the empirical FeP04 tube FLC in Figure 106. The influence in modifying the friction coefficient from 0.01 to 0.05 is also shown. The higher axial end feed rate was found to develop both more negative minor strain but also a higher level of major strain for the critical strain path. Increasing the friction

coefficient had the opposite effect on the negative minor strain but was found to significantly increase the major strain level. In general, the higher values of friction coefficient were found to confine the strain path of the element from the corner radius expansion zone to one of plane strain stretch.

Figure 107 illustrates the FLD (strain) process signatures for the SS 304 tube hydroform FE models using a feed rate of 0.02mm/Bar (1mm/ms). The results demonstrate the strong difference in forming modes experienced by the different regions of the hydroformed tube as a direct result of the different friction conditions. The figure indicates the strong shift from very low major strain to a high negative minor strain for the tube guide region with increasing friction. This is in agreement with the trend found experimentally. The expansion zone also has a strong shift in deformation, from one of between tensile and pure shear to one of plane strain. This was also found in the experimental hydroforming trials.

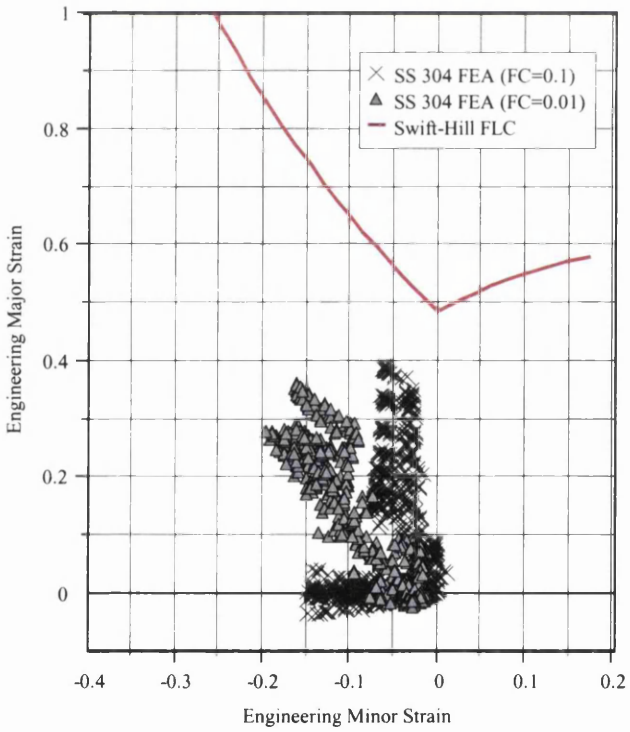

Figure 107: Influence of friction on FLD (strain) process signature for SS 304 tube FE model (Feed rate = 1mm/ms (0.02mm/Bar), maximum pressure of 1000Bar).

Figure 108 illustrates the influence of metal properties on the strain path and the level of forming severity. This was demonstrated from the critical strain paths of FeP10 hydroforming models based on different metal descriptions, i.e. sheet and tube. The model based upon the sheet properties demonstrated a high degree of safety with the final tube strains well below the Empirical sheet FLC in strong contrast to the model based upon the tube properties, despite both models displaying near identical strain paths.

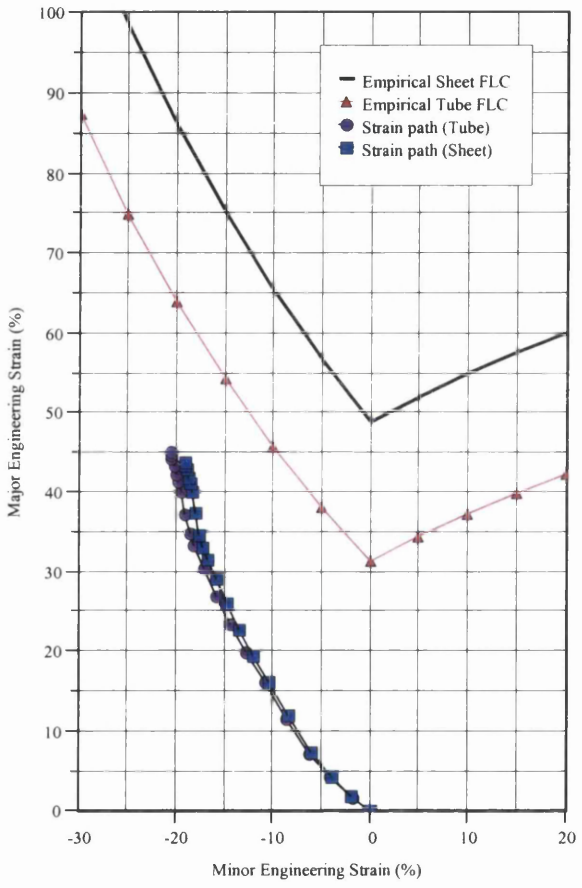

Figure 108: FEA results illustrating the influence of material properties on strain path and forming severity for element at centre of corner radius at section A-A (FeP10 coil and tube, FC =0.01, feed rate = 1.25mm/ms (0.025mm/Bar), maximum pressure of 1000Bar).

6.6.4 Validation of FEA Tube Hydroforming Process Models

In general, very good correlation was obtained between the experimental results and the FE models developed. Where the correlation was poor, the FEA was still capable of illustrating the trend anticipated.

- ***Strain profiles***

The predicted strain profiles, LA, LB and A-A were generally found to correspond well with experimental results for all of the metals and the range of processing conditions used. However, the FE models consistently overestimated the level of strain determined practically for the SS 304 and FeP04 tube metal (>2.5%). Interestingly, the converse was true of the HSLA FE models and experimental results. The difference in the strain profiles was reversed with the measured values displaying greater strain magnitudes than the FE models. Whilst differences were found in the profiles, the differences in strain magnitude was within the capability of the camera-microscope system, which has an associated error of approximately 4% [182]. Expectedly, the experimental strain profiles A-A would be lower, due to difficulties in accurately measuring the strains at the corner radii with the camera system. As a result the measured values at the component corners underestimated the actual strain due to the curvature of the surface. The underestimated can be seen from Figure 109 for the FeP04 tube.

The introduction of the weld mechanical properties in to FeP04 tube model weld region, Figure 109, provided a reasonable representation of the actual measured strain profile for hydroformed tube. Although this difference was observed, the overall strain profile of the FEA results was found to provide a greater degree of accuracy when the weld was integrated into the model.

Interestingly, from the experimental strain profiles measured at section A-A, the strains corresponding to the corner radii of the 70mm wide bottom face of the component, displayed lower levels of strain. These corner radii were found to exhibit a lower degree

of corner fill than the upper most and this was found for all of the hydroforms at pressures above 700Bar.

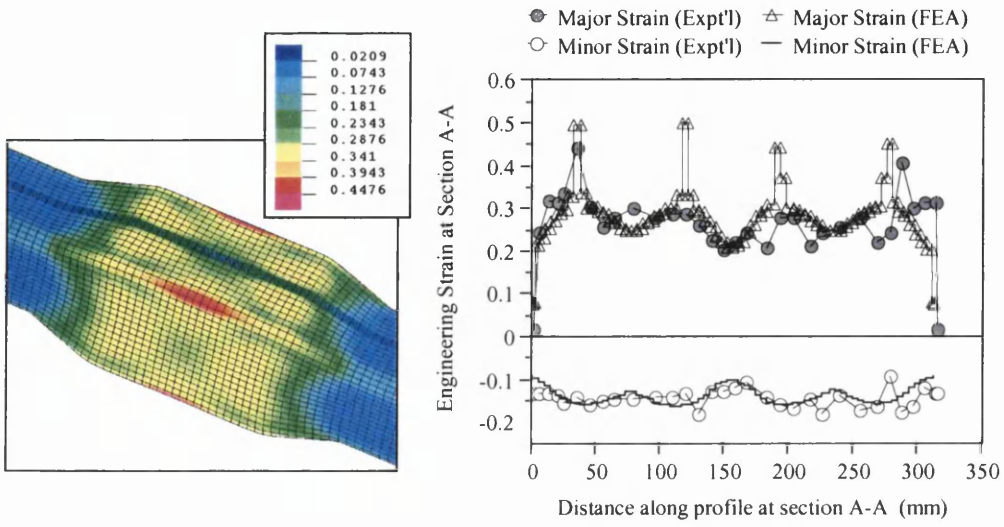

(a) (b)

Figure 109: FeP04 tube hydroform to 1000 Bar, feed rate = 1.25mm/ms (0.025mm/Bar) (a) FE model major strain contour plot of tube hydroform at expansion zone, (b) Experimental versus FE model major & minor strain profiles at section A-A, (FE model incorporated tube parent and weld mechanical properties and FC = 0.01).

The strain profiles at section A-A also strongly illustrate that with increasing pressure, the degree of strain developed on the flat sides of the component was less than the increase in strain at the corners. For the stainless steel experimental hydroforms, the changes in strain were of the order of 2% and 4% for the flats and corner radii, respectively for the change in pressure from 700 to 1000Bar. Whilst, a change took place the difference was small. This was partly due to the final size of the corner radii that was achieved, as a result of the high rate of work hardening. The small difference was also attributable to the high n-value of the 304 stainless steels tube and very low friction behaviour experienced, allowing for a much improved strain distribution. Even at the pressure of 700 Bar an increase in strain was possible at the die wall illustrating that the 'die lock' condition was minimal.

In general, the stainless steel FEA results based upon the strain profiles (LA), shown in Figure 110 to 112 were found to correlate extremely well with the experimental data.

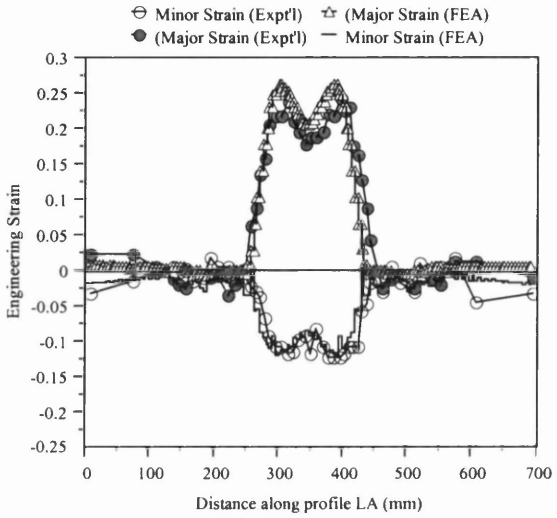

Figure 110: Comparison of FE model and experimental strain profile (LA) for stainless steel (304) tube at 900Bar, feed rate = 0.0125mm/Bar (FE model FC=0.01).

However, better correlation was found at higher pressures and with greater levels of end feed. The poorest correlation found between the FEA results and the experimental measurements for profile LA was for the experimental hydroforming conditions of 700 Bar in combination with 0.004mm/Bar feed rate, shown in Figure 112.

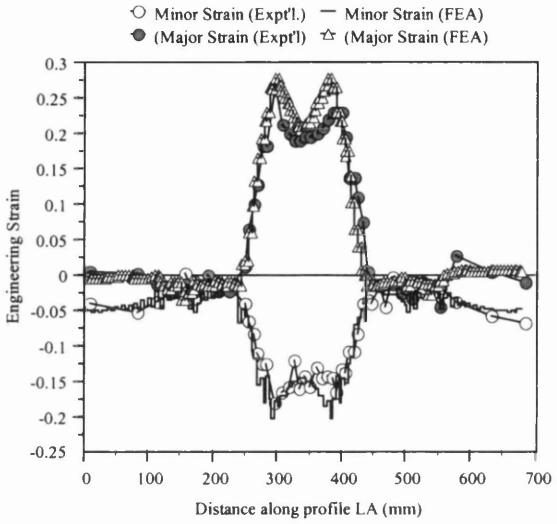

Figure 111: Comparison of FE model and experimental strain profile (LA) for stainless steel (304) tube at 900Bar, feed rate = 0.025mm/Bar (FE model FC=0.01).

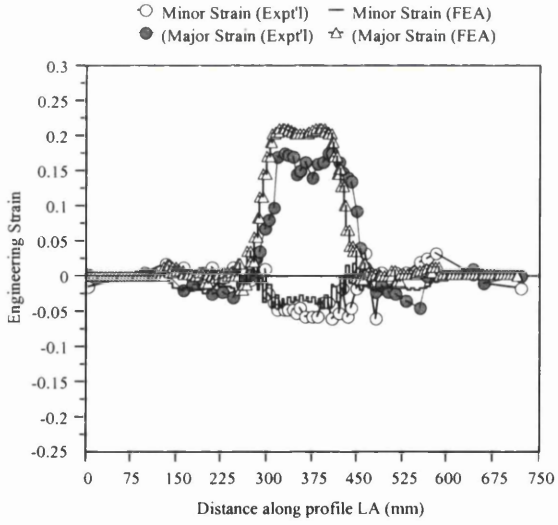

Figure 112: Comparison of FE model and experimental strain profile (LA) for stainless steel (304) tube at 700Bar, feed rate = 0.004mm/Bar (FE model FC=0.01).

The major strain at the centre of the expansion section of the experimental hydroform was some 8% strain lower than the results predicted from the FE model.

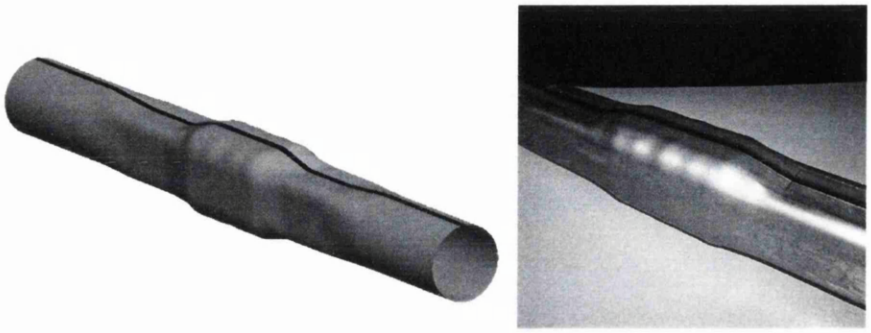

Figure 113: Comparison of FEA and experimental images of HSLA tube at 500Bar (Feed rate = 0.025mmBar, FEA FC =0.01).

The wrinkling behaviour displayed by the HSLA tube material was accurately predicted by the corresponding FE model, see Figure 113.

- ***Component Corner Radii***

The minimum internal radius of the experimental hydroforming die tool manufactured for the research programme was 5mm. To evaluate the response of the different steel tubes to different hydroforming conditions on the developed external component corner radius. Corner radius measurements were performed on the steel tubes, hydroformed in the experimental research trials, and in the FE models at internal pressures up to 1000Bar.

The predicted component corner radius fill for the stainless steel tube FE models using axial feed rates of 0.025mm/Bar, 0.0125mm/Bar and 0.004mm/Bar are plotted against the experimental data obtained, Figure 114. Reasonable agreement was found between the experimental results and the FE models for the 0.0125mm/bar and 0.025mm/Bar feed rates. However, the experimental data obtained from the 0.004mm/Bar feed rate displayed a wide departure between the experimental and FE results. The FE model trend

observed was a smaller corner radius was achieved for an increasing feed rate. The result illustrates a limitation of the FE model used. The influence of feed rate on corner filling was low, with less than 5mm difference in corner radius between 0.004mm/Bar and 0.025mm/Bar FE models.

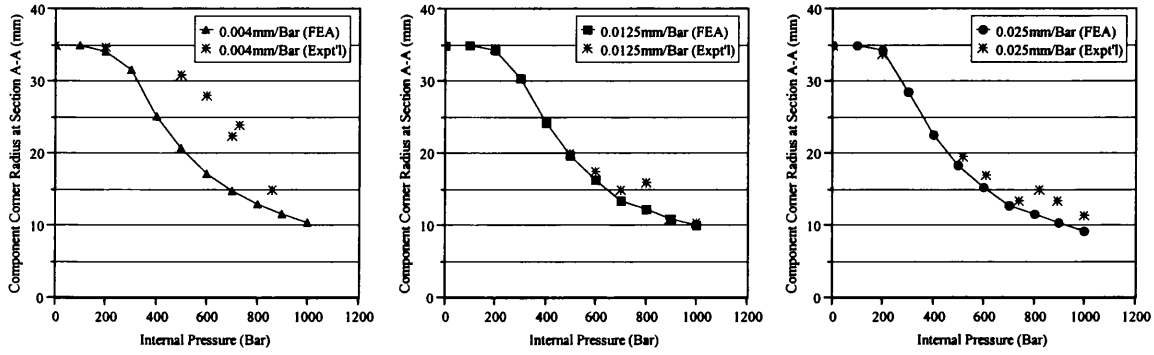

(a) (b) (c)

Figure 114: Corner radius versus internal pressure relationship for type 304 stainless steel tube using (a) 0.004mm/Bar feed rate, (b) 0.0125mm/Bar feed rate and (c) 0.025mm/Bar feed rate.

Figure 115 demonstrates the combined influence of material yield strength, work-hardening characteristics and thickness on hydroform corner fill experienced by the FeP04 and stainless steel tube hydroform models. Greater levels of corner fill were achieved for the lower strength, thinner wall FeP04 tube material.

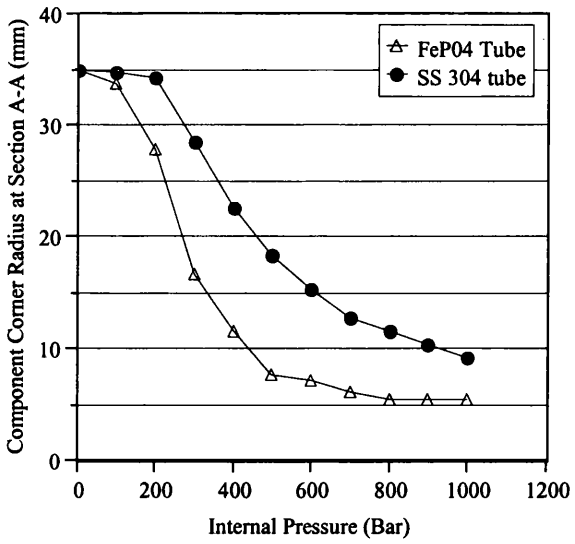

Figure 115: Comparison of predicted external corner radius for FeP04 tube and type 304 stainless steel tube FE models (1.25mm/ms or 0.025mm/Bar feed rate, FC = 0.01).

The influence of material properties and tube wall thickness on the minimum external corner radius was further illustrated by means of the analytical model proposed by Bikert [34], Figure 116. Although there was a difference in the initial tube thickness, the difference between the stainless steel and FeP04 material properties influenced the corner radius development. The stainless steel tube, which had both a higher initial material yield strength and a higher work-hardening rate, was found to achieve less die corner radius filling than the FeP04 tube for the same internal pressure. Consequently, the stainless steel tube material would require greater pressures and energy to achieve the same corner radius as the FeP04 tube.

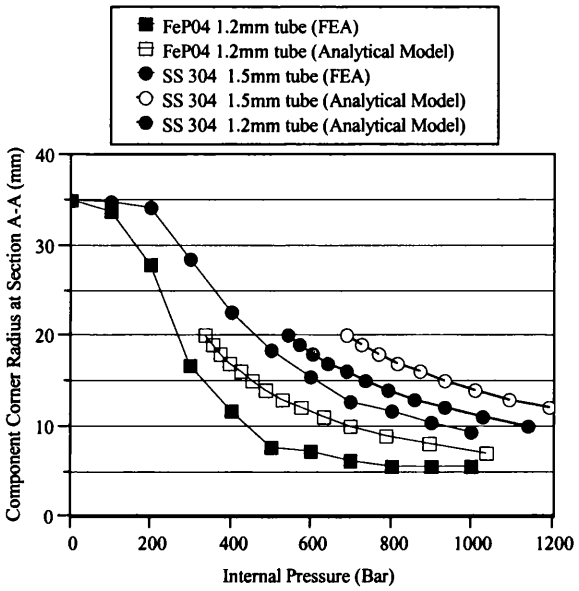

Figure 116: Comparison of corner radius-internal pressure relationship from FE model results with analytical data calculated from model proposed by Birkert [34] - FE feed rate = 1.2mm/ms (0.025mm/Bar), FC =0.01.

- **TWT Hydroform Model**

In order to determine the suitable internal pressure for forming the TWT under a 0.004mm/Bar feed rate, the analytical models were utilised in conjunction with the FE model. The maximum safe processing pressure, was determined based upon an internal pressure which would develop thinning levels below the safe thinning limit but also be free from potential die witness line related issues at 1000Bar. The area subject to high thinning levels was the expansion region of the tube. This region of the TWT FE model was analysed for thinning. The maximum pressure utilised in the experimental trials was therefore 700Bar.

In order to validate the FE TWT hydroform model, a comparison of the major and minor strain profiles for section LA was performed, Figure 117. The comparison between the strain profiles demonstrated reasonable correlation based upon the maximum forming pressure and feed rate used for the TWT (700Bar, with an end feed rate of 0.004mm/Bar).

The strain profiles measured displayed close correlation to results obtained for the stainless steel tube material, which was hydroformed under the same processing conditions (Figure 112). In both cases, singular tube and TWT, the maximum minor strain achieved was at the centre of the tube with a magnitude of approximately -5%. For the same region, the tubes experienced a major strain magnitude of some 20%.

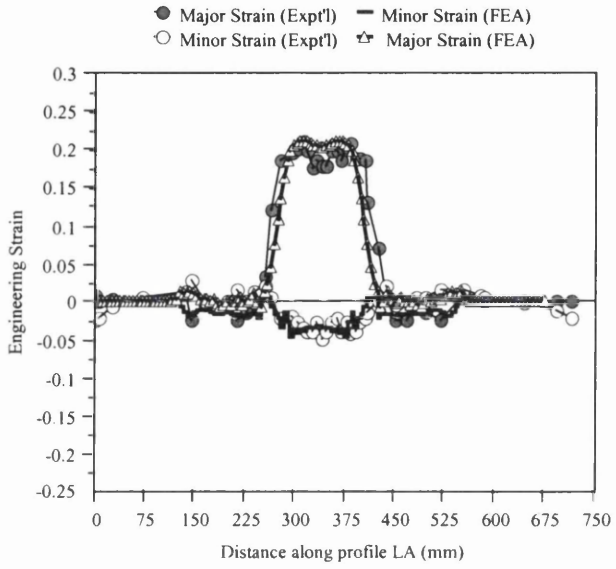

Figure 117: Comparison of FE and experimental strain profiles along section LA for TWT at 700Bar, feed rate = 0.004mm/Bar (FE model FC=0.01).

7.0 Discussion

7.1 Coil and Tube Material Characterisation

7.1.1 Dimensions

The conventional steel coil thickness was found to vary greatly across the width, based upon the limited number of measurements made. However, although within the specified tolerance, the steel was found to border this limit in each case. Interestingly, the FeP04 coil material illustrated quite different thickness readings, which ultimately would mean that the tube produced from the coil would be different depending upon the slitting position that it was taken from. The coil exhibited a wide distribution of properties across the coil width. This coupled with thickness variability can ultimately lead to very different tube products from the same coil, ignoring the potential coil variation along its length.

The coil thickness measurements for the hot rolled metals were only from the slit coil but were close to the expected material thickness ordered. The hot rolled HSLA steel was found to be out of specification at the front end of the coil. However, despite this fact the majority of the tube would have been discarded at the tube mill, due to the coil join with the slit coil in front. This is stated as the coil join disturbs the high frequency welding process, and produces tubes with weld imperfections. However, the quantity of tube discarded does depend on how the long the welding conditions are interrupted. The tube manufacturing was found to have a profound effect on the thickness uniformity of the tube metal. The weld line was found to be thinnest region of all the tubes except for the stainless steel due the difference in welding process used. With the exception of the HSLA tube, the thickness variations may not be significant to affect the tube hydroforming process, e.g. tube end sealing. However, the HSLA thickness and tube diameter variations may have more influence upon the tube bending process, with the tube blank more prone to internal scoring from the close fitting internal mandrel and potential damage to the tooling.

Interesting in almost all cases the tube material was found to be thicker than the coil metal, which may have been a manufacturing effect, although the difference in position through coil could have also given rise to such effects. Therefore, whilst the thickness increase due to tube manufacturing was likely it was not conclusive found from the measurements performed. This would be difficult to establish practically as coil thickness traces are usually obtained from the coil centre-line and therefore do not account for any cross coil thickness variation. What could be concluded from the measurements was that the tube manufacturing process increased the thickness variability, very locally. This was almost certainly due to highs and lows in the level of contact made with the roll forming dies, resulting in roll-forming witness lines. The variations in wall thickness may have lead to non-uniform variations in strain distribution of the tube during hydroforming, in addition to any introduced from frictional influences or tool geometry.

Although the coil materials displayed a thickness drop-off at the coil edges the tube material was welded satisfactorily, and the welds were considered sound, based upon the tests that were performed.

No problems, such as pinching on tool closure, were identified during the experimental tube hydroforming trials, which may have related to the tube diameter variations.

7.1.2 Mechanical Properties

Not only were tube thickness variations found to fluctuate locally but the mechanical properties were also. All of the tubes were found to display non-uniformity around the tube circumference in terms of the material properties. The material having the least variation was the stainless steel tube, although lower elongation was found at the weld-line compared with the remainder of the tube. The degree of change in mechanical properties was also profound for the conventional steels and a drop in formability was observed in every case. The formability indicators that were found to illustrate the most significant changes were the yield or 0.2% proof strength, yield to tensile ratio, n-value, uniform elongation and to a slightly lesser extent, the total elongation.

Of greatest significance was the influence of tube manufacture upon the FeP10 mild steel, which displayed a dramatic reduction in formability, indicated by the strong changes to the formability indicators. Although it was initially thought that the affect was specific to the tube mill operation, it was later discovered that these changes were grade dependent as similar affects were observed in an independent research programme. The independent research programme involved ERW tube (100mm and 106mm in diameter) manufactured from 2.6mm hot rolled, mild steel coil [183]. Interestingly, it has been found that by adding Boron to the chemistry of this family of steels, the strong reduction in formability parameters can be minimised [184].

Interestingly, the HSLA coil, which displayed similar chemistry, front mid and end of coil, also exhibited a high degree of uniformity in terms of mechanical properties, despite the thickness variations. This indicated that the coil processing conditions were uniform, as was established, based upon the Intranet data observed.

It was also not possible to determine whether or not the tube mill speed had a significant effect upon the residual formability of the tube as only the normal operating conditions were used, which was partly dictated by the welding requirements.

7.1.3 Surface Texture

As a consequence of tube manufacture, strong influences were observed and are clearly illustrated in Figures 6.26 to 6.32 showing the 3D surface roughness representations for both coil and tube metals. The influences are also depicted in Figures 6.9a & b and 6.25, which illustrate the changes in all surface parameters that were determined for coil and tube. In principal, the trend observed was a reduction in average or r.m.s. surface roughness as a result of tube manufacture. This was almost certainly attributable to the flattening of the soft surface asperities or removal of hard asperities on passing of the steel coil through the tube roll forming tools. A second strong trend observed was found in the differences between the coil and tube surface textures. This trend was the increase in average total asperity height, which was found to increase in all cases. It is believed that this was either due to an increase in peak height, as for FeP10, or an increase in

depth, as in the cases for FeP04 and HSLA. The visual characteristics of this trend may be seen from the differences between the 3D surface roughness representations. The reason for such significant changes in the surface asperity peaks or troughs may be attributable to surface galling as a result of material pick up on the rotating roll forming tools. This would be in addition to uneven and therefore local points of tool contact with the coil material in processing the tube. From the tube material obtained for this particular test programme, distinct surface quality imperfections were noted that were attributable to the ERW tube manufacturing process.

The process imperfections included:

- Tram lines or roll forming lines, indicating local points of contact with the tools
- Gouge marks, possibly as a cause of tool pick-up
- Roll-forming tool scuff marks
- Scratches

During the processing of the FeP04 tube material on the tube mill, the cause behind scuff-marks, found on the exiting tube metal, was due to small imperfections (holes) in the surface of the roll forming tools. On rotating, these holes would cause sharp acicular marks on the tube surface at regular intervals. The removal of the scuff-marks was achieved by improving the surface of the tooling. This was achieved by polishing the roll-forming tools during operation, using a fine emery cloth. The initial cause of the imperfections was unknown. It may have been attributable to poor coil joining practices, or pick up of foreign material from coil handling. The same scuff-marks were also observed on the other steel tubes, except for the stainless steel material. A typical gouge mark may be seen in Figure 6.31, illustrating the 3D surface roughness of the HSLA tube metal. Such surface imperfections, may play a significant role in the reduction in material formability, but also may have an impact upon component painting or coating processes. For improved paint finish, a smooth surface finish is required. In each instance, the surface quality of the ERW tube manufactured was not satisfactory for A-Class (Outer body) component and provided a poor surface for painting, which would have been undesirable for exterior or visible component surfaces.

Additional surface imperfections may have been introduced into surface of the tubes from poor coil handling, either at the steel distributor or at the tube mill.

7.1.4 Sheet Forming Limit Curves

The experimentally derived FLCs did not compare well positioning of the analytical models examined. In particular, the plane strain intercept of the experimental curves was located to the right of plane strain, typically by some 5-10%. However, the tensile FLD data was found was found to follow the analytical data more closely. It is believed that the observed difference in the fit was due to the strain path influences of the FLC test method used. Therefore, the experimental FLC would be less appropriate to evaluate tube hydroformed components subjected to linear strain path deformations, and in particular plane strain deformation.

The fact that the position of the minimum FLD_0 value can vary, indicates that the FLC is not an intrinsic material property and may be influenced by the component strain path. The level of deviation from a linear path will largely be governed by geometry although friction and test or process conditions may also play a significant role. Dry et al [185] found that the FEA models of the FLC tests correlated very well with the experimental FLCs. Therefore, the FLC used to assess a component should be representative of the component geometry and process conditions to be able to achieve the highest degree of accuracy in predicting failure. However, this is not practical and therefore the laboratory determined FLC remains suitable for the general assessment of many automotive pressed components.

In contrast to the experimental FLCs, the analytical models were found to have FLD_0 located at the plain strain position, i.e. at zero minor strain.

7.2 Small Scale Evaluation of Dry Film Lubricants using MSD Test

The dry film lubricants used in the MSD tests for each of the three coils had a profound effect upon the forming behaviour of the metal. Strikingly, the lubricant caused a significant modification to the forming modes experienced and consequently the percentage draw and fracture height. The material that was most influenced by the dry film lubricants was the FeP04 cold rolled mild steel. It is uncertain how much of the difference between the metals related to the r-bar and lower yield (0.2% proof) strength and how much related the thickness. The FeP04 coil material possessed significantly higher r-vales, a lower yield strength and lower thickness than the other two steels. Under the lighter blank-holder loads this material was found not to fail at all and instead the cup draw out from the blank-holder region. Interestingly, with the exception of the FeP04 coil, the lubricant performance was found to be particularly similar, although in almost all cases Hydrodraw 625 was found to enable greater levels of percentage draw and higher values of fracture height. Experimentally, the lubricant was found to improve the strain distribution o the sample and the greater levels of draw relate to lower friction values, which reduced the degree of material restraint, imposed by the blank-holder.

The results clearly indicated that the dry film lubricants were able to maximise the sample material performance in each case, by improving strain distribution, but also reducing frictional restraint of material toward the die. The higher friction conditions, relating to the samples tested in the unlubricated condition, clearly illustrated a constraint on the minor strain (positive or negative) which confined the deformation mode to one of essentially plane strain stretch, which has the lowest forming limit.

The fracture height of the MSD samples was found to be proportional to the punch radius. Therefore, the results of the MSD tests also strongly illustrate that the process or FLD signature of a part is strongly dependent upon metal, lubrication (friction), forming parameters but also the tool geometry.

7.3 Experimental Tube Hydroforming Trials

- ***Initial Hydroforming Trials***

The results of the tube hydroforming trials illustrated the significant difference in the response of the tube metals to the different hydroforming process conditions, despite the difference in wall thickness between the metals. The results also demonstrated how sensitive the experimental hydroform geometry was to the various feed rates applied. This was mapped by the substantial difference in strain mode observed, which consequently resulted in different outcomes. A large part of the variation observed in strain modes, found from using the different processing conditions, was due to the component geometry along with the frictional conditions. If the severity of the hydroform expansion zone were to have been lower, the FLD process signatures would be similar to the extent that there was not expansion region, then the FLD signature would be identical due to the far more limited range of available process conditions. Moreover, failures du to the onset of necking would not take place, making it increasingly more difficult to determine the FLC.

Due to the large uncertainties of tube manufacture the practical trials reinforce the necessity to conduct trials on the tube formability to develop a suitable knowledge base of the required products.

Interestingly, the dry film lubricant appeared to provide a friction coefficient that appeared independent of steel tube surface texture and more importantly internal pressure, and behaved similar to a hydrodynamic lubricant according to the Stribeck curve.

The hydroforming trials that were performed enabled the verification of the analytical FLC models reviewed. Additionally the trials supported the development of the FEA models that were developed.

- ***Corner radius development***

The development of a hydroformed component corner radius is achieved with significant increases of internal pressure, resulting in local strain and therefore potentially excessive local thinning.

The relationship between the corner radius and internal pressure was found to approximate an exponential curve. The relationship was also influenced by tube end feed rate. At lower feed rates a wide range of scatter was observed, due to difficulty in maintaining adequate sealing conditions. However, with increasing feed rate increases uniformity was observed. With the higher feed rates, smaller corner radii were observed which may be explained by the lower combined stress required to cause yielding of the tube metal, assuming that the deformation follows an isotropic hardening nature.

- ***Verification of the Analytical Tube FLC models***

The approximations of the tube FLC from the assumed strains in tube manufacture and original sheet FLC (Table 6.4), was found to provide a reasonable indication for the FeP04 and HSLA tube metal. In strong contrast the FeP10 tube FLC determined using this method was not sufficiently accurate and would not be suitable for the forming evaluation of a tube hydroformed component. This illustrates that a tube FLC, derived experimentally or from a hydroform test would provide the most accurate means of assessing the hydroforming process.

Whilst the analytical models exhibited reasonable agreement with the experimental hydroforming data there were differences. In particular the FeP10 tube analytical FLCs were found to differ from the test data, with the FLCs underestimating the forming limit.

Whilst an exact reason is not known for the differences observed for this and the other metals, a number of influences may have caused the differences. In particular, influences

such as strain rate hardening and normal stress influences may have contributed to the differences observed. These factors were not considered in the analytical models evaluated.

Strain Rate Hardening

The 80mm thickness mechanical properties of the coil and the tube metals were obtained for a specific nominal strain rate, developed by the tensile testing equipment (0.01/s). This strain rate was only valid for the range of deformation between proof stress and uniform elongation. The strain rate developed beyond uniform deformation was not considered, as the strain distribution was not uniform. The strain rate would therefore require measuring for discrete regions of the sample beyond uniform deformation. During the experimental tube hydroforming trials the average strain rate of the hydroforms was of the order of 0.015/sec and therefore was not significantly different from that of the tensile tests. This is in strong contrast to the strain rate hardening that could be expected from press forming of sheet metal. However, during the first 6 seconds of the hydroforming process, the strain rate for the stainless steel (and other tube materials) was higher. With a feed rate of 0.004mm/Bar, the strain rate was 0.0275/s, due to the large initial expansion. However, the strain rate gradually reduced for the majority of the hydroforms due to the contact with the walls of die cavity. For the hydroforms subjected to higher levels of axial end feed, in spite of the average decrease in strain rate, the corner regions possessed slightly increased levels of strain and therefore strain rate. The maximum strain rate for the corner regions corresponded to the FeP04 tube material, where the average strain rate was 0.0225/s.

For steels that possess positive strain rate sensitivity, an increase in strain rate may ultimately reduce the tendency for strain localisation and provide a more uniform strain distribution [186] and thereby increasing the forming limit.

Normal Stress

An additional phenomena that may have influenced the component strain distribution, in addition to the strain rate and frictional behaviour, was the possible influence of a normal force or normal stress component acting through the thickness of the deforming tube. The normal force or stress may have acted to raise the forming limit.

Other Factors

Another possible reason or source error in experimental FLC data, obtained from the hydroforming trials was the variability of the tube material properties, including through and cross coil, coupled with the associated thickness variations. Additional factors, such as tube roll-forming marks, externally or internally, may also have contributed to the initiation of the necks, as observed with the hot rolled mild and high strength steels. The other experimental contributors may have included a lack of uniformity of the lubricant employed and the accuracy of the strain analysis, particularly for the corner regions of the components.

Although the tube tensile and hydroform data was somewhat limited, it clearly illustrated that an analytical FLC could be utilised to good effect, where the component would be subject to essentially linear strain paths. The analytical FLC would therefore be suitable in the FEA of a tube hydroformed component when the deformation consists of essentially linear strain paths.

The stainless steel tube experimental data obtained was found to fit reasonably with the Swift-Hill FLC and the Empirical FLC where the maximum terminal n-value was considered to be no more than 0.21, unlike Andersson [187], who used the actual full n-value from the tensile tests. Subsequently, Andersson found that the Empirical FLC, proposed by Keeler and Brazier, overestimated the experimental data.

7.4 FEA of the Tube Hydroforming Process

As with the experimental hydroforming trials, the FE models illustrated that a critical tube inflation pressure range existed, dependent upon the tube metal. This critical range was found to be between 200 and 400Bar for the FeP04, FeP10 and stainless steel tube and 300 and 500Bar for the HSLA tube. It was during these pressure ranges that the greatest increase of thinning took place prior to necking, and ultimately determined the final degree of thinning the component possessed, even using the high feed rate of 0.025mm/Bar.

- ***Influence of Friction***

The Coulomb friction coefficient used in the FE models had a profound influence on the level of thinning of the hydroforms studied. In no instance was a medium to high friction coefficient found to benefit the hydroforming conditions, as it can have in some circumstances when press forming. In fact quite the opposite was found. The influence of increasing the friction coefficient was found to cause increasing levels of thinning, resulting in predicted splitting or excessive thin out conditions, i.e. thinning above the safe limit. Whilst each of the metals displayed differing responses to the feed rates and friction values the overall trend was the same. The thinning tendencies of the tube hydroforming models can be explained by the influence of the feed rates and friction coefficient on the strain path or process signature. Figure 107 illustrated that increasing the end feed rate would proportionally increase the negative minor strain of the hydroformed model, due to higher compressive loads being applied.

The influence of increasing friction reduced the magnitude of minor strain developed as the frictional resistance effectively reduced the compressive loads. When the frictional resistance was high i.e. a friction coefficient of 0.15, coupled with increasing pressure, the end result was a thickening of the tube wall in the guide regions, which increased with increasing tube feed rate. This action was found to therefore prevent the required material feeding or flow to the centre expansion region, necessary to prevent material 'thin-out'. In addition to inhibiting material flow into the die cavity form the tube ends, increasing the friction coefficient increased the major strain locally, tending the strain

path for the element (critical strained region) towards the FLC. This effect was a result of the poor strain distribution around the hydroform at section A-A, resulting from the higher friction value. The lower friction values also increased the strain uniformity of the component, and therefore the thickness, by allowing the material against the flat walls of the die to continue to strain as opposed to locking against the die cavity wall. This is referred to as a 'die lock' condition and is observed under conditions of high frictional coefficient or geometry related factors.

Due to the low friction, dry film lubricant (Hydrodraw 625) used in the experimental hydroforming trials, the FE model reliability increased as the friction coefficient remained consistent for all of the materials and process conditions used. The FE analysis correlated best with using the friction coefficient of 0.01. This frictional coefficient was lower than the value determined by Masseria [188], who determined that for the friction strip draw test, using the FeP04 steel using the Hydrodraw 625 lubricant, a dynamic friction coefficient of 007. This value was comparable to the results of the test performed using Mo_2S as the dry film (0.08). If the friction coefficient of 0.01, used in the FE models, was representative of the friction coefficient in practice, this would reinforce the findings of Eichhorn [134] who determined that the friction coefficient in tube hydroforming was lower than found in strip tests.

- ***Influence of Material***

The strain path the FE hydroforms were not only influenced by the processing conditions and the friction coefficient but also by the material properties. Figure 108 illustrated the difference in strain path for the FeP10 hydroform modelled using sheet and a tube material data. Interestingly for the strain path of the element considered, the FeP04 tube material displayed a moderately more negative minor strain than the FeP04 sheet metal, using the same friction coefficient (0.01) and a feed rate of 1.25mm/ms (0.025mm/Bar). This is believed to be due to the differences in yield or proof strength between the coil and tube. The model using the coil properties was "softer" and therefore would thicken at lower compressive loads than the model using the tube properties. Therefore, the higher

yield value lead to an increase in the minor strain as more material was forced into the die cavity, instead of being "consumed" by thickening.

The influence of material properties was also strongly illustrated by the FeP04 sheet versus tube models, which found that the sheet metal, despite having a moderately higher degree of formability failed due to wrinkling and splitting for the entire range of processing conditions. It is believed that this was due to the difference in 0.2% proof strength, where the sheet material had a lower value and was therefore softer and more susceptible to wrinkling. In the case of the FeP10 FE models, the model using sheet properties was predicted to form safely under all of the processing conditions, whilst the model using tube properties would only form safely using a feed rate of close to or above 1.25mm/ms (0.025mm/Bar).

These results illustrate a number of important implications. Firstly it has illustrated the necessity to have accurate tube hardening curve data to accurately represent the tube materialin the FE model. Based upon the FEA, using the sheet properties, the component would have not been feasible under the particular tube hydroforming conditions and geometry. The other important implication is that from a metals property perspective, the softer, lower yield strength associated with the parent sheet steel is not necessarily ideal for the tube hydroforming process and in this instance the tube properties, as work-hardened, were more favourable. The significance of this is that steel suppliers who are developing new tube manufacturing capabilities, to meet the newly emerging tube market of high D/t ratio tubes may produce tube which are not favourable for the tube hydroforming process due to the potentially lower work-hardening effects of the processes.

The importance of having accurate tube hardening curve data was also demonstrated by the results of the stainless steel FE models comparing the different hardening curve input types.

Interestingly, as found in practice the difference in material properties was found to have a profound influence on the level of corner fill. The stainless steel tube having a higher work-hardening rate than the FeP04 tube was observed to possess significantly larger corner radii for the same internal pressure. This was also observed experimentally.

Further improvements to model accuracy were found when the weld properties were integrated into the FE model as illustrated by Figure 6.85. In the case of the stainless steel this was not found necessary. However, the extent of material characterisation may be limited and the degree of the model development required may also be lengthy. Therefore, it is important to establish the key properties and the degree of accuracy required from the model, which may only be possible through further research.

- ***Influence of Processing Conditions***

The FE models developed in this research project provided suitably accurate predictions of the hydroforming behaviour of the entire range of materials. The limitation of the process simulations was found to exist at the lowest feed rate of 0.004mm/Bar, where the models did not account for a potential loss in sealing force and therefore a low pressure increase. The 0.004mm/Bar feed rate models for the conventional steels also prematurely predicted necking failure at significantly lower pressures, 200-300Bar less than found in practice. However, despite the underestimation of pressure, the experimental hydroforms, with the exception of the stainless steel metal, all failed using 0.004mm/Bar before reaching 1000Bar. It would appear that this is an area for the Pam-stamp™ code to develop further.

The tube FE models were found to provide an accurate description of the hydroforming process and the influence that the material properties would have. In comparing the strain profiles, good correlation was generally observed. However, it is not possible to indicate the level of error in the simulation due to the large number of practical factors, which may have clouded these errors. These factors include the variability in the tube properties and wall thickness. However, of potentially more significance was the degree of accuracy possible using the Camera CSA (circle strain analysis) equipment. Whilst it was

found to be consistent, errors due to the component geometry, such as corner radii created difficulties in accurately determining the surface strain, due to difficulties in positioning the camera probe. It has been previously estimated that the CSA performed may be accurate to within 4% strain [189]. Therefore, although the experimental data represents the true findings, the surface strain data was subjected to a number of potential influences, which may have resulted in small errors.

Summary

The geometry of the tooling for a hydroformed component can be used to closely control the thinning and deformation mode that the tube is subjected to and potentially the final formed properties. Frictional influences are more significant in the high pressure tube hydroforming process as the increasing internal fluid pressure acts as increasing blank-holder load would in a pressing process. From the experimental trials performed, the hydroform geometry used was found to be extremely sensitive to both friction and end feeding influences, which the FE models predicted. Based upon the high degree of correlation between the experimental and FEA results, this research project has illustrated that FEA can be used effectively in the development of hydroforming tooling design, process conditions and selection of optimum steel grades and frictional conditions.

8.0 Conclusions

The objectives of the research project have been to investigate the fundamentals of the tube hydroforming process, establish the influence of steel properties and to investigate the ability of numerical models, including FEA, to predict this process. The findings would contribute to the overall research effort required to enable greater implementation of this technology for future vehicle generations.

This thesis has presented the findings of the research project, including the use of invaluable small-scale test techniques to determine the mechanical tensile and forming behaviour of the tube and parent coil metals. This was further reinforced by large-scale experimental hydroforming trials, utilising the Anton Bauer Hyprotec high-pressure tube hydroforming unit. This enabled the identification of influence of the hydroforming process conditions on the tube metals studied and how the steel properties influenced the process. Finite element models of the process were developed indicating the current state-of-the-art capability to aid in the design and manufacture of automotive tube hydroforming components.

8.1 Influence of ERW Tube Manufacture on Strip Steel Properties

A detailed survey was performed to establish the influence of ERW tube manufacture on the original strip steel products. The principal focus was to establish the potential effects on the intrinsic material properties but this also included the influence of ERW production on the material thickness and surface characteristics. Consequently, it was possible to establish how the steel tube material would perform under hydroforming conditions.

8.1.1 Tube Properties and Dimensions

- It was found that whilst general reductions in steel formability are likely on ERW processing, the changes may not be significant. The changes in formability could be estimated in some instances, e.g. FeP04 and HSLA. However, the changes that were determined could not be predicted with any certainty for the full range of metals studied as the change or response to tube manufacture appeared to be more strongly influenced by the specific steel grade than the D/t ratio of the tube metal.

- The most significant changes to the strip steel mechanical properties were an increase in the 0.2% proof /yield strength, and decreases in the n-value, uniform and the total elongation values

The reduction in the key formability parameters translated to a reduction in the analytically derived FLCs.

- The behaviour of the hot rolled, mild steel (FeP10) was found to exhibit the most dramatic change in formability.

- ERW tube manufacture was found to increase the variability of the steel tube mechanical properties and wall thickness.

- Improvements in strip steel processing quality is essential to achieve consistent and uniform coil properties, in terms of both mechanical properties and coil dimensions, so that the tube product may be more consistent.

- ERW tube manufacture was found to be suitable for producing tube for subframe and chassis applications but had significant limitations in availability and quality for B-I-W applications.

8.1.2 Surface Texture

By evaluating the changes in surface texture new or improved means of tube processing, texture rolling or hydroforming lubricants may be identified. This research project identified a number of key changes in the surface characteristics of the strip steels.
The key texture changes that were found included: -

- ERW tube manufacture significantly decreased the mean and r.m.s. roughness of the original steel coil metals.

- ERW tube manufacture significantly increased the average total asperity height of the original steel coil metals.

- ERW tube manufacture introduced numerous surface imperfections, which resulted in a product with a non 'A'-class finish, therefore indicating that this tube material type would only be suitable for non 'A'-class components applications.

8.1.3 Small Scale Evaluation of Dry Film lubricants using MSD Test

The MSD test provided the means to evaluate the influence of the dry film lubricants on the forming characteristics of the strip steel products studied. The dry film lubricants were found to:

- Reduce friction between the die plates, punch and the sample.

- Increase the percentage draw and fracture height for the same given blank-holder load compared to unlubricated material.

- Improve strain distribution.

- Increase drawing and biaxial deformation of the FeP04 steel.

- Increase biaxial deformation of the FeP10 and HSLA steels.

The behaviour observed in the MSD tests provided a strong indicator of how the lubricants would behave under tube hydroforming conditions. The hot rolled steels both had higher yield strengths, and lower r-values allied to a heavier material thickness, which resulted in the low draw characteristics observed.

8.2 Experimental Tube Hydroforming Trials

From the experimental tube hydroforming trials it was found that friction and tube end feed, governed by the feed rate, were critical parameters in attempting to achieve hydroformed tubes free of wrinkles, necks or splits. The principal reason for the sensitivity to these two parameters was due to the die design, which demanded a high level expansion of the starting tube perimeter. In the absence of or at low levels of tube end feed, as used in the experimental trials, tube wall thin-out would result for all the conventional steels when subjected to the strain levels required to achieve the design geometry of the hydroformed component.

The general intrinsic material properties of the HSLA slit coil material, which caused the low level of draw in the MSD tests caused the low degree of draw in the tube hydroforming process, resulting in an inability for the material to flow resulting in body wrinkling of the hydroform. These intrinsic properties were due to a combination of high yield strength, very low r-values and the heavier material thickness of 2.0mm. The increased thickness and yield strength would have meant that the tube did not have the same degree of die wall contact and therefore less axial (column) stiffness, resulting in wrinkling.

- The hydroform design geometry used in the experimental trials had a major influence the forming behaviour and capability of the tube material as substantially higher levels of strain and internal pressures were achieved compared with those possible under "free forming" conditions.

- Insufficient axial end feed was found to cause excessive thinning resulting in tube splitting.

- Medium to high friction had the same influence as a low feed rate, in terms of on the level of component thinning.

- The experimental data was found to display good correlation with the Analytical FLC models proposed, which include: -
    - Empirical or Modified Swift-Hill tube FLC for conventional steels.
    - Swift-Hill or Empirical FLC for normalised 304 stainless steel tube.

The tube hydroform tool geometry, frictional effects and processing conditions are all critical in controlling the flow of the tube material in the die cavity and therefore on whether the outcome of the process is successful or not.

8.3 FEA of the Tube Hydroforming Process

The FE models created using Pam-stamp™ software accurately described the tube hydroforming process for a wide range of steels and processing conditions. One of the key factors in the close correlation was due to the simplification of the hydroforming process but also due to the extensive metals characterisation that was performed to ensure accurate material representation on the FE models.

More accurate FE models of the tube hydroforming process were obtained using :

- Tube material stress-strain curve data, as opposed to steel coil data.
- Experimental stress-strain data when Krupkowsky curve fit is significantly different.
- Full anisotropy parameters or r-bar where unavailable.
- Incorporate weld properties where appropriate but not essential.
- Use appropriate analytically derived FLC (Empirical, Swift-Hill or Modified Swift-Hill where appropriate) based upon tube mechanical properties.

If sheet material properties are used to represent ERW or other tube mechanical properties in FE models of tube hydroforming, then unreliable results can be expected. This may have major consequences such as delays to prototyping or production.

The dry film Hydrodraw 625 provided a very low friction coefficient, practically which corresponded well to the models using a friction coefficient of 0.01 for all of the metals and processing conditions used during hydroforming, thereby enabling a robust FE model to be generated. The reason behind this was that one of the factors influencing the hydroforming process was made consistent.

9.0 Practical Implications

From the research programme undertaken in this thesis, a number of practical implications have been identified which strip steel, tube, lubricant and hydroformed component manufacturers should consider in the design of a hydroformed component.

- ***Influence of ERW Tube manufacture***

The ERW tube manufacturing process modifies the mechanical properties of the steel tube. This modification was found to be an increase the yield / 0.2% proof strength and generally a reduction in the formability over the original strip steel. The modifications, whilst likely to be influenced by D/t ratio may be strongly influenced by the steel grade. The modifications cannot be easily predicted as the roll forming process that shapes the slit coil to form a tube is complex which subjects the tube materialto potentially many forming modes. These include plane bending (including reversals) in forming the slit coil into a general W or U shape. The tension in the slit coil being passed through the rolls during ERW tube manufacture may also cause some degree of materialstretch. Additionally, after welding the tube may be subjected to radial compression due to the sizing operation required to fix the tube diameter. This is achieved by passing the tube through a series of squeeze rolls and usually a die. Tube straightening is also performed to ensure that for a given length the tube meets required specification. In addition to the variable strain modes, local contact between the slit coil and roll forming dies may cause local work-hardening effects. The welding operation itself may induce work-hardening in the parent slit materialclose to the weld region due to the effect of the welding squeeze rolls which push the slit coil edges together to form the tube. In the design of a tube hydroformed component, it is important for the materialsupplier and the manufacturer to appreciate that the original strip steel properties are unlikely to be retained and therefore to design the component accordingly.

Due to the complexity of the roll forming process the accurate prediction of the formability of the ERW tube blanks was not possible based upon the parent coil properties and could potentially result in significant errors depending upon the steel grade. Differences in the set-up of the rolls on a tube mill that is not dedicated to the

rolling of one tube type, may also have influences on the final tube product properties. The differences in the mill set-up though are likely to depend upon the incoming slit coil, although subtle differences in the shit operators could also lead to differences.

- ***FLC Applicability to Tube Hydroformed Components***

In using appropriate analytical FLC models it was possible to predict steel tube formability limits reasonably accurately when hydroforming, particularly when the tube is formed into relatively simple component geometry. Applicability of the analytical FLC models would be limited to essentially linear strain paths on their own. For complex components, thinning analysis or manipulation of forming limit stress diagrams using analytical FLCs may be more appropriate. The Empirical and modified Swift-Hill FLC models were found to be suitable for the conventional steels studied and it is believed that this would potentially extend for a wider range of D/t ratios and steel grades. For the 304 stainless steel tube the Swift-Hill would provide a suitable forming limit for linear strain paths.

The selection of the appropriate steel for a tube hydroform application does not purely involve meeting the required performance requirements but also the hydroforming requirements.

- ***Surface Texture and Lubrication***

The surface texture of conventional steels may be modified significantly during ERW tube manufacture. In the experimental hydroforming trials the surface texture appeared to play an almost insignificant role with low friction behaviour being observed for the full range of hydroforming pressures used and for all of the steels used. This was partly due to the solid/EHP lubrication regime that Hydrodraw 625 provided. This behaviour would be similar to the Hydrodynamic Stribeck behaviour. However, from the reported results of the hydroforming friction tests, surface texture could play a more significant role in the adherence of the lubricant to the steel tube surface. Therefore when using oil-based or similar lubricants in conjunction with ERW tube, the lubricant performance may either be enhanced or reduced. Consequently, it is important for the steel supplier to identify the

mechanism behind the surface texture changes to be able to supply steel with an optimal texture and lubricant combination for particular hydroforming conditions.

- ***FEA of the Tube Hydroforming Process***

The FE models that were developed produced accurate results, particularly for processing conditions having medium to high end feed levels. The accuracy of the models was limited to the assumptions made, including material models for anisotropy, isotropic hardening form and strain-hardening curves, in addition to the simplification of the physical processing conditions. These engineering assumptions are the strongest limitations of the models developed and must be borne in mind in the development of real automotive tube hydroformed components to ensure successful forming. Similar assumptions may result in similar errors to those observed. An improved model accounting for pressure loss could be devised. However, such a model is unlikely to be able to consider the plastically deformed tube end, due to cone sealing, if it is constructed using shell elements. However, if 3D brick elements were utilised then this phenomenon could be accounted for, which would give rise to a more accurate minimum sealing force. However, models using 3D brick elements have considerably longer computation times and would not be suitable for the FE analysis of component feasibility and optimisation, when considering a new vehicle development programme. For now, the analyst must be aware and understand the implications of the model limitations.

The FE models developed exhibited a strong sensitivity to the material properties used to represent the tube blanks. This sensitivity may have been exacerbated by the very low friction conditions but also by the die geometry analysed. Interestingly the FE results indicate that by utilising the sheet properties to represent the tube blank, errors in predictions would result, i.e. in certain circumstances necking/splitting failure would be predicted when in practice it would not and vice-versa. Further improved FE model accuracy was achieved by incorporating the tube weld-line, although in practice this would increase model size, complexity and computation times and would therefore be avoided where possible.

Aside of the analytical FLC models that could easily imported into the Pam-Stamp™, or other similar codes, for post-process analysis it was found that thinning analysis provided a robust failure criterion, which could establish the forming severity of a tube hydroformed component. The limitation of the thinning analysis is that where regions thicken significantly they may or may not be subjected to wrinkling/ section folding, which may go undetected without component visualisation. Under such circumstances the component would not result be subjected to excessive thinning/necking but would still be considered to have failed as it did not achieve the desired component geometry.

The degree of accuracy established will provide further confidence in the reliability of the results of FE models of the tube hydroforming process. This fact is important, as a major role of FE modelling of forming processes is targeted at component feasibility studies.

- ***New Tube Manufacturing Processes***

By examining the influence of using original coil properties in the hydroforming process models, it was possible to illustrate that new tube manufacturing techniques (for higher D/t ratio tubes produced with almost unchanged mechanical properties) would not necessarily improve the suitability of a component for tube hydroforming. In the case of FeP04 material, at 1.2mm or less, the increase in yield strength was found to be of benefit in preventing wrinkling during tube hydroforming. However, in contrast, the more formable tube (modelled using the coil material properties), the tube may was susceptible to wrinkling/folding, preventing successful outcome. This affect may have repercussions during pre-bending, pre-forming and tube hydroforming and significantly limit the application of the new steel tube products. It will therefore be imperative to design the hydroform component according to the tube product used or tailor the tube product according to the design constraints.

The research project also identified that significant quality improvements are necessary in coil processing to improve coil profile and properties to ensure a consistent tube product. Additionally, suitable new steel grades may be manufactured for the purpose of tube hydroforming. Such tube hydroforming steels are likely to have high average

anisotropy, which provides a high draw and reduced thinning tendency, but also steels with a high stretch capability (n-value) coupled with suitable strength. Until such steels are manufactured, a major emphasis to provide suitable steel tube hydroforms for B-I-W structures will be placed upon the alternative tube manufacturing technologies. Stainless steel exhibits high formability characteristics and good hydroforming behaviour due to its high n-value. However, the base price of this material may prevent widespread application of this material into the body structure, although critical structures may be considered as a result of their high work-hardening rate. However, there are also issues of welding stainless steels to conventional steels providing further restrictions for their implementation.

10.0 Recommended Further Research

The use of tube hydroforming for automotive applications is likely to increase as requirements for reduced vehicle mass, spurred by demands for improved fuel efficiency and lower emissions, grows.

A number of areas of research, highlighted in the critical review of literature, indicated key enabling technologies, such as tube manufacture, the forming processes, FEA and assembly and joining technology. Part of the manufacturing element of producing a tube hydroformed component was addressed in the project undertaken, having determined a number of essential facts relating to steel formability and its influence and interaction with the tube hydroforming process and how FEA may be utilised to predict the forming process.

Whilst a number of guidelines for forming evaluation and FEA of the hydroforming of steel tube have been identified, a number of areas for research that were either not conclusive from this project or require further detailed investigation, some of which were highlighted in the chapter 9.0.

The principal areas include expanding upon the steel grades studied (in ERW tube form) in this project for high volume under body and lower body automotive applications, such as trip and Ultra high strength steels for chassis frame rails.

10.1 Full Process

10.1.1 Tube Manufacture

However, yet further work is necessary to be able to simulate the full "through" process forming operations, including tube manufacture. By understanding the ERW tube making processes better it will be possible to optimise this process, in terms of line-speed or flower pattern for example, or the steels grades used or the processing conditions of the

original coils. This last comment is particularly valid in the case of cold rolled grades, which undergo a skin pass or temper rolling process to eliminate the development of Luders bands. This is not necessary for ERW slit coil as the tube making process is effectively a skin pass process, although potentially more severe. Therefore, it would be possible to supply coil without having been temper rolled and thereby achieving a greater level of formability in the final tube product.

Due to the mechanical property changes in strip steel found in this research project it is necessary to understand how a wide range of steel grades (beyond those studied) will respond when subjected to ERW tube making, particularly hot rolled high strength and ultra-high strength steels such as TRIP steel. This is stated as, depending upon their response, these steels may have significant design limitations on the scope of suitable automotive applications based upon the sectional designs and therefore the subsequent formability requirements.

As the new tube manufacturing technologies are still emerging to cater for the large D/t ratio tube for B-I-W applications, which cannot be achieved on ERW tube mills, it is essential to identify their process limitations as early as possible and to be able to design out the limitations. This may be achieved either by means of pre-process technology, the tube hydroforming process, hydroform die tool design or through the optimal selection of the steel grade.

Tailored Welded Tube (TWT)

Whilst the manufacture of a unique Tailored Welded Tube (TWT) configuration was developed in this thesis, TWT technology provides the potential to produce complex tube hydroformed components. With the added benefits of laser welded blank technology, i.e. mass and cost reduction, by only utilising the required thickness / strength of steel where necessary, TWT hydroforms may provide enhanced weight reduction and improved component performance over conventional pressings and single piece (single thickness) tube hydroforms. Additionally, TWT s consisting of different, dedicated coated strip steel products for the different vehicle regions could also be realised. Before full realisation of

the benefits of hydroformed TWT technology is achieved, substantial research is required to enable the production of automotive quality components. This technology is likely to see fruition in the manufacture of front longitudinal (crash-rails) and similar components.

10.1.2 Pre-process steps

The pre-process steps to produce a tube hydroformed component may be developed further. Although the tube bending process and tooling has comparatively a higher degree of maturity than tube hydroforming, there may be particular requirements and opportunities for development for use in applications having tube produced using the new technologies. These developments may involve specialised tooling or innovative techniques. The pre-forming process, which is currently a crude operation, requires research in how to utilise this process to optimise the tube hydroforming process, by improving material flow or wall thickness distribution. With more difficult sections where end feed is restricted this process may be critical in producing a successful component. New techniques/innovations to aid in the pre-process of the steel tube are required to cater for the low to medium volume B-I-W production, best suited to the tube hydroforming process cycle. For the steel suppliers the main focus should be on the developing suitable pre-process techniques for tube produced using the new technologies.

10.1.3 Tube Hydroforming

Whilst a broad understanding of the tube hydroforming process is developing, some of its limitations and effects on components for assembly and performance are less well known or understood. The nature of the forming process, depending upon die geometry, will induce a significant level of work-hardening into the metal. Whilst this cold-work effect may increase the yield strength of the component and potentially have some benefits to impact performance, in terms of a higher peak load, the component durability is likely to deteriorate [45]. However, the influence of pre-strain on fatigue life has only been examined for sheet material and no reported results of fatigue behaviour have been published so far. Therefore, the control of the tube hydroforming process to aid or

influence the component performance is of critical value in the future development of this automotive technology.

In terms of forming evaluation further development of the forming limit curve or forming limit stress curve is necessary as is the requirement to ensure the appropriate hardening models are employed in FE models, particularly with complex, multi-process stage hydroformed components.

10.2 FEA of the Tube Hydroforming Process

The majority of features that are likely to require improvement in the forming analysis of tube hydroforms are the introduction of material model improvements and integration of suitable failure criteria. Aside of material behaviour, improvements in the accuracy of tube hydroform models need and will continue in many forms, including the element formulation or material model "type". Significant improvements or advancements in all areas will only be achieved through collaborative research programmes between the software developers, the material suppliers, the component manufacturers and the end users. Furthermore, simulation tools to assist in rapid evaluation of hydroform component feasibility is necessary as under the current methods, the analysis time is tool long, and provides a major risk to the design and development of a component or design scheme.

10.3 Friction and Lubrication in Tube Hydroforming

The high-pressure tube hydroforming process develops high frictional forces between the tube blank and the walls of the die cavity, which increase proportionally to the applied internal pressure. Therefore, for tube hydroforming applications a very low friction condition is required to sufficiently lower the friction forces, thus enabling improved flow of material into the die cavity. Lower friction will also improving the strain and thickness distribution in the circumferential and longitudinal directions, maximising the capabilities of the steel. In all likelihood, an increasing number of solid, dry film or wax, lubricants will be developed by lubricant suppliers and utilised to meet these low friction

requirements. This will require further developments from Hydroform press manufacturers to design and produce systems, which are compatible with the lubricants.

Therefore, it is important to ensure that the final surface texture provides a suitable surface on which the lubricant can adhere to. Research is therefore necessary to determine the surface texture characteristics necessary to provide suitable lubricant adherence to the tube blank and is likely to be achieved through joint partnerships with lubricant suppliers. Research may ultimately be required to develop new textures, tube processing methods or lubricants to meet the needs of the hydroform manufacturer.

10.4 Influence of Tube Hydroform Manufacture On Coating Performance

Whilst the influence on coating performance is largely understood for conventional coated sheet steels that are pressed and spot or laser welded into assemblies, additional consideration and investigation must be performed for components that are likely to be tube hydroformed based upon coated strip steel products. The reason for this is due to the complexity and severity of the forming processes involved, outlined in this thesis.

Although the typical coating behaviour during pressing is either to powder or flake, depending on the forming conditions, coating and substrate, the tube hydroforming conditions are unique and the potentially high hydrostatic loads that hydroforming may subject a tube to may result in unique behaviour of the coating system. It is therefore necessary to examine current coating system behaviour, in terms of hydroforming and corrosion performance. It may therefore be possible to determine if existing coatings require developing for particular tube hydroforming applications or if new coating systems require development.

References

[1] Anon, World Automotive Manufacturing, Issue No.24 April 2000.

[2] Anon, Automotive Emerging Markets, Issue No. 33 May 2000.

[3] Peterson, P. T., 'Holistic Design – The Key to Light Vehicle Structures', Proc. International Symposium on Automotive Technology and Automation, 1996.

[4] Daniels, J., 'World Vehicle Forecasts & Strategies – Automotive Technology, Informa Publishing Group Ltd, p27 , ISBN 1 84083 165 0.

[5] Wells, P., and Nieuwenhuis, P., 'The challenge of globalisation and technological change', Automotive Materials, Financial Times Automotive, p 9.
ISBN 1 85334 912 7.

[6] Anon, Automotive World, June 2000.

[7] Anon, 'Manufacturing Flexibility Expected to Save DaimlerChrysler Corporation More Than $3 Billion in Production Launches Throughout 2004', PR Newswire, 8th June 2000.

[8] Anon, Select Committee on Trade and Industry, Appendices to the Minutes of Evidence - Appendix 7 – Memorandum submitted by Honda Europe Ltd , July 7th 2000.

[9] Vasilash, G. S., 'Honda's Hat Trick', Automotive Manufacturing & Production, October 2000.

[10] Anon, Automotive Engineering International, February 2000.

[11] Sinclair, S., 'The World Car – The Future of the Automobile Industry', W.W.Norton, 1979.

[12] Anon, Energy Policy and Conservation Act (P.L. 94-163), 1975.

[13] Anon, EC Directive 89/458/EEC.

[14] King, J., 'The Future of Steel in The Automotive Industry', South Wales Metallurgical Society Paper Presentation', 8th August 1997.

[15] Fekete, J. R., 'Overview of Metal Pressing', Sheet Metal Pressing Development and Applications', SP-1221-SAE International, February 1992, pp125-137.

[16] Wells, P., and Nieuwenhuis, P., 'The Challenge of globalisation and technological change', Automotive Materials, Financial Times Automotive, p 117.
ISBN 1 85334 912 7.

[17] Anon, Sollac Products and Services Brochure, SOLLAC, September 1996.

[18] Engel, B., Drewes, E-J., 'From 450Mpa Dual-Phase to 1,100MPa Complex Phase Steels: Development of A New Generation of Automotive Sheet Steels', IBEC '97. Proc. International Body Engineering Conference and Exposition, Automotive Body Materials, pp127, Detroit MI. USA, 1997.

[19] Takechi, H., 'Present Stage Practical usage of High Strength Steel Sheets for Automobiles in Japan', SAE Technical Paper No. 865053, 1986.

[20] Llewelln, D.T., 'Steels: Metallurgy and Applications', 2nd Edition, Butterworth-Heinemann Ltd, Oxford, ISBN 0 7506 2086 2, Chapt. 2, p34-59.

[21] Anon, 'Ultra-light steel car enters Phase II', Automation and Materials Processing, November 1996.

[22] Van Shaik, M. A. M., 'The Ultralight Steel Autobody Project – From a clean sheet of paper to a marketing tool for steel', Proc. International Symposium on Automotive Technology and Automation, 1996.

[23] Walker, E.F., Lowe, K., 'Ultra light Steel Auto Body', Proc. Materials for Lean Weight Vehicles', Institute of Materials, Gaydon, November 1995.

[24] Anon, 'Scrap and the steel Industry', Committee on raw Materials (Brussels 1997), International Iron and steel Institute publication, p49-56. ISBN 2 930069 295.

[25] Anon, 'Steel – the automotive material of the future', Automotive Manufacturing (C498/31/240/95), IMechE Seminar, Mechanical Engineering Publication, 1996. ISBN 86058 0238.

[26] Anon, 'Aluminium – making light volume car production', Automotive Manufacturing (C498/31/240/95) IMechE Seminar, Mechanical Engineering Publication, 1996. ISBN 86058 0238.

[27] Anon, Automotive Engineering Plastics, Pentech Press, London 1991. ISBN 07273 01152

[28] Bursa, M., ISATA magazine, April 2000 (Issue 9), p12-13.

[29] Anon, Patent Specification, Ref. Number: 676, 048 UK, May 26th 1950. No 13354/50.

[30] Anon, Patent Specification, Ref. Number: 701,547 UK, August 22nd, 1952, No 19818/51.

[31] Dohmann, F., and Hartl, C., 'Hydroforming – A Method to Manufacture Light-Weight Parts', Journal of Materials Processing Technology 60, 1996, p669.

[32] Personal communication with R. Schonnenbeck and W. Zimmermann (Technical Development Managers Siemplekamp Pressen Systeme (SPS) 21st July 2000.

[33] Siegert, K., Aust, M., 'State-of-the-Art of Hydroforming Tubes, Extrusions and Sheet Metals in Europe', 'Innovations in Tube Hydroforming', ERC / NSM International Conference and Exhibits on Tube and Sheet Hydroforming Technology, Manufacturing of Lightweight components. Detroit, MI, USA, June 2000.

[34] Bikert, A., 'Factors Influencing the Design of Hydroforming Tools', Proceedings of the International Body Engineering Conference, IBEC '99, 1999-01-3182, 1999.

[35] Mason, M., 'Hydroforming of High Strength Steel Tubes for Body and Frame Applications', Proceedings of 29th International Symposium on Automotive Technology and Automation, Florence, Italy June 1996, 96NM147, pp143-155.

[36] Dohmann, F., Hartl., C., 'Liquid Bulge Forming as a Flexible Production Method', Journal of Material Processing and Technology (1994), Vol. 45, p379-380.

[37] Limb, M. E., and Limb, A., M'Hydraulic Forming of Tubes and the Feasible Working Region', Sheet Forming, International Congress on materials Engineering, Birmingham, UK, September 1981, pp1-12.

[38] Anon, German Patent: DE 42 14 557 A1, Verfahren zum hydraulischen Aufweiten von geschlossenen Hohlprofien, Bundesdruckerei, November 1993.

[39] Tube hydroforming – research and practical application', Dohmann, F., and Hartl, Ch., Journal of Materials Processing Technology 71, (1997) 174.

[40] Mason, M., 'Hydroformed Tubes for Automotive Body Structure Applications', Simulation and Development in Automotive Simultaneous Engineering, SAE 930575, March 1993, pp59-64.

[41] Bruggeman, C., 'Hydroforming of Structure Parts for Personal Cars', Proceedings of the International Conference on Hydroforming, Fellbach, Germany, October 1999, pp 407- 424. ISBN 3–88355-285-2.

[42] Hannibal, T.A., Dieffenbach, J.R., ' Hydroformed Structural Elements: An Economic Evaluation of the Technology', IBEC '98, 980451, 1998.

[43] Walia., S., Gowland, S., Hemmings., J., Beckett, M., and Wakelin, P., 'The Engineering of a Body Structure with Hydroformed Components', Proceedings of the International Body Engineering Conf., IBEC '99, 1999-01-3205, 1999.

[44] Schulz, W-D., 'Presentation of a Hydroforming Volume Production Line for Engine Cradles', Proceeding of the Hydroforming Congress: Hydroforming for Large Volume Production, November. 1997. Germany.

[45] Boyles, M.W., Davies, G.M., 'Through Process Characterisation of Steel for Hyrdoformed Body Structure Components', Proceeding of International Body Engineering Conference 1999, IBEC '99, 1999-01-3205.

[46] Longhouse, B., 'Applied Pressure Sequence Hydroforming', Proceeding of 3rd Annual Automotive Tube Fabricating Conference, Dearborn, MI. USA, May 1998.

[47] Lassl, G., Hanicke, L., and Holm, S., 'Development of a Hydroform-Intensive Car Body Structure', Proceedings of International Body Engineering Conference - Advanced Technologies & Processes, 1997, IBEC '97 , pp11-1854.

[48] Lassl, G., Hanicke, L., and Holm, S., 'Lighter Car Body In Aluminium with Hydroforming Technology, R&D Result', Proceedings of International Body Engineering Conference - Advanced Technologies & Processes, 1996, IBEC '96, pp119-126.

[49] Leitloff, F.U., Pohler, D., and Gutierrez, V.A., 'Tolerances in Hydroforming – Process Layout and Tool Design', Proceedings of the International Conference on Hydroforming, Fellbach, Germany, October 1999, pp37-45. ISBN 3–88355-285-2.

[50] Personal communication with Derek Payne (UK Vari-form Representative) 6th October 2000.

[51] Prelog, H., Reicelt, J., and Wenzel, M., 'Hydroforming Frame Components – From Concept to High Volume Production', Proceedings of the International Conference on Hydroforming, Fellbach, Germany, October 1999,pp. 481-485, ISBN 3–88355-285-2.

[52] Wesel, F.W, 'Other Hot Forming Processes' – section 8.5 steel manual,., Verein Deutscher, Eisenhuttenlaute, Cerlag Stahleisen GmbH, Dusseldorf, Germany. ISBN 3-514 00455-2.

[53] Linnert, G.E., Continuous Upset Seam Welding, Chapter 6, Welding Metallurgy *(carbon and alloy steels)*, American Welding Society, Miami, Florida, USA.

[54] Smith, W., and Roberts, J., 'High Frequency Welding', ASM Handbook, Vol. 6 Welding , Brazing and Soldering, p.252-253.

[55] Anon, BS 3889 Part 2a, British Standard Specification for Eddy Current Testing BSI.

[56] Anon, BS 6323: Part 1: 1982 British Standard Specification for Seamless and Welded Tube for Automobile, Mechanical and General Engineering Purposes. General requirements, BSI.

[57] Nichols, K., 'Destructive Testing of Welded Tubulars', Tube & Pipe Technology September/October issue 1998.

[58] Anon, BS 6323: Part 5: 1982 British Standard Specification for Seamless and Welded Tube for Automobile, Mechanical and General Engineering Purposes. Specific requirements for electric resistance welded steel tubes, BSI.

[59] Anon, 'VAI Tube and Pipe Mill Technology Receives an Order for a Tube Welding Line in Russia', VAI press release, Linz, March 23rd 2001.

[60] Anon, VOEST-ALPINE Industrieanlangenbau GmbH & co Homepage : www.vai.at

[61] Bollinger, E., Jhtten, D.W., 'Tubes for Hydroforming, Proceedings of the International Conference on Hydroforming, Fellbach, Germany, October 1999, pp97-104. ISBN 3–88355-285-2.

[62] Blaszk, J., Bea, M., Trotha, L, and Stockinger, F., 'Laser Tube Cutting and High Productivity Laser Welding; Benefits, Challenges, Solutions' Tube & Pipe Technology, November/December Issue 1998.

[63] Burke, P., 'Hyfo' - Corus Internal Presentation, Welsh Technology Centre, June 2000.

[64] Gerlach, J., Kneiphoff, U., and Wonneberger, I., 'Thin-Walled Tailored Tubes for Body Structures – Production, Testing and Application', ERC / NSM International Conference and Exhibits on Tube and Sheet Hydroforming Technology, Manufacturing of Lightweight components. Detroit, MI, USA, June 2000.

[65] Stange, R., 'Tube and Pipe Bending – principals, methods, tooling and developments', Form No. 85163, 1997, p8.

[66] Kervick, R., J., and Springborn, R.K., 'Cold bending and Forming of Tubes and Other Sections', American Society of Tooling Manufacturing Engineers Publication, Dearborn, Michigan, USA, 1966, p76.

[67] 'Design Guidelines for Hydroformed Components', Jones, R., Twelves, M., Edgar, K., Proceedings of the Materials for Lean Weight Vehicles Conference, Gaydon, England, 1999.

[68] Birkert, A., and Neubert, J., 'Tool and Part Design for Tube Hydroforming', Proceedings of the International Conference on Hydroforming, Fellbach, Germany, October 1999, pp. 47-60, ISBN 3–88355-285-2.

[69] Osen, W, 'Specific Design Concepts for Hydroforming Presses', Proceedings of the International Conference on Hydroforming, Fellbach, Germany, October 1999, pp. 139-148, ISBN 3–88355-285-2.

[70] Anon, Schuler Metal Forming Handbook, Chapter 5, p429, Springer-Verlag Berlin Hiedelberg, 1998, ISBN 3-540-61185-1.

[71] Bieling, P., 'Mechanically locked Hydroforming Machines for High Volume Production', Proceedings of the International Conference on Hydroforming, Fellbach, Germany, October 1999, pp. 161-171, ISBN 3–88355-285-2.

[72] Osen, W., 'Specific Design Concepts for tube Hydroforming Presses', Proceedings of the International Conference on Hydroforming, Fellbach, Germany, October 1999, pp. 139-148, ISBN 3–88355-285-2.

[73] Nottrott, A., 'Siempelkamp Pressen System GmbH & Co., Krefeld, 'Hydroforming Machines and Plants', Proceedings of the International Conference on Hydroforming, Fellbach, Germany, October 1999, pp. 149-160, ISBN 3–88355-285-2.

[74] Anon, Schuler Hydroforming Brochure, 'Launching High Pressure Tube Hydroforming for Volume Production', 2000.

[75] Lewis, C., and gleave, M., 'A Spot of Welding on the Side', Welding and Metal Fabrication', June 1999, Vo. 67. No5.

[76] Personal communication with Matthew Gleave (Research Officer, BSSP WTC, Port Talbot) 20th October 2000.

[77] Personal communication with Kevin Edgar (Corus Tubes, PMD Manager), October 29th 2000.

[78] Zimmerman, W., and Lucke, H.U., 'Reducing Part Costs for Hydroforming', Tube & Pipe Journal November / December 1998, p98-102.

[79] Bruggemann, C., 'Hydroformed Body Side Structure in the '97 Buick Park Avenue: Introducing New Technology to Current Production in a Complex product Environment', IBEC '97, Proceedings of Advanced Technologies and Processes, 1997, p1-5.

[80] Personal communication with Ray Barrow (Quality Manager, Tyco Tube Ltd), January 12th 2000.

[81] Slater, R.A.C., Engineering Plasticity, Theory and Application to Metal Forming Processes. The Macmillan Press Ltd., 1977. p120-134. ISBN 0 333 15709 5

[82] Askeland, D. R.,'The Science and Engineering of Materials', 2nd SI Edition, Chapman & Hall,1990, ISBN 0-412-34260-X, Chapt 6, p152-153.

[83] Llewelln, D.T., 'Steels: Metallurgy and Applications', 2nd Edition, Butterworth-Heinemann Ltd, Oxford, ISBN 0 7506 2086 2, Chapt. 2, p35.

[84] Llewelln, D.T., 'Steels: Metallurgy and Applications', 2nd Edition, Butterworth-Heinemann Ltd, Oxford, ISBN 0 7506 2086 2.Chapt. 2, p15.

[85] Hollomon, J.H Tans AIME **162** (1945) pp268.

[86] Swift, H. W., and Chung, S.Y., Proc. Inst. Mech. Eng. **165**. 1951 pp199.

[87] Backofen, W.A., 'Deformation Processing', Addison-Wesley Publishing Company Inc., 1972, Chapt.10, p 202.

[88] Backofen, W.A., 'Deformation Processing', Addison-Wesley Publishing Company Inc., 1972, Chapt. 10, p207.

[89] Backofen, W.A., 'Deformation Processing', Addison-Wesley Publishing Company Inc., 1972, Chapt. 10, p215.

[90] Marciniak, Z., 'Tensile Instability Phenomena', Plasticity and Metal-Forming Technology, Elsevier Applied Science, 1989. ISBN 1851 66 2723.

[91] Hearn, E.J., 'Mechanics of materials', Vol.1 2nd Edition, prgamon Press 1985, ISBN 0 08 0311318, Chapt. 9, p198-199.

[92] Rees, D. W. A., 'Mechanics of Solid Structures', M°Graw-Hill Book Company, 1990. ISBN 0 07 7072227, p. 704.

[93] Thomsen, E.G., Yang, C.T., and Kobayash, S., 'Mechanics of Plastic Deformation in Metal Processing', The Macmillan Company, 1965, Chapt.6, p90.

[94] Backofen, W.A., 'Deformation Processing', Addison-Wesley Publishing Company Inc., 1972, Chapt. 3, p50.

[95] Hill, R., 'Mathematical Theory of Plasticity', Clarendon Press, Oxford. 1950, p325.

[96] Anon, 'Basic Formability', FTi course publication, March 1997, Chapt.2, p29.

[97] Keeler, S.P., 'Determination of Forming Limits in Automotive Pressings', Sheet Metal Industries, September 1965, p686.

[98] Goodwin, G.M., 'Application of Strain analysis to Sheet Metal Forming Problems in the Press Shop', SAE Technical Paper 680093, 1968, pp280.

[99] Anon, 'Basic Formability', FTi course publication, March 1997, Chapt6., p9.

[100] Keeler, S., 'Circle Grid System – A Valuable Aid for Sheet metal Formability', SAE Technical Paper 680092, 1968.

[101] Keeler, S.P., and Eisenbach, E.R., 'Metal thinning Analyses Supplement Circle Grids', Proceeding of the International Body Engineering Conf., IBEC '97, p47-53.

[102] Pearce, R., 'Sheet Metal Forming', Adam hilger Publishers, ISBN 0-7503-0101-5, Chapt. 12, p147.

[103] Anon, ASM Handbook 9th Edition. Vol.1, p550.

[104], Nakazima, K., Kikuma, T., and Hasuka, K., 'Study on the Formability of Steel Sheets', Yamata Technical Report No. 264. p 141.

[105] Hecker, S., 'Simple Technique for the Determining Forming Limit Curves', Sheet Metal Industries, November 1975.

[106] Keeler, S. P. and Brazier, W. G, 'Relationship between Laboratory Material Characterisation and Press-Shop Formability', Proc. Of Microalloy 75, New York, 1975. pp.517-530.

[107] Backofen, W.A., 'Deformation Processing', Addison-Wesley Publishing Company Inc., 1972, Chapt.10, p 208.

[108] Montfort, G., 'Summary of Experimental FLD Work', Benelux Deep Drawing Research Group (BDDRG), BDDRG Working Group, LiPge, May 14, 1997.

[109] Anon, SO 12004: 1997 (E) Metallic materials – Guidelines for the determination of forming-limit diagrams.

[110] Kergen, R., and Lescart, J.C., 'Analysis of the tube formability in perspective of tube hydroforming', Proceedings of the WG IDDRG, Birmingham, 1999.

[111] CimetiPre, R., 'Influence of Some Parameters on the Forming Limit Curve', British Steel Internal Placement Student Report, January 1999.

[112] Delaby, B., 'Forming Limit Stress Curves', British Steel Internal Placement Student Report, January 1999.

[113] Darlington, R., A., Parker, J.D. and Godwin, J., 'Forming Evaluation of Complex Tube Hydroformed Components', Darlington, Ironmaking and Steelmaking, 2000 Vol.27, No.6pp 461-468.

[114] Levy, B., 'Recommendations on the Use of Forming Limit Curves for Hydroforming Steel', International Conference on Hydroforming, Fellbach, Germany, October 1999, pp 77- 95. , ISBN 3–88355-285-2.

[115] Hora, P., Skiekerud, M., and Longchang, T., 'Possibilities and Limitations of FEM-Simulation in Hydroforming Operations', International Conference on Hydroforming, Fellbach, Germany, October 1999, pp 407- 424.

[116] Personal communication with John Godwin (Principal Research Officer, British Steel, Welsh Technology Centre).

[117] Visit to Addison International, 20th May 1998.

[118] Personal communication with Kevin Edgar (Project Engineer, Corus Automotive Engineering - CAE, formerly Bristish Steel's Automotive Engineering Group - AEG), 16th November 1999.

[119] Coulomb, C.A, 'MJmoires de mathJmatique et de physique de l'acadJmie royale des sciences', 1781 p161.

[120] Amontons, G., 'De la resistance causJe dans les machines', Histiore de l'academie royale des sciences avec les mJmoires de mathJmatique et de physique, 1699, p206.

[121] Schey, J.A., 'Frcition in Sheet Metal Forming', Society of Automotive Engineers – Sheet metal Pressing Development Applications, SP-1221, paper 970712, pp87-106.

[122] Meuleman, D.J, and Zoldak, J.J, 'The interactions of coated steels, Die materials and forming Lubricants, Society of Automotive Engineers – International Congress and Exposition, Paper 860432, Detroit, 24-25 February, 1986.

[123] Anon, BS ISO 4287:1997, General Product Specifications (GPS) – Surface texture: Profile method – Terms, definitions and surface texture parameters.

[124] Emmens, W.C., 'Tribology of Flat Contacts and its Applcations in Deep Drawing', PhD Thesis, University of Twente, November, 1997, ISBN 90-3651028-7.

[125] Anon, BSEN 10130 (1991) : British Standard Specification for Cold Rolled low carbon steel flat products for cold forming – technical delivery conditions, BSI.

[126] Personal communication with John Aitchison (Research Officer BSSP, Welsh Technology Centre, Port Talbot), June 22nd 2000.

[127] Lundh, H., Bustad, P-A., Carlsson, B., Endberg, G., Gustafsson, L., and Lidgren, R., 'Sheet Steel Forming Handbook', SSAB Tunnplat AB, 1998, ISBN 91-971592-9-8, Chapt.6, p15-16.

[128] Schey, J.A , 'Tribology in Metalworking', ASM, Metals Park, 1983.

[129] Schipper, D.J., 'Transitions in Lubrication of Concentrated Contacts', PhD Thesis, University of Twente, 1998.

[130] Scheers, J., Vermeulen, M., De MarJ, C., 'The influence of surface texturing on the tribological behaviour of sheet steel', Proceedings Sibetex 3 Seminar, Zelzate, Belgium, October 1996.

[131] Le Roche, Y., Berard, J.Y., Duval, J.L., Mouatassim, El., Pasquale, E.Di.,'Coupled Sheet Metal Forming and Fatigue Simulation', Proceedings of the 20th IDDRG Bienniel Congress June 17-19, 1998, Brussels Belgium, CRM, p126.

[132] Personal communication with Dr. Dean Cartwright (Research Officer, Welsh Technology Centre, Port Talbot), 9th July 1999.

[133], Limb, M.E., Chakrabarty, J., Garber, S., Roberts, W.T., 'Hydraulic Forming of Tubes'Sheet Metal Industries, November 1976, p419-425.

[134] Eichhorn, A., 'Innovative developments Concerning Hydroforming of Tubes', Proceedings of the International Conference on Hydroforming, Fellbach, Germany, October 1999, pp. 391-405, ISBN 3–88355-285-2.

[135] Prier, M., Engel, B., 'Process Development using Process Modelling', 'Innovations in Tube Hydroforming', ERC / NSM International Conference and Exhibits on Tube and Sheet Hydroforming Technology, Manufacturing of Lightweight components. Detroit, MI, USA, June 2000.

[136] FEA Information Homepage : www.implicitfea.com

[137] Anon, Microfield User Manual Version 3.0, Appendix A - Finite Element Methodology and Conventions, Rockfield Software.

[138] Engel, B., 'Process Orientated Control of Hydroform Production Lines', Proceedings of the International Conference on Hydroforming, Fellbach, Germany, October 1999, pp 191- 200. ISBN 3–88355-285-2

[139] Neugebauer, R., Putz, M., Leihkauf, J., and Schulze, B., 'Continuous Simulation of Hydroforming', International Conference on Hydroforming, Fellbach, Germany, October 1999, pp 201- 220, MAT-INFO, ISBN 3–88355-285-2.

[140] Zienkiewicz, O.C., 'The Finite Element Method', McGraw-Hill Book Company, 1977.

[141] Hora., P., Skrikerud.,M., and Longchang, T., 'Possibilities and Limitations of FEM Simulations in Hydroforming Operations', International Conference on Hydroforming, Fellbach, Germany, October 1999, pp 407- 424, MAT-INFO, ISBN 3–88355-285-2.

[142] Hughes, D., Bettles, J.L., 'A Comparison of the Capabilities of Explicit and Implicit ABAQUS Finite Element Analysis Codes for the Simulation of Sheet Metal Forming Processes', British Steel Strip Products, Internal Tech. Note, WL/PA/TN/1202H/5/92/12, Nov. 1992.

[143] Anon, Pamstamp Version 2.0 Training Manual, Mark 92, ESI.

[144] Anon, Pamstamp Software user update, EUROPam '99', Darmstadt, Germany, 1999.

[145] Solver reference manual, PAM-Stamp Version 2000, PAM SYSTEM INTERNATIONAL S.A.

[146] Pam-Generis™ reference manual, PAM-Stamp Version 2000, PAM SYSTEM INTERNATIONAL S.A.

[147] Personal communication with Tony Busvine (Director VPS) May 23rd 2000.

[148] Anon, LS-DYNA Product Brochure, CAD-FEM GmbH, 1998.

[149] Autoform GmbH Homepage : www.autoform.de, June 2000.

[150] Personal communication, Miller, B. (Wilde & Partners)

[151] Brun, R., Lai, M., Li, X., and Messina, A., 'Cutting Lead-Time And Development Costs Of Hydroformed Parts By FEM Simulation', IBEC '97, Conference

Proceedings of Body Assembly & Manufacturing, Detroit, MI, USA, 1997. pp 97-101.

[152] Meuleman, D., Liu, S.D., and Thompson, K., 'Analytical and Experimental Examination of Tubular Hydroforming Limits', SAE International Congress and Exposition, (980449) Detroit, MI, USA, 1998 pp138-150.

[153] Srinivasan, T.M., Shaw, J.R. and Thompson, K., 'Tubular Hydroforming: Correlation of Experimental and Simulation Results', SAE International Congress and Exposition, (980448) Detroit, MI, USA, 1998 pp130-137.

[154] Yoshida, T., and Kuriyama, Y., 'Effects of Material Properties And Process Parameters On Deformation Behaviour in Tube Hydroforming', IDDRG2000 21st Biennial Congress Proceedings, Ann Arbor, MI, USA, 2000, pp 43-52.

[155] Kergen, R., Lescart, J.C., and Duroux, P., 'Analysis of the Tube Formability in perspective of Tube Hydroforming', IDDRG 2000 21st Biennial Congress Proceedings, Ann Arbor, MI, USA, 2000, pp 33-41.

[156] Willinghofer, S., 'Forming Simulation: An Aid in part Development and Process Optimisation for Suspension Components', EUROPam '99, Conference Proceedings, Darmstadt, Germany, 1999.

[157] Darlington, R. A., Hughes, D. and Rees, M., 'Design Considerations for Pre-bending of Tubes for the Production of Hydroformed Components', EUROPam '99'. Darmstadt, Germany, 1999.

[158] Liu, J., Hahn, D., 'Optimisation of Process and Tool Development for Tube Hydroforming Using Computer Simulations', Innovations in Tube Hydroforming Technology, ERC/NSM Conference on Tube Hydroforming Technology. Conference proceedings, Detroit, MI, USA, 2000.

[159] Dutton, T., Iregbu, S., Sturt, R., Kellicut, A., Cowell, B., and Kavikondala, K., 'The Effect of Forming on the Crashworthiness of vehicles with Hydroformed Frame Siderails', IBEC '99, Conference Proceedings 1999-01-3208, Detroit, MI, USA, 1999.

[160] Karima, M., Qian, Y., and Cattran, D., 'Towards Further Understanding of the Mechanics of Tube Hydroforming', IBEC '98, Conference Proceedings of Body Assembly & Manufacturing, (982276), Detroit, MI, USA, 1998. pp 47-52.

[161] Hora, P., Skiekerud, M., and Longchang, T., 'Possibilities and Limitations of FEM-Simulation in Hydroforming Operations', Proceedings of the International Conference on Hydroforming, Fellbach, Germany, 1999, pp 407- 424. ISBN 3–88355-285-2.

[162] 'Automotive Design, KBE', Automotive Aspects March 2000 Corus Automotive Communications.

[163] Hecker, S. S., 'Simple Technique for Determining Forming Limit Curves', Sheet Metal Industries, Vol 52, November 1975, pp671-676.

[164] Anon, BSSP, WTC, Product Engineering Operating Procedure CP 04/0P/03

[165] Anon, BSSP, WTC, Product Engineering Operating Procedure CP 04/OP/02

[166] Sauer, W., J., Gotera, A., Robb, F., and Huang, P., 'Free Bulge Forming of Tubes under Internal Pressure and Axial Compression', Proc. 6th North American Metal Working Research Conference, Gainsville, Florida, USA, April 1978, p228-235.

[167] Bleck, W., Deng, Z., Papamatellos, K.,and Gusek, C., 'A comparative study of the forming-limit diagram models for sheet steels', Journal of Materials Processing Technology 83 (1998) 223-230.

[168] Asnafi, N., and Skogsgardh, A., 'Theoretical and experimental analysis of stroke-controlled tube hydroforming', Materials Science and Engineering (2000) 95-110.

[169] Cartwright, D., Drake, P. R., Godwin M. J., 'Effect of low cost press tool materials on formability of sheet steel' Ironmaking and Steelmaking 1998 Vol. 25, No. 2, p131-135.

[170] Altair Hypermesh® (v3.1) user manual.

[171] Gere, J.M., and Timosheko, S.P., 'Mechanics of Materials', 4th Edition, PWS Publishing Company, 1990, ISBN 0-534-93429-3, Chapt. 1, p23-24.

[172] Gere, J.M., and Timosheko, S.P., 'Mechanics of Materials', 4th Edition, PWS Publishing Company, 1990, ISBN 0-534-93429-3, Appendix – Physical Properties.

[173] Personal communication with Dave Ling (ESI UK technical support representative), July 1998.

[174] Pam-SYSTEM™, Pam-GENERIS™ Reference Manual, PAM-STAMP™ Version 1998.

[175] Kaye and Laby, Tables of Physical and Chemical Constants, Sixteenth Edition, 1995, Longman, England.

[176] Personal Communication, Damian Dry (Research Engineer, Engineering Doctorate Scheme – Wales) June 2000.

[177] Forming Technologies Incorporated FTi, Sheet Metal Formability: from product design to die tryout course notes. Rev 3 –19 Jul 99.

[178] Anon, BSEN 10130: 1991 Cold rolled carbon steel flat products for cold forming.

[179] Anon, ASM International (Steel Designations Book) ISBN 0 87170-635-0

[180] Anon, BS 4659: 1989, British Standards specification for tool and die steels.

[181] Anon, Anton Bauer CAD release drawings for manufacture of hydroform die tools, April 1996.

[182] Philip John Scriven, ''Formability and Processing of Laser Welded Blanks for Automotive Applications', Eng.D Thesis, University of Wales, Cardiff, 1997.

[183] Personal communication with Mike Boyles (Manager Automotive Applications, Corus, R,D& T, Welsh Technology Centre), 8th August 2001.

[184] Personal communication with Ray Barrow (Quality Manager, Phoenix Steel Tube) 23rd March 2001.

[185] Dry, D., Hughes, D., and Owen, R., 'Laser Weld Properties in the Finite Element Analysis of Press Formed Tailored Blanks', 3rd International Conference on Materials for Lean Weight Vehicles, November 1999.

[186] Sing, W. M., Rao, K. P., and Hua, M., 'Role of Process Variables in the Modification of the Forming Limit Stress Curve', Journal of Material Processing Technology 45 (1994), pp545-550.

[187] Andersson, R., 'Effects of Composition and the Production Process on the Formability of Austenitic Stainless Steels' Licentiate Thesis, 1999, Lulea Univerity of Technology, 1992: 42, ISSN: 1402 - 1757.

[188] 'Tribological Study – Friction and lubrication on the high pressure hydroforming process', Masseria, F., Internal placement student report, June 2000.

[189] Scriven P., 'Formability and Processing of Welded Blanks for Automotive Applications', EngD Thesis, October 1997.